Department of Pharmaceutical Sciences

The Synthesis and Characterisation of Modified Polyethylenimine Polymers for Gene Delivery.

Anthony Brownlie

May 2002

Abstract

Polyethylenimine (PEI) has previously been shown to be an efficient gene delivery vector in both *in vitro* and *in vivo*. Despite this efficient transfection response PEI suffers from high toxicity when administered *in vivo*. We report the synthesis of four modified PEI polymers for use as gene delivery vectors. PEI was modified through attachment of Palmitoyl groups to give P-PEI, the attachment of Palmitoyl and Polyethylene glycol groups to give PP-PEI, the quaternisation of PEI and P-PEI to give QPEI and QP-PEI respectively. The successful modification of the PEI polymer was confirmed using various analytical techniques Nuclear Magnetic Resonance, Fourier Transform Infrared spectroscopy, Ultra Violet spectroscopy and Gel Permeation Chromatography Multi Angle Laser Light Scattering. The polymers ability to interact with plasmid DNA and their subsequent morphologies were also investigated. P-PEI was found to self assemble into a vesicular structure upon sonication. This vesicular structure was retained upon complexation with DNA (~200nm). PP-PEI was found to produce worm like structures when sonicated (~700nm). QPEI was shown to produce small tightly packed spheres with DNA (~50nm). The condensation of DNA by QPPEI produced flattened vesicular structures (~200nm). PP-PEI (~700nm) and QPPEI (200nm) were also sonicated in the presence of cholesterol to produce vesicular structures.

In vitro studies showed the modified polymer/DNA complexes were found to be more resistant to degradation in the presence of plasma proteins and blood erythrocytes, with the exception of QPEI. Haemolytic activity of the modified polymers was found to be very low and less than that of the parent PEI polymer. MTT assays showed that the modified polymer/DNA complexes were less cytotoxic than PEI alone. The modified polymers were found to be less efficient transfection agents *in vitro*, with the best modified polymer (QPPEI) producing around 60% of the response shown by PEI. *In Vivo* studies using a green fluorescent protein marker revealed P-PEI, QPPEI and QPPEI/cholesterol to be more efficient transfection agents than the parent molecule PEI.

Acknowledgements

I would like to thank my supervisor Dr Ijeoma Uchegbu for all her help and advice during my PhD studies. I would also like to thank Dr Andreas Schatzlein for his help during my time spent at the Beatson laboratories.

Thank you also to everybody in the lab for giving me somebody to talk and moan to, especially Lee, Maureen, Alistair, Lubna and anyone else I have left out.

Last but not least, thanks to my mum and dad for supporting me throughout my time at university, giving me money and letting me stay in their house.

Table of Contents

Chapter 1: Introduction to Gene Therapy

1.1: Introduction to Gene Therapy

The term 'gene therapy' can be applied to any clinical use of recombinant DNA technology to modify somatic cells i.e. the introduction of genetic information into a patients cells to enable the production of beneficial proteins to rectify or control a disease [1]. A stricter use of the term denotes only the replacement of defective or missing genes. Gene therapy derives from the observation that certain diseases are caused by the inheritance of a single functionally defective gene. These diseases that have the potential to be treated through replacement with a standard functional copy of the gene [2]. Diseases that have become targets for gene therapy include acquired multifactorial diseases such as cancer [3], arthritis [4] and AIDS [5], as well as monogenetic disorders such as cystic fibrosis [6] and muscular dystrophy [4]. The use of gene therapy is intended to help overcome certain limitations found with the use of protein drugs, such as low bioavailability, poor pharmacokinetics and high production costs.

At the present time the majority of approved gene therapy protocols involve cancer patients. Around 68% of existing protocols are for the treatment of different tumours [1]. The current clinical trials use a variety of different approaches to achieve their goal (Figure 1). The combination of gene therapy with cellular immuno-therapy was derived from evidence that the immune system may be able to eliminate human tumours. The immune response can be manipulated with immune stimulating cytokines [7, 8] or the

expression of tumour antigens in engineered cells [9, 10], in order to induce tumour regression. Another approach is the use of suicide genes introduced directly into cancer cells to generate cell death. This approach suffers from the difficulty of selectively targeting cancer cells whilst avoiding killing normal tissues. Because of this problem suicide gene therapy has been limited to local cancer therapy such as brain tumours [11]. Tumour suppressor genes take part in critical cell functions such as signal transduction, gene transcription and cell death [12, 13]. The substitution of mutated or deleted tumour suppressor genes with a working copy could restore the original suppressor function [1].

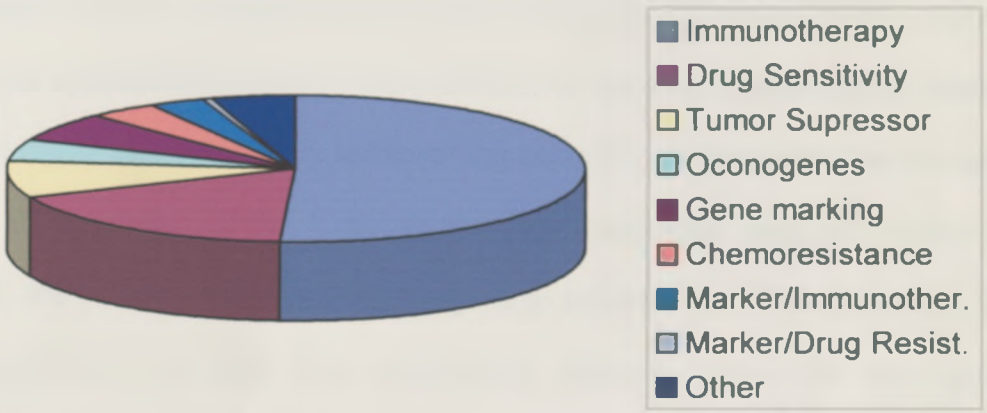

Figure 1: Different approaches to treatment of cancer using gene therapy. The immunotherapy approach represents around 50% of approved trials [1].

A fourth approach to gene therapy is through the marking of genes. Studies have shown that the contamination of gene marked tumour cells can contribute to relapse following autologous stem cell transplants [14]. This approach is being investigated in studies of myeloblastic leukaemia, chronic myeloid leukaemia and neuroblastoma. The use of this approach in clinical trials is being aimed at understanding whether somatic transduction can be safe and whether the transduced genes can be durably expressed, and whether the transduction process could affect cell properties. Gene therapy is also being combined with chemotherapy [15]. Multi-drug resistant genes are transferred into normal cells in order to allow the use of higher doses of chemotherapeutic drugs. This permits more intensive chemotherapy sessions with an increased therapeutic ratio [16]. Tumours of the central nervous system have proved very difficult to treat by conventional means alone, these difficulties have led to efforts to treat them through gene therapy [17]. The location of the tumours hampers successful surgical treatment, whilst the effects of chemotherapy are blocked by the presence of subpopulations of cells that temporarily withdraw from the cell cycle protecting the tumour. The reduced permeability of the blood-brain barrier also hinders drug treatments.

A variety of both viral and non-viral vectors for gene delivery are currently available. Viral based gene therapy involves the use of attenuated or defective viruses created by genetic engineering. These vectors work by utilizing the highly evolved pathways of infection to deliver and express

genes in the body and are designed not to cause viral disease [18]. These infection pathways provide the viruses with access to a number of different target cells, uptake via receptor-mediated endocytosis and efficient intracellular trafficking from the endosomes to the nucleus. Certain viral vectors such as retrovirus and adenovirus, are capable of permanently integrating their genomes into the host chromosomal DNA or replicating and persisting as an extra-chromosomal element within the nucleus. Several viruses such as, retrovirus, adenoviruses, adeno-associated viruses and herpes viruses have been investigated for *in vivo* gene delivery. Each of these vectors has their own unique biological properties as well as different clinical applications and safety concerns. Non-viral vectors have been developed in response to the problems and risks associated with viral vectors (Table 1), such as the induction of an inflammatory or immunogenic response, the inability to administer a repeat dose, problems with control of long-term expression and some viruses can only take genes of around 5-8Kbases [19].

Non-viral vectors fall into three main classes, cationic lipid-based carriers (lipoplexes) [20, 21], cationic polymer-nucleic acid complexes (polyplexes) [22, 23] and naked DNA. Non-viral vectors have several advantages over viral vectors such as, having none of the safety problems of viral vectors, being easy to prepare, purify and store, and the fact that the molecular structure and purity of the vectors can be determined with a high degree of accuracy. Non-viral vectors also do not suffer from DNA size limitations.

Gene delivery system	Delivers genes of a limited size	High level of sustained gene expression	Scale up problems	Safety problems
Cationic liposomes	No	No	No	No
Cationic polymers	No	No	No	Some reports of toxicity
Naked DNA	No	No	No	No
Retroviruses	Yes	Yes	Yes	Possible mutagenesis
Lentivirus	Yes	Yes	Unknown	Possible mutagenesis
Adenoviruses	Yes	Yes	No	Yes
Adeno associated viruses	Yes	Yes	Yes	Yes

Table 1: Summary of properties for viral and non-viral gene delivery vectors [19].

1.2: Viral Vectors

1.2.1: Retrovirus Vectors

Retroviruses are enveloped viruses approximately 10Kb in size and consist of a single stranded RNA molecule [24]. The virus consists of three genes: Gag, for core proteins, Pol, for reverse transcriptase and Env, for viral envelope proteins. Once the virus has entered a cell, their genomes are reverse transcribed into double stranded DNA that integrates into the host genome and is expressed as a protein. Most retroviral vectors are derived from murine leukaemia viruses (MLV) that contain double stranded RNAs that can replicate through a DNA intermediate in host cells [25]. The recombinant virus can use either an ecotropic envelope, which can recognize mouse cells, or an amphotropic envelope, which recognizes human and other cells. The functional Gag, Pol and Env genes are removed and replaced with the transgene of interest [18]. The DNA produced by this modification is then incorporated into the host genome during cell replication. Retroviruses can only integrate into replicating cells, with the exception of the human immunodeficiency virus (HIV), which can integrate into non-replicating cells [26]. This factor clearly restricts the use of retroviruses as vectors for gene delivery. Other limitations of retroviral vectors include the limited capacity of insert DNA (~8Kb) and the current achievable viral titres (about 10^7), which is low when compared to that needed to treat large tumours [18]. The generation of recombinant replication competent viruses also constitutes a risk to health. Retroviruses can also be deactivated by the C1 complement

protein and anti-alpha galactoysl epitope antibodies, which are both present in human serum [24].

1.2.2: Adenoviral Vectors

Adenoviruses are non-enveloped viruses that contain a linear double stranded DNA genome [27]. The virus life cycle does not require dividing cells as the virus replicates as episomal elements in the nucleus of the host cells, which excludes the insertional problems associated with retroviruses. Most adenoviruses are based on the Ad5 virus and are double stranded DNA viruses that are capable of high levels of transduction. Adenoviruses (Figure 2) are larger and more complex than retroviruses or adeno-associated viruses, as only a small fraction of the viral genome is removed from the vector [28].

Adenoviral virons are icosahedral in shape around 70 to 100nm in diameter (Figure 1.2.2). The double stranded DNA and core proteins are surrounded by a protein shell composed of capsid proteins [29]. The capsid contains 252 surface projections called capsomers, with 12 vertices. There are eleven structural proteins numbered from protein 2 to 12. The three capsid proteins, which actively participate in the virus entry into the cells, are fiber (protein 3), penton base (protein 5) and hexon (protein 2). There are at least 4 inner core proteins that are known to take part in the viral DNA replication [4].

Despite the fact that adenoviral vectors have been widely used for gene therapy, they have several disadvantages [27]. Adenoviruses have 47 serotypes and their large diffusion in humans often results in a strong

immune response in the host due to the presence of viral proteins and sometimes the immune response is even higher in case of previous exposure to the virus. Reports of severe reaction and even deaths have been found when using high doses of the virus. Also, unlike retroviruses the duration of expression is very limited [27].

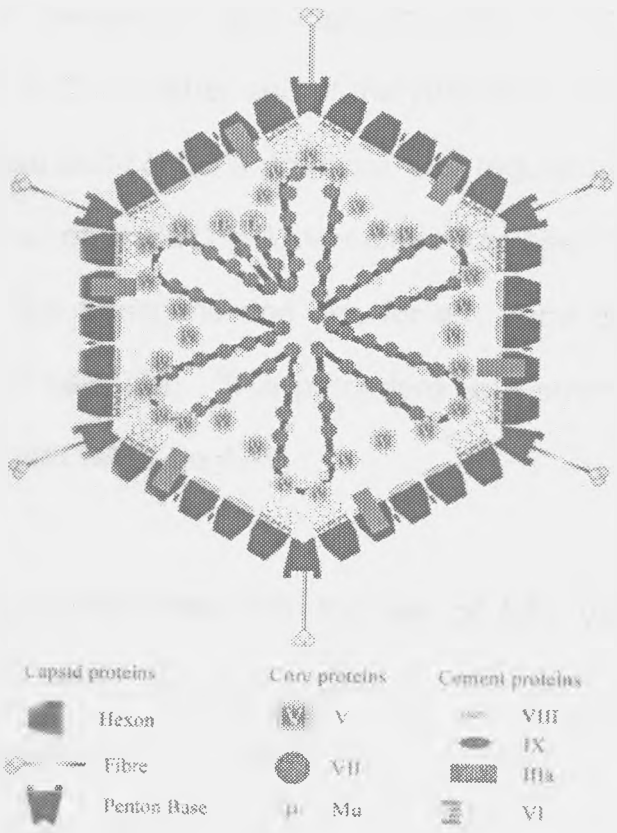

Figure 2: Structure of adenovirus. The locations of the capsid and cement components are reasonably well defined. In, contrast, the disposition of the core components and the virus DNA is largely theoretical [28].

1.2.3: Adeno-associated Vectors.

The adeno-associated virus (AAV) is a small, simple, nonautonomous virus that contains linear single stranded DNA [30]. The AAV virus is widespread in the human population but is not associated with any disease and requires co-infection with adenoviruses in order to replicate. The viral genome consists of two genes, rep, encoding a family of overlapping proteins involved in replication and integration, and cap, encoding a family of three viral structural proteins [31]. At either end of the viral DNA is a sequence named the Terminal Repeat that contains promoter and regulatory sequences. The conventional method of producing AAV vectors has been to co-transfect two plasmids: one for the transgene and one for structural genes cap/rep, into adenovirus infected cells [32]. This procedure was prone to contamination with adenoviruses and wild-type AAV.

The main drawbacks associated with the use of AAV vectors are a small packaging capacity, which limits the size of the transgenes that can be delivered, and the presence of the integrating vector carries the risk of insertional mutagenesis [31], prevalence of seropositivity of antibodies against wild-type AAV, and difficulty in producing sufficiently high titres as required for human clinical trials [31].

1.2.4: Lentiviral Vectors

Lentiviral vectors are based on the lentivirus HIV-1, first discovered during the outbreak of AIDS and the ensuing research into HIV [1]. Lentiviral vectors are a subclass of retroviruses that are able to infect both proliferating and non-proliferating cells and are capable of high levels of transgene expression [1]. These viruses are constructed from the core of HIV-1 and the surface protein from stomatite vesicular virus. The lentivirus is capable of transfecting genes in nearly all types of cells, with high levels of transfection. Reports of lentiviral vectors combined with gene marking have shown prolonged *in vivo* expression in muscle, liver and neuronal tissue [33, 34]. Gene marking is used to show how well a vector can transfect genes, and the effect the transfection process has on the transfected cells Despite the promising *in* vivo results lentiviral vectors present safety problems for both clinical staff and patients with the risk of the potential generation of recombinant viruses even more deadly than the parental HIV virus [1].

1.3: Non-Viral Vectors

1.3.1: Naked DNA

The simplest approach to non-viral gene therapy is the use of DNA without a carrier. DNA has not been shown to give good transfection results for cells *ex vivo*. Efficient gene transfection has been shown after local injection of plasmid DNA *in vivo* most notably in muscle [35] and skin [36]. Intravascular injection of plasmid DNA usually results in poor expression in the major organs. Although the rapid injection of a large volume of DNA (1.5 to 3.0ml) through the portal or tail vein of mice, was shown to give a high level of gene expression in the liver, which increased with increasing volume of DNA. The level of expression was found to be comparable to that of the intravenous administration of adenoviral vectors. Despite this high transfection efficiency the procedure is unsuitable for clinical applications.

The observation that the administration of protein antigen encoded plasmids into muscle or skin in mice leads to humoral and cellular immune responses directed to the antigen [18] has increased the study into naked DNA vaccines. Methods have been developed in order to improve the gene transfer of naked DNA, for example the gene gun [37] and electroporation methods [38, 39]. Use of these physical methods allows the DNA to penetrate the cell membrane directly and bypass the endosome/lysosome and avoid any enzymatic degradation. The 'gene gun' method of DNA delivery uses a high-pressure helium stream to deliver DNA, coated onto

gold particles, directly into the cytoplasm [37]. This method has shown reasonable transfection for a variety of cell lines *ex vivo* and *in vivo* a moderate transfection efficiency in skin cells.

Electroporation is the application of a high voltage to a mixture of DNA and cells in suspension [40]. The cell-DNA suspension is placed between two electrodes and exposed to an electrical pulse and the DNA enters the cells through holes formed in the cellular membrane during the electrical pulse. The DNA is trapped within the cytoplasm until the pulse is stopped. The best results have been found using rapidly proliferating cells, although electroporation of mammalian cells has proved to be ineffective, as most cells do not survive being exposed to the high voltage. More recent devices and electroporation procedures have been shown to produce less cell damage *in vitro* and substantial improvements in the level of gene expression in the skin and tumours of mice [41].

1.3.2: Liposomes

Liposomes were first described as models for cellular membranes and were then applied to the delivery of substances to cells [21]. Liposomes are self-closed colloidal particles in which bilayered membranes composed from self-aggregated lipid molecules encapsulate a fraction of their surrounding medium into their core. Liposomal formulations can be described as large, small, multi, oligo and unilamellar liposomes (Figure 3) [20].

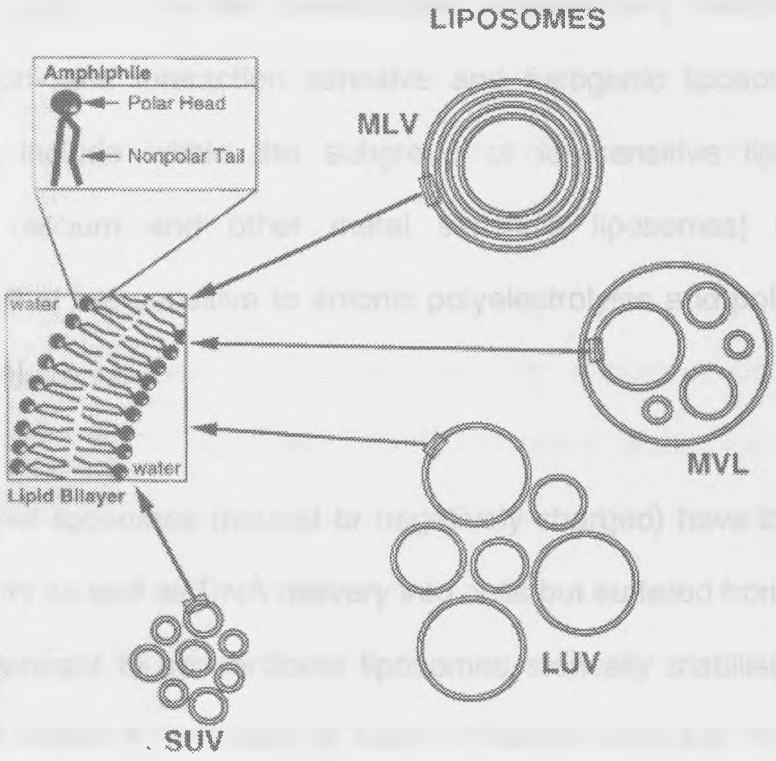

Figure 3: Schematic representation of liposomes. Small (below 50-80nm) and large (80-1000nm) vesicles can be distinguished while with respect to lamellarity unilamellar, oligolamellar and multilamellar liposomes are defined. Multivesicular liposomes are large uni- or oligolamellar vesicles with smaller vesicles entrapped [21].

Smaller unilamellar liposomes are more frequently used for medical applications [42]. Using these formulations a new classification can be used based on their interaction characteristics such as, non-specific, inert, specific and reactive liposomes [43]. Non-specific liposomes cover all conventional liposomes in which *in vitro* but not *in vivo* behaviour can be controlled. Inert liposomes do not interact with their surroundings because of steric stabilization due to the polymer coating of the surface [43]. Specific liposomes are those capable of interacting as determined by surface attached ligands. The last classification includes very reactive liposomes such as ion- and interaction sensitive and fusogenic liposomes. These liposomes include within the subgroup of ion-sensitive liposomes (pH sensitive, calcium and other metal sensitive liposomes) and cationic liposomes that are sensitive to anionic polyelectrolytes and polyanions such as DNA [44].

Conventional liposomes (neutral or negatively charged) have been used for drug delivery as well as DNA delivery into cells but suffered from poor results [21]. In contrast to conventional liposomes sterically stabilised liposomes have been shown to be stable in blood circulation and can to some extent evade rapid uptake in systemic circulation [45]. Other liposomal formulations include virosomes, a liposome containing fusogenic viral proteins [46]. Efficient DNA encapsulation has been found to be problematic and they tend to produce large particles. Virosomes suffer from immunogenetic problems as well because of the presence of the viral or bacterial proteins [46].

Liposomes are generally constructed from phospholipids (Figure 4), with sterols such as cholesterol added to improve the mechanical properties of bilayers [20]. Both natural and synthetic lipids are used. Natural lipids tend to be zwitterionic, neutral or anionic. Cationic lipids tend to be synthetic as they are practically non-existent in nature [47]. Nature has produced several thousand different lipids, with the most abundant lipids being either lectithins (phosphatidylcholines) or sphingomyelins [21]. They contain a choline head group attached either via a glycerol or sphingosine backbone to two fatty acid chains and tend to be zwitterionic at a physiological pH [21]. Neutral lipids are glycolipids that normally contain one or more sugar groups attached to the backbone [21]. Anionic lipids contain charged groups either on the polar head or on the phosphate group [21].

Sterols are amphiphilic molecules that are important components of biological membranes [43]. They provide increased mechanical strength and improved thermal properties and phase behaviour of membranes, and in doing so reduce or eliminate the drastic fluidity changes with temperature variation and are often used in liposome preparations [21]. Non-phospholipid synthetic lipids are mostly non-ionic lipids. They usually have (poly)-glycerol or poly (oxy) ethylene oxide polar heads attached to carbon chains. Cationic lipids can be distinguished between single chain and double chain lipids [21] (Figure 1.3.2b). The most commonly used ones are quaternary ammonium salts containing a long chain fatty acid. They are able to form liposomes

either in mixtures with both zwitterionic and neutral lipids, cholesterol or an anionic surfactant at unbalanced ratios.

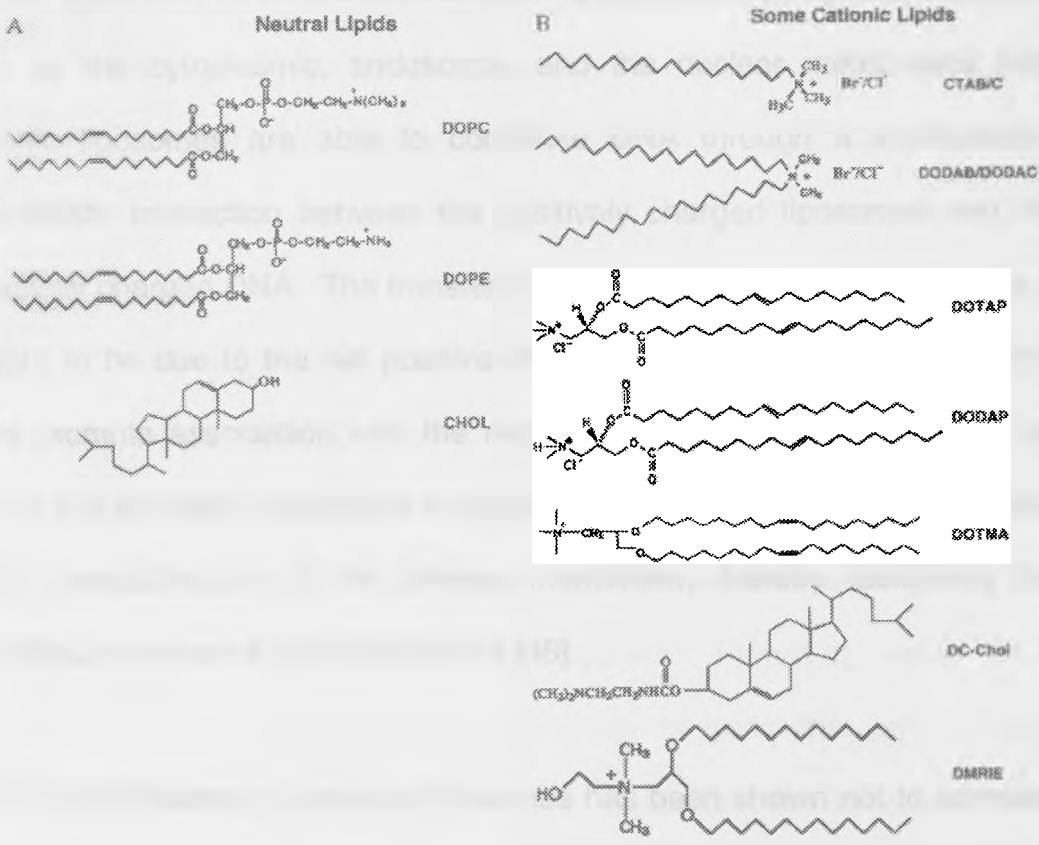

Figure 4: Chemical formula of various lipids. Neutral lipids: DOPC dioleoyl phosphatidyl choline, DOPE: DO phosphatidyl ethanolamine. Chol: cholesterol, cationic lipids: CTAB/C: cetyl trimethyl ammonium bromide/chloride, DODAB/DODAC: dioctdecyl dimethyl ammonium bromide/chloride, DOTAP: 1,2-diacyl-3-trimethylammonium propane, DODAP: 1,2-diacyl-3-dimethyl ammonium propane, DOTMA: [2,3-*bis* (oleoyl)propyl] trimethyl ammonium chloride, DC-Chol: 3B[N-(n',N' – dimethylaminoethane)-carbamoyl] cholesterol, DMRIE: dimyristoyl.[21]

Gene transfer using lipoplexes is strongly reliant upon their physico-chemical properties and on the cellular internalisation mechanisms. The use of cationic liposomes to mediate transfection is hampered by several obstacles such as the cytoplasmic, endosomal, and the nuclear membranes [48]. Cationic liposomes are able to condense DNA through a spontaneous electrostatic interaction between the positively charged liposomes and the negatively charged DNA. The transfection ability of the resulting lipoplexes is thought to be due to the net positive charge exhibited by the complex that could promote association with the negatively charged surface of cells as well as the fusogenic properties exhibited by the lipoplex can induce fusion and/or destabilisation of the plasma membrane, thereby facilitating the intracellular release of complexed DNA [48].

The *in vitro* efficiency of cationic liposomes has been shown not to correlate with results gained from *in vivo* administration [21]. This can be attributed to the differences in requirements for a good *in vitro* and *in vivo* transfection agent. Such factors as, the physical chemistry of surface receptors and the cell propensity for endocytosis are significantly more complex than those found in cell culture. In order to improve *in vivo* transfection efficiency different approaches have been studied. The inclusion of cholesterol in the liposome bilayer has been shown to inhibit the effects of serum and improve cell binding and uptake. The inclusion of cholesterol also promotes stability allowing increased doses of both lipid and DNA to be delivered and expressed [48-50].

Liposomes have also been modified through the attachment of polyethylene glycol (PEG) [51]. The attachment of PEG helps avoid the tendency to form large aggregates shown by lipoplexes, as well as reducing their blood clearance and prolonging their circulation. The inclusion of PEG has also been shown to alter the biodistribution of lipoplexes to target tissues such as tumours rather than the lung and heart [51].

The *in vivo* response of cationic liposomes was first reported in 1989 using a mouse model [52, 53]. Lipoplexes were administered intravenously (i.v.), intratracheally (i.t.) and intraperitoneally (i.p.). Gene expression was seen in the lung for up to a week with i.v. and i.t. administration, while expression was not seen in the reticuloendothelial system. Promising results from studies using marker genes led to the study of gene therapy in model animals [54, 55]. The delivery of the cystic fibrosis transmembrane conductance regulator gene (CFTR) to airways and deep alveoli via i.t. administration in cystic fibrosis transgenic mice, to correct the ion transport [56] defect led to the conclusion that this approach would be efficacious in humans. Another study reported the delivery of human CFTR gene to mutant mice by nebulisation and 50% correction of ion transport in the same mice was also reported [57].

A number of protocols for gene therapy involving liposomes have been approved and performed in humans [21]. The gene expression and safety profile of lipoplexes was evaluated in 5 melanoma patients [58]. PCR and

immunostaining showed the presence of DNA and expressed proteins in tumours respectively. Liposomes have also been complexed with the CFTR gene and administered intranasally into nine cystic fibrosis patients. Six of the patients were given placebo formulations. Nasal biopsies showed no histological or immuno-histological changes and no other adverse effects were observed and partial improvement in Cl^- transfer was observed in patients [59]. Low levels of expression were observed and lasted only for a few days although the safety of these formulations indicated that this approach could lead to more feasible therapies. To date there have been a large number of clinical protocols using liposomal formulations for the treatment of cystic fibrosis, cancer and cardiovascular disease [21], which demonstrate the importance of this technology.

As research into gene therapy with liposomes continues, the emphasis is moving towards complicated engineered designs that incorporate the many functions required to bypass the various extra- and intracellular barriers, rather than simple electrostatic complexes [44]. A complex with a condensed DNA core, surrounded by a lipid bilayer with fusogenic agents and an outer steric polymer layer that can be shed, with exposed ligands is currently the goal of some research groups (Figure 5). This design would provide stability as well as reducing non-specific interaction and increasing selectivity through the exposed ligands.

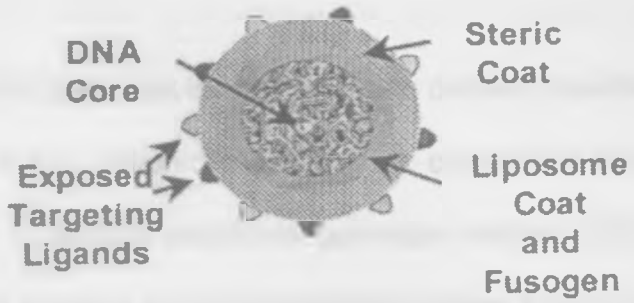

Figure 5: Schematic of the ideal liposomal complex containing the elements for improved gene delivery [44].

1.3.3: Cationic Polymers

The use of cationic polymers to mediate gene delivery has been studied for a number of years and cationic polymer/DNA complexes have been termed polyplexes [22]. Cationic polymers generally contain protonable amines. The amount and position of the protonable amines varies between different polymers. Linear polymers like poly-L-lysine (Figure 6) tend to have positive charges located on sides groups, while branched polymers like polyethylenimine and dendrimers have their positive charges on the backbone [60].

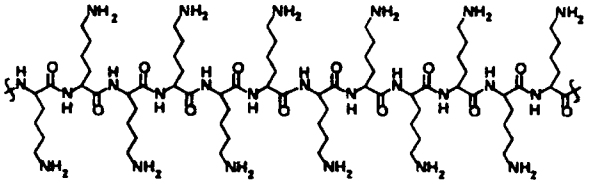

Figure 6: Chemical structure of ploy-L-lysine.

Of the cationic polymers poly-L-lysine is probably the most widely investigated [61, 62]. The development of polyplexes based on oligolysines and synthetic polypeptides was due to the fact that these polylysine compounds are amines and are available in a number of different molecular weights and the varied size distributions of the polyplexes. Reports of in vivo gene expression using polylysine are limited. The first report of *in vivo* expression was by Wu *et al* [63]. Asialo-orosomucoid polylysine complexes were administered intravenously to rats. The highest levels of gene

expression was found in the liver after 24 hours, while no expression was observed after 96 hours. Perales *et al* [64] reported the intravenous administration of galactosylated polylysine complexes of around 15nm in diameter, which prolonged expression for up to 20 weeks. Hashida *et al* [65] also reported the elimination of a galactosylated polylysine from blood circulation in a matter of minutes, with preferential uptake by the liver. Polylysine has also been targeted to the lung. Ferkol *et al* [66] reported specific gene expression in respiratory epithelium and submucosal glands in mice. Polylysine was coupled to a Fab (immunoglobulin) fragment with specificity for a receptor highly expressed in lung epithelium cells.

As poly-L-lysine exhibits poor *in vitro* and *in vivo* results, research has been focused on improving the polymer to increase its suitability for *in vivo* use, through use of liphophilic components, target specific ligands and with endosome disruptive peptides [60]. Brown *et al* [67] reported the conjugation of hydrophilic and hydrophobic chains to polylysine and polyornithine. The modified polymers were able to self assemble into vesicular systems upon sonication. The new complexes were found to be less cytotoxic than the parent polymer complexes. An improved *in vitro* gene expression was found in human tumour cell lines without the presence of receptor specific ligands and lysosomotropic agents.

Transferrin-polylysine complexes have been reported in an *ex vivo* phase I study in the presence of inactivated adenoviral particles [68]. The

subcutaneously administered cancer vaccine consists of the individual patients melanoma cells, which are transfected *ex vivo* by a transferrin-poly-L-lysine complex/adenovirus formulation to produce interleukin-2.

1.3.4: Polyethylenimine

Polyethylenimines (PEI) consist of a large family of hydrophilic polyamines of varying molecular weight and degrees of chemical modification [69]. PEI's are synthesised by cationic ring opening polymerisation of ethylenimine (arzidine) via a nucleophilic addition mechanism [70]. PEI's produced in this way are believed to be highly branched, possessing primary, secondary and tertiary amine groups in a ratio of approximately 1:2:1 (Figure 7). Other literature has reported a ratio of 1:2.4:1 [71]. The branching sites of PEI are separated largely by secondary amine groups, with one branch occurring for every 3-3.5 nitrogen atoms along a linear chain. This branching distribution yields spherical shaped molecules, which may possess many charged nitrogens. The charge density will vary according to the position of the equilibrium with various proton sources.

A

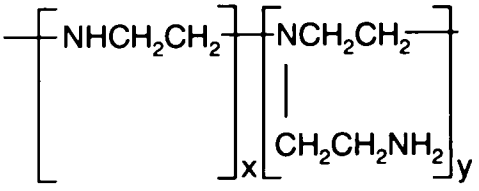

B

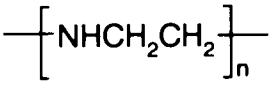

Figure 7: Chemical structures of A: Branched PEI and B: Linear PEI.

Gene Delivery Potential

PEI was first tested for its gene delivery potential by Boussif *et al* in 1995 [72]. Molecules such as lipopolyamines [73] and polyamidoamine dendrimers [74] have been proved to be efficient transfection agents. The reason for their high efficiency was thought to be due to the fact that they possess a substantial buffering capacity below physiological pH. This observation led to the testing of PEI, which has a substantial buffering capacity at virtually any pH [72]. PEI was shown to be a highly efficient transfection agent in both *in vitro* and *in vivo* tests [72], with a low cytotoxicity although other groups have reported high toxicity when using PEI [75]. Since PEI was first shown to have good gene delivery potential, the number of examples in the literature reporting PEI's potential has increased rapidly. Abdallah *et al* [76] reported that PEI was used to introduce genes into the mature mammalian brain *in vivo*, with transfection and duration of expression results proving to be much higher than any previously reported non-viral method. Boletta *et al* [77] were able to deliver DNA to the rat kidney using PEI. The complexes were injected into the renal arteries of rats and allowed to remain in contact with the kidney for ten minutes. Goula *et al* [78] reported the transfection of genes via the intravenous route, into several organs. The heart, spleen, liver and kidneys were found to contain low levels of gene expression, but the lungs showed much higher levels of expressed genes.

Effects of molecular weight.

As PEI is available in many different molecular weights, several groups have been investigating the transfection efficiency of PEI of differing molecular weights. Abdallah *et al* [76] investigated the *in vivo* transfection efficiencies of PEI in the mature mouse brain comparing the effects of three different molecular weights of PEI (25, 50 and 800kDa). It was found that the 3 preparations gave different levels of transfection, with the lower molecular weight polymers giving a higher transfection efficiency than the higher molecular weight PEI's. In particular the 25kDa polymer gave the highest levels of transfection. Godbey *et al* [79] also investigated the *in vitro* transfection efficiency of different molecular weight PEI's (600, 1200, 1800, 10,000 and 70,000 Da). They found that PEI's of molecular weights of 1800 Da and under gave no transfection at all. The fact that the larger PEI molecules gave higher transfection efficiencies was thought to be due to the fact that the larger PEI molecules either affords better entry of the complexes into cells or they offered more protection to the plasmids they were carrying.

Although the two groups had differing results an optimum molecular weight was found to lie between 10-70KDa. Godbey *et al* [79] put the discrepancy down to differences in the experimental setup, such as using different ratios of PEI nitrogens to DNA phosphates, the different cell types used by the two groups and the fact that Abdallah *et al* [76] worked *in vivo* while Godbey *et al* worked *in vitro*.

Fischer *et al* [80] reported the synthesis of a PEI of molecular weight 11·9 Kda, characterised through ^{13}C NMR and laser light scattering size exclusion chromatography. This new low molecular weight polymer was compared with a higher molecular weight polymer (800KDa) to clarify the effects of molecular structure and mass as well as cytotoxicity. The low molecular weight polymer exhibited a low degree of branching and was less cytotoxic over a wide range of concentrations, than the higher molecular weight PEI. The low molecular weight PEI also gave *in vitro* transfection efficiencies up to two orders of magnitude higher than those of the higher molecular weight PEI [81]. The different reports in the literature show the use of a lower molecular weight polymer reduces toxicity but also compromises transfection efficiency, while increasing molecular weight increases transfection but toxicity also increases. An optimal ratio of toxicity vs. transfection efficiency seems to arise with polymers ≤ 25Kda. Linear PEI has been shown to be less toxic than the branched version and in some cases has improved transfection efficiency. There are yet to be reports detailing a direct comparison of linear and branched PEI with the same molecular weight so no conclusion on whether or not one is better than the other can be made as a lower molecular weight linear polymer may give reduced toxicity over a higher molecular weight branched polymer.

Modification of PEI

Hydrophilic polymers such as polyethylene glycol (PEG) have been attached to liposomes in an effort to reduce protein binding to the liposome/DNA complex [21]. These modifications have resulted in a prolonged half-life of the modified liposome in blood when compared to the unmodified liposome. This method of reducing protein binding has been applied to PEI. The first report of PEG modified PEI in the literature was by Holmberg *et al* [82]. The modified complex was shown to be able to reject fibrinogen from the surface of the complex.

Ogris *et al* [83] investigated the *in vivo* and *in vitro* effects of PEGlyated-transferrin-PEI/DNA. The complex showed a strong reduction in plasma protein binding and erythrocyte aggregation. The modified complex also exhibited improved stability, reduced surface charge, increased half-life in the blood and reduced toxicity. Non-PEGylated complexes were administered intravenously to tumour bearing mice resulting in gene expression in the tail and lung, with severe toxicity in some mice. The PEGylated complexes were found to express the reporter gene in the tumour without any significant toxicity. Vinogradov *et al* [84] reported on the use of PEG-PEI complexes for the delivery of chemically modified oligonucleotides (ODNs), in particular antisense phosphorothioates (PS-ODNs). The PEG-PEI complexes were compared to PEG-polyspermine (PEG-PSP) complexes. PEG-PEI proved to be stable at physiological pH and ionic

strengths. The complexes also proved to be more stable than PEG-PSP when in the presence of low molecular mass electrolytes. Based on the stability of the PEG-PEI complexes, as well as the small size of the complexes (-ca 32nm), PEG-PEI appears to have good potential for the delivery of PS-ODNs.

PEI has also been shown to have been chemically modified with epichlorhydrine or ethoxylated, without any loss of *in vitro* transfection activity [85]. This shows PEI to be a promising structural base for forming more sophisticated viral-like vectors that could include supplementary functions such as cell specific targeting ligands. Zanta *et al* [86] have reported that neutral PEI/DNA complexes bearing galactose residues transfect efficiently in specific hepatocyte-derived cell lines in the presence of serum and in the absence of any extra membrane-disrupting agent.

PEI has been used in liposomal formulations in an attempt to improve DNA encapsulation and delivery of DNA to liver cells [87]. The inclusion of PEI in the formulations caused an increase in the percent liposomal encapsulation of the large DNA molecules as well as buffering lysosomal activity, thus protecting the compacted DNA from degradation. To try to incorporate some of the attributes of viral delivery systems and to further increase the cellular uptake and nuclear delivery of genes, adenovirus particles have been attached to polymer/DNA complexes [88]. When adenovirus particles are added to transfection systems as free particles they can enhance the cellular

uptake of DNA [88]. Baker *et al* [88] have shown that a PEI-adenovirus system gives improved transfection results over PEI and adenovirus particles on their own. Although the inclusion of viral particles within a formulation facilitates improved transfection, immunological problems can still occur from the presence of viral particles.

There are many membrane-modifying agents that have been used to increase the efficiency of gene delivery using polycation/DNA complexes. Compounds such as endosomolytic peptides, glycerol and bacterial proteins have been used with ligand polylysine complexes and have improved transfection efficiencies up to more than 1000-fold *in vitro* [89]. PEI, which is a more efficient molecule for gene delivery, has only been enhanced by around 10-fold using membrane modifying agents. This is thought to be due to PEI's own membrane destabilising properties [89].

Godbey *et al* [90] have reported a modified PEI transfection procedure that has significantly increased the polymers *in vitro* transfection efficiency by around 16%. The modified procedure removed any free polycations from the transfecting solution through centrifugation of the complex solution and removal of the supernatant containing un-complexed PEI, reducing the toxicity associated with the free polymer. The composition of the PEI complexes that are administered to cells was modified, allowing improved PEI packing around the plasmid to yield a greater buffering capacity without any change in the surface charge of the complexes.

An important property of polycation/DNA complexes is their size. Complexes of small size (<100nm) have been considered to be a critical parameter for *in vivo* delivery because of known physical restrictions, for example in the vascular system, dimension of fenestrations (through which the material must pass to gain access to the target cells) and diffusion in the tissues. Tang *et al* [91] have examined complexes between PEI and DNA using electron microscopy. The complexes were found to have diameters of around 50nm, compared to polylysine/DNA complexes, which had diameters of around 1000nm. Although there are large differences in the size of the complexes, they had similar toroidial structures.

Ogris *et al* [92] investigated the effect of complex size on *in vitro* transfection efficiency. Transferrin-conjugated and unmodified PEI (800 kDa) were found to form extremely large complexes with DNA (up to 1000nm) unless the individual components were mixed at a highly positive nitrogen/phosphate charge ratio. This was thought to be due to the fact that transferrin is a very soluble negatively charged plasma protein which when incorporated in sufficient amounts, would stabilise complexes in solution also at electroneutrality. It was found that the smaller, stable complexes show a significant decrease in transfection experiments when compared to the larger complexes. This was thought to be due the enhanced uptake and endosome destabilising activity of the larger complexes.

Despite increasing reports on both the promising *in vitro* and *in vivo* use of PEI to date there has yet to be any reports of clinical trials using PEI as the transfection agent. While PEI is an effective transfection agent the toxicity of PEI [75] precludes its use in humans.

1.4: Aims and Objectives

The aim of this work was to investigate the effects of molecular modification of the gene delivery polymer PEI (25KDa). The synthesis of four new PEI derivatives, constructed from the attachment of palmitoyl and PEG chains, as well as the quaternisation of the parent polymer and the palmitoyl modified polymer, are reported in Chapter 2. This chapter aslo reports on the structural characterisation of the polymers. A number of analytical techniques such as NMR, FTIR, elemental analysis, gel permeation chromatography and a TNBS UV assay were used in conjunction with one another to both confirm and determine the degree of modification made to each polymer.

The aims of chapter 3 is to investigate the physiochemical properties of each polymer after interaction with a plasmid DNA reorter gene. The DNA condensation efficiency of the polymers was measured using an ethidium bromide exclusion assay. Photon correlation spectroscopy was used to measure the size of polymer/DNA complexes, the surface charge of the complexes was measured using zeta potential analysis. The polymer/DNA complexes were also visualised by negative staining electron microscopy.

The objective of chapter 4 was to use a variety of *in vitro* techniques to try and predict as well as explain the behaviour of the complexes when adminstered *in vivo*. The interaction of the complexes with proteins and

blood erythrocytes were investigated as well as the haemolytic properties of the modified polymers. Cell toxicity was investigated using a MTT assay in two different cell lines. The *in vitro* transfection efficiency of the polymers was also measured in the same cell lines. Finally the *in vivo* transfection efficiency in mice was measured using an immuno-histochemical assay.

Chapter 2: Synthesis and Structural Characterisation

2.1: Introduction

2.1.1: Polymer Synthesis

Hydrophobic Modifications

The primary amine groups of PEI are chemically active and therefore present a suitable site for the attachment of pendant chains to the parent polymer. In the literature there are only a few reports of PEI being modified with amphiphillic side chains. The first such report of synthesising PEI with amphiphillic side chains was by Klotz *et al* in 1969 [93] in the investigation of bio-macromolecular interactions. PEI was modified by the attachment of butryl, hexanoyl and lauroyl aliphatic groups, as well as carbobenzoxytyrosine or carbobenzoxytryptophan aromatic residues. All the modified PEI's were conformationally compact, water-soluble polymers capable of efficiently complexing with methyl orange.

A modified amphiphilic PEI polymer was synthesised for the purpose of cytoplasmic delivery of the aqueous content in liposomes through endosomes [94]. The modified polymer, cetylacetyl(imidazol-4-ylmethyl)PEI (CAIPEI, Figure 8), was incorporated into the bilayer of liposomal vesicles. The protonation of the polymer, CAIPEI, at an acidic pH endowed the modified polymer vesicles with the abiltiy to fuse with negatively charged liposomes.

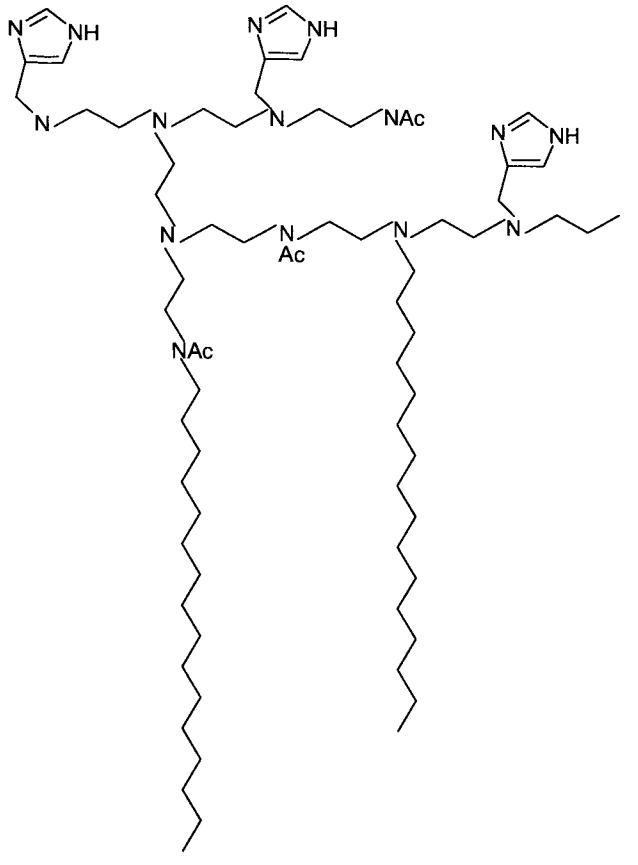

Figure 8: Chemical structure of cetylacetyl(imidazol-4-ylmethyl)PEI (CAIPEI) [94].

The properties of amphiphilic PEI's based on long chain alkyl halides have also been investigated [95] through the synthesis of various octadecyl-alkylated PEI's. The n-alkylated PEI's were either highly viscous or solid substances depending of the degree of alkylation. With an increase in the alkylation by the long-chain hydrocarbons a first order endothermic transition was found to occur. This was thought to be due to a crystallisation of the side chains, which became stronger with an increasing degree of alkylation. These modified PEI's were found to have a wide range of stabilization

properties in oil as demonstrated through the micro-emulsion polymerisation of styrene and the preparation of gold colloids.

.

PEG Modification of PEI

In the second modification of PEI, we followed the approach of attaching both hydrophobic (palmitoyl) and hydrophilic (PEG) groups to PEI. We used the method as described by Brown *et al* (2000) [67]. Brown *et al* reported the coupling of both palmitoyl and PEG groups to polylysine and polyornithine homopolymers. These polymers were able to self-assemble into vesicles upon probe sonication when in the presence of cholesterol. The polymeric vesicles were found to be less toxic than the parent polymers with a significant increase in *in vitro* transfection.

Methoxypolyethylene Glycol (mPEG) is a linear, hydrophillic, uncharged, flexible polymer based on the CH_2CH_2O repeat unit, and is prepared by ring opening polymerisation of ethyleneoxide. It is available commercially in a variety of molecular weights and has a low order of toxicity in oral, parenteral and epidermal applications [96]. When administered intravenously to humans, mPEG's of molecular weights ranging from 1000-6000 Daltons are promptly excreted, predominantly via the kidney. Modification with mPEG tends to produce a steric barrier to interactions with proteins and phagocytes

which leads to an extensively improved circulating life, decreased immunogenicity and antigenicity, and a negligible reduction in biological activity [97].

The literature lists several instances of cationic polymers being modified with PEG conjugates. Choi *et al* reported the synthesis of PEG grafted polylysine and lactose-PEG grafted polylysine [98, 99]. Both these modified polymers showed an increased solubility and an increased *in vitro* transfection. Kabanov *et al* [100] and Wolfert *et al* [101] have developed A-B type block polycations as vectors for oligonucleotide and gene delivery. This vector consists of one hydrophilic polymer region (PEG) combined with one polycationic polymer region (polylysine). The block copolymer is able to form a complex with DNA, whilst maintaining a low cytotoxicity, which is comparable to the cation alone but exhibits an increased solubility.

Quaternary ammonium modification of PEI

For the quaternisation of PEI and Palmitoyl-PEI, we used a modified method as described by Domard *et al* [102]. The quaternisation of compounds with methyl iodide, such as chitosan, have given rise to an increased solubility [103]. The quaternisation reaction was conducted in several stages in order to increase the yield of the quaternary chitosan derivatives. An inorganic base was used to fix the iodhydric acid formed during the reaction and to avoid the protonation of the unreacted primary amine groups.

Murata *et al* [104] investigated the viability of a quaternary chitosan-galactose conjugate for use as a gene delivery vector. The quaternary conjugate was shown to have a reduced cytotoxic activity with an increase in *in vitro* transfection efficiency.

To date there are only a few reports of quaternary PEI in the literature. In each case the quaternary PEI has been described for use as a stationary phase for high performance anion exchange chromatography [105, 106].

In this section we report the synthesis of 4 new polyethylenimine based polymers. PEI has been modified through the addition of palmitoyl side chains, the addition of both palmitoyl and PEG side chains and through the quaternisation of both PEI and Palmitoyl-PEI.

2.1.2: Nuclear Magnetic Resonance Analysis

A spectroscopic technique for the study of polymers must produce high resolution, narrow line width spectra that provide selectivity and structural information. It must possess sufficient sensitivity to detect and monitor very low levels of structure in the polymers, as small structural changes produce much larger effects on the physical and mechanical properties. In the field of polymer analysis and characterisation, Nuclear Magnetic resonance (NMR) has become the leading technique [107]. An important area of activity is to determine the chemical structure of polymers and to develop techniques to facilitate such determination. In NMR analysis of polymers there are two available methods. For solvent soluble polymers, the most commonly used technique is through solution state (one dimensional or multidimensional) NMR [108-110]. For crosslinked polymers or thermosets, solid state NMR can be used [107].

For the polymers that we have synthesised we have used solution state NMR for their structural characterisation [111]. The studies were carried out using both ^{1}H and ^{13}C NMR with use of both one-dimensional and two-dimensional techniques.

^{13}C NMR has been used as far back as 1973 to study the structure of various branched PEI's to give an insight into their structure [112] and there are several examples of the use of ^{1}H NMR in the characterisation of modified

PEI polymers [113]. Both ^{1}H and ^{13}C NMR have been instrumental in the structural analysis of various quaternary compounds [114, 115].

NMR is the experimental study of the energy levels of certain atomic nuclei of molecules. When placed in a magnetic field, the magnetic properties of the nuclei will dominate. Nuclear spin is a characteristic possessed by all atomic nuclei [116]. There are certain atomic nuclei that possess an odd number of either protons or neutrons and have a nonzero spin. Examples are the principal isotopes of hydrogen, sodium and phosphorus. As the positively charged nucleus spins on its axis, a magnetic moment is created by the moving charge and will align in a magnetic field. The nuclei of primary interest to polymer chemists are the proton (^{1}H), deuteron (^{2}H), ^{13}C and ^{19}F [107]. In NMR spectroscopy the sensitivity and effectiveness are regulated by two factors, the natural abundance of the isotope and its gyromagnetic ratio (the ratio of the magnetic moment of a system to its angular momentum). For example, the ^{1}H isotope is 100% naturally abundant and has a high gyromagnetic ratio, which makes ^{1}H the most sensitive nucleus for NMR study. On the other hand, with a natural abundance level of only 1.1% and a gyromagnetic ratio one quarter that of hydrogen, the ^{13}C nucleus is 1.6×10^{-2} times less sensitive than hydrogen for use in NMR.

The nuclear spin of the nuclei generates a small magnetic field, and these dipoles are randomly orientated unless placed in the presence of an applied magnetic field. Upon placing a sample in a homogeneous magnetic field, the

dipoles will align with the line of induction or the force of the applied magnetic field. The majority of the protons magnetic moments will be randomly pointed due to the fact that the molecules are in constant thermal motion, and that the molecules are interacting with one another [116]. However, the average magnetisation will be preferentially aligned along the magnetic field. The average of all these magnetic moments is termed the thermal equilibrium magnetisation, and is proportional to the intensity of the NMR signal and directly proportional to the magnitude of the applied field.

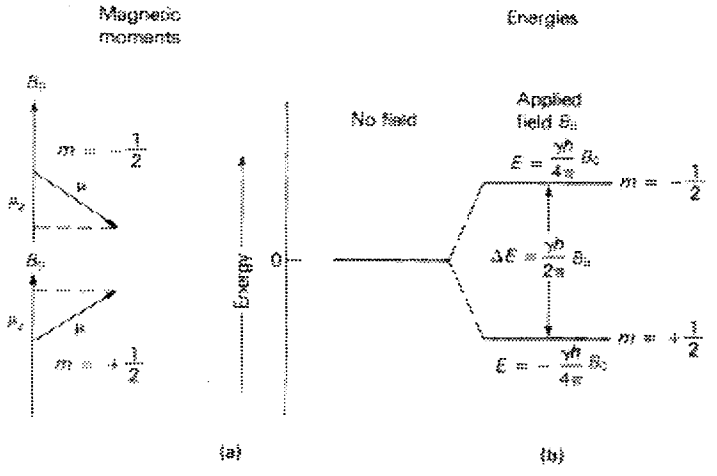

Figure 9: Magnetic moments and energy levels for a nucleus with a spin quantum number of ± ½ [116].

Nuclei with a spin of ½ have two energy states (Figure 9). They can be aligned with the field (lower energy) or aligned against the field (higher energy). All nuclei that have spins greater than ½ possess asymmetrical charge distributions and multiple energy levels. In general, there are 2I+1

nuclear energy states that correspond to magnetic quantum number values of I, (I-1), (I-2), ---, -I. The energy difference falls in the radiofrequency range (107-108 Hz). The nuclei can be induced into a higher state through the absorption of a radiofrequency pulse of the appropriate frequency and strength. This radio frequency, *rf*, is produced by using an alternating current of variable frequency that is passed through a coil whose axis lies perpendicular to the applied magnetic field in the *xy* plane [107].

The introduction of the alternating current gives rise to an oscillating magnetic field, which is also perpendicular to the applied field. As the frequency of the oscillating field is varied, there is a point at which it exactly matches the processional frequency of the nuclei, and energy from the radiofrequency is absorbed by the nuclei. When this absorption occurs, the system is said to be in resonance. This absorption of energy is the resonance phenomenon. When in resonance, energy is transferred from the nuclei, which causes a change in the spin orientation of the nuclei.

The *rf* field provides the nuclei with the quanta of energy necessary to move to the higher energy levels. When the proper *rf* pulse is applied, the nuclei begin to move in phase. As the *rf* pulse continues, more and more nuclei fall in line and process in phase with the rf magnetic field. After a certain period of *rf* exposure, the magnetisation becomes coherent. The protons then proceed as a coherent group in the *xy* plane rather than as randomly phased

individuals in the *z* direction. The synchronisation of radiowaves produces a coherent *rf* signal that can be detected over the random background [107]. Once the *rf* field is turned off, the magnetisation can return to its original equilibrium value through the emission of energy or by the transfer of energy to the surrounding molecules. As the probability of spontaneous emission depends on the frequency to the third power, and at radio frequencies, this term is therefore too small to be significant. So all NMR transitions are stimulated. The stimulated process by which the energy is lost to the environment is called relaxation [116].

The 90^0 *rf* pulse, also known as the read pulse, is produced by passing an oscillating electric current through the transmitting coil that surrounds the sample. The field generated by the *rf* pulse is perpendicular to the applied magnetic field. A short pulse of *rf* radiation of *t* seconds duration is equivalent to the simultaneous excitation of all the frequencies in the range rf_0 (*t-1*, where rf_0 is termed the carrier frequency of the nuclei under study). Because the pulse duration lasts only microseconds, the bandwidth is sufficiently large to excite all of the resonant nuclei in the sample.

As the nuclei receive the pulse, they draw closer to each other and become a bundle of processing nuclei that has a net magnetisation in the *xy* plane (Figure 10). After receiving the pulse, the nuclear spins initially group about the static field and the local magnetic fields of adjacent molecules, the nuclei proceed at different frequencies and quickly lose their coherence and fall out

of phase. The precession phase of the nuclei is not totally random and a net component of magnetisation is generated in the xy plane. This component induces a voltage in the receiving coil that surrounds the sample.

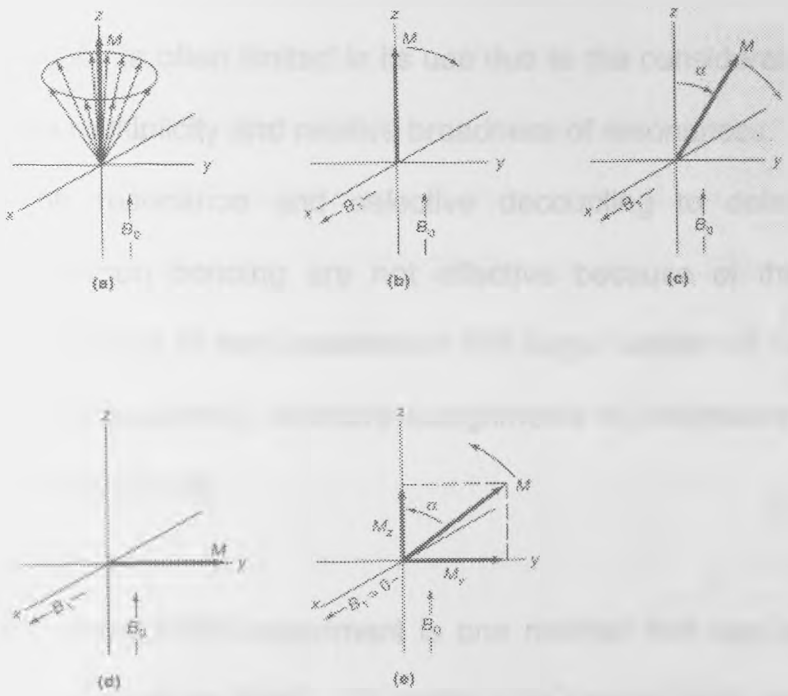

Figure 10: Behaviour of magnetic moments in a rotating field of reference 90-deg pulse experiment. (a) Magnetic vectors of excess lower energy nuclei just before pulse, (b), (c), (d) Rotation of the sample magnetisation vector M during lifetime of pulse, (e) Relaxation after termination of the pulse [116].

The signal observed in the time domain is called a free induction decay because it is measured free of a driving *rf* field. It is a decaying voltage

because the net nuclear magnetic field decays when the nuclei return to their equilibrium value [107]. The term induction is used because a current is induced in the receiver coil. This signal is collected as a function of time, amplified, and then processed to give the detected NMR signal.

NMR spectroscopy is often limited in its use due to the considerable overlap arising from the multiplicity and relative broadness of resonances. The usual methods of off resonance and selective decoupling to determine the multiplicity of carbon bonding are not effective because of the inherent limitation of selectivity in the presence of the large number of overlapping resonances. Consequently, structure assignments to resonance are often difficult and arbitrary [110].

The two-dimensional NMR experiment is one method that can be used to overcome such limitations [116]. To make a 2-D experiment out of a 1-D experiment, the evolution time is stopped incrementally through a range of values, and a series of Free Induction Decays (FID's) are stored, each with a different evolution time. After the first Fourier Transformation, the resulting first domain spectra are aligned parallel to one another to form a matrix of data points. Transposition of the matrix gives a new series of data points that can be subjected to a second Fourier Transformation. This process is done for each data point of the original first domain spectrum. When the resulting spectra from the second Fourier Transformation are again arrayed in a matrix, the chemical shifts can be aligned along one axis, and the frequency,

which is dependant on the phase or amplitude modulation that developed during the evolution period, can be aligned on the other axis [116].

The resolution in the two dimensional spectrum is better than in either the ^{13}C or ^{1}H spectrum alone, but the sensitivity is lower. In 2-D NMR experiments, the resolution increases as the square of the field strength. At the higher static field strengths that are available on modern NMR experiments, the advantages of 2-D NMR experiments further increase. One such 2-D technique is the long-range ^{1}H-^{13}C COSY spectrum, also known as Heteronuclear Multiple Bond Connectivity (HMBC). It gives a 2-D spectrum with ^{13}C Chemical shifts on one-axis and ^{1}H chemical shifts on the other axis [116].

2.1.3: Fourier Transform Infrared Spectroscopy Analysis

One of the most useful and often used spectroscopic techniques is Infrared (IR) Spectroscopy. The success of IR is due to a number of reasons. The IR spectroscopy is a rapid and sensitive technique, with sampling methods that are easy to use. The instrumentation used is inexpensive, the operation of the equipment is straightforward, and service and maintenance of the equipment are not difficult. Finally, interpreting the spectra is not particularly problematical and is easily learned [107].

A major limitation of IR spectroscopy occurs when trying to obtain quantitative results. Measurements made in IR spectroscopy give precise information about the relative ranking of the amount of specific structure in a series of samples, making exact and conclusive quantitative IR measurements a demanding process [117].

Molecules consist of atoms held together by valence forces. These atoms vibrate by thermal energy, giving every molecule a set of resonance vibrations that correspond to the resonance modes of mechanical structures. Accordingly when imposing radiation is passed through the material it is absorbed at frequencies which correspond to the molecular modes of vibration, and a plot of transmitted radiation intensity versus frequency shows the absorption bands. IR spectroscopy measures the vibrational energy levels of molecules [116]. The distinguishing band parameters measured in

IR spectroscopy are frequency (energy), intensity (polar character), band shape (environment of bonds) and the polarization of the various modes, that is, transition-moment directions in the molecular structure. The IR spectrum is often called the fingerprint of a molecule. Due to the distinguishing vibrational energy levels created for each molecule and its isomers, the IR spectrum registers the most specific information concerning the molecule [116].

IR spectroscopy is a technique that can be used to provide both chemical specificity and selectivity. As an identification tool, it has no close spectroscopic competitor.

Fourier Transform Infrared Spectroscopy

IR spectra were originally measured using a dispersive instrument containing an optical element, which consisted of either a grating or a set of prisms, which geometrically dispersed the IR radiation. A scanning mechanism passes the dispersed radiation over a slit system that isolated the frequency range falling on the detector. This allowed the spectrum or the energy transmitted through a sample as a function of frequency to be recorded. The dispersive method of IR spectroscopy is highly limited in its sensitivity as the majority of the available energy does not fall on the open slits and therefore does not reach the detector. The sensitivity of IR spectroscopy was improved with the introduction of a multiplex optical device, called the

Michelson interferometer, which allowed the continuous detection of all the transmitted energy simultaneously. The resulting IR instrumentation is called a Fourier Transform Infrared Spectrometer (Figure 11) [117].

Light covering the frequency range of 5000-400cm^{-1}, is split into two beams. Either one beam is passed through the sample, or both are passed, but the second beam is made to traverse a longer path than the first beam [118]. The two new beams are recombined to produce an interference pattern that is the sum of all the interference patterns created by each wavelength in the beam. The differences in the two paths are systematically changed and the interference patterns change to produce a detected signal that varies with optical path difference. The resulting pattern is known as the interferogram and looks nothing like a spectrum. Fourier transformation of the interferogram, using a computer built into the machine, converts it into a plot of absorption against wavenumber, which resembles the usual spectrum obtained by the traditional method [118]. FTIR offers several advantages over the traditional method, and a few disadvantages. The whole spectrum is measured in a few seconds, as it is not necessary to scan each wavenumber successively. Because it is not dependant upon a slit and a prism or a grating, high resolution in FTIR is easier to obtain without sacrificing sensitivity [119].

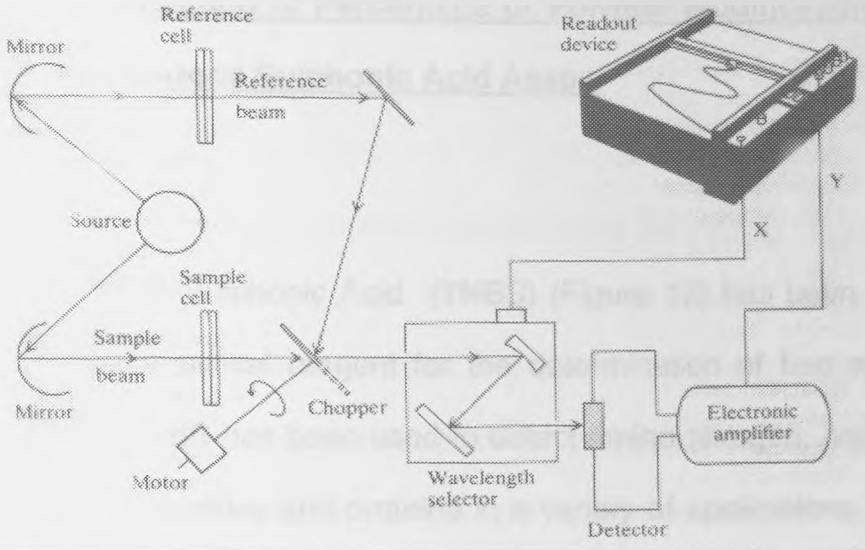

Figure 11: Schematic of an infrared spectrophotometer [119].

2.1.4: Determination of Percentage of Polymer Modification by a 2,4,6-Trinitrobenzene Sulphonic Acid Assay.

Trinitrobenzene Sulphonic Acid (TNBS) (Figure 12) has been shown to be an effective analytical reagent for the determination of free amino groups [120, 121]. TNBS has been used to detect amino nitrogen, primary amines, amino acids, peptides and proteins in a variety of applications. It has been shown to be a selective reagent for primary amine groups [120, 121].

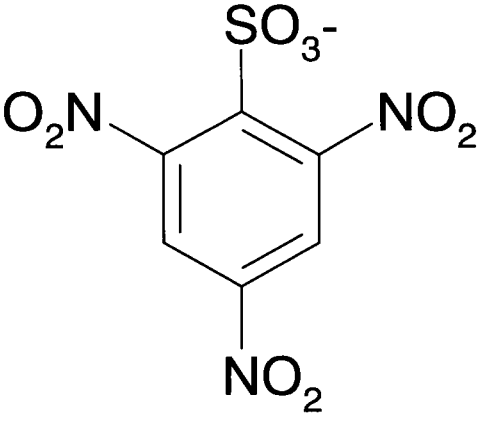

Figure 12: Structure of 2,4,6-TrinitroBenzene Sulphonic Acid.

We used a modified method reported by Snyder and Sobocinski (1975) [122]. The polymer is allowed to react with TNBS in a buffered medium, giving N-Trinitrophenyl-polymer derivatives, the concentration of which is measured by molecular absorption spectroscopy. Snyder and Sobocinski stated that the concentration of primary amine groups could be directly related to the

absorbance of the trinitrophenylation reaction mixture after a short incubation period of 15 to 30 minutes.

This method is used as a means of evaluating the degree of modification of the modified PEI homopolymer. The number of primary amine groups that have been modified in the various polymer synthesis procedures were measured by a comparative titration of the free primary amine groups in both the unmodified and modified PEI, using 2,4,6-trinitrobenzene sulphonic acid.

2.1.5: Elemental Analysis

Elemental analysis was performed on each of the polymers. This simple procedure gives the proportion of elements in each compound as percentage value. The elemental analysis allows us to calculate the modifications made to each polymer and compare it the values gained from the NMR analysis and the TNBS assay.

2.1.6: Molecular Weight Determination.

In the solid state, most polymers will take on some sort of a semi-crystalline structure. This crystalline structure is destroyed when we dissolve the polymer in a suitable solvent. For very crystalline structures, we may need to use very polar solvents and/or high temperature to destroy the crystalline structure and get the polymer into solution. Dissolving the polymer correctly into the solvent is a critical step in obtaining the correct molecular weight for the polymer [123]. Sufficient time must be allowed to ensure the polymer has dissolved into a true solution. Highly crystalline, high molecular weight polymers may take several hours to dissolve, and high temperature may be required. The polymer solution should be filtered unless there is a chance of shear.

For GPC (or size exclusion) analysis of polymers, steric interaction between the polymer and the crosslinked gel packing material is the main separation mechanism [118]. GPC is performed in isocratic mode. Figure 13 depicts a cross section of a porous polymeric gel packing material. The solid spheres represent different sizes of the eluting polymer as the sample travels down the column in the eluent. The larger sized particles are excluded from the small pores, and the smaller sized particles are able to permeate the pores. The larger ones elute first, and the smaller ones elute last [118].

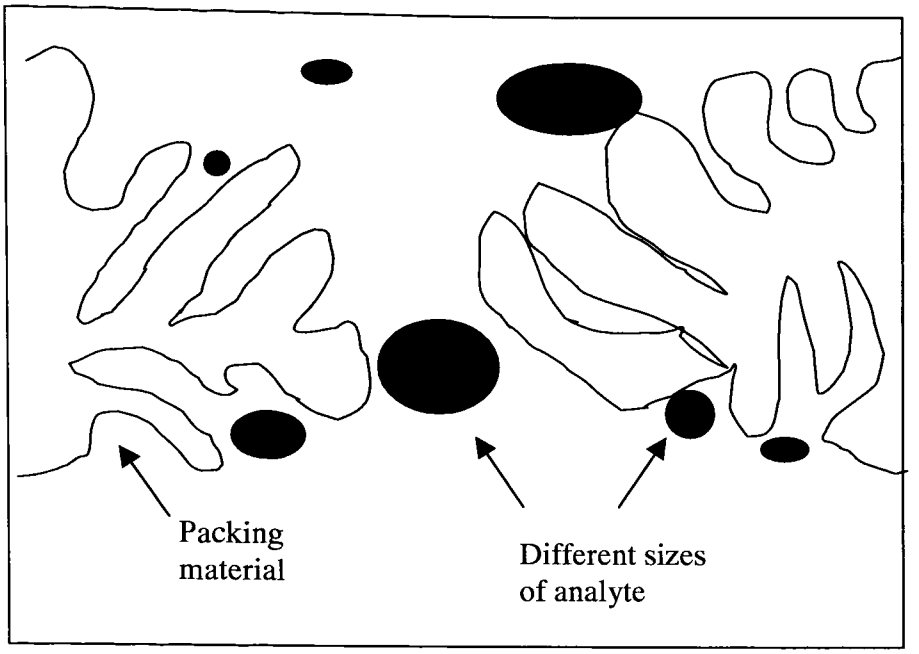

Figure 13: Cross section of a porous polymeric packing material.

Detectors in GPC Analysis

There are many detectors used in polymer chromatography. The main concentration detector for polymer chromatography is the refractive index (RI) detector, but ultraviolet (UV) and evaporative light scattering (ELS) detectors can also work well under the right circumstances (such as gradient analysis). For added information, we can use molecular weight sensitive detectors coupled with a concentration detector. Viscometry and laser light scattering detectors are used by many to gain more insight into polymer structural information. There are several detectors that have been used for compositional analysis, including multi-wavelength UV, RI + UV, FTIR and Mass spectroscopy.

The concentration detector responds to concentration *C*. The RI detector responds to *C* times the specific refractive index increment, dn/dc. The molecular weight sensitive detectors respond to molecular weight multiplied by a function. For viscometers, this function is [n], the intrinsic viscosity. For light scattering, the response is simply *M(C)*, and for mass spectroscopy, the response is *1/M* (Where M is molar mass). This is why mass spectroscopy is not very useful for high molecular weight polymers [118].

Combining molecular weight sensitive detectors with the RI detector provides more information and insight into polymer Mw and structure. There are three main combinations used in GPC analysis:

1. Refractive Index/Viscometer.
2. Refractive Index/Light Scattering.
3. Triple detection with Refractive Index/Viscometer/Light Scattering.

Some of the specific advantages we gain with these multi-detector combinations are:

1. Improved detector performance at the high Mw (molecular weight) end.
2. Absolute or true Mw distribution.
3. Macromolecular architecture and conformation (such as important branching information).

Since the light scattering response is proportional to *C x M*, there is no need to run a set of narrow standards to calibrate the column set. The light scattering apparatus does, however need to be calibrated.

One of the interaction modes observed in aqueous GPC is due to intra molecular interactions. Polyelectrolytes that have ionic groups present (anionic or cationic) will repel each other, causing the polymer chains to expand, resulting in early elution. This effect is independent of column chemistry, and addition of 0.05M-0.10M salt (like $NaNO_3$) will effectively shield this interaction.

Specific Refractive index increment

The quantity *dn/dc*, also called the specific refractive index increment describes how much the refractive index of a polymer solution changes with respect to the concentration of the solute. Measurement of *dn/dc* is essential for the absolute characterization of the molar mass, since it is a term used in the molar mass calculation [124].

Polymers with larger values of dn/dc scatter more light at the same mass than those having smaller values. Therefore, knowing the dn/dc permits the deduction of molar masses from the light scattering data. Because *dn/dc* changes with wavelength it is important to measure it at the same wavelength as the light scattering apparatus. Moreover it is also

advantageous to measure *dn/dc* offline since determining this quantity on-line makes numerous assumptions about the total mass that has eluted [124].

To measure dn/dc, a series of dilutions of the sample are made. These dilutions are then injected into the RI detector and data collection is automatically performed using the DNDC software. The software (ASTRA) then calculates the dn/dc based upon the signal strength from the RI (*dn*) and the concentrations of the dilutions (*dc*) [125].

Laser Light Scattering

Laser light scattering is a non-evasive technique that can be performed in either the batch or chromatography mode [126]. In either instance the sample may be recovered at the end of the study. Unlike molecular weights that are estimated from gel size exclusion chromatography data alone, the molecular weight obtained from light scattering is not dependant upon either the stokes radius of the polymer nor a calibration curve that depends upon running several standards.

Batch Mode Laser Scattering Study

A batch mode experiment is carried out by injecting the sample directly into the flow cell and then measuring the amount of scattered light at several angles. The data collected for each sample is processed simultaneously

using the Zimm formalisation [127]. The experiment may be repeated at various polymer concentrations to give the weight average molar mass (*Mw*), radius of gyration $\langle r^2 \rangle$ and the second virial coefficient *A2*, which is a measure of macromolecule-solvent interactions. When performed in micro-batch mode, a typical experiment requires several samples of polymer at different concentrations in a volume of at least 1ml each [127].

Chromatography Mode Light Scattering Study

During a chromatography mode light scattering study the laser light scattering is coupled with HPLC size exclusion chromatography (SEC) [126]. Coupling light scattering to a fractionation step avoids the ambiguity that can otherwise result from a batch mode experiment, in particular, the fact that light scattering provides the weight average *Mw* of all species present in solution. The *Mw* determination depends only upon the light scattering and refractive index detector, with the refractive index detector being used to determine the concentration of the polymer at each slice of the chromatogram that is analysed [126]. Since the *Mw* determination is completely independent of elution position, non-globular shape and/or interaction with the SEC support have no impact on the *Mw*'s determined by light scattering.

Zimm plot

The Zimm plot allows you to calculate the weight average molar mass, z-average rms radius, and the second viral coefficient, as well as their standard deviations [123]. When ASTRA analyses the batch data for a Zimm plot, it assumes that each peak region is a plateau. It combines all the data points within each peak into a single value for each scattering angle, keeping a specified percentage of low values for use in propagating errors, and analyses each concentrations data for noise. The respective uncertainties are plotted on the graph as error bars. Noisy detectors are weighted less, just as in chromatography calculations. The Zimm plot shows the second viral coefficient vs. the z-average rms radius. The intersection of the two projections on the y-axis gives the weight-average molar mass.

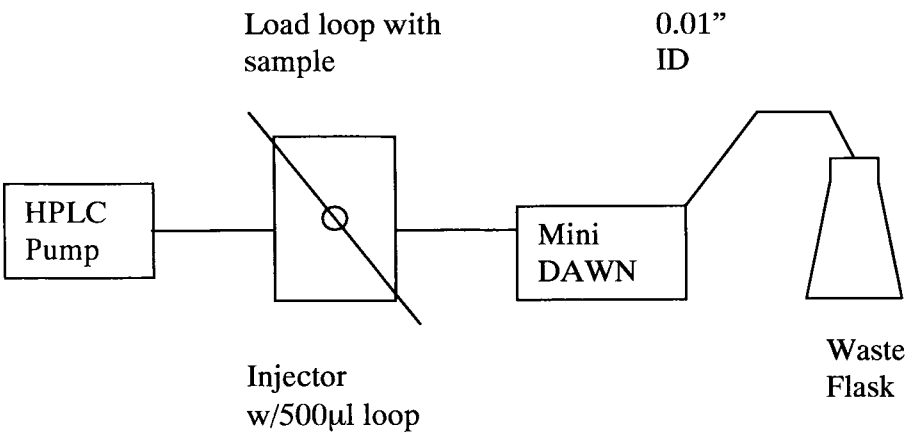

Figure 14: HPLC pump with injector. Mobile phase from the pump pushes the sample from the injection loop into the miniDAWN.

2.2: Methods and Protocols

2.2.1: Materials

Material	Supplier
Amberlite-93 resin	Fluka, UK
Deuterium oxide	Sigma, UK
Methyl-d_3-alcohol	Sigma, UK
1-methyl-2-pyrolidinone	Sigma, UK
Methyl iodide	Sigma, UK
Methoxypolyethyleneglycol p-nitrophenyl carbonate	Sigma, UK
Sodium Bicarbonate	Sigma, UK
Sodium hydroxide	Sigma, UK
Sodium iodide	Sigma, UK
Sodium tetraborate	Sigma, UK
Palmitic Acid N-hydroxysuccinimide	Sigma, UK
Polyethylenimine	Aldrich, UK
Potassium Bromide	Sigma, UK
Trinitrobenzene sulphonic acid	Sigma, UK

Table 2: List of Materials

2.2.1: Synthesis of Polymers

Palmitoyl-Polyethylenimine

Polyethylenimine (PEI) (100mg, Mw~25,000) and sodium bicarbonate (67mg) were dissolved in a mixture of absolute ethanol (24ml) and water (76ml). Palmitic acid N-hydroxysuccinimide (70mg) was dissolved in absolute ethanol (53ml). This solution was then added drop wise to the PEI solution, and the mixture was left to stir for 72 hours whilst protected from light. The ethanol in the mixture was then removed by rotary evaporation. The solution was then washed with diethyl ether (3x100ml). After washing the solution was dialysed against water (5L), with six changes of water over a period of 24 hours, using a dialysis membrane with a pore size of 12 to 14 Kd. Once the dialysis was completed the solution was frozen using liquid nitrogen and the frozen liquid was then freeze-dried. The resulting polymer was named Palmitoyl Polyethylenimine (P-PEI). Reproducibility was confirmed within 5-10% using NMR analysis.

For the synthesis of palmitoyl-polyethylenimine we used a modification of a method reported by Uchegbu *et al* [128].

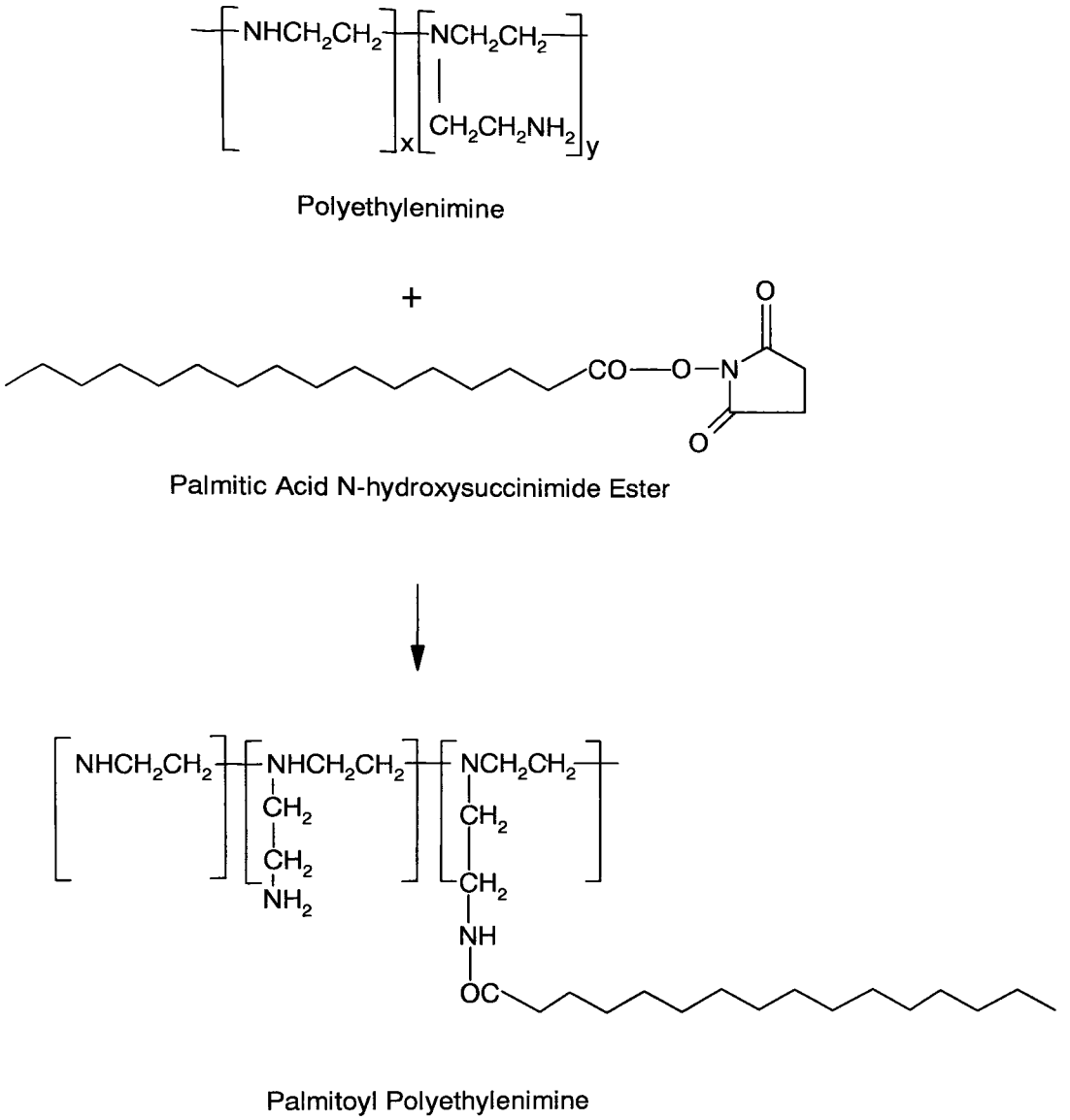

Figure 15: Synthesis Diagram of Palmitoyl Polyethylenimine

Palmitoyl-Polyethylene glycol- Polyethylenimine

Polyethylenimine (100mg, Mw~25,000) was dissolved in 0.08M sodium tetraborate (60ml). Over a 3h period and with stirring methoxypolyethylene glycol p-nitrophenyl carbonate (200mg, Mw~5,000) was added in three portions. This reaction mixture was left to stir for 15 hours at room temperature whilst protected from light. The reaction mixture was then dialysed against water (5L) with six changes of water over a 24h period. Sodium hydrogen carbonate (260mg) was then dissolved in the dialysed liquid. Palmitic acid N-hydroxysuccinimide (68mg) was dissolved in absolute ethanol (76ml), this solution was then added drop wise to the dialysed liquid over a period of 1 hour with stirring. The reaction mixture was then left to stir for 72 hours at room temperature whilst protected from light. This mixture was subsequently dialysed against water (5L) with six changes over a 24-hour period. The dialysed solution was then freeze-dried, and the freeze-dried material was then dissolved in chloroform (100ml). The chloroform solution was filtered and the filtrate evaporated under reduced pressure at 30-40°C until the volume had been reduced to about 5ml. This solution was then added drop wise to diethyl ether (200ml) and the precipitate was collected by filtration. The precipitate was then freeze-dried. The resulting polymer was named Palmitoyl Polyethylene glycol Polyethylenimine (PP-PEI).

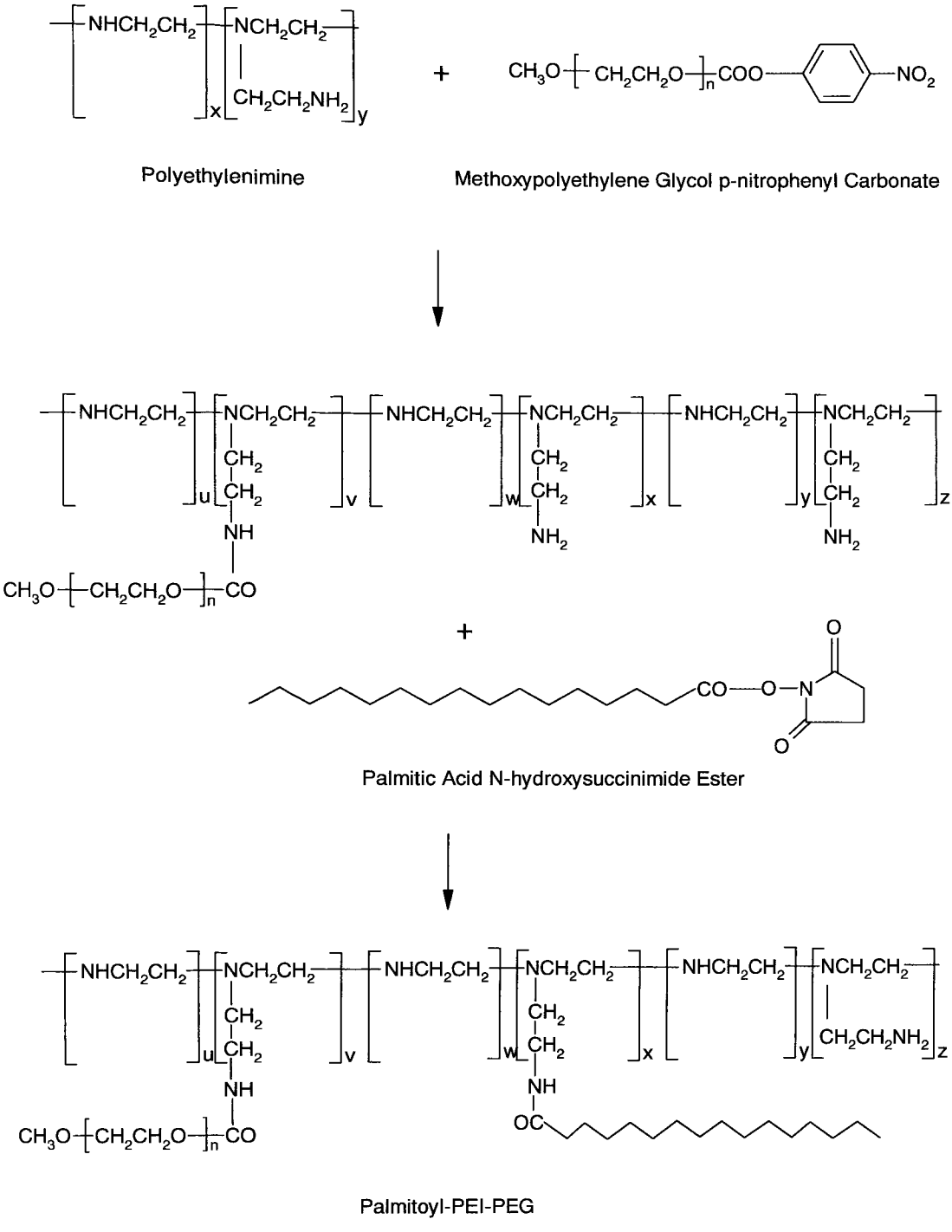

Figure 16: Synthesis Diagram of Palmitoyl Polyethylene glycol Polyethylenimine.

Quaternary Ammonium Polyethylenimine

Polyethylenimine (315mg, Mw~25,000) was dispersed in 1-methyl-2-pyrolidinone (50ml) for a period of 12 hours at room temperature whilst protected from light. Methyl iodide (1.3ml), sodium hydroxide (114.4mg) and sodium iodide (128.7mg) were added to the reaction mixture. The solution was then stirred under a stream of nitrogen for 3 hours at 36°C. The reaction mixture was added drop-wise to diethyl ether (200ml). A precipitate was formed and was left to settle overnight.

Once the precipitate had settled the solution was poured off and the precipitate was washed with diethyl ether (2x100ml) and ethanol (2x100ml) before being dissolved in water (100ml). The resulting solution was then dialysed against water (5L), with six changes over a period of 24 hours.

A column was packed with Amberlite-93 resin (30ml), which was washed with 1M hydrochloric acid (100ml). Water was passed through the column until a neutral pH was achieved. The sample solution was passed through the column and the resulting solution was then freeze-dried until all traces of water were removed. The resulting polymer was named Quaternary Polyethylenimine (Q-PEI)

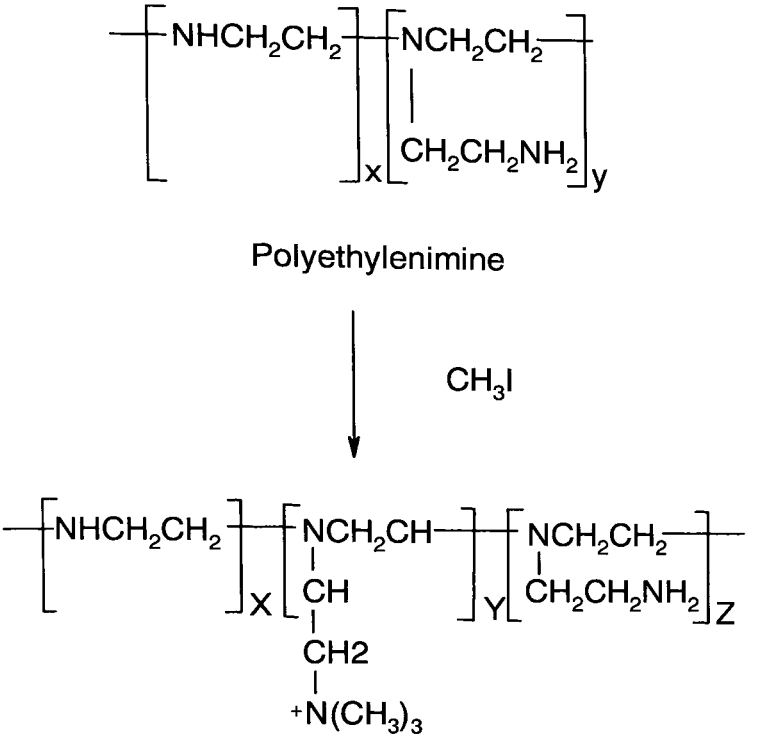

Figure 17: Synthesis Diagram of Quaternary Ammonium Polyethylenimine. Main chain quaternary ammonium modification could also take place.

Quaternary Ammonium Palmitoyl Polyethylenimine

Palmitoyl Polyethylenimine (314mg) was dissolved in methanol (50ml) for a period of 12 hours at room temperature whilst protected from light. Methyl iodide (1.3ml), sodium hydroxide (114.4mg) and sodium iodide (128.7mg) were added to the reaction mixture. The solution was then stirred under a stream of nitrogen for 3hours at 36°C. The reaction mixture was added drop wise to diethyl ether (200ml) and the precipitate that formed was allowed to settle overnight. The solution was poured off and the precipitate washed diethyl ether (2x100ml) and absolute alcohol (2x100ml). The precipitate was then dissolved in a water/methanol mixture (1:1 v:v, 100ml) and the resulting solution dialysed against water (5L), with six changes over a 24 hour period. A column was packed with Amberlite-93 resin (30ml), which was washed with 1M hydrochloric acid (100ml). Water was passed through the column until a neutral pH was achieved. The sample solution was passed through the column and the resulting solution was then freeze-dried. The resulting polymer was named Quaternary Ammonium Palmitoyl Polyethylenimine.

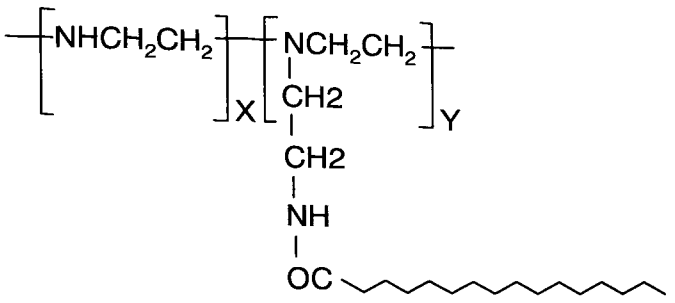

Palmitoyl Polyethylenimne

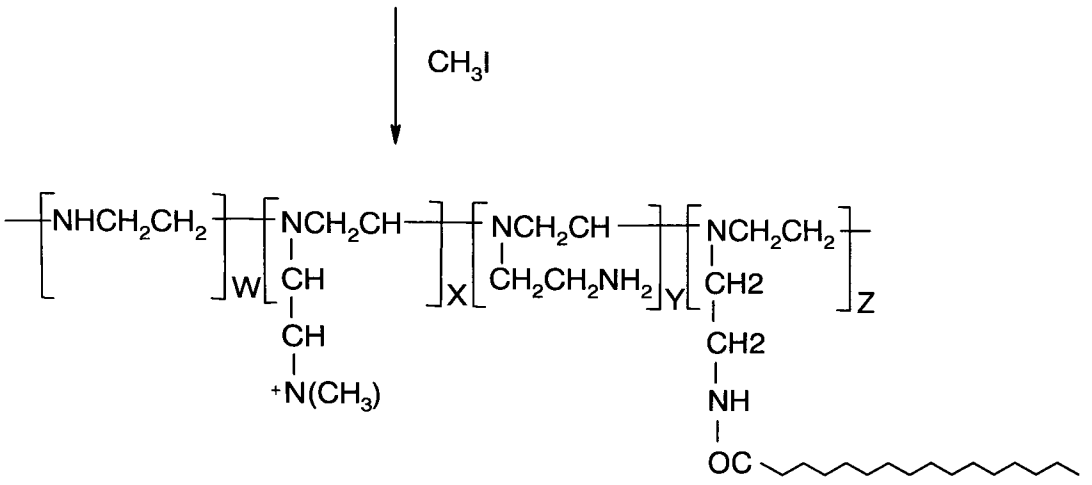

Quaternary Ammonium Palmitoyl Polyethylenimine

Figure 18: Synthesis Diagram of Quaternary Ammonium Palmitoyl Polyethylenimine. Main chain quaternary ammonium modification could also take place.

2.2.2: NMR Analysis

^{1}H NMR analysis (with integration), ^{13}C correlation and HMBC spectroscopy experiments were performed on solutions of Polyethylenimine, Quaternary Polyethylenimine in D_2O. Palmitoyl Polyethylenimine and Palmitoyl Polyethylene Glycol Polyethylenimine were analysed in $CDCl_3$. Quaternary Palmitoyl Polyethylenimine was analysed in deuterated methanol (Bruker AMX 400MHz spectrometer, Bruker Instruments, UK).

2.2.3: FTIR Analysis

Samples of Palmitoyl Polyethylenimine, Palmitoyl polyethylene glycol PEI and Quaternary Palmitoyl PEI were prepared for analysis using potassium bromide discs. 1mg of the sample was transferred to a sample tube. 250mg of potassium bromide was then added to the sample tube. The sample mixture was then agitated to ensure complete mixing. The sample mixture was then ground to a fine powder with a mortar and pestle. The powder was then compressed to form the disc prior to analysis (Mattson 5000 FTIR Spectrometer, Mattson UK)

Both Polyethylenimine and Quaternary polyethylenimine presented as a liquid. 1mg of the sample was cast evenly onto a sodium chloride disc, which was then analysed using the same technique as for the potassium chloride disc.

2.2.4: TNBS Assay

Polyethylenimine Calibration Series

Polyethylenimine (10mg) was transferred to a 5ml volumetric flask, which was then made up to the mark using 0.1M sodium tetraborate solution as dilutent (Stock Solution). 25, 50, 75, 100, 150, and 200μl aliquots of the stock solution were transferred to 10ml volumetric flasks, which were then made up to the mark using sodium tetraborate: methanol (70:30 v/v) to give six calibration solutions of concentrations 5, 10, 15, 20, 30, and 40μl/ml of PEI.

Palmitoyl-PEI and Palmitoyl Polyethylene glycol-PEI

P-PEI (5mg) was transferred to a 10ml volumetric flask, which was then made up to the mark with methanol. 1ml of this solution was then diluted to 10ml with methanol. 3ml of the second solution was further diluted to 10ml with 0·08M Sodium tetraborate solution.

Quaternary Polyethylenimine

Quaternary polyethylenimine (10mg) was transferred to a 5ml volumetric flask, which was then made up to the mark with methanol. 1ml of this solution was then diluted to 10ml with methanol. 3ml of the second solution was further diluted to 10ml with 0·08M Sodium tetraborate solution.

Quaternary Palmitoyl Polyethylenimine

Quaternary palmitoyl polyethylenimine (10mg) was transferred to a 5ml volumetric flask, which was then made up to the mark with methanol. 3ml of this solution was further diluted to 10ml with 0·08M Sodium tetraborate solution.

Reagent Blanks

The reagent blanks consisted of 0·08M Sodium tetraborate: methanol (70:30 v/v).

Analysis of Samples

Sample solutions (3ml) were transferred to a sample tube. 0·03M TNBS solution (75μl) was added to the sample solution, which was then agitated to ensure complete mixing. The solution was then allowed to stand at room temperature for 30 minutes. The solutions were then analysed on a spectrophotometer at 438·0nm, (Unicam UV-1, Unicam Ltd, UK)

2.2.5: Elemental Analysis

The simultaneous determination of C,H,N and Cl was performed using a Perkin Elmer 2400 analyser. The sample was wrapped in tin foil and was combusted at 1800°C in pure oxygen. The combustion products were catalysed and interferences were removed before being swept away into the detector zone where each element is separated and eluted as CO_2, H_2O, NO_2 and ClO_2. The signals were converted to a percentage of the elements. Oxygen content is estimated from other element percentages.

2.2.6: Molecular Weight Determination.

Dn/Dc Measurements

5mg of polymer was transferred to a 50ml volumetric flask, which was then made up to the mark with the appropriate solvent (Table 3) to give a 0.1mg/ml solution. Serial dilutions of this stock solution were then made to give 0.02, 0.04, 0.06 and 0.08mg/ml solutions. The solutions were then filtered using 0.22μm nylon filters.

A Rheodyne 7725 sample injector was used to load the samples. The *dn/dc* values of the varying solutions were measured using a Waters 2410 refractive index detector at 850nm. The data was processed using Wyatt DNDC for Windows v5.00 software.

Laser Light Scattering Measurements

Solutions of Palmitoyl PEI, Palmitoyl Polyethylene Glycol PEI and quaternary palmitoyl PEI were prepared and loaded as described for *dn/dc* measurements. The molecular weights of the polymers were measured by static laser light scattering (Wyatt Mini Dawn) equipped with a 20mV semiconductor diode laser (vertically polarised, λ = 690nm) at three angles of 45^0, 90^0, and 135^0. The molecular weights were obtained from Zimm plots processed using Astra for Windows v4.70 software.

Gel Permeation Chromatography – Laser Light Scattering (GPC/LLS) Measurements.

GPC/LLS measurements of Polyethylenimine and Quaternary polyethylenimine were performed using a mobile phase of 0.5M Sodium Chloride, on a PSS Hema-Bio 300 column (300x8mm, particle size = 10μm, exclusion limit for dextran = 3,000,000).

200μl of each sample (5mg/ml) was injected onto the columns using a Waters 717 auto-sampler and measurements were performed at room temperature.

Polymer	Solvent
Polyethylenimine	0.05M Sodium Chloride
Palmitoyl Polyethylenimine	Methanol
Palmitoyl Polyethylene Glycol PEI	Chloroform
Quaternary Polyethylenimine	0.05M Sodium Chloride
Quaternary Palmitoyl PEI	Methanol

Table 3: Solvents used for *Mw* determinations

2.3: Results and Discussion

2.3.1: NMR Analysis

Polyethylenimine

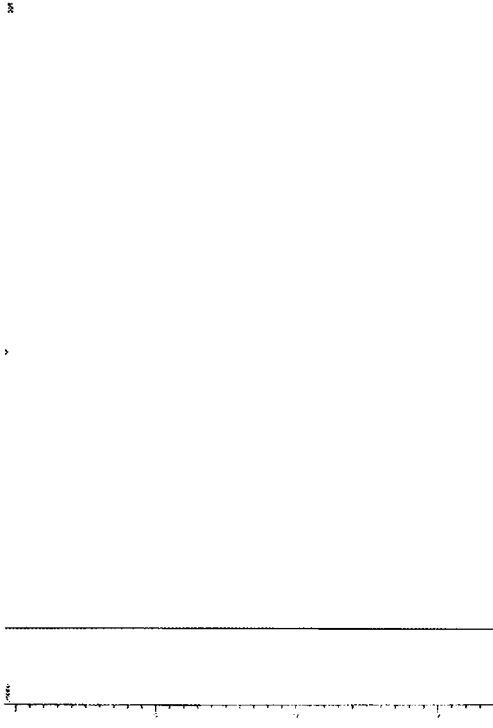

Figure 19: ^{1}H NMR spectra of PEI.

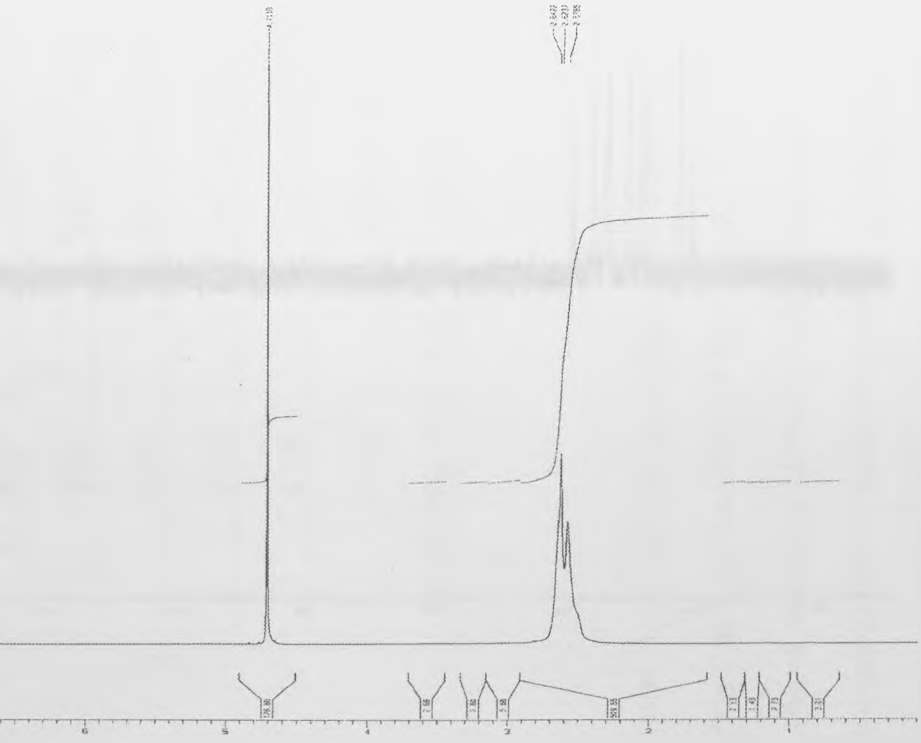

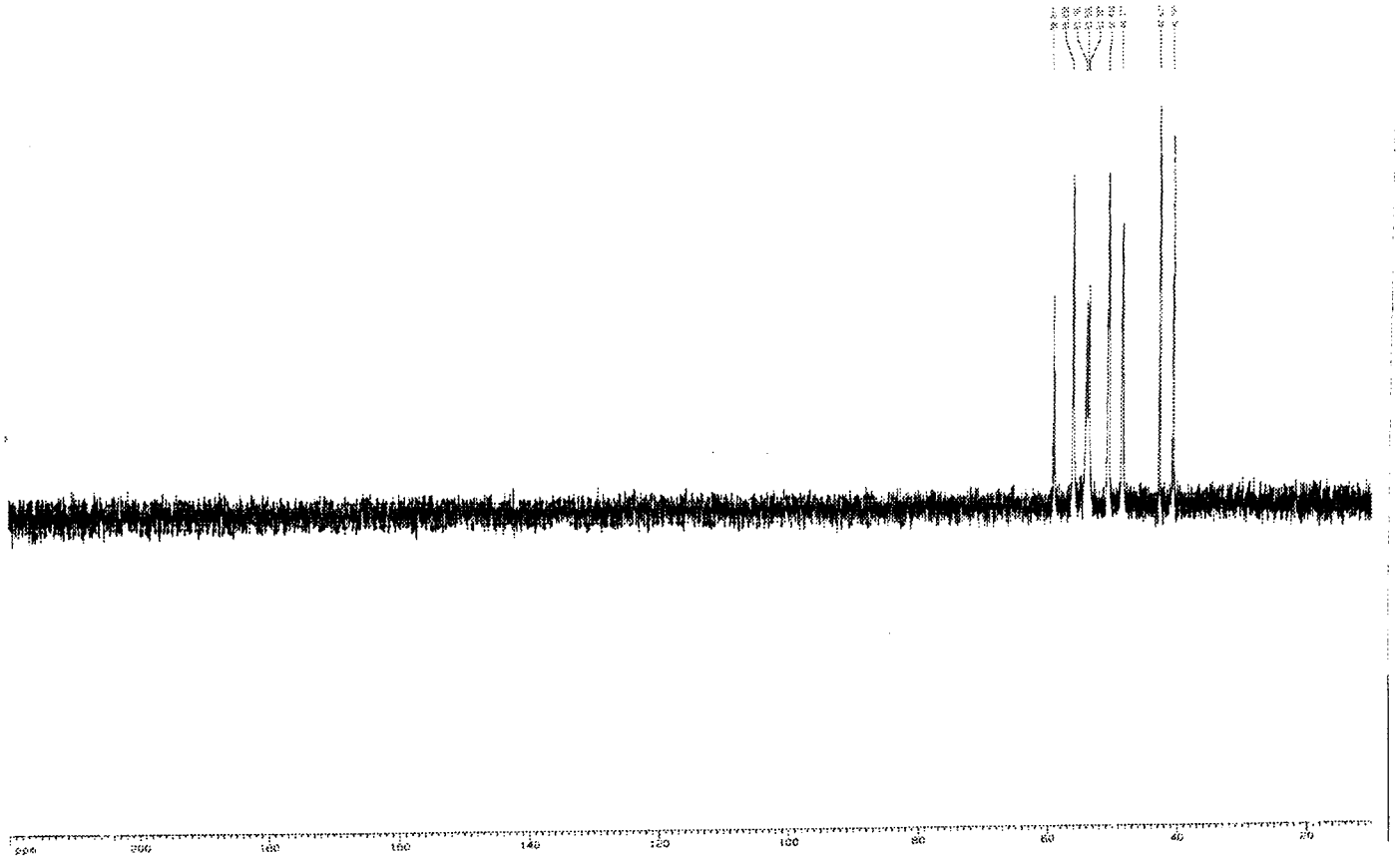

Figure 20: ^{13}C NMR spectra of PEI

The ^{1}H NMR spectrum (Figure 19) for PEI shows all CH_2 signals resonating between δ = 2.5 and 2.7ppm. Therefore, methylene groups with different amine substituents cannot be sufficiently separated for quantitative analysis. The ^{13}C spectrum (Figure 20) shows the structural elements of PEI to have well separated signals in the typical area of between 37 and 54ppm. The eight signals of the corresponding methylene groups were assigned as indicated (Table 4).

Assignment	Chemical Shift (ppm)
NH_2-**C**H_2-CH_2-N	40.52
NH_2-**C**H_2-CH_2-N	42.6
NH-**C**H_2-CH_2-N	49.3
NH-**C**H_2-**C**H_2-NH	50.4
NH-**C**H_2-CH_2-NH_2	53.3
N-CH_2-CH_2-N	53.5
N-**C**H_2-**C**H_2-N	55.8
N-**C**H_2-CH_2-NH_2	58.8

Table 4: Carbon assignments of PEI.

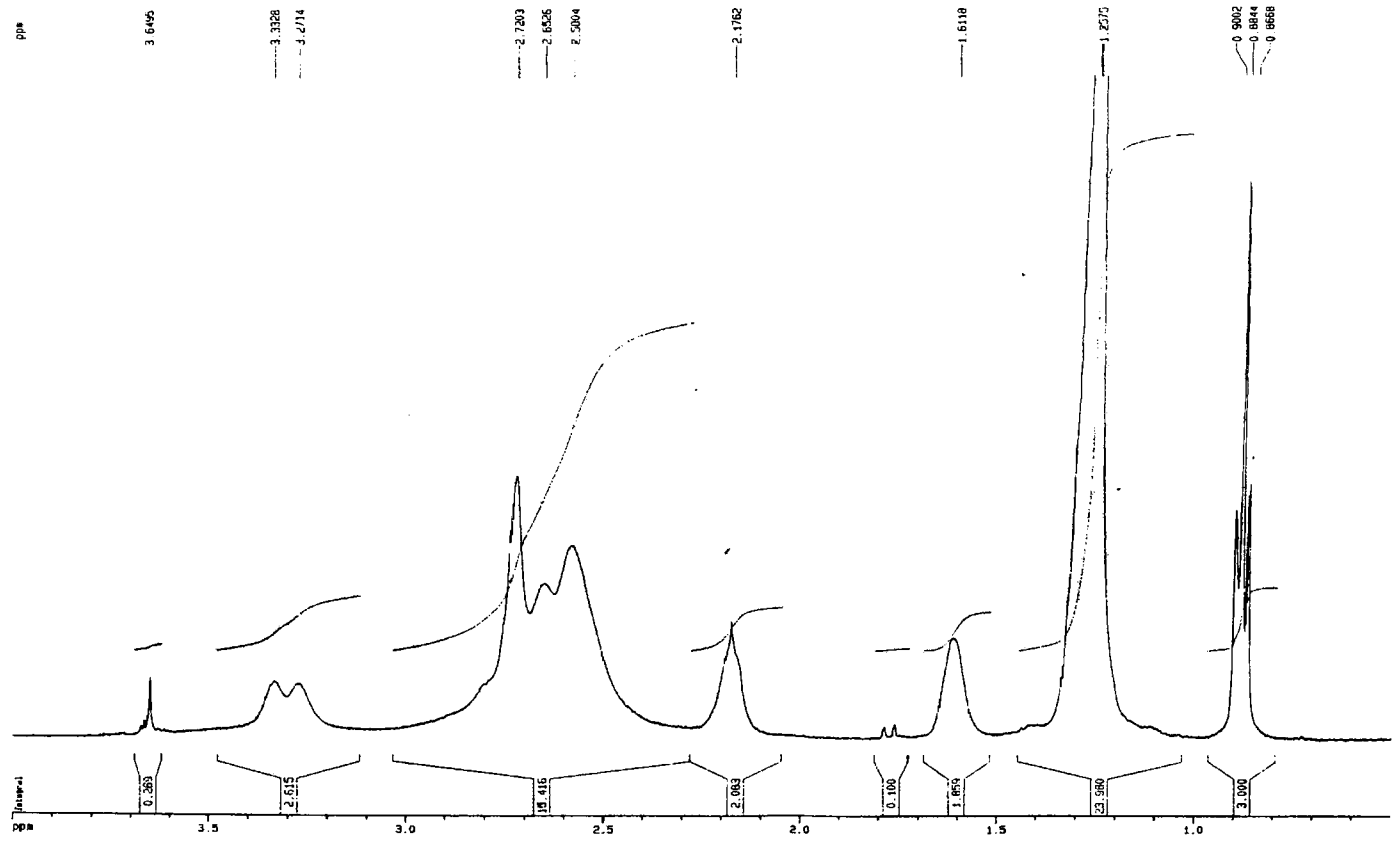

Figure 21: ^{1}H NMR spectra of Palmitoyl Polyethylenimine.

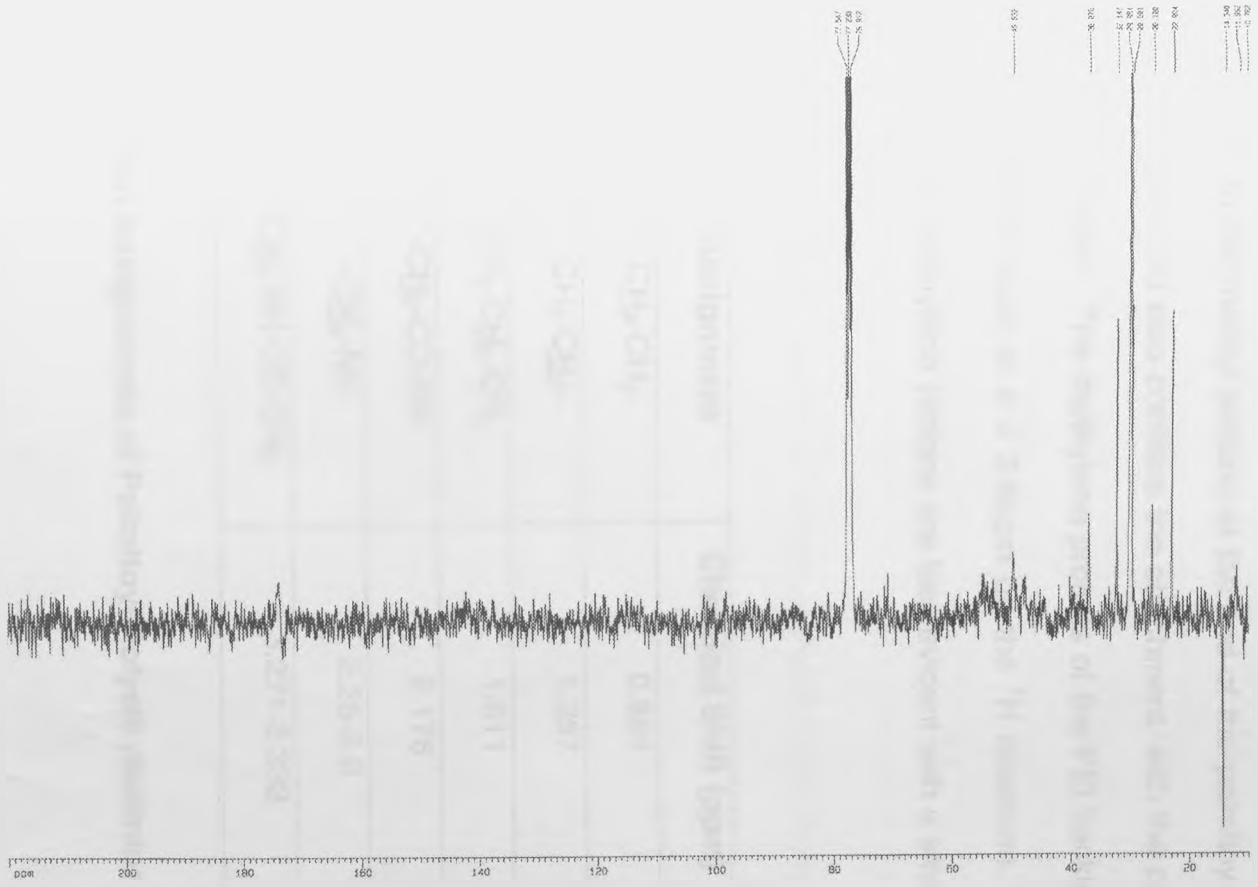

Figure 22: ^{13}C NMR Spectra of Palmitoyl Polyethylenimine. ^{13}C jmod C, CH_2 up; CH, CH_3 down

Modification of the PEI chain is seen by the downfield shift of the methylene backbone protons to δ = 3.0-3.5ppm, due to the attachment of a carbonyl group to the PEI nitrogen (Figure 21). The presence of the palmitoyl side chain can be further confirmed by the presence of a triplet peak at δ = 0.884ppm, due to the methyl protons at the end of the palmitoyl chain. The ^{13}C spectra (Figure 22) also confirms the attachment, with the presence of a signal at δ = 14.3ppm. The methylene protons of the PEI backbone present as a large mulitplet peak at δ = 2.6ppm on the ^{1}H spectrum. On the ^{13}C spectrum the PEI methylene protons are less evident with a small signal at δ = 49ppm.

Assignment	Chemical Shift (ppm)
$C\underline{H}_3$-CH_2	0.884
CH_3-$C\underline{H}_2$-	1.257
CH_2-$C\underline{H}_2$-CH_2	1.611
-$C\underline{H}_2$-CO-NH	2.176
-$C\underline{H}_2$-NH	2.25-3.0
-$C\underline{H}_2$-NH-CO-CH_2	3.271-3.332

Table 5: Proton Assignments of Palmitoyl Polyethylenimine.

Assignment	Chemical Shift (ppm)
CH_3-CH_2	**14**
CH_3-**C**H_2	**22**
CH_2-CO-NH	**26**
CH_2-**C**H_2-CH_2 (Palmitoyl)	**29**
CH2-**C**H2-CH2-CO	**32**
CH2-CH2-CH2-CO	**36**
NH-**C**H_2-**C**H_2-NH	**49**
Solvent Peak	**77**

Table 6: Carbon Assignments of Palmitoyl Polyethylenimine.

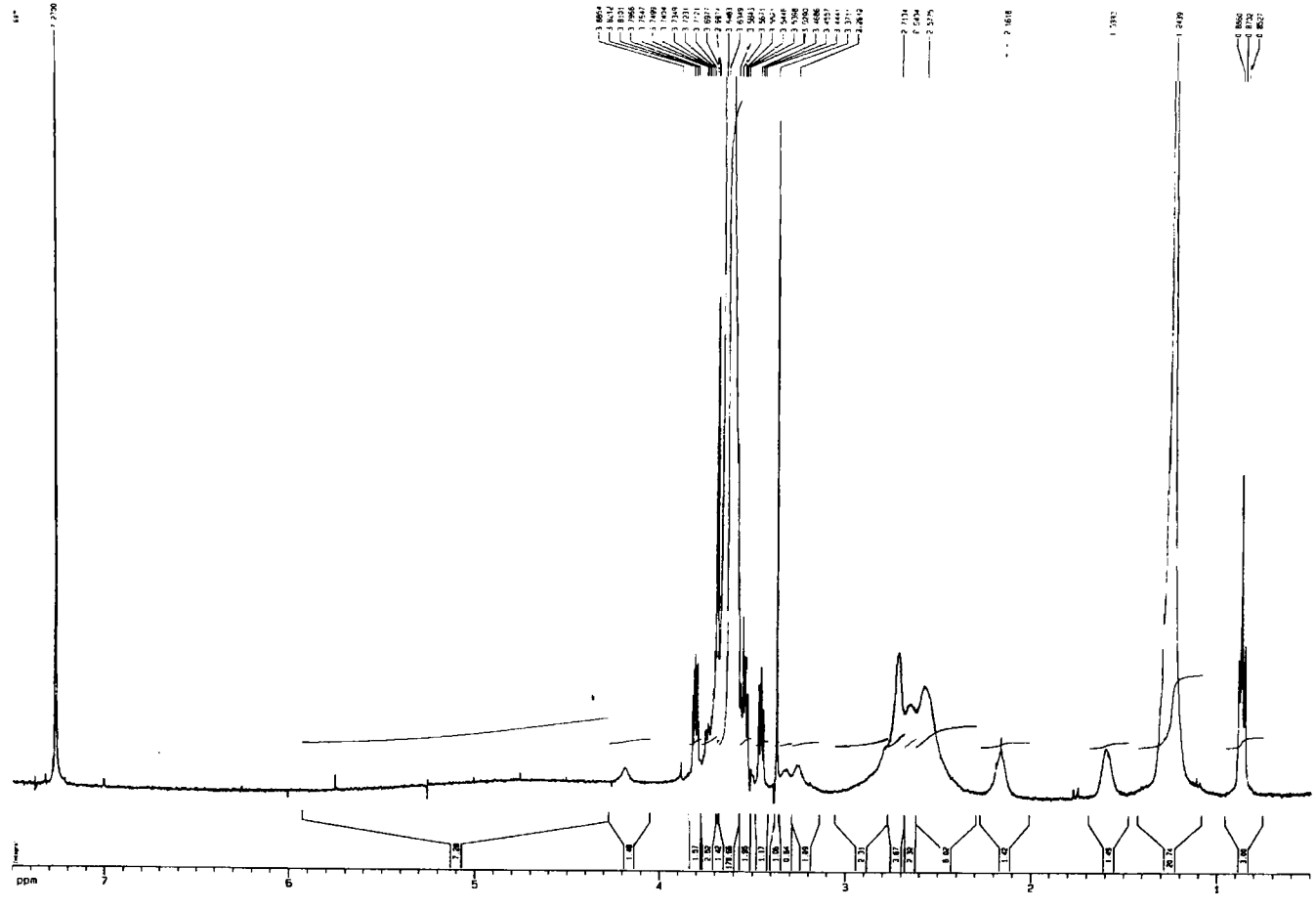

Figure 23: ^{1}H NMR Spectra of Palmitoyl Polyethylene glycol Polyethylenimine.

Figure 24: ^{13}C NMR Spectra of Palmitoyl Polyethylene glycol Polyethylenimine. ^{13}C jmod C, CH_2 up; CH, CH_3 down

Once again the modification of the PEI backbone is confirmed through the downfield shift of the methylene protons to δ = 3.2-3.4ppm, due to the carbonyl modification of the adjacent primary amines. The attachment of the palmitoyl side chains to the PEI backbone is further confirmed by the triplet peak at δ = 0.884ppm, due to the methyl protons of the palmitoyl chain (Figure 23). This is also confirmed by a signal at δ = 14.321ppm on the ^{13}C spectrum. Attachment of the PEG groups can be confirmed by the presence of a peak at δ = 3.37ppm due to the methyl protons of the methoxy-PEG (CH_3-O) group. The ^{13}C spectrum confirms the attachment shown by a signal at δ = 59ppm (Figure 24).

Assignment	Chemical Shift
$C\underline{H}_3$-CH_2 (Palmitoyl)	0.884
CH_3-$C\underline{H}_2$ (Palmitoyl)	1.257
CH_2-$C\underline{H}_2$-CH_2	1.611
$C\underline{H}_2$-CO-NH	2.176
$C\underline{H}_2$-NH	2.25-3.0
$C\underline{H}_2$-NH-CO-CH_2	3.271-3.332
$C\underline{H}_3$-O (PEG)	3.37
CH_2-$C\underline{H}_2$-O (PEG)	3.52-3.75

Table 7: Proton Assignments for Palmitoyl PEG PEI.

Assignment	Chemical Shift
$\underline{C}H_3$-CH_2	14
CH_3-$\underline{C}H_2$	22
$\underline{C}H_2$-CO-NH	26
CH_2-$\underline{C}H_2$-CH_2 (Palmitoyl)	29
CH_2-CH_2-$\underline{C}H_2$ (Palmitoyl)	32
$\underline{C}H_2$-CH_2-CH_2 (Palmitoyl)	36
N-$\underline{C}H_2$-CH_2-NH	49
$\underline{C}H_3$-O (PEG)	59
CH_2-$\underline{C}H_2$-CH_2 (PEG)	71
Solvent Peak	77

Table 8: Carbon Assignments of Palmitoyl PEG PEI

Figure 25: ^{1}H NMR Spectra of Quaternary Ammonium Polyethylenimine.

Figure 26: ^{13}C NMR Spectra of Quaternary Ammonium Polyethylenimine. ^{13}C jmod C, CH_2 up; CH, CH_3 down.

Comparison of the polyethylenimine ^{13}C spectrum (Figure 20) with that of the quaternary ammonium product (Figure 26), it can be seen that modification of the PEI chain has taken place. This can be seen by the downfield shift of the CH_2 peaks (δ=2.8-3.28ppm), indicating an increase in the electro-negativity of the backbone and terminal nitrogen's of the polymer. The ^{13}C spectrum shows the presence of CH_3 peaks at both 50 and δ = 52ppm, which can be attributed to the quaternary ammonium groups, $N^+(CH_3)_3$. The presence of tertiary amino groups, $N(CH_3)_2$, can be detected at δ = 40ppm.

Assignment	Chemical Shift (ppm)
$N(C\underline{H}_3)_2$ (tertiary)	2.3
$C\underline{H}_2$-$C\underline{H}_2$ (PEI backbone)	2.8-3.28
$N^+(C\underline{H}_3)_3$ (main chain quaternisation)	3.5
$N^+(C\underline{H}_3)_3$ (quaternary)	4.05
Solvent Peak	4.6

Table 9: Proton assignments of QPEI.

Assignment	Chemical Shift (ppm)
NH_2-CH_2-$\underline{C}H_2$-N	35
NH_2-$\underline{C}H_2$-CH_2-N	39
$N^+(\underline{C}H_3)_2$ (backbone)	43
$N^+(\underline{C}H_3)_2$ (tertiary)	47-49
NH-CH_2-$\underline{C}H_2$-NH_2	52
N^+-$\underline{C}H_2$-CH_2-N	55
$N^+(\underline{C}H_3)_3$ (quaternary)	60-63

Table 10: Carbon assignments for QPEI.

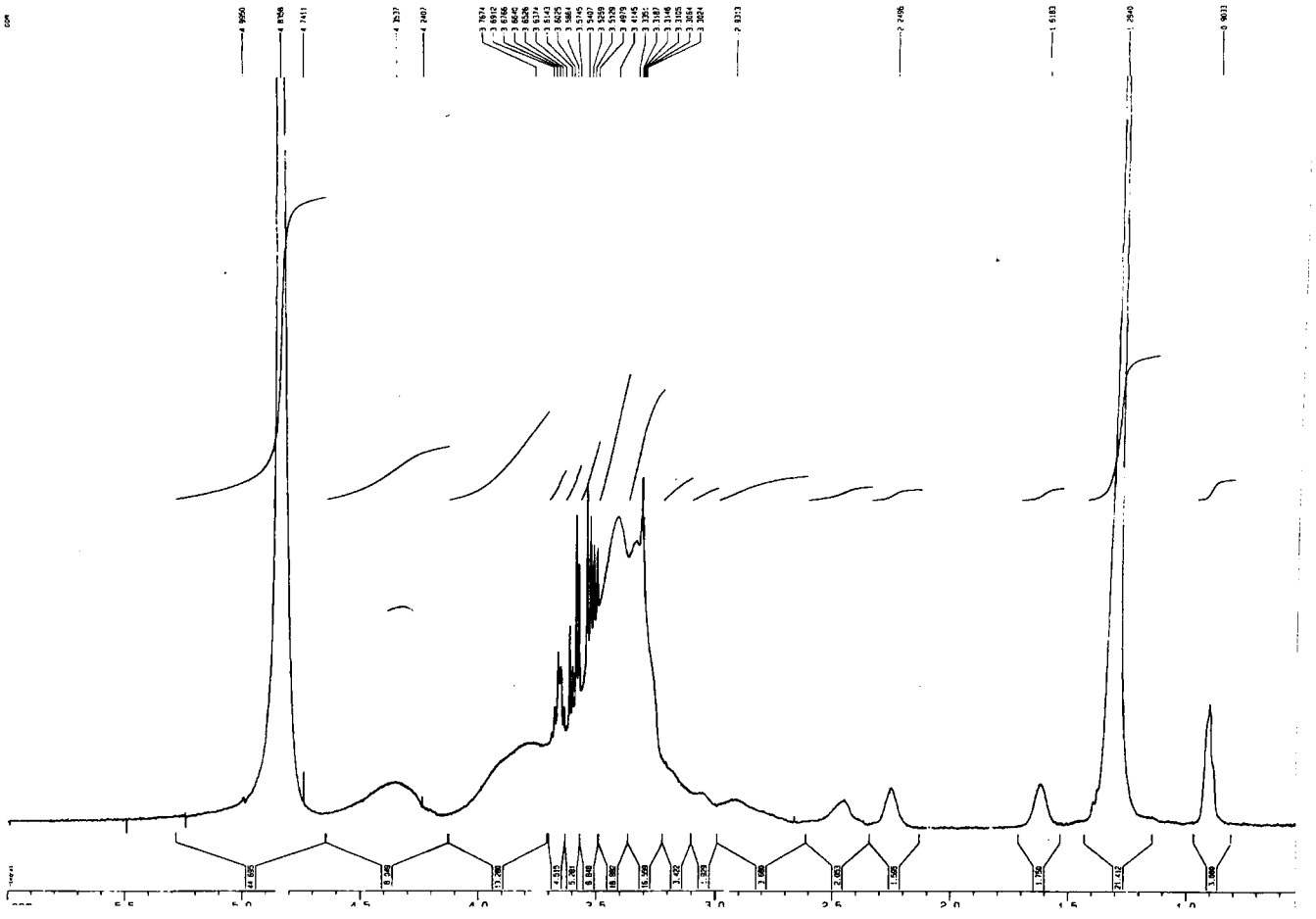

Figure 27: ^{1}H NMR Spectra of Quaternary Ammonium Palmitoyl Polyethylenimine.

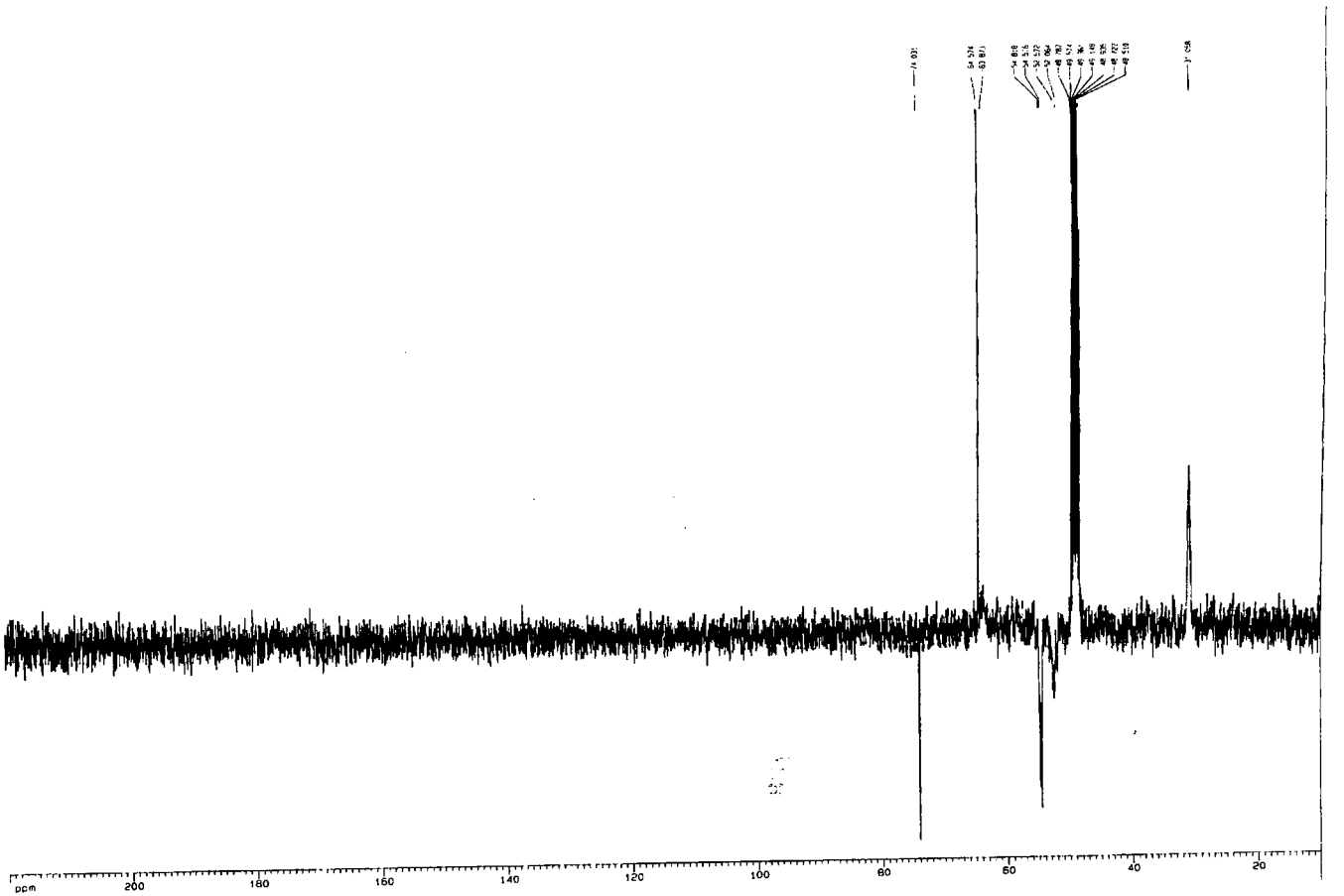

Figure 28: ^{13}C NMR Spectra of Quaternary Ammonium Palmitoyl Polyethylenimine. ^{13}C jmod C, CH_2 up; CH, CH_3 down.

The ^{13}C spectrum of the Palmitoyl-PEI quaternary derivative shows extensive modification (Figure 28) when compared to its parent polymer (Figure 20). Again, the downfield shift of the CH_2 peaks is evident. The quaternary ammonium groups can be detected with signals at both δ = 53 and 56ppm, whilst the tertiary ammonium groups give a signal at δ = 41ppm. The ^1H (Figure 27) spectrum shows a decrease in the amount of palmitoyl groups attached to the PEI chain possibly due to cleavage of theses groups during the quaternisation reaction.

Assignment	Chemical Shift (ppm)
$C\underline{H}_3$-CH_2 (Palmitoyl)	0.903
$C\underline{H}_2$-CH_3 (Palmitoyl)	1.29
CH_2-$C\underline{H}_2$-CH_2 (Palmitoyl)	1.61
$C\underline{H}_2$-NH	2.24
N-$C\underline{H}_2$-$C\underline{H}_2$-N (PEI backbone)	3.0-3.5
$C\underline{H}_3$ (quaternary)	3.7
-CH_2-NH-CO-CH_2	4.3
Solvent Peak	4.8

Table 11: Proton assignments for QPPEI

Assignment	Chemical Shift (ppm)
$\underline{C}H_3$-CH_2	14
CH_3-$\underline{C}H_2$	31
$\underline{C}H_2$-CH_2 (Palmitoyl)	48-49
$N^+(\underline{C}H_3)_2$	52
$N^+(\underline{C}H_3)_3$	54
$\underline{C}H_2$-CH_2-NH_2	63-64

Table 12: Carbon assignments for QPPEI

2.3.2: FTIR Analysis

Calculation of PEI Branching Density

Li *et al* [71] reported a method for calculating the branching density of PEI using FTIR. By comparing the spectra of two PEI's of differing molecular weights a difference at the band of 1595cm^{-1} was observed (Figure 29). This difference can be attributed to the vibration of primary amine (NH_2) scissoring. The intensity of CH_2 vibrations at 1460cm^{-1} can be used as an internal reference and the relative intensity ratio of NH_2 to CH_2 for each polymer can be calculated. There are $(2 + \mathrm{db} \times \frac{\mathrm{Mn}}{43})$ primary amine groups for each branched PEI chain, where Mn = number average molecular weight and db = branching density, the number of primary amine groups over that of monomeric units (CH_2CH_2N) is $\frac{2 + \mathrm{db},25 \times \frac{\mathrm{Mn},25}{43}}{\frac{\mathrm{Mn},25}{43}}$, which is proportional to the measured intensity ratio, where $Mn_{,25}$ = 10 × 10^{3}gmol^{-1} = 10,000, $Mn_{,7}$ = 0.6 × 10^{3}gmol^{-1} = 600, 43 = molecular weight of one monomer unit, ratio of primary amines to CH_2 = for 25kDa = 0.56 and ratio of primary amines to CH_2 = for 7kDa = 0.95.

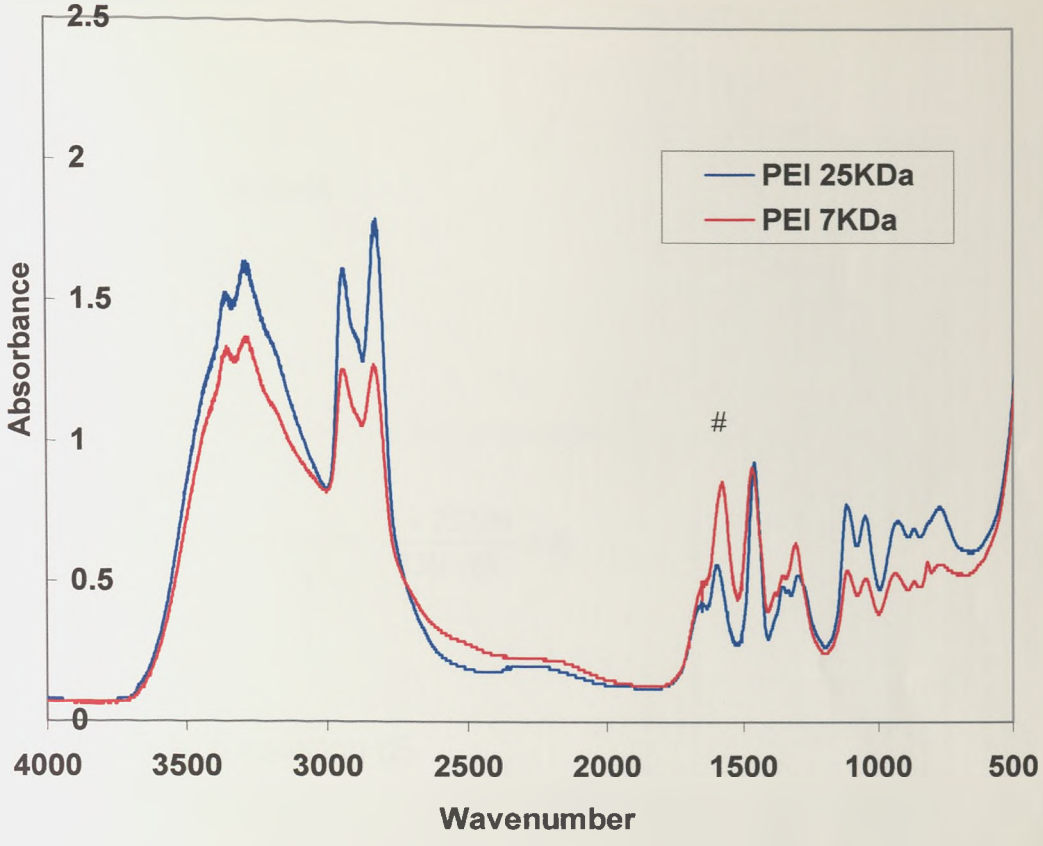

Figure 29: Fourier Transform Infrared Spectra of Polyethylenimine (25KDa and 7KDa). # indicates difference between polymers at 1595 cm^{-1}.

PEI 25kDa

$$\frac{2 + db,25 \times \frac{Mn,25}{43}}{\frac{Mn,25}{43}} \propto 0.56 \qquad (1)$$

PEI 7kDa

$$\frac{2 + db,7 \times \frac{Mn,7}{43}}{\frac{Mn,7}{43}} \propto 0 \cdot 95 \qquad (2)$$

Therefore,

$$\frac{2 + db \times \frac{10,000}{43}}{\frac{10,000}{43}} = K0 \cdot 56 \Rightarrow \frac{2 + 233db}{130 \cdot 23} = K \qquad (3)$$

Substitute for K in equation (2)

$$\Rightarrow \frac{2 + db \times \frac{600}{43}}{\frac{600}{43}} = \frac{2 + 233\,db}{130 \cdot 23} \times 0 \cdot 95 \Rightarrow \frac{2 + 14db}{14 \times 0 \cdot 95} = \frac{2 + 233db}{130 \cdot 23}$$

$$\Rightarrow \frac{2 + 14db}{13 \cdot 3} = \frac{2 + 233db}{130 \cdot 23}$$

$$\Rightarrow 130 \cdot 23(2 + 14db) = 13 \cdot 3(2 + 233db)$$

$$\Rightarrow 260 \cdot 46 + 1823 \cdot 22db = 26 \cdot 6 + 3098db$$

$$\Rightarrow \quad 233 \cdot 86 = 1275 \cdot 68\,\text{db}$$

$$\Rightarrow \quad \text{db} = \frac{233 \cdot 86}{1275 \cdot 68}$$

$$\Rightarrow \quad \text{db} = 0 \cdot 183$$

Number of primary amine groups $= 2 + \text{db} \times \frac{\text{Mn}}{43}$

$$= 2 + \left(0 \cdot 183 \times \frac{10{,}000}{43}\right)$$

$$= 44 \cdot 558$$

Number of monomeric units $= \frac{\text{Mn}}{43} = \frac{10{,}000}{43} = 232 \cdot 5$

Therefore PEI (25KDa) has 233 monomeric units with 45 branching points, i.e. 10 monomeric units with 2 branching points (Figure 30).

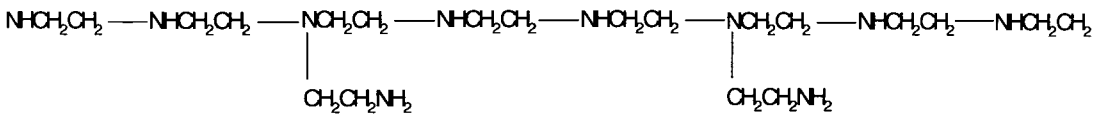

Figure 30: Polyethylenimine chain with two branching points.

Molecular weight of PEI Chain with 2 branching points = 430·682g

Therefore molecular weight of PEI with one branching group, i.e. 1 primary amine group = 215·341g

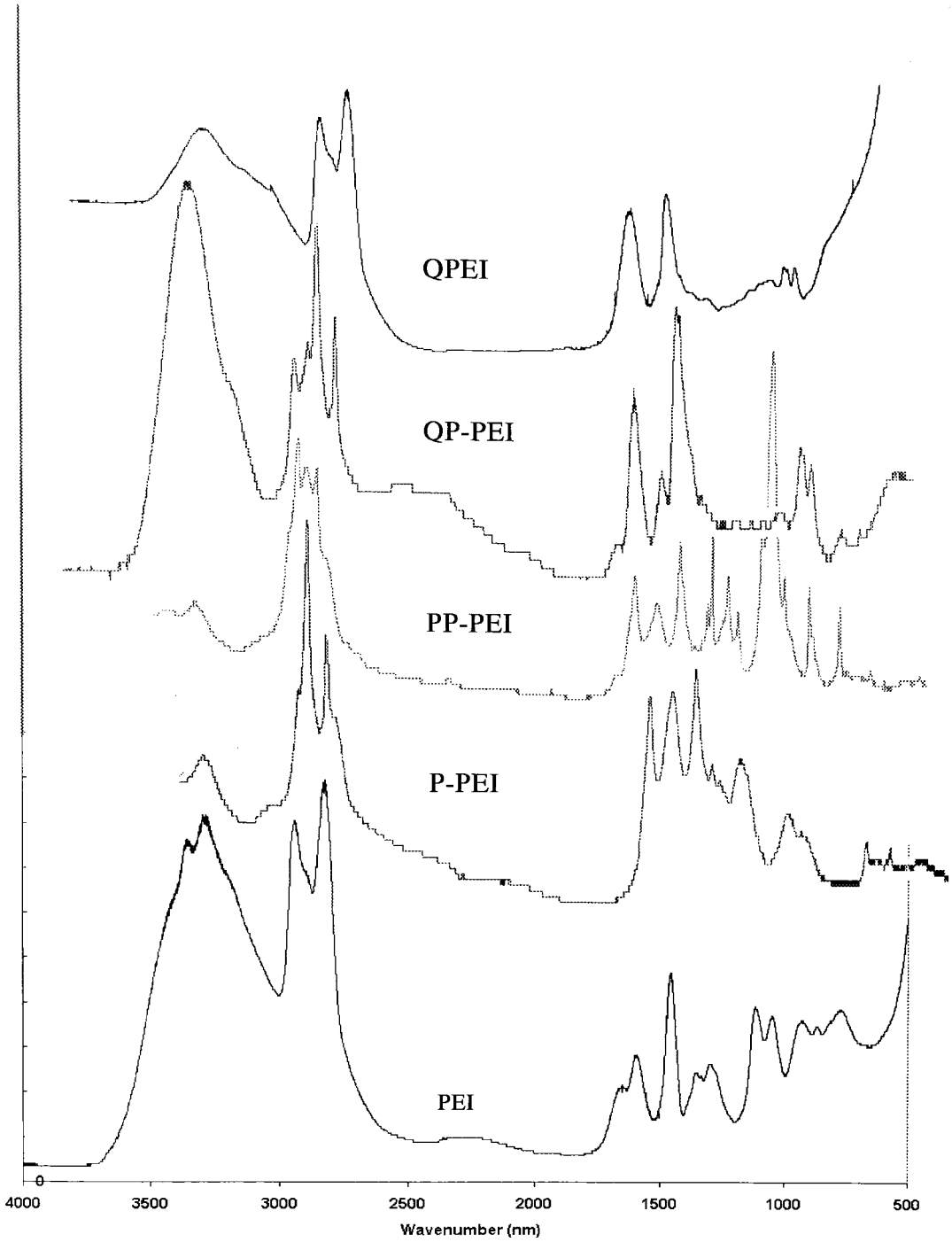

Figure 31: FTIR spectra of PEI, P-PEI, PP-PEI, QP-PEI and QPEI.

The FTIR spectra further confirm the modifications made to the parent PEI polymer and yielded characteristic fingerprint regions for each of the polymers (Figure 31). The P-PEI and PP-PEI spectra show a decrease in absorption at ~3400nm, indicating a reduction in the number of primary amines available on each of the modified polymers as compared to PEI. The attachment of specific ligands to the polymer is clearly visible. The attachment of palmitoyl and PEG chains are confirmed by the presence of a peak at ~1600nm due to the CONH groups. The end groups of the ligands can also be identified, the OCH_3 group on the PEG chains is shown by a peak at ~2800nm. The CH_3 end group of the palmitoyl chain results in a peak at ~1390nm. The confirmation of the quaternary structure of QPEI and QPPEI are not confirmed by the FTIR spectra, as the two compounds produced a lack of characteristic frequencies.

2.3.3: TNBS Assay

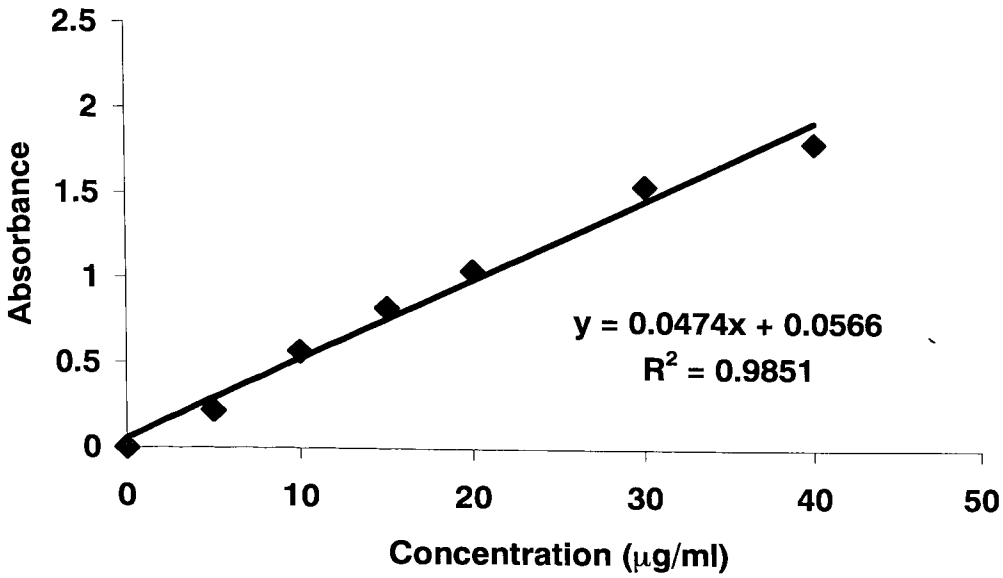

Figure 32: Polyethylenimine Calibration Series (Absorbance at 438·0nm).

Assay of Palmitoyl Polyethylenimine.

At 438·0nm P-PEI gave an absorbance of 0·177 ± 0·01 (n=3)

From PEI calibration series: $\text{Absorbance} = 0 \cdot 0474 \times \text{Concentration} + 0 \cdot 0566$

$$\text{Concentration} = \frac{0 \cdot 177 - 0 \cdot 0566}{0 \cdot 0474} = 2 \cdot 54 \mu g / ml$$

5mg of P-PEI was diluted to 15μg/ml, therefore: 15μg of P-PEI contains 2·54μg of PEI monomer, therefore 1g of P-PEI contains 169mg of PEI monomer, i.e. 0.8mmoles of primary amines.

Assay of Palmitoyl Polyethylene glycol Polyethylenimine.

At 438.0nm PP-PEI gave an absorbance of 0·115±0.002 (n=3)

From PEI calibration series: $\text{Absorbance} = 0 \cdot 0474 \times \text{Concentration} + 0 \cdot 0566$

$$\text{Concentration} = \frac{0 \cdot 115 - 0 \cdot 0566}{0 \cdot 0474} = 1 \cdot 232 \mu g / ml$$

5mg of PP-PEI was diluted to 15μg/ml, therefore: 15μg of PP-PEI contains 1·232μg of PEI monomer, therefore 1g of PP-PEI contains 82·1mg of PEI monomer, i.e. 0.38mmoles of primary amines

Assay of Quaternary Polyethylenimine.

At 438.0nm quaternary polyethylenimine gave an absorbance of 0.231±0.032.

From PEI calibration series: $\text{Absorbance} = 0 \cdot 0474 \times \text{Concentration} + 0 \cdot 0566$

So if Absorbance = 0.231, then concentration = 0.231-0.0566/0.0474 = 3.67μg/ml.

10mg of QPEI was diluted to 6μg/ml, therefore: 6μg of QPEI contains 3.67μg of PEI monomer, thèrefore 1g of QPEI contains 611mg of PEI monomer, i.e. 2.9mmoles of primary amines.

Assay of Quaternary Palmitoyl Polyethylenimine

At 438.0nm quaternary palmitoyl polyethylenimine gave an absorbance of 0.588±0.0023.

From PEI calibration series: $\text{Absorbance} = 0 \cdot 0474 \times \text{Concentration} + 0 \cdot 0566$

So if Absorbance = 0.588, then concentration = 0.588-0.0566/0.0474 = 11.21μg/ml.

10mg of QPPEI was diluted to 60μg/ml, therefore: 600μg of QPEI contains 11.21μg of PEI monomer, therefore 1g of QPPEI contains 186 mg of PEI monomer, i.e. 0.8mmoles of primary amines.

2.3.4: Elemental Analysis.

	Carbon	Hydrogen	Nitrogen	Oxygen	Chloride
PEI	54.89	12.09	32.10		
P-PEI	50.92	10.88	16.85	21.35	
PP-PEI	53.68	10.18	8.63	27.51	
QPEI	36.17	9.34	15.11	15.76	23.62
QPPEI	46.28	10.01	11.32	20.08	12.31

Table 13: Measured Percentage values of each element in the respective polymers.

From the elemental analysis we can calculate the number of available nitrogens per gram of polymer.

PEI has 22.2mmoles of nitrogens available per gram of polymer ((%of nitrogen x 10)/14).

Therefore,

Polymer	mmoles of nitrogen per gram of polymer
P-PEI	12.0
PP-PEI	6.1
QPEI	10.8
QP-PEI	8.1

2.3.5: Molecular Weight Analysis

DN/DC Analysis

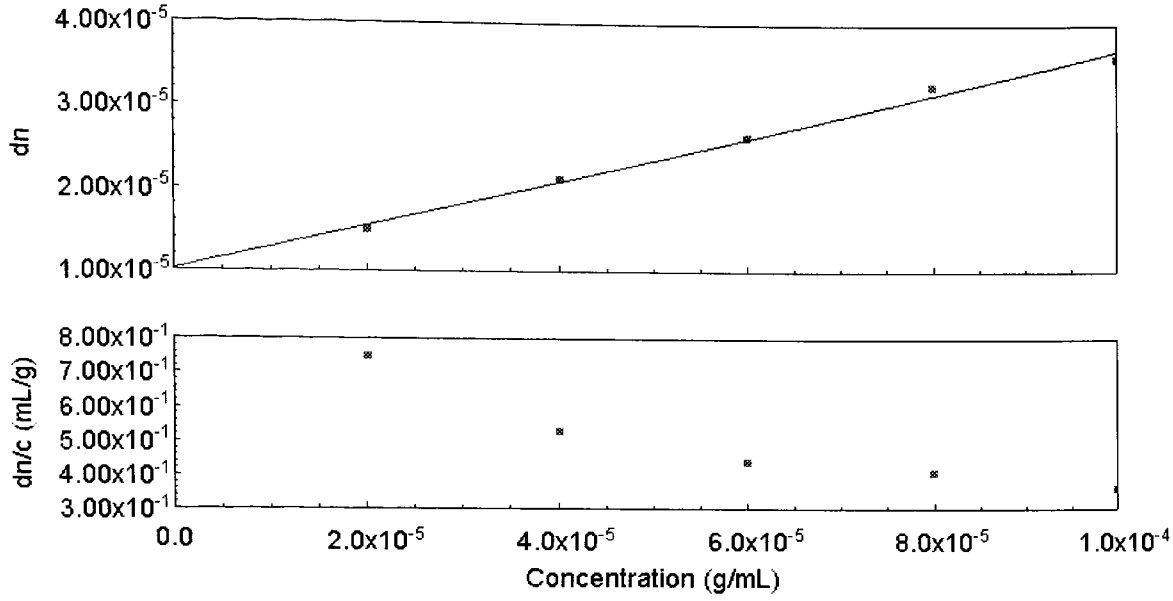

Figure 33: Dn/Dc Plot of PEI.

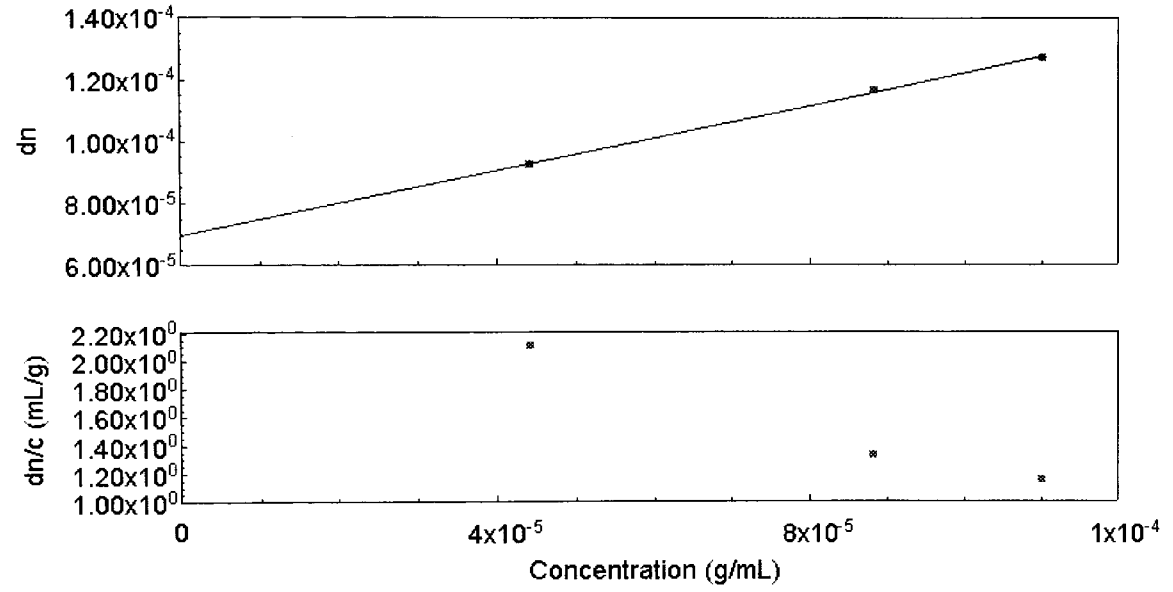

Figure 34: Dn/Dc Plot of P-PEI.

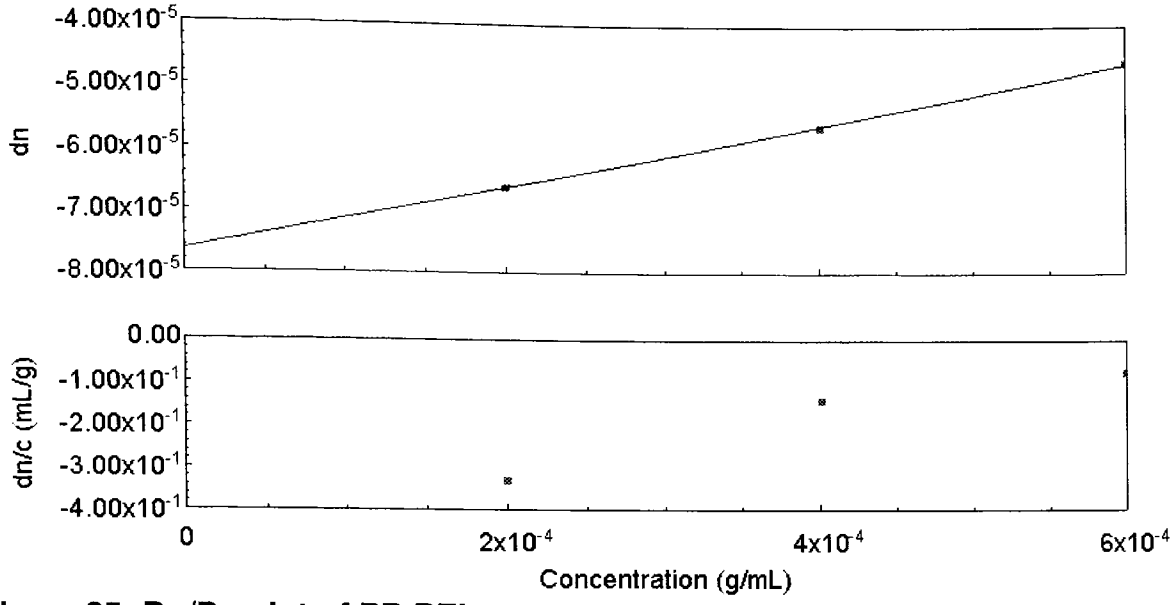

Figure 35: Dn/Dc plot of PP-PEI.

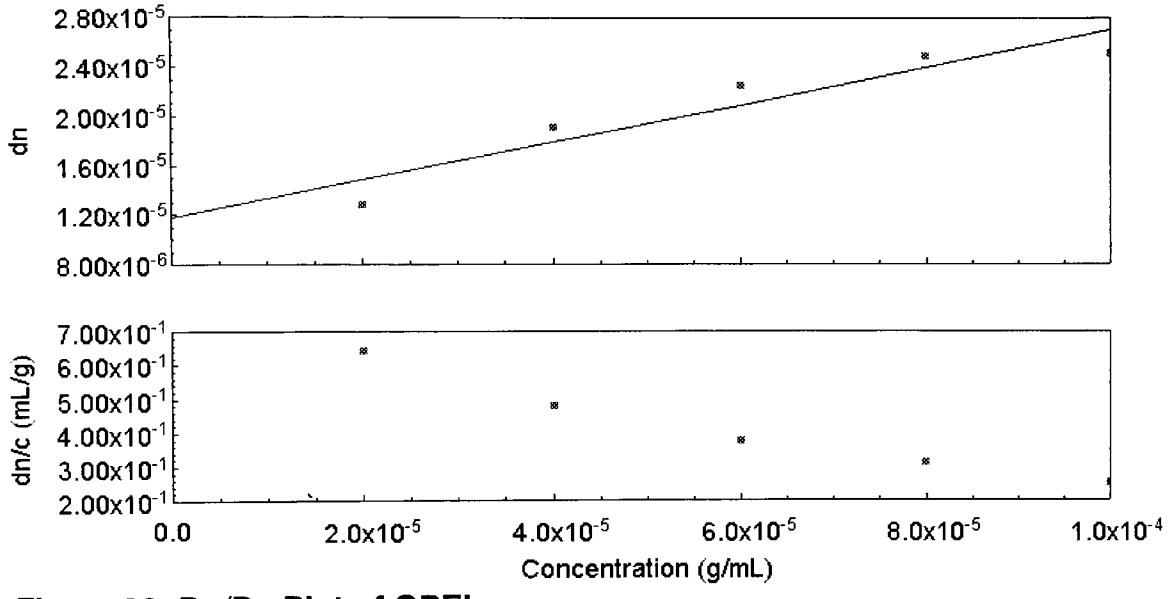

Figure 36: Dn/Dc Plot of QPEI.

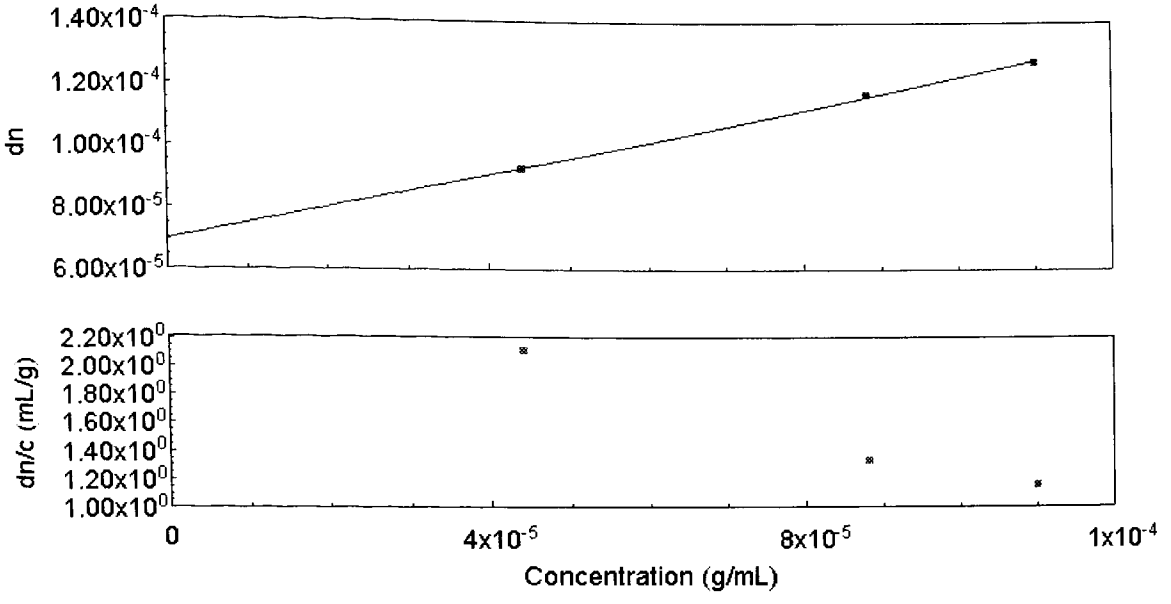

Figure 37: Dn/Dc Plot of QPPEI.

Molecular Weight Determination

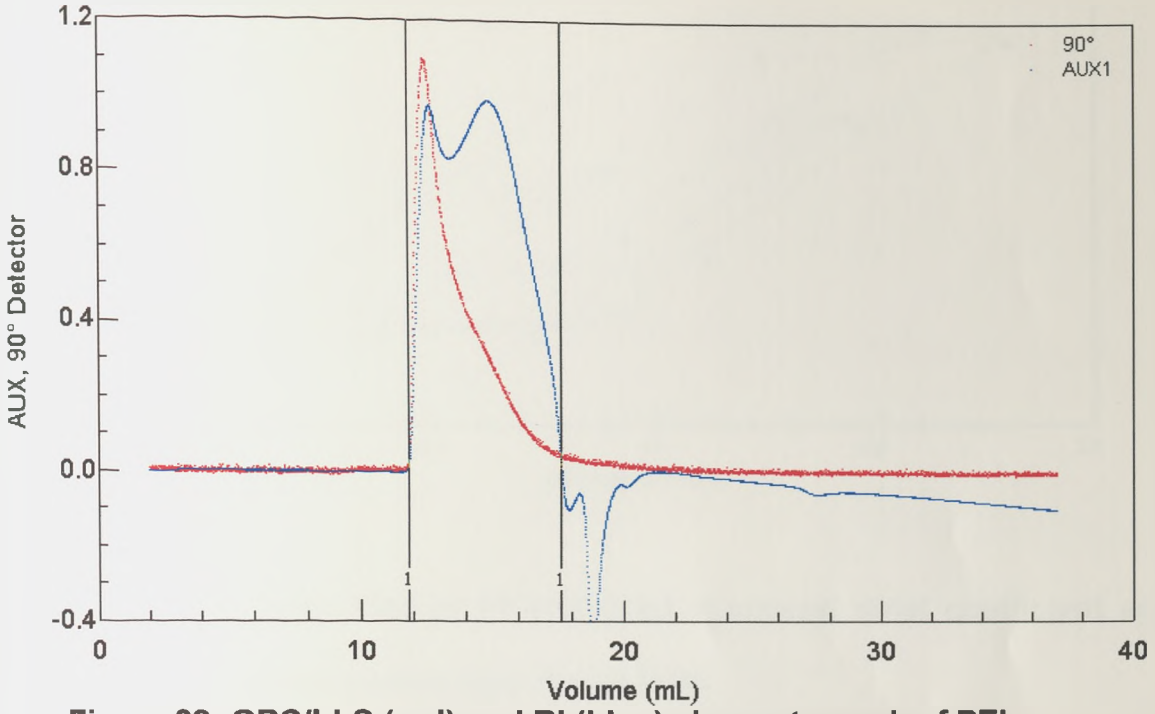

Figure 38: GPC/LLS (red) and RI (blue) chromatograph of PEI

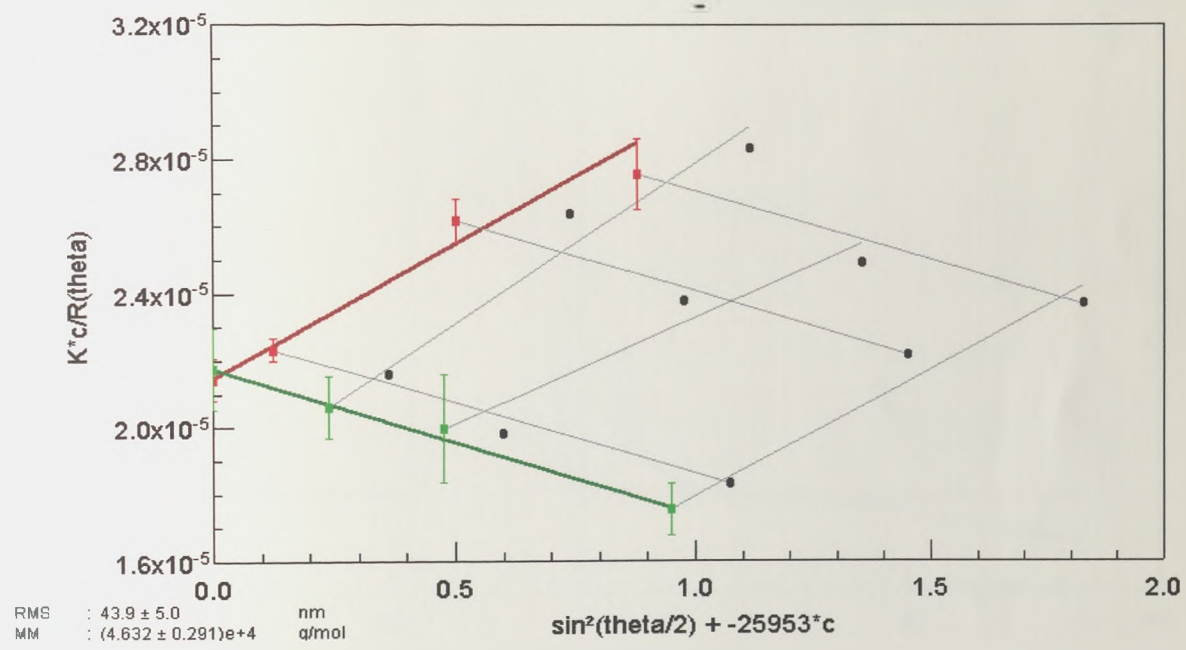

Figure 39: Zimm Plot of P-PEI (Red = second virial coefficient and green = z-average rms radius).

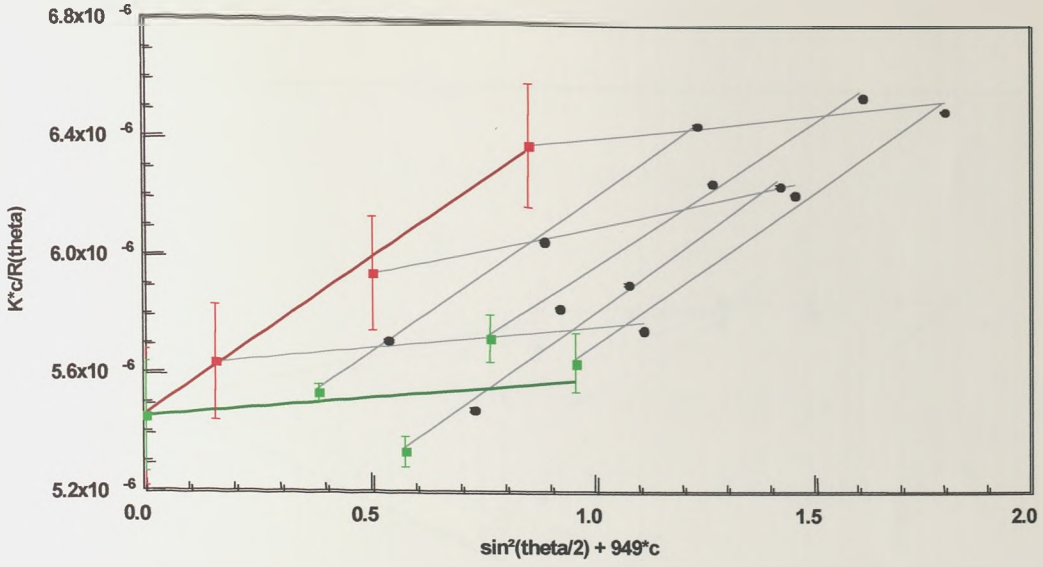

Figure 40: Zimm Plot of PP-PEI (Red = second virial coefficient and green = z-average rms radius).

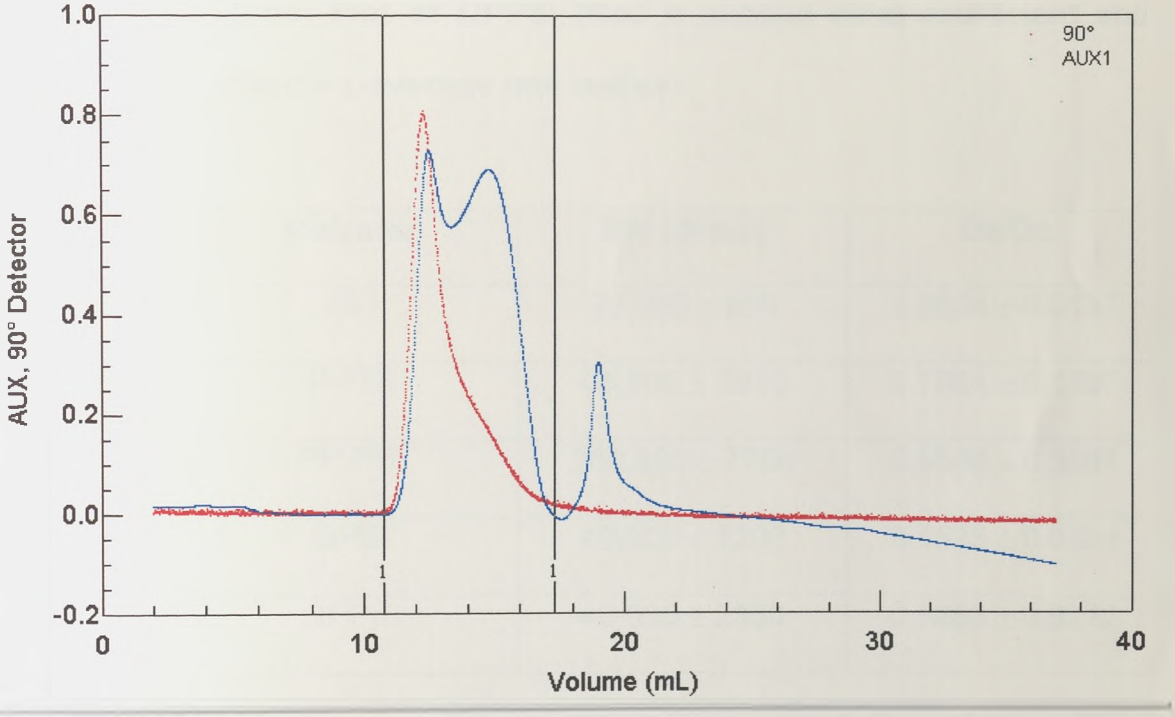

Figure 41: GPC/LLS (red) and RI (blue) chromatograph of QPEI

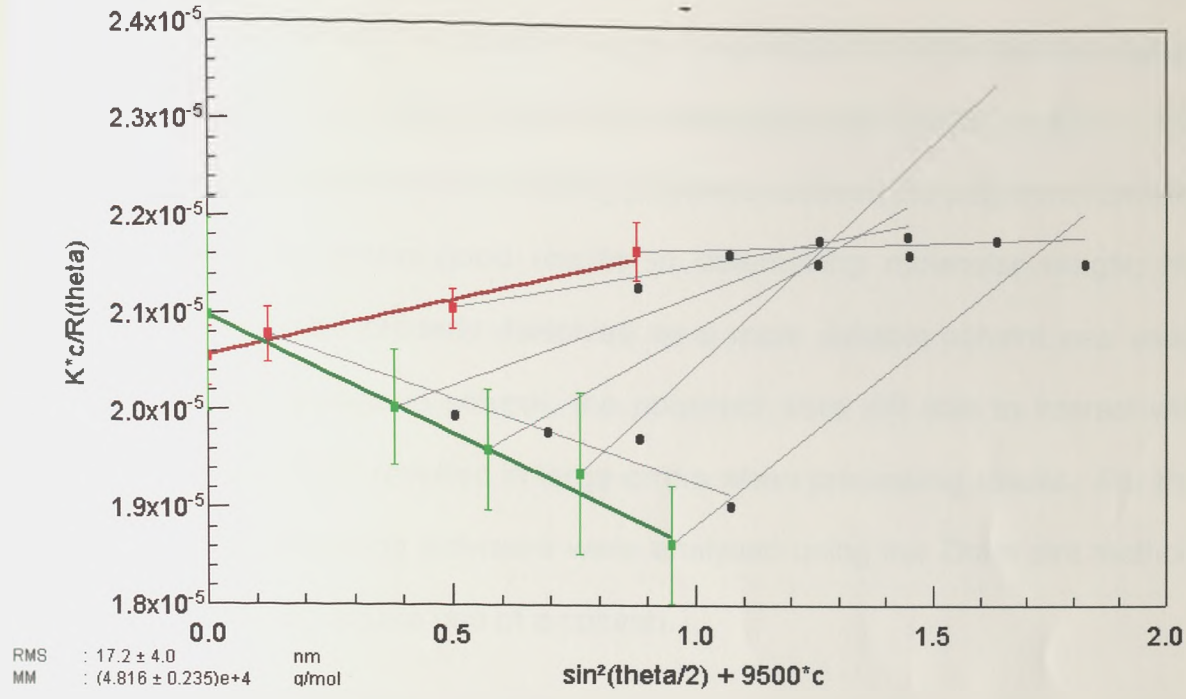

Figure 42: Zimm Plot of QPPEI (Red = second virial coefficient and green = z-average rms radius).

Polymer	Mw (g/mol)	Dn/Dc
PEI	23,000 ± 850	0.2664 ± 0.0137
P-PEI	46,000 ± 2910	0.7964 ± 0.1597
PP-PEI	260,000 ± 7700	0.0506 ± 0.0007
QPEI	49,000 ± 1200	0.1525 ± 0.0324
QPPEI	48,000 ± 2350	0.5283 ± 0.0212

Table 2.3.5: Summary of Dn/Dc and Mw Results.

The modified polymers were analysed using several techniques and solvents. Both the unmodified PEI and QPEI were dissolved in a salt solution, the use of this solution was to help mask the highly positive nature of the polymers and any subsequent interactions with the GC column. The amphiphillic nature of the remaining polymers reduced the polymers solubility in water. To obtain good results in determining molecular weight, the polymer must be properly dissolved so a more suitable solvent was used. Despite this change in solvent, the polymers were still able to interact with the column, which resulted in large errors when processing results. For this reason the remaining polymers were analysed using the Zimm plot method, which does not require use of a column.

2.4: Discussion of Results

Each of the techniques used to analyse the modified polymers must be used in conjunction with each other to give a complete picture of the modifications made. The NMR and FTIR data can be used to confirm the modifications made to the parent PEI polymer and can to a certain extent give the level of branching and modification of the polymers. The TNBS assay gives information on the level of modification made to the polymer primary amines. The elemental analysis also provides information on the modifications made to the polymers.

P-PEI

From the NMR data, the integrals on the ^1H spectrum (Figure 21) show a ratio of 3 palmitoyl CH_3 protons to 15.416 PEI CH_2 protons i.e. a ratio of 1 palmitoyl group to 7.2 unmodified CH_2 groups. The ratio of methylenes attached to a carbonyl group to unaltered methylenes is 2.6:15.4, approximately 1:6 (Figure 21). One palmitoyl methyl group (3.0) appears to correspond to one altered methylene group (2.6). One palmitoyl group should correspond to four CH_2 groups. This shows that the NMR data is underestimating the level of palmitoylation and therefore cannot be used in calculating the degree of modification in the P-PEI polymer.

From the TNBS Assay we know that for every 1000mg of PEI 169mg are present as unmodified primary amine groups. From the FTIR results we also know that for every 5 CH_2CH_2N there is 1 $CH_2CH_2NH_2$

∴ Since there is 1 primary amine per 5 CH_2CH_2N groups, the Mw of 1 Palmitoyl Polyethylenimine unit (Figure 30) is (5x42)+239 = 448

∴ 831mg of Palmitoyl Polyethylenimine contains $\frac{831}{448}$ such units = 1·85moles

169mg of Polyethylenimine contains $\frac{169}{210} = 0 \cdot 8$ Polyethylenimine units with a primary amine.

∴ The ratio of palmitoyl amide groups to unmodified primary amines = 1.9:0.8

∴ 1 palmitoylated unit is accommodated by $\frac{2 \cdot 7}{1 \cdot 9} = 1 \cdot 42$ polyethylenimine units

= 7·1 CH_2CH_2N units, therefore for every 7.1 nitrogens, 1 is palmitoylated

∴ **%Palmitoylation of amine groups = 14.1 mole%**

From the elemental analysis data the number of moles of each element in the unmodified PEI can be calculated for N=2 :

Carbon	Hydrogen	Nitrogen
4	10.6	2

And for P-PEI

Carbon	Hydrogen	Nitrogen
7	18.2	2

Therefore we can remove the values, which are known to be attributed to the unmodified PEI to give:

Carbon	Hydrogen	Nitrogen
3	7.2	0

For each $CH_2CH_2NHCH_2CH_2NH_2$ we have 3 moles of carbon. Each palmitoyl group has 16 moles of carbon ∝ 33 moles of hydrogen. Therefore each primary amine has $\frac{3}{16}$ = 0.187 palmitoyl groups or each nitrogen is modified 9.375%.

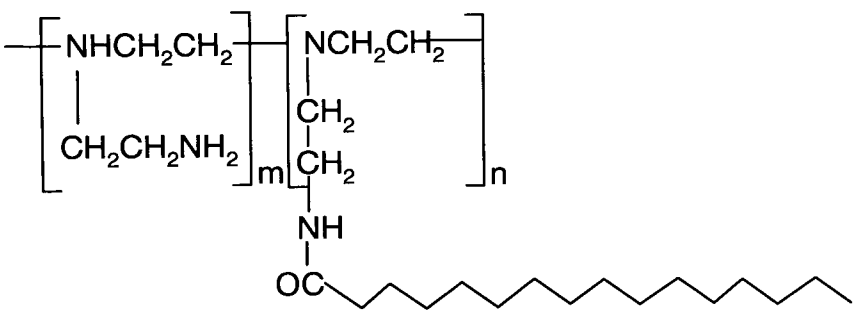

Figure 43: Suggested chemical structure of PPEI, where m= 41 and n = 4.

PP-PEI

From the integration values on the ^1H spectrum, the ratio of Palmitoyl chains to PEG chains is given as 3 palmitoyl methyl protons to 188 PEG protons. The total number of PEG protons = 5000 (Mw of PEG) = (5000/44) x4 = 455 protons. Therefore there are only 188/455 = 0.413 moles of PEG to 1 mole of palmitoyl.

From the TNBS assay we know that for every 1000mg of PEI 82 mg are present as unmodified amine groups. From the FTIR results we also know that for every 5 CH_2CH_2N there is 1 $CH_2CH_2NH_2$

$\therefore$ 1000mg of PP-PEI contains $\frac{82}{215}$ = 0.38 moles of primary amine groups

918mg of PP-PEI contains both palmitoyl and PEG PEI at a ratio of 1:0.41

$$\text{moles of palmitoyl/PEG groups} = \frac{918}{1x(215+239)+0.41(215+5000)}$$

$$= \frac{918}{2592} = 0.354 \text{ moles.}$$

Therefore we have 0.38moles of unreacted primary amine PEI to 0.35 moles of reacted PEI primary amines. But the ratio of palmitoyl:PEG = 2.4:1,

Therefore, the ratio of Palmitoyl-PEI:PEG-PEI:unreacted PEI = 0.25:0.1:0.38.

Since 1 primary amine is accommodated by 5 nitrogens, the ratio of nitrogens in each group = 1.25:0.50:1.9

% Palmitoylation of nitrogens = $\frac{0.25}{1.25+0.50+1.9} x100 = 6.9\%$

% PEGylation of nitrogens = $\frac{0.5}{1.25+0.50+1.9} x100 = 2.7\%$

From the elemental analysis data, the number of amide groups in PP-PEI can be calculated as 6.1 mmoles per gram of polymer. As 9.6% of the amide groups on the PP-PEI polymer are modified the number of available mmoles of nitrogen per gram of polymer can be given as 5.51 mmoles.

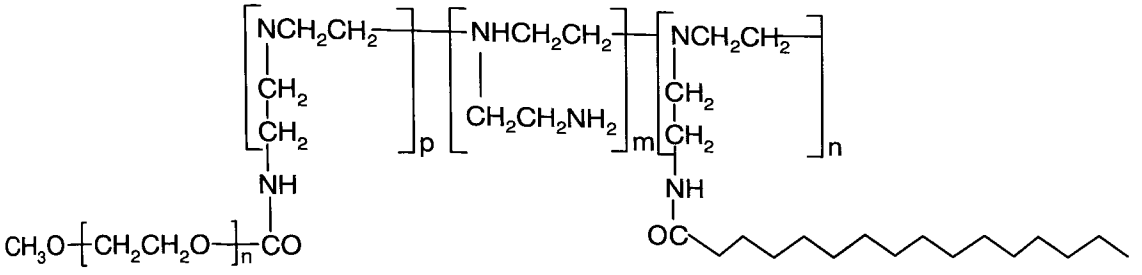

Figure 44: Suggested chemical structure of PP-PEI, where p=1, m= 41 and n= 3.

QPEI

The NMR and FTIR data were able to confirm the modification to the PEI parent polymer. The TNBS assay was used to calculate the level of primary amines as 2.9mmoles per gram of polymer. The elemental analysis was used to calculate the level of available nitrogen's in the polymer as 10.8 mmoles per gram of polymer, these two results show that not all of the primary amines were modified. The ^{13}C NMR spectrum of QPEI (Figure 2.3.1h) shows a mixture of both tertiary and quaternary amines. It was not possible to calculate the individual tertiary and quaternary modifications from the ^{1}H NMR spectra (Figure 2.3.1e) as the peaks were not sufficiently

isolated. The ^{13}C NMR spectra also shows the quaternisation of the main PEI backbone has also taken place.

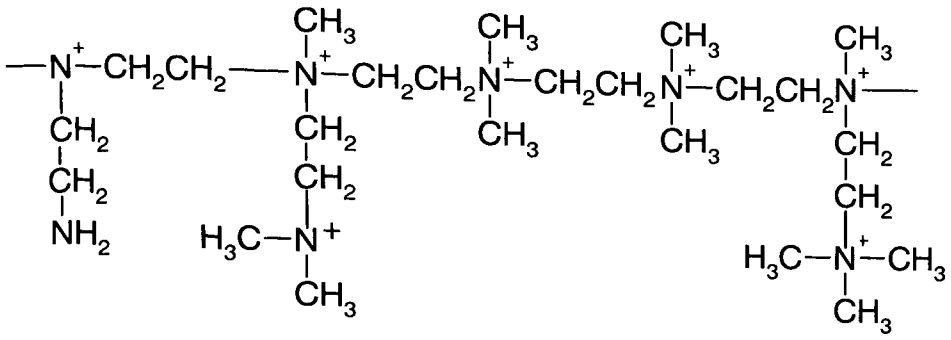

Figure 45: Suggested chemical structure of QPEI, showing tertiary and quaternary modification of primary amines and the PEI backbone.

QPPEI

As the NMR data for P-PEI overestimated the degree of palmitoylation, we cannot use the NMR to calculate the modification of QPPEI.

The degree of modification can be calculated using the elemental analysis data and the fact that $5CH_2CH_2N$'s are composed of one primary amine.

% of elements in QP-PEI	No of moles of each element in 1000g	Relative no of moles for N =10
C = 46.3	39	48.3
H = 10	100	124
N = 11.3	8.07	10

For N = 10 we have 20 carbons present on a section of the PEI chain. Therefore if both primary amines are modified we would have a ratio of C:N of $C_{52}N_{10}$ but instead we have a ratio of $C_{48}N_{10}$ and we know that the starting level of palmitoylation of P-PEI is 14.1%. Therefore only 1:7 nitrogen's are palmitoylated. Therefore we can assume that in the region of 1:10 primary amines will be palmitoylated if we subtract C_{16} + C_{20} from C_{48} we are left with C_{12}, the remaining primary amines are most likely to be converted into a quaternary ammonium group. Therefore we have a quaternisation of the PEI backbone nitrogen's (Figure 46) and some tertiary amines as shown in the lack of unaltered methylenes when compared to 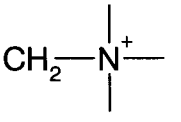 or 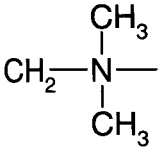 .

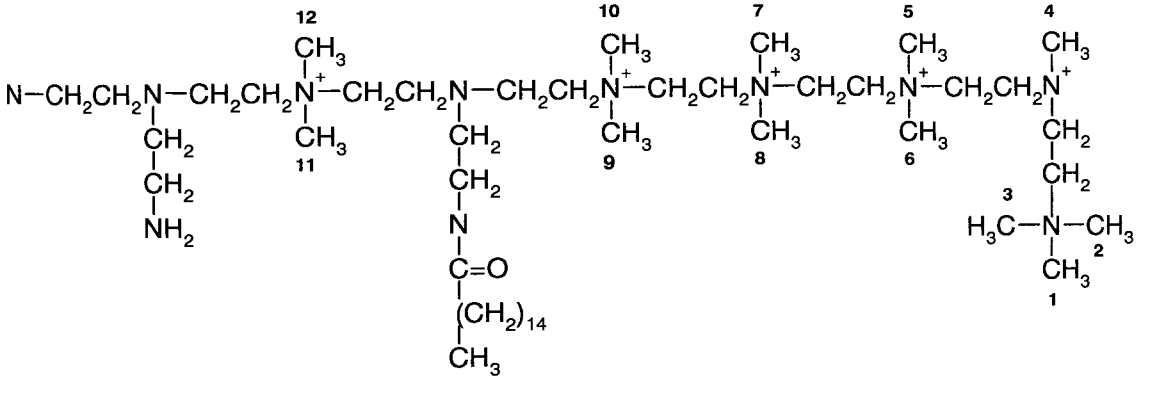

Figure 46: Suggested chemical structure of QPPEI.

The TNBS data shows that there are 0.8 mmoles of unmodified primary amines. This proves that not all the primary amines were converted and so the level of backbone quaternisation may approach 100%. From the elemental analysis data, the number of amide groups in QP-PEI can be calculated as 8.1 mmoles per gram of polymer. As 14.1% of the amide groups are modified the number of available mmoles of nitrogen per gram of polymer can be given as 6.95 mmoles.

Polymer	%MPEG per mole of nitrogen	%Palmitoyl per mole of nitrogen	Available mmoles of Nitrogen for complex-ion with DNA per gm of polymer	Molecular weight g $mole^{-1}$	Elemental analysis found
PEI	-	-	22.2	23,000	C=54.9 H=12.1 N=32.1
P-PEI	-	14.1	9.8	46,000	C=50.92 H=10.88 N=16.85 O=21.35
PP-PEI	3.3	8	5.51	260,000	C=53.7 H=10.2 N=8.6 O=27.5
Q-PEI	-	-	10.8	49,000	C=36.2 H=9.3 N=15.1 O=15.8 Cl=23.6
QP-PEI	-	14.1	6.95	48,000	C=46.3 H=10.0 N=11.3 O=20.1 Cl=12.3

Table 14: Summary of polymer structural characterisation.

Using the modification values from the NMR, FTIR, TNBS and elemental analysis experiments to calculate the molecular weight (Mw), we can see that the GPC-Malls experiments have overestimated the polymwers Mw's. Using the FTIR results we can calculate the Mw of PEI to be 10,000g/mol, whereas the GPC-Malls calculated it to be 23,000g/mol. The same overestimation is seen with P-PEI and PP-PEI, with calculated Mw values of 18,000g/mol and 19,000g/mol respectively, whereas the measured GPC-MALLS values are 46,000g/mol and 260,000g/mol. This overstimation may be attributed to the lack of solubility shown by the polymers due to their mixed hydrophobic and hydrophillic natures.

2.5: Conclusions

In this section we were able to report the successful modification of the polymer PEI to produce four novel polymers for use as gene delivery agents, namely, palmitoyl-PEI (P-PEI), Palmitoyl-PEG-PEI (PP-PEI), quaternary ammonium PEI (QPEI) and quaternary palmitoyl PEI (QP-PEI). Similar modifications have previously been made to PEI, through attachment of hydrophobic side chains or quaternisation of the polymer, although no reports have been made to their use as gene delivery vectors and no reports exist of hydrophilic and hydrophobic modifications made to the same polymer batch. The modifications made to each of the polymers were confirmed through a variety of analytical techniques. NMR and FTIR analysis were used to confirm the structural characteristics of each of the polymers. A TNBS assay and elemental analysis of the polymers were used in conjunction with the spectroscopic data to measure the degree of modifications made during the synthesis and the resulting available sites for DNA binding. The molecular weight of the modified polymers was also measured through GPC analysis although when compared to the calculated Mw values the measured values were shown to be overestimated. The analysis of QPEI and QPPEI proved to be difficult due to the presence of tertiary amines. Future work could focus on the use of exhaustive quaternisation techniques to overcome this.

The detailed analysis shows that the modified polymers are structurally different (Table 14) to the parent PEI polymer, with varying degrees of

modification. These modifications should provide interesting changes to the physical and biological behaviour of the modified polymers.

Chapter 3: Physical Characterisation of Polymer/DNA complexes

3.1: Introduction

3.1.1: DNA Condensation.

DNA exists in aqueous solutions in linear, circular or supercoiled formations, which can all be approximated by a random coil structure or a rigid worm-like structure [21]. A random strand of DNA can occupy between 10^3 and 10^6 times the physical volume of the condensed coil and is therefore too large to access into its biological location, unless there is some kind of condensing or binding process taking place [22]. The volume in which DNA molecules occupy can be reduced up to a million fold, by condensing the DNA. Molecules of DNA of sizes varying from 400 to 40,000 base pairs and longer have been condensed by multivalent cations (hexamine Co^{3+}, La^{3+}) [129], positively charged polyelectrolytes (polylysine) and polycations (spermidine $^{3+}$) [129, 130].

The effect of DNA condensation can be accounted for by known and calculable free energies such as mixing, bending, hydration and electrostatics [129]. The most dominant of these forces is electrostatics, as the condensation of DNA cannot take place unless 90% of the DNA phosphate charge is neutralised.

Most condensation procedures result in similarly shaped complexes, such as doughnut shaped toroids or rods [129]. Only the very smallest of DNA

segments cannot be condensed into the aforementioned structures, but tend to form amorphous aggregates [129]. This requirement for a minimum DNA length can be explained by the requirement for nucleation. If the nucleus is an intermolecular dimer, the number of interactions required to stabilise the dimer at a low concentration of DNA is inadequate below a few hundred base pairs. This is because the DNA molecules are too short to provide the free energy required for condensation, therefore the nucleus will be unstable and unable to add more molecules to build a complete condensed particle.

The structure of complexes produced from cationic polymer DNA condensation is dependent upon the polymer structure rather than the DNA structure [91]. The size of the polymer/DNA complex was found to be linked to the concentration of DNA used in the formulation of the complexes i.e. the complex size was increased with an increase in the concentration of DNA [22].

The condensation efficiency of cationic polymers was shown to be affected by molecular weight and structure. High molecular weight polymers such as polylysine (27KDa), PEI (25KDa), intact and fractured dendrimers were all able to condense plasmid DNA, producing small toroids of 40 to 60nm in diameter [88]. Although the condensation efficiencies of the polymers proved to be similar, the transfection efficiencies extended across a large range.

To measure the condensation efficiency of the modified polymers we used an Ethidium bromide exclusion method as described by Brown *et al* (2000) [67]. Ethidium bromide (Figure 47) has a strong affinity to bind to DNA at a site called the 'fluorescence' site. When bound at this site a large and specific increase in the fluorescence of ethidium bromide is observed [131]. When a cationic polymer condenses DNA, the numbers of sites available for ethidium bromide binding are greatly reduced. By measuring the reduced fluorescence of the condensed DNA compared to the fluorescence of free DNA, the condensation efficiency of the polymers can be measured.

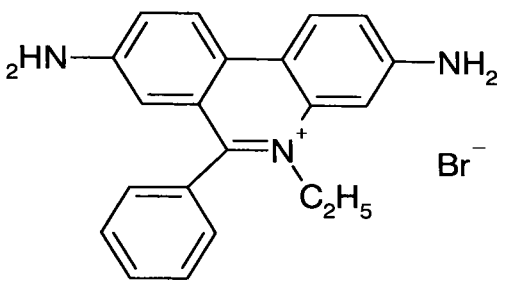

Figure 47: Chemical structure of ethidium bromide (3, 8-diamino 6-phenyl-5-ethylphenanthridinium).

3.1.2: Photon Correlation Spectroscopy

Photon Correlation (PCS) is a measurement of Brownian motion and the relation of this measurement to the size of a particle [132, 133]. Brownian motion is the random movement of particles due to the bombardment by the solvent molecules that surround them. The size of a particle may be calculated using the Stokes-Einstein equation [132, 134];

$$d(H) = \frac{kT}{3\pi\eta D}$$

Where, d (H) = hydrodynamic diameter, D = Diffusion coefficient, K = Boltzmann's constant, T= Absolute temperature and η = Viscosity.

The larger the size of a particle, the slower its Brownian motion will be [135]. The velocity of a particle can be defined by a property known as the diffusion coefficient. The measured diameter in PCS is referred to as the hydrodynamic diameter, as it is the diffusion of a particle in a fluid, which is being measured [136, 137]. The diameter that is obtained is the diameter of a sphere that has the same translational diffusion coefficient as the particle.

PCS instruments are equipped with a monochromatic coherent Helium-Neon Laser with a fixed wavelength of 633nm. This laser is used as a light source, which converges to a minimum size in the sample by means of a focusing lens [137]. The scattered light is detected by a photomultiplier. Fluctuations

in the intensity of scattered light are converted by a correlator. This generates the autocorrelation function, which is passed to a computer where the appropriate data analysis is performed [138] (Figure 48).

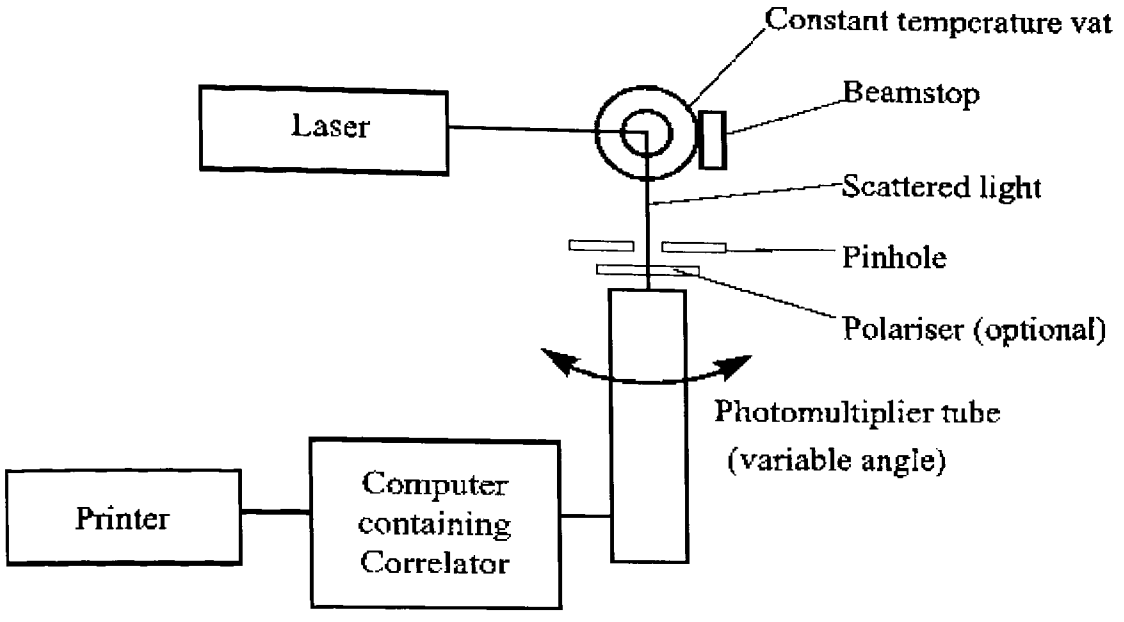

Figure 48: Schematic representation of Photon Correlation Spectroscopy Instrumentation.

Many systems take measurements at a single angle (90°), which is sufficient for the interpretation of the size distribution. However certain sizes of a particle will have a scattering intensity minimum at 90^0 and the reduced signal to background ratio will increase the measurement error [138]. In these cases measurement at second angle will improve the results. Using the maxima and minima in the intensity versus angle diagram enhances the detection of particle sizes in these circumstances.

Illumination of the sample cell results in a speckle pattern [139] (Figure 49). The pattern is stationary in both size and position as the whole system is stationary. The sections of light in the pattern are where the light is scattered from the particles, arrives with the same phase and interfere constructively to form a bright patch. The dark spaces are the additions of the scattered light, which are mutually destructive and cancel each other out.

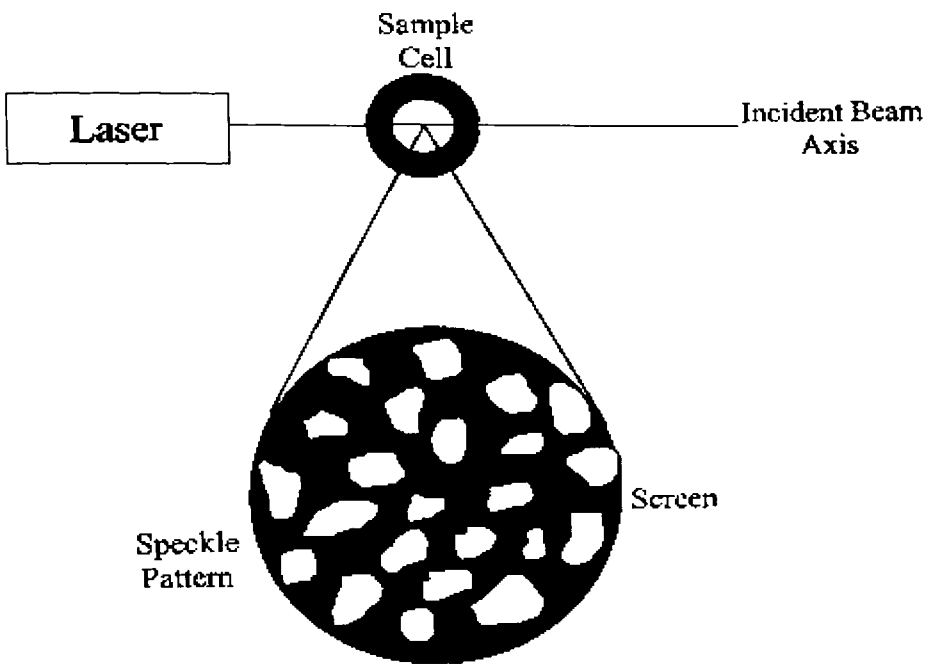

Figure 49: Schematic representation of a speckle pattern.

For a system of particles undergoing Brownian motion, a speckle pattern is observed where the position of each speckle is seen to be in constant motion. This is observed because the phase addition from the moving particles is constantly evolving and forming new patterns. The rate at which

the intensity fluctuations occur will depend on the size of the particles [139]. Smaller particles cause the intensity to fluctuate more rapidly than the large ones. These intensity fluctuations are detected with the use of a coherent detector. In any one instant a single speckle of light could be in view and could change to a dark space in the next instant. This change gives rise to a large fluctuation in the observed scattering intensity [139]. A photomultiplier whose aperture is of the same order as the size of one speckle can be described as coherent.

The spectrum of frequencies contained in the intensity fluctuations, which arise from the Brownian motion of particles, can be measured using a digital correlator [137]. A correlator is a signal comparator, which measures the degree of similarity between two signals, or one signal with itself at varying time intervals. Comparing the intensity of a randomly fluctuating signal, with itself at a point in time and then at a later time, there will be no correlation between the two signals. Correlation between the two signals will only occur if the time between sampling points is extremely small i.e. in milliseconds. As this sampling time increases the correlation will decrease with time until there is no correlation. Large particles change slowly with time and therefore correlation will decrease slowly. Smaller, faster moving particles cause the correlation between signals to decrease more quickly [137].

The correlator decides upon the length of the sample time used to sum a number of photon pulses. The incoming pulses are counted by an input

counter, and at the end of each sample time, the total count in that sample time is passed into a shift register, the contents of which are moved along by one channel. To make room for this information the contents of the last channel 'fall off the end' and are discarded. The count in the first shift register channel is then multiplied by the count in each of the other shift register channels in turn, each product being added to the appropriate store channel. The total count in the next sample time is treated in the same way and so on [138].

The z-average or harmonic intensity averaged particle diameter, can be obtained from the correlation function, by using various algorithms [140]. The PCS software offers several algorithms. Monomodal (Cumulants Analysis) allows the calculation of the z-average diameter and the polydispersity of distribution only, the log of the correlation function G is plotted against time and the slope of the fitted line is related to the z-average particles size. Multimodal analysis allows for exponential sampling, with a medium resolution and is used for samples with differing size populations. CONTIN analysis is most suitable for smooth distributions, with a low resolution. NNLS (non-negative least square) is based on a standard textbook algorithm and provides the highest resolution of all the algorithms. The choice of algorithm depends upon the type of information required and which algorithm gives the most reproducible results from repeat sets of data.

3.1.3: Zeta Potential Analysis

Zeta potential is an important parameter in the characterisation of the polymer/DNA complexes. The charge of a complex can help define how a complex will act in both *in vitro* and *in vivo* situations. Zeta Potential (ζ) is the measurement of the surface charge density of a particle, and can be affected by both the pH and the salt content of the medium of choice. The use of electrophoresis in a capillary cell to measure zeta potential is a long-standing technique. Better quality data can be achieved from using the stationary layer technique to take measurements. However, when using the stationary layer technique there are a number of practical considerations that have to be taken into account, which can result in a loss of potential accuracy and resolution. When particles with a net charge are placed in an electric field, they will migrate towards the electrode with the opposite charge. This movement is termed electrophoresis (Figure 50) [141]. The terminal velocity of micron-sized particles is reached in a matter of microseconds, due to their low inertia. The velocity of the particle is determined by the associated charge (zeta potential), the viscosity of the medium and the applied field. The velocity in a field of 1 volt/cm is known as the particle mobility. The zeta potential can be calculated from this value using the Henry equation [142].

$$\varsigma = \frac{4\pi\eta\mu e}{\varepsilon}$$

where, ζ = zeta potential, μ_e = electrophoretic mobility, η = viscosity, å = dielectric constant.

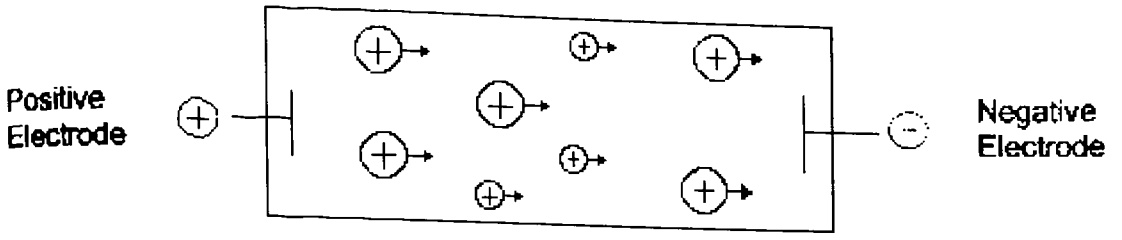

Figure 50: Electrophoresis of charged particles.

Electro-osmosis is the movement of liquid containing ions, next to a charged surface when a field is applied along the surface (Figure 51) [143]. In a quartz cell the velocity of the electro-osmotic flow is the same order of magnitude as the particle mobilities that are being measured. This flow takes in the region of 10's of milliseconds to establish, much longer than electrophoresis.

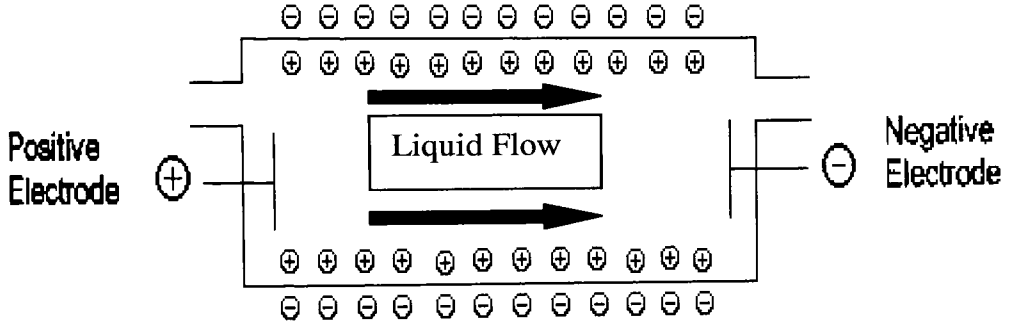

Figure 51: Electro-osmosis of ions through an open cell.

In a capillary, which is closed at both ends, the liquid flow along the cell wall returns through the centre of the cell. The true particle mobility can be found by measuring particle mobility at the point where the fluid flow along the cell

wall cancels out with the return flow in the centre of the cell (Figure 52) [144].

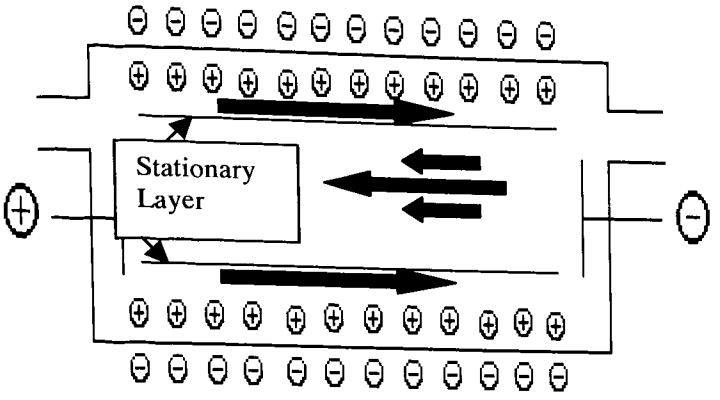

Figure 52: Stationary layer in a closed cell.

This position is called the stationary layer or the stationary level. The use of this method can give increased resolution and accuracy [145].

By avoiding electro-osmosis, at any point in the cell the mobility of the particles would give the true mobility. Neutralising or shielding the charge on the cell walls with a coating can achieve this effect, but this method is difficult to apply and lasts for only a few measurements at most. Another method is fast field reversal (FFR). This method reverses the applied field rapidly enough that electro-osmosis becomes insignificant. Use of this technique gives an accurate mean, but has a resolution lower than that of the standard stationary layer method [145].

An alternative method is the Mixed Mode Measurement technique [146]. This method combines the best properties of both stationary layer and FFR techniques in a capillary cell. The mixed mode measurement gives improved

resolution, an insensitivity to cell alignment and reduced sensitivity to cell wall contamination. An additional feature is that the zeta potential of the cell wall can be measured. The mixed mode measurement consists of both slow field reversal and fast field reversal measurements [146]. The technique uses a new cell that positions the measurement zone in the middle of the cell, rather than at the stationary layer. As the measurement zone is further from the cell wall, there is a reduction in flare from the nearby surface. The alignment of the cell becomes less important, and the cell wall charge can be calculated.

An FFR measurement is performed at the cell centre, which gives an accurate determination of the mean value. A zero field measurement i.e. particle mobility is measured without a charge being applied, is then performed in order to measure the effect of Brownian motion broadening. Finally a slow field measurement is made. This measurement increases the resolution although the electro-osmosis effect shifts the mobility values. The mean zeta potentials can be calculated from the FFR measurements and the electro-osmotic flow can be determined by subtracting the slow field reversal measurements. This value can then be used to normalise the slow field reversal distribution and the electro-osmosis value is used in the calculation of the cell wall zeta potential [146].

3.1.4: Electron Microscopy

Most Transmission Electron Microscopes (TEM's, Figure 53) use a thermonic triode electron gun, which produces an intense beam of high-energy electrons that are directed down the microscope column [147]. This electron beam is focused down to a small spot by means of a series of deflector coils and condenser lenses. The beam is projected onto the specimen in such a way that the illuminated area and the convergence angle can be controlled. Particular groups of electrons can be selected by the operator to contribute to the final image. The specimen image is then projected onto a fluorescent screen for recording [148].

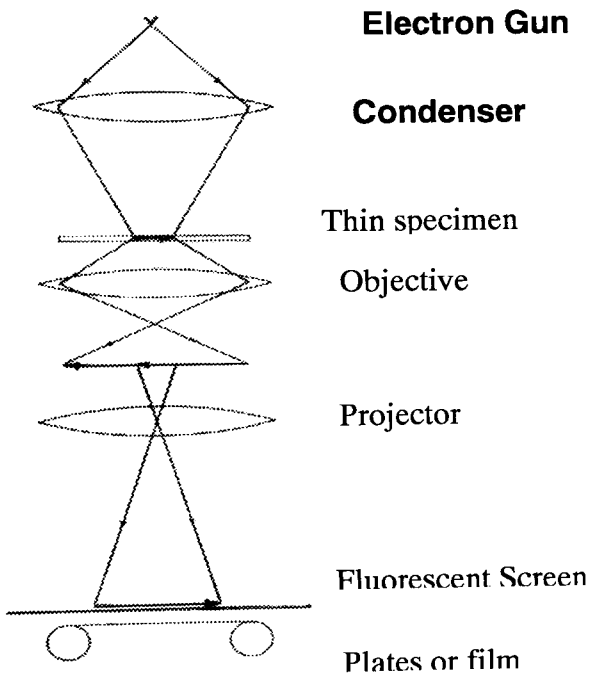

Figure 53: Schematic diagram of the major components of the optical system in a Transmission Electron Microscope.

Negative Staining of Samples

A heavy metal salt solution is applied to the specimen grid and the solution dries down around the specimen [149]. As a result the specimen itself remains electron-translucent whilst its immediate surroundings do not. Typical negative-staining solutions are uranyl acetate (1-4% w/v), phosphotungstic acid (1-2% w/v) and uranyl formate (1-4% w/v). A drop of the particle suspension is usually pippeted onto a support film. The particle suspension is mixed with the staining solution before applying to the film.

3.2: Methods and Protocols

3.2.1: DNA Condensation

40μl of Ethidium bromide (10mg/ml) was transferred to a 1L volumetric flask. The flask was then made up to the mark with distilled water, to give a final concentration of 0.4μg/ml.

Various polymer solutions were prepared as described in section 3.2.2. The concentration of DNA solution was set at 100μg/ml. 250μl of polymer solution was added to 250μl of DNA solution to give 500μl of the final complex.

Ratio of Polymer/DNA (w/w)	Concentration of Polymer Solution
40:1	4mg/ml
20:1	2mg/ml
10:1	1mg/ml
5:1	0.5mg/ml
2.5:1	0.25mg/ml
1:1	0.1mg/ml

Table 15: Ratios of Polymer/DNA complexes used in DNA condensation.

50μl of complex solution was added to 950μl of Ethidium bromide solution in a 1ml fluorescence cuvette and the fluorescence measurement was read immediately. Measurements of each solution were taken at time intervals of 0, 1, 2, 4, 6, and 24hours ($\lambda_{excitation}$ = 526nm, $\lambda_{emission}$ = 592nm, Perkin-Elmer LS-50B spectrofluorimeter, Perkin-Elmer, UK). Complex solutions were left at room temperature between measurements.

The results are expressed as Relative units (RU), where RU = Measured intensity/Intensity of DNA Blank. The DNA blank consisted of 25μl Dextrose + 25μl DNA solution + 950μl Ethidium Bromide.

3.2.2: Photon Correlation Spectroscopy

Optimal Polymer/Cholesterol Ratios.

10mg of either PP-PEI or QPPEI was sonicated with varying amounts of cholesterol in 2ml of 5% Dextrose solution, using a probe sonicator (3 x 2min). The sample was packed in ice during probe sonication to prevent overheating.

Preparation of polymer solutions

P-PEI, PP-PEI and QPPEI were probe sonicated (3 x 2min) in a 5% dextrose solution. The sample was packed in ice during probe sonication to prevent overheating. Both P-PEI and QPEI were water-soluble and were dissolved in a 5% dextrose solution.

Preparation of Polymer/DNA complexes

A volume of the DNA solution was slowly added drop wise to an equal volume of polymer solution.

Preparation of DNA Solutions

The plasmid (pCMV sport β-gal) was grown in E.coli and the plasmid was purified using a QIAGEN Endotoxin free Giga Plasmid kit (QIAGEN, Hilden, Germany) according to the manufacturers instructions. The purity of the plasmid was confirmed by agarose gel electrophoresis.

Sizing of Polymer/DNA Complexes

The sizes of the polymer/DNA complexes were measured using a Malvern Zetasizer 3000 (Malvern Instruments, UK). All measurements were performed at 25^0C, using CONTIN analysis. Before each measurement, standards (polystyrene latex beads, 300nm, Sigma Co., UK) were run. All z-average data obtained from the standards agreed with that stated by the manufacturer.

3.2.3: Zeta Potential Analysis

All polymer/DNA complexes were prepared as described in section 3.2.1. The zeta potentials were determined using a Zetasizer 3000 (Malvern Instruments, UK). Sampling time was set at 30 seconds, with 3 measurements per sample. The viscosity of the disperse phase was set at 0.893 Centipose and the dielectric constant was 79. All measurements were performed at 25°C. At the start of each measurement, standards (Malvern Zetasizer standard, Malvern Instruments, UK) were run. All zeta potential data obtained from the standards agreed with that stated by the manufacturer.

3.2.4: Electron Microscopy

The electron microscopy of the polymer/DNA complexes was performed using negative staining. Droplets of the complexes were mixed in equal volumes with 1% uranylformate on a specimen support grid and immediately dried down using filter paper. The negatively stained samples were then imaged on a LEO 902 energy-filtering electron microscope at 80kV

3.2.5: Materials

Material	Supplier
Cholesterol	Sigma, UK
Dextrose	Sigma, UK
Endotoxin free Giga plasmid kit	Qiagen, Germany
Ethidium Bromide	Sigma, UK
Polystyrene latex beads	Sigma, UK
PCMV Sport β-Gal plasmid	Life Technologies, UK
Uranyl formate	Sigma, UK
Zetasizer Standard	Malvern Instruments, UK

Table 16: List of materials

3.3: Results

3.3.1: DNA Condensation

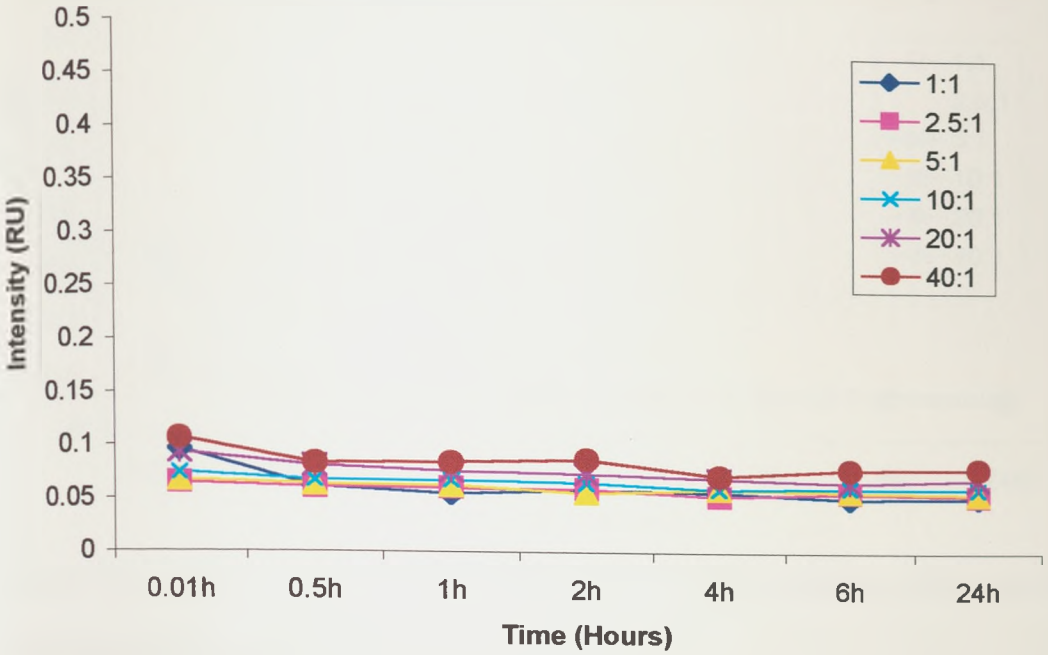

Figure 54: DNA Condensation of P-PEI at different polymer/DNA ratios.

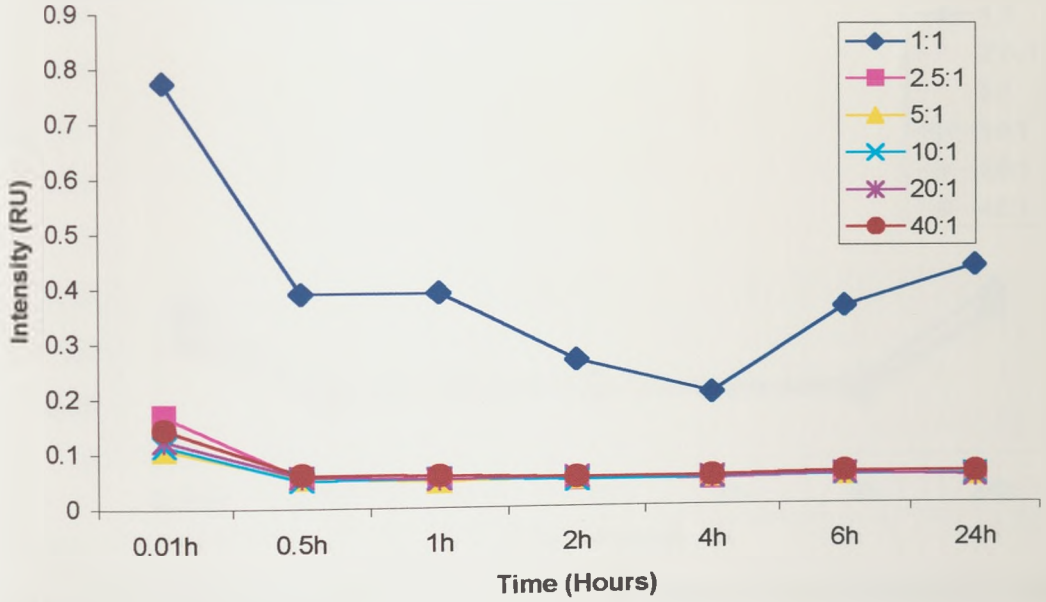

Figure 55: DNA Condensation of PP-PEI at different polymer/DNA ratios

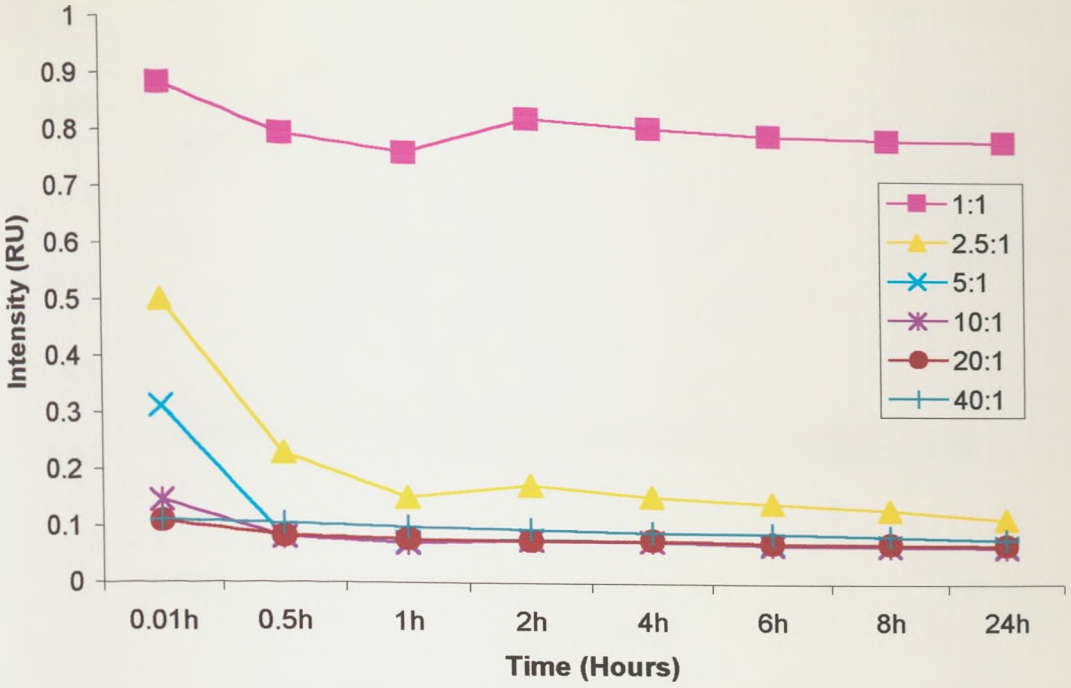

Figure 56: DNA Condensation of PP-PEI/Cholesterol (2:1, w/w) at different polymer/DNA ratios.

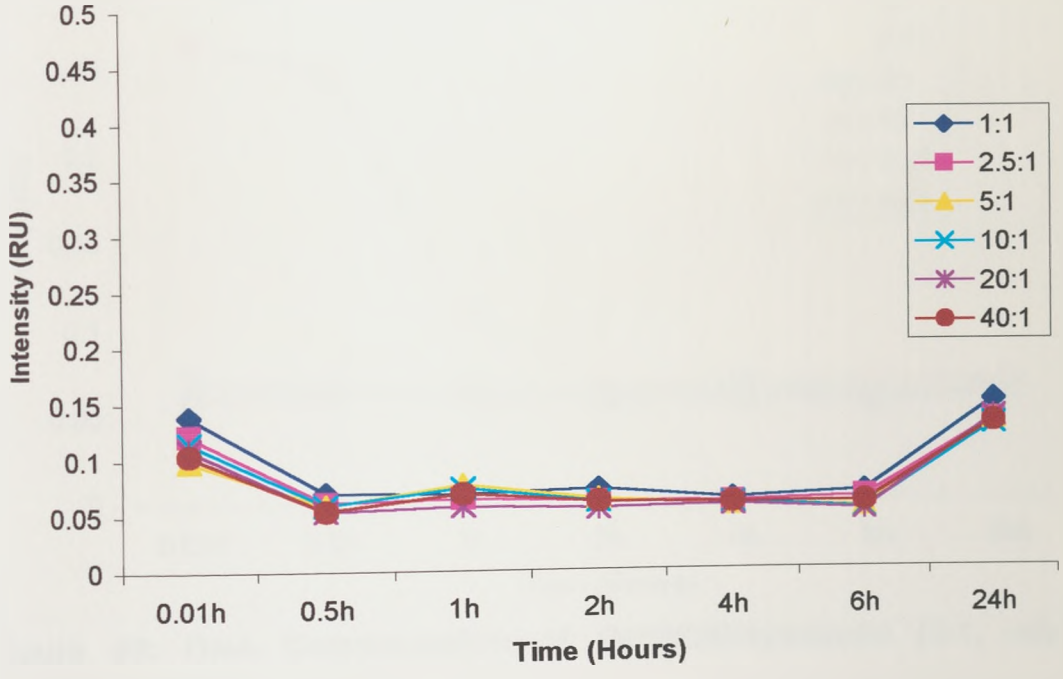

Figure 57: DNA Condensation of QPEI at different polymer/DNA ratios.

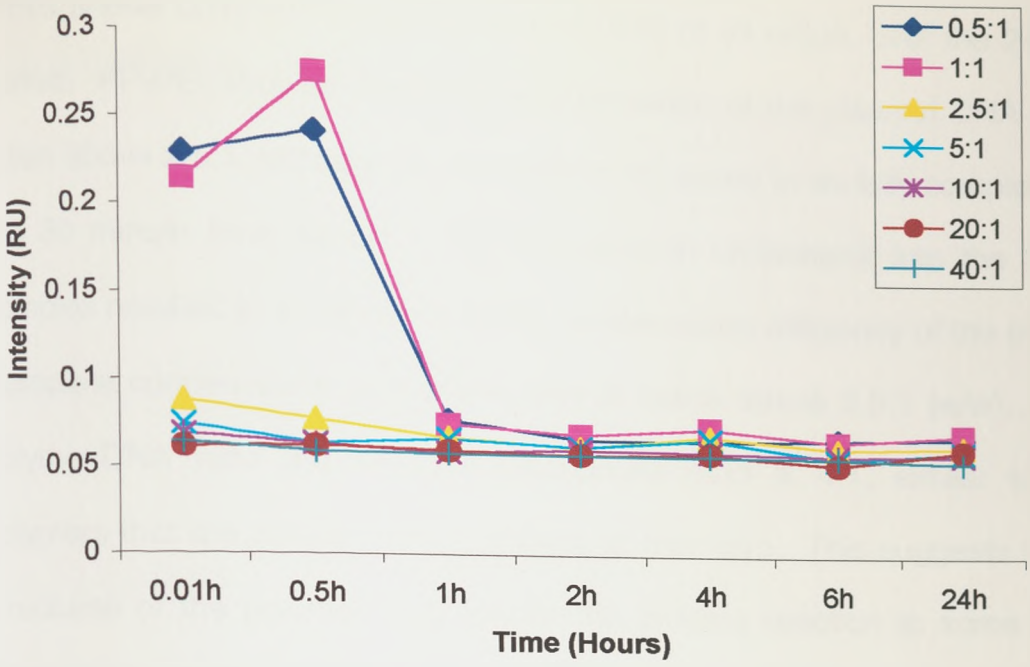

Figure 58: DNA condensation of QPPEI at different polymer/DNA ratios.

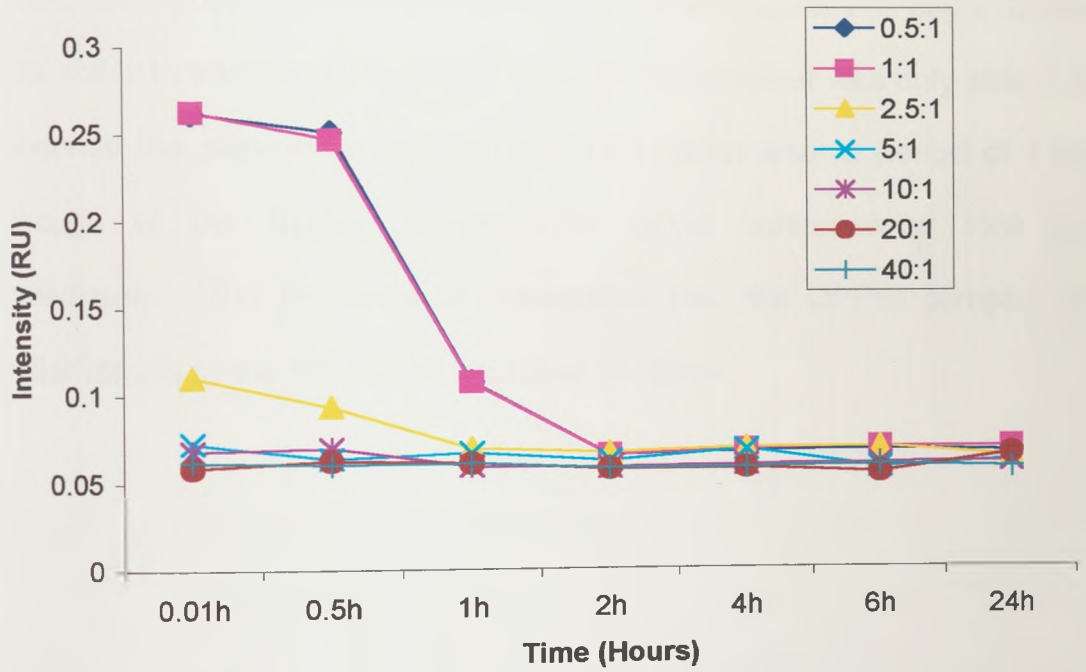

Figure 59: DNA Condensation of QPPEI/Cholesterol (2:1, w/w) at different polymer/DNA ratios.

P-PEI shows complete condensation of DNA at all ratios, over the 24h time period. PP-PEI showed complete condensation of the plasmid DNA only at ratios above 2.5:1, although condensation appeared to be fully complete after the 30 minute time period. The inclusion of cholesterol into the PP-PEI complex resulted in a decrease in the condensation efficiency of the polymer. Complete condensation took place only at ratios above 2.5:1 (w/w). At this polymer/DNA ratio the nitrogen phosphate ratio is 4:1, similar to other polymers that are able to fully condense at this ratio. This suggests that the structures of the polymer may hinder the binding reaction to some extent. The QPEI polymer was able to completely condense the plasmid at all the ratios tested, although there seemed to be a slight decrease after the 6h period. The quaternisation of the P-PEI polymer results in a slight decrease in its ability to condense the DNA. The QPPEI polymer was only able to fully condense the plasmid at the ratio of 0.5:1 (w/w) after a period of 1 hour, although at the higher polymer/DNA ratios condensation took place immediately. The presence of cholesterol into the QPPEI complex gave similar results to the PP-PEI/Cholesterol complex.

3.3.2: Photon Correlation Spectroscopy

Optimal PP-PEI/Cholesterol Ratio

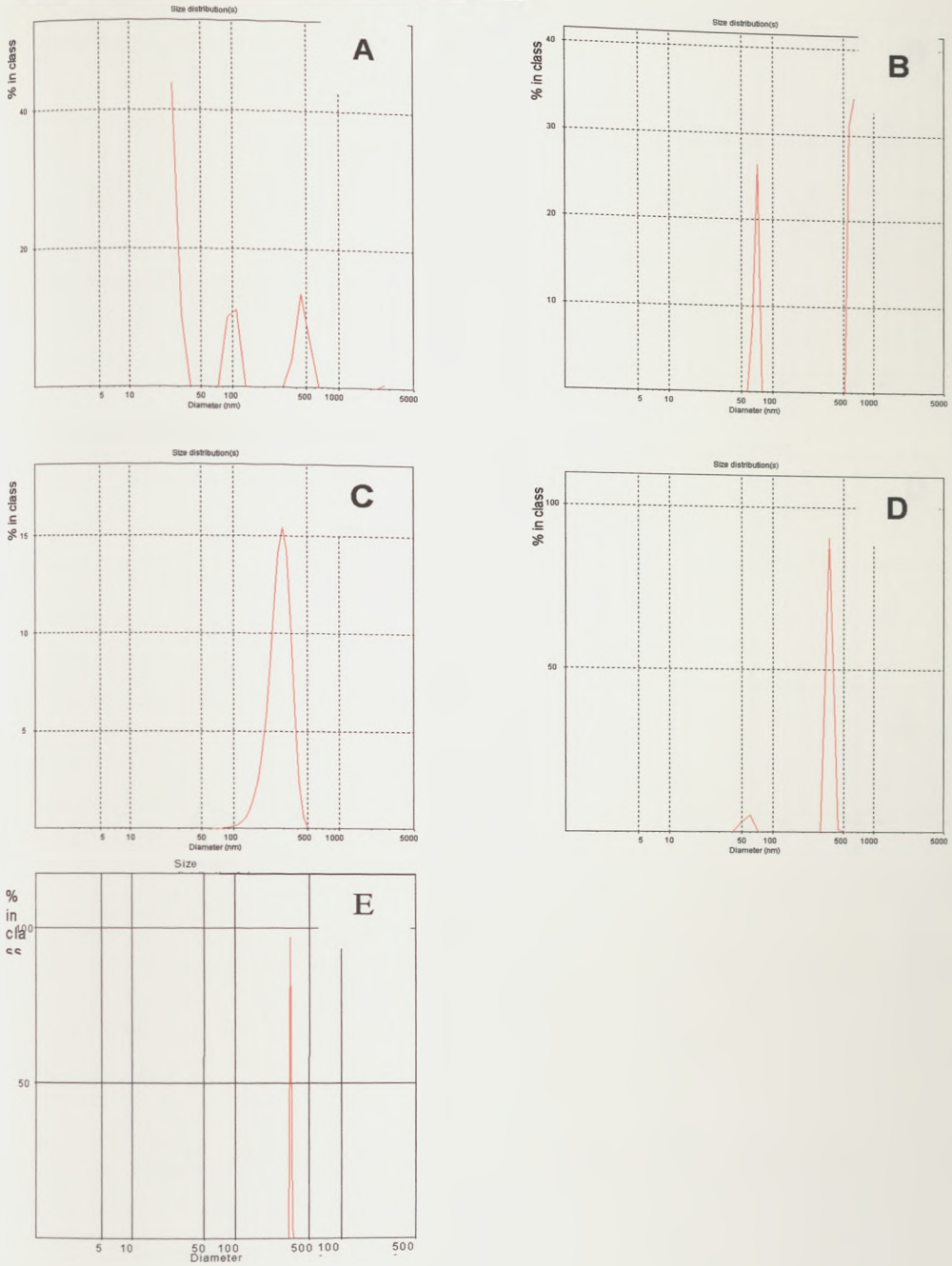

Figure 60: Intensity size distributions of PP-PEI (10mg) with varying amounts of cholesterol. A: 1mg, B: 2mg, C: 3mg, D: 4mg, E: 5mg

Optimal QPPEI/Cholesterol Ratio

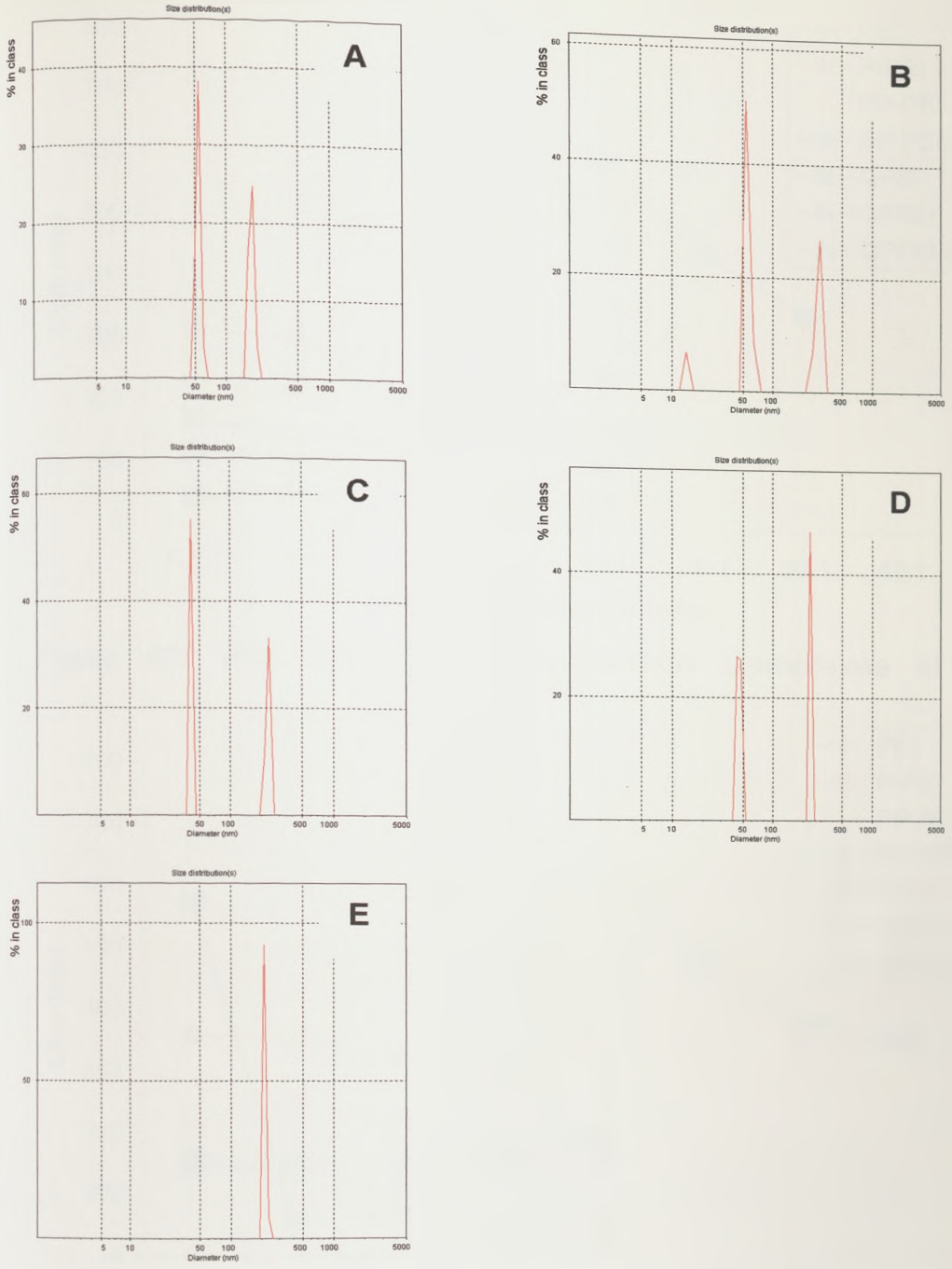

Figure 61: Intensity size distributions of QPPEI (10mg) with varying amounts of Cholesterol; A: 1mg, B: 2mg, C: 3mg, D: 4mg, E: 5mg

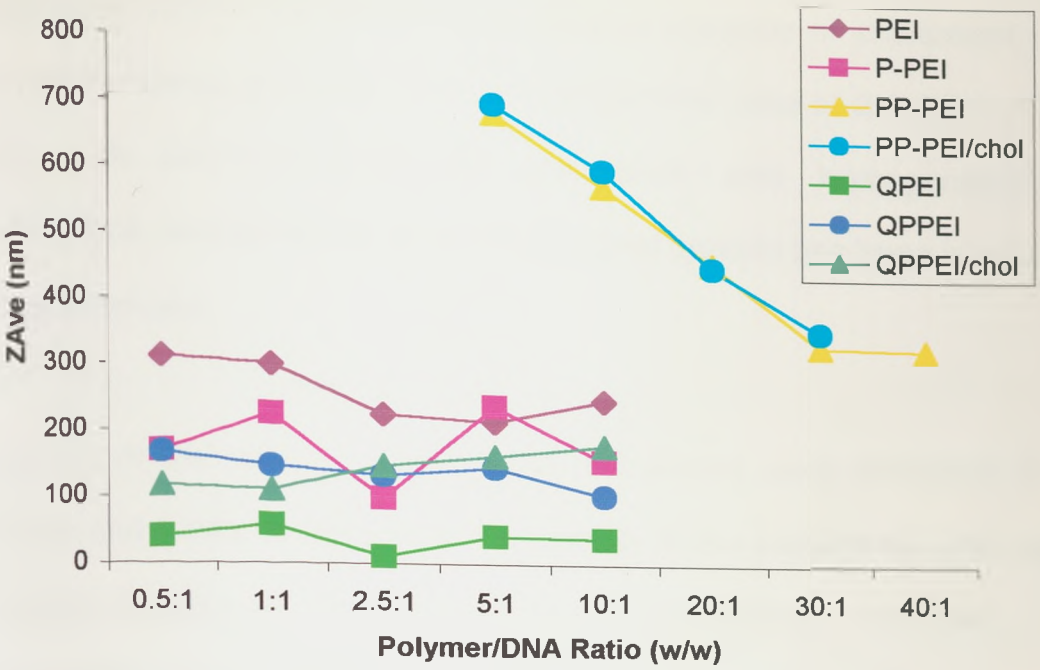

Figure 62: PCS Sizing of Polymer/DNA Complexes at T=0.05h.

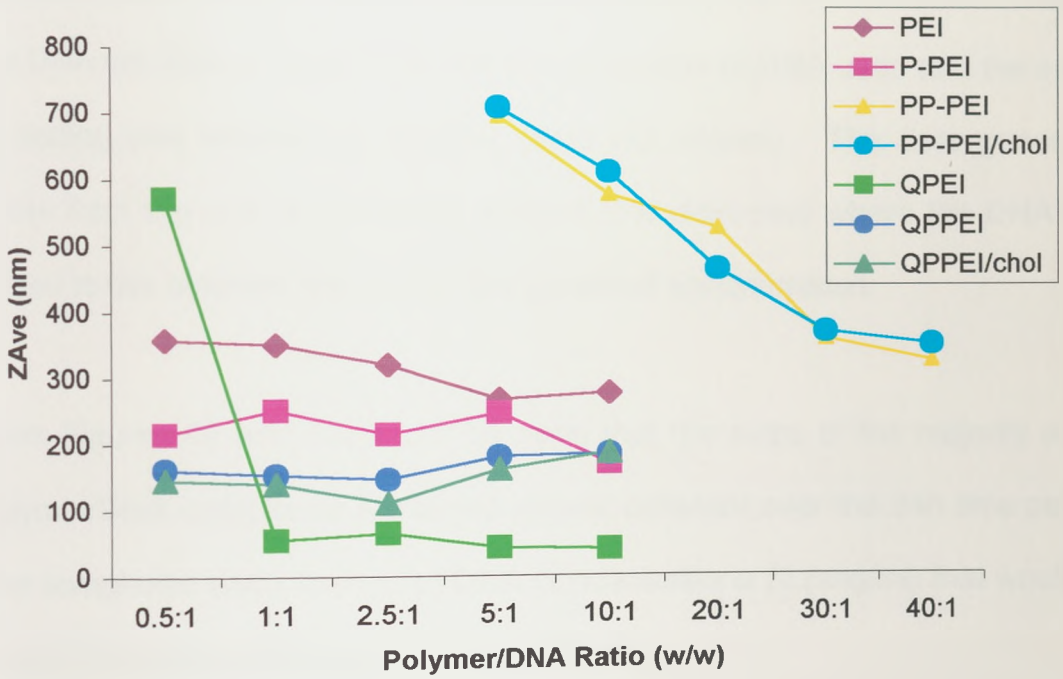

Figure 63: PCS Sizing of Polymer/DNA Complexes at T=24h.

Figures 60 and 61 show the intensity size distributions of PP-PEI and QPPEI probe sonicated in the presence of varying amounts of cholesterol. Both polymers showed an optimal polymer/cholesterol ratio of 2:1 (w/w). At this ratio both polymers produced complexes with homogeneous size distributions, indicating that all the cholesterol present has been incorporated into the complex.

The size of the various polymer/DNA complexes were measured at time t=0.05h and t=24h, to determine the stability of the complexes. The sizes of PEI/DNA complexes have been reported previously. The size of the complexes were found to vary considerably depending upon many factors such as, the choice of solvent, whether the polymer solution was added to the DNA solution or vice versa, the concentration of DNA used and the speed of adding one solution to another (data not shown). The data generated arose from the use of a specific solvent (5% dextrose) where the DNA was added to the polymer solution at the specified concentration.

From Figures 62 and 63, it can be seen that the sizes of the majority of the polymer/DNA complexes remained almost constant over the 24h time period. The complexes were formed at DNA concentrations (0.5mg/ml) that would be used for *in vivo* experiments (see chapter 4).

PP-PEI produced much larger complexes when mixed with DNA. The complex sizes ranged from ~700nm (5:1 w/w) to ~300nm (40:1 w/w). The

PP-PEI/DNA complexes decreased in size with an increase in the amount of polymer used in the formulation of the complexes. At the concentrations used in formulation, PP-PEI could only form stable complexes at ratios above 5:1. The PP-PEI/Cholesterol/DNA complexes produced similar results to the PP-PEI complexes, with no reportable differences in size.

Both QPPEI/DNA and QPPEI/Cholesterol/DNA complexes were found to be stable in size over the 24h period. The complexes were found to be similar in size over the different ratios and again the inclusion of cholesterol into the complex produces no reportable differences to the complexes not containing cholesterol. QPEI mixed with DNA to produce complexes with sizes of ~40nm. The complexes were shown to be stable over time, except at the ratio of 0.5:1 (w/w). After 24h the complex had increased in size from ~40nm to ~600nm.

3.3.3: Zeta Potential Analysis

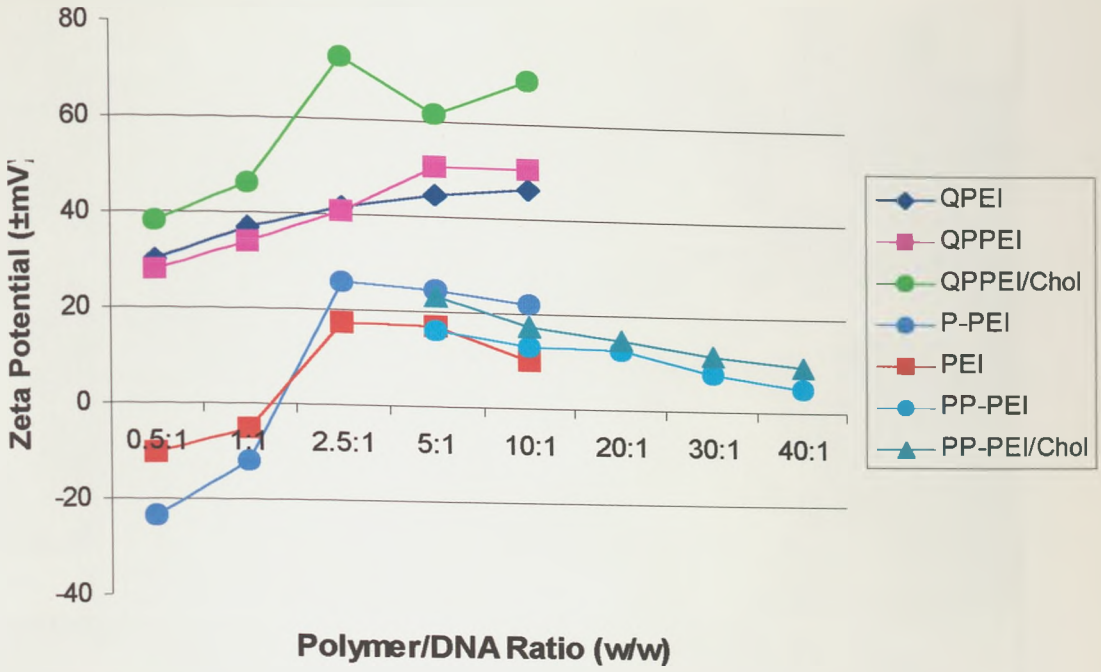

Figure 64: Zeta Potentials of polymer/DNA complexes (t=1h).

Polymer (1mg/ml)	Zeta Potential (mV)
QPEI	+50.8
QPPEI	+60.3
QPPEI/Cholesterol	+75.8
P-PEI	+30.5
PEI	+35.2
PP-PEI	+20.6
PP-PEI/Cholesterol	+27.8

Table 17: Zeta potential values for uncomplexed polymers in a 5% glucose solution.

3.3.4: Electron Microscopy Analysis

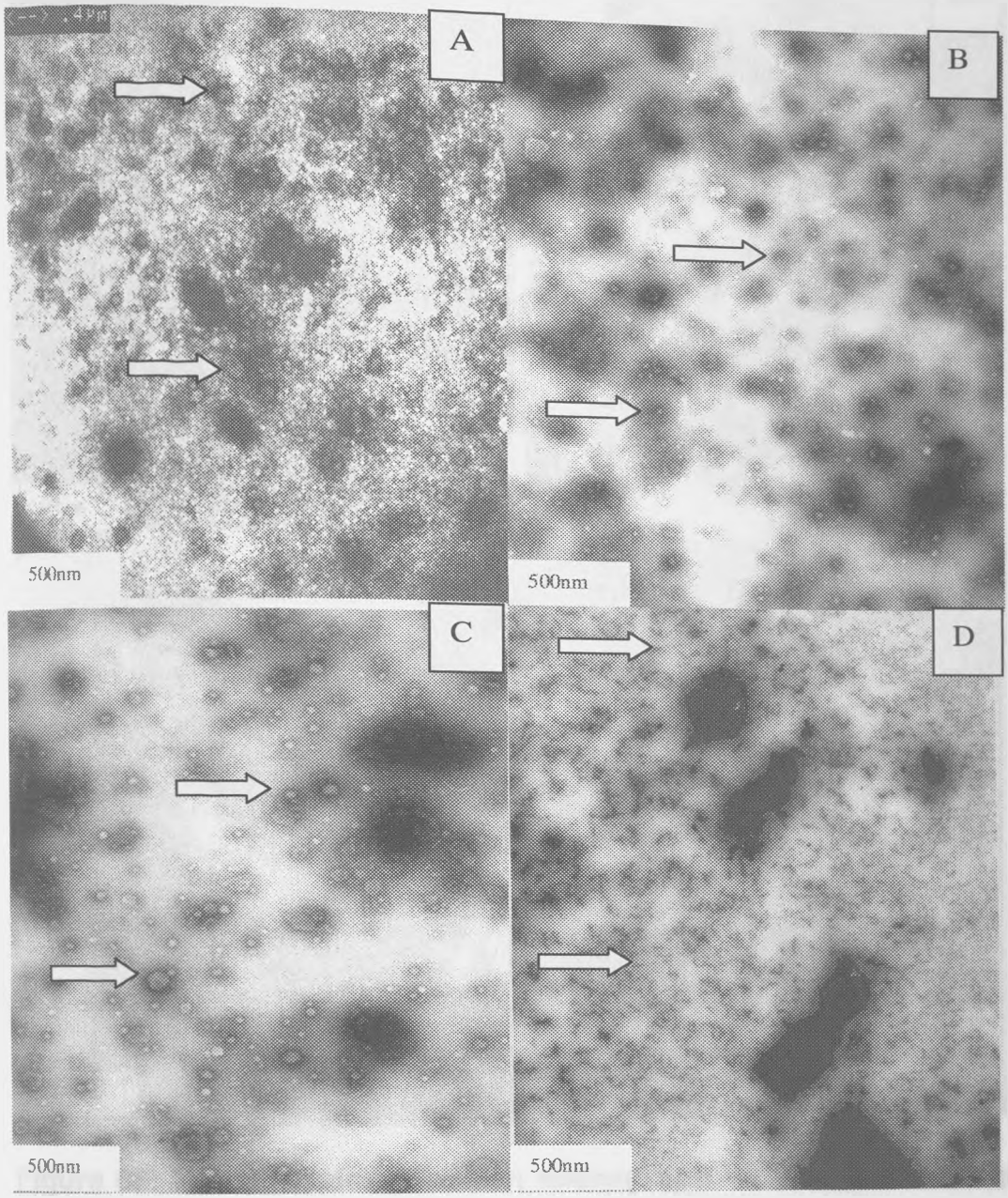

Figure 65: Transmission electron micrographs with negative staining of A: P-PEI vesicles, B: P-PEI/DNA complexes (2:1, w/w), C: P-PEI/DNA complexes (5:1, w/w), D: PP-PEI tubules (as indicated by arrows)

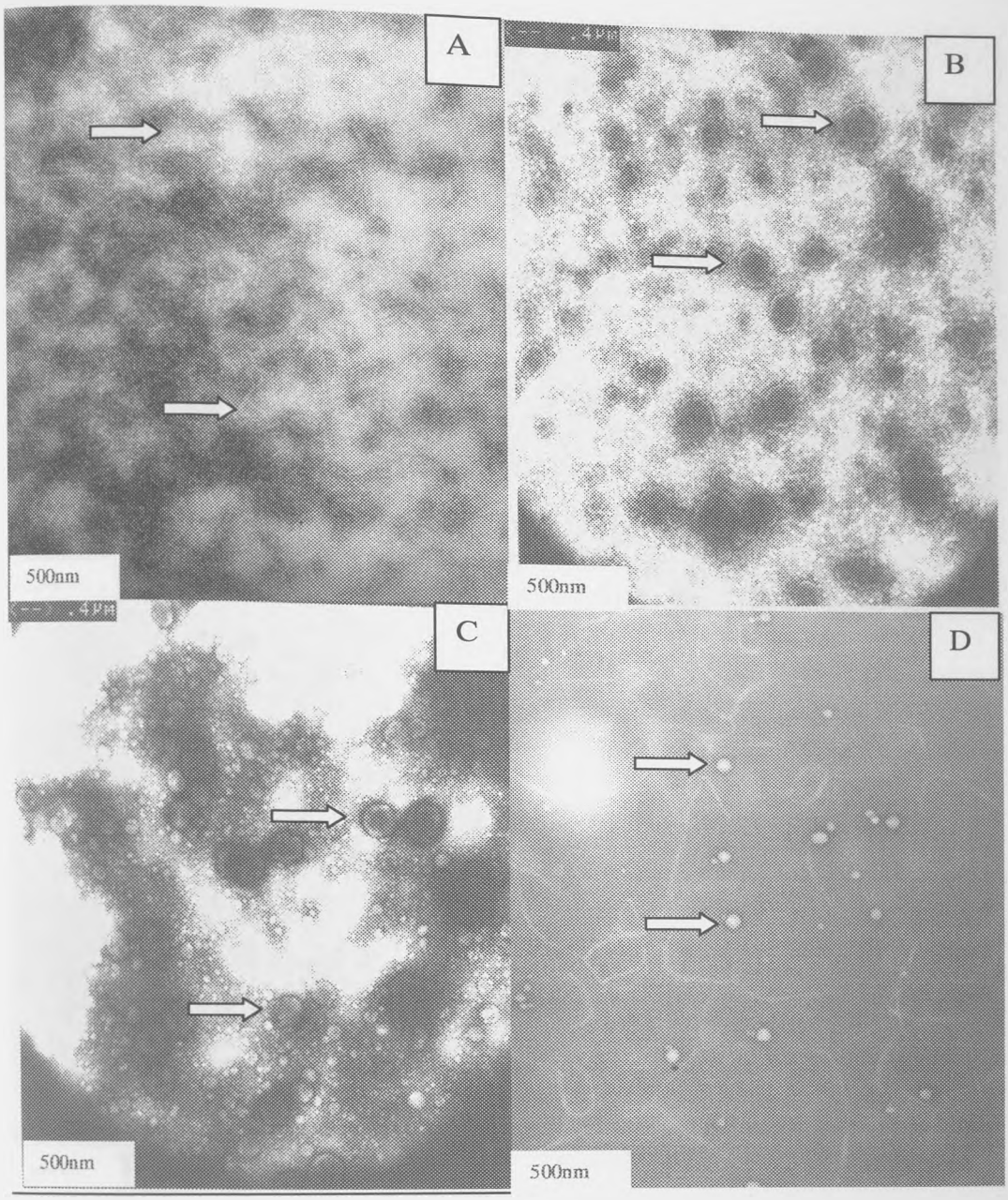

Figure 66: Transmission electron micrograph with negative staining of A: PP-PEI/DNA tubules, B: PP-PEI/Cholesterol vesicles, C: PP-PEI/cholesterol/DNA vesicles, D: QPEI/DNA complexes (as indicated by arrows)

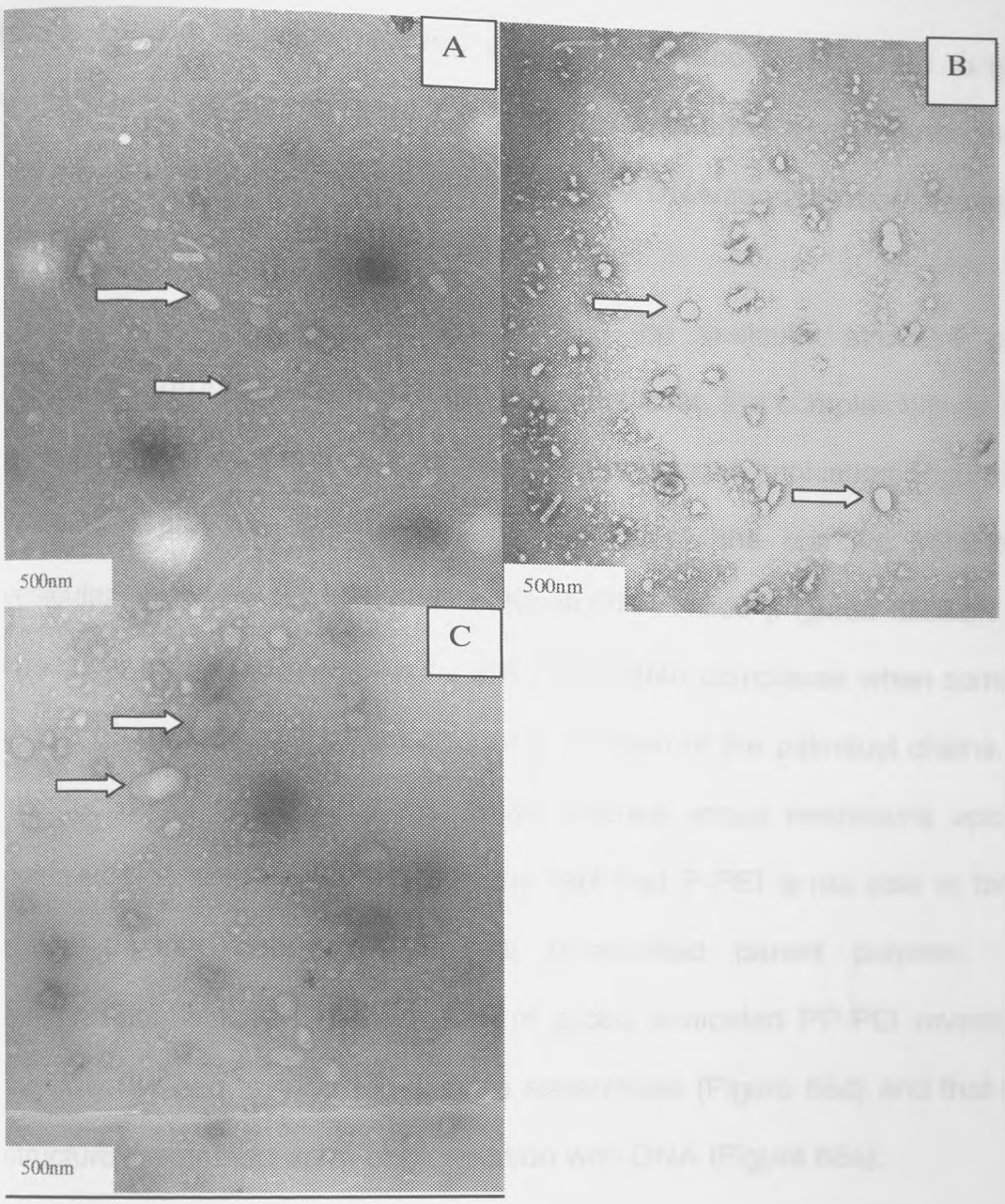

Figure 67: Transmission electron micrograph with negative staining of A: QPPEI/DNA complexes, B: QPPEI/cholesterol complexes, C: QPPEI/cholesterol/DNA complexes (as indicated by arrows)

In this section negative staining electron microscopy was used to give a physical view of the polymer/DNA complexes, in order to give further insight into the dimensions of the complexes and the DNA condensation process.

The negative staining technique shows the vesicular structure of the complexes through a stained interior and exterior, the complex bilayer is not stained. P-PEI was able to form vesicles upon probe sonication (Figure 65a). When the polymer was complexed with DNA the complex retained its vesicular shape, even at higher polymer/DNA ratios (Figures 65b&c). This change in morphology shown by the P-PEI/DNA complexes when compared to that of unmodified PEI is due to the addition of the palmitoyl chains. The introduction of these side chains will impose space restrictions upon the complexation process resulting in the fact that P-PEI is not able to form as tightly packed complexes as its unmodified parent polymer. The transmission electron micrographs of probe sonicated PP-PEI reveals that the polymer had formed tubular-like assemblies (Figure 65d) and that these structures remained upon complexation with DNA (Figure 66a).

The condensation of DNA with QPEI revealed that the polymer had formed tightly packed complexes, almost like solid spheres (Figure 66d), similar to that of the unmodified PEI [91]. The QPEI polymer contains only short sides chains that are not long enough to hinder its complexation with DNA, thus the formation of small tightly packed complexes. QPPEI also formed complexes that looked like flattened vesicles (Figure 67a). The presence of cholesterol

upon probe sonication of the polymer resulted in a heterogeneous mixture of shapes (Figure 67b). The formation of vesicular complexes proved to in the majority, although some rod-like shapes can be seen. Upon condensation of DNA, the polymer/DNA complex produced much larger vesicular complexes (Figure 67c). The inclusion of cholesterol could result in a strengthened bilayer resulting in the formation of vesicles, although this was not tested.

3.4: Discussion of Results

DNA Condensation

Despite the modifications made to the PEI polymer, all the modified polymers were able to condense plasmid DNA. The fact that some of the polymers take longer to reach complete condensation of the plasmid suggests that the binding process is governed by a kinetic component. The reduction in the number of available nitrogen's in the modified polymers shows that the binding process is not only governed by electrostatic forces but also a degree of twisting and bending by the plasmid DNA to reach those binding sites not readily accessible.

The inclusion of cholesterol in two of the formulations resulted in a reduction of condensation efficiency, with the lower polymer/DNA ratios taking longer to completely condense the plasmid DNA. The inclusion of cholesterol into the PP-PEI and QPPEI complexes may result in a reduction of the number of charge sites available for condensing the DNA, which would account for the decrease in condensation efficiency when compared to the polymers not containing cholesterol. We hypothesis that not all of the PEI nitrogen's are involved with the DNA binding process and may even be inaccessible to DNA (Figure 68).

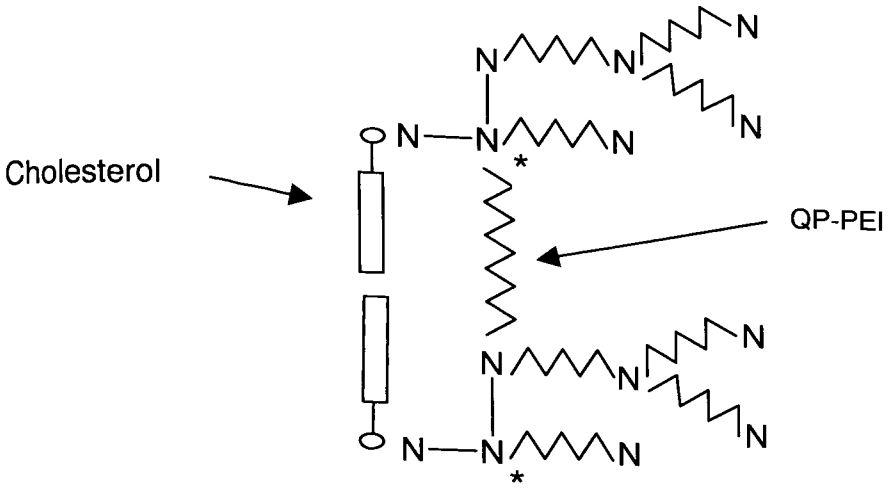

Figure 68: Schematic representation of cholesterol incorporated into the QPPEI formulation. The * represents possible sites that are inaccessible to DNA.

As the condensation of DNA is thought to controlled by electrostatic forces resulting from counter ion release, a minimum number of charge sites on the polymer are required to before condensation will take place. Several groups have shown that the minimum number of consensus polycations charges for DNA condensation number between six and eight [23, 150]. For branched PEI (25KDa), DNA has been shown to be fully complexed at a theoretical positive:negative (nitrogen:phosphate) charge ratio of ± 0.4.

The structure of the polymer involved also influences the DNA condensation procedure [91]. Polymers containing charge ratios that lie close to the polymer backbone are more efficient in the condensation of DNA and show increased stability to competitive displacement by anions.

This difference in morphologies can be explained through the different chemical structures of the polymers. The palmitoylation of PEI to produce P-PEI has resulted in a polymer that can self assemble into a vesicular structure upon ultrasonication. The vesicular structure of P-PEI was retained upon complexion with plasmid DNA. We hypothesis that the Palmitoyl chains of P-PEI form the bilayer of the vesicle, with the remaining free amine groups present on the vesicle interior.

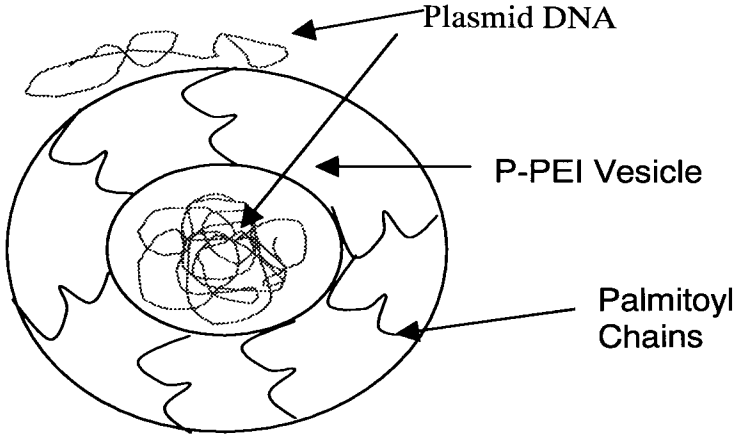

Figure 69: Schematic representation of the P-PEI/DNA vesicular complex.

The worm-like structures of the PP-PEI/DNA formulation may be formed through steric hindrance from the PEG chains. These chains may be present at the end of the tubule resulting in a stabilising effect at the high curvature ends of the molecule (Figure 70).

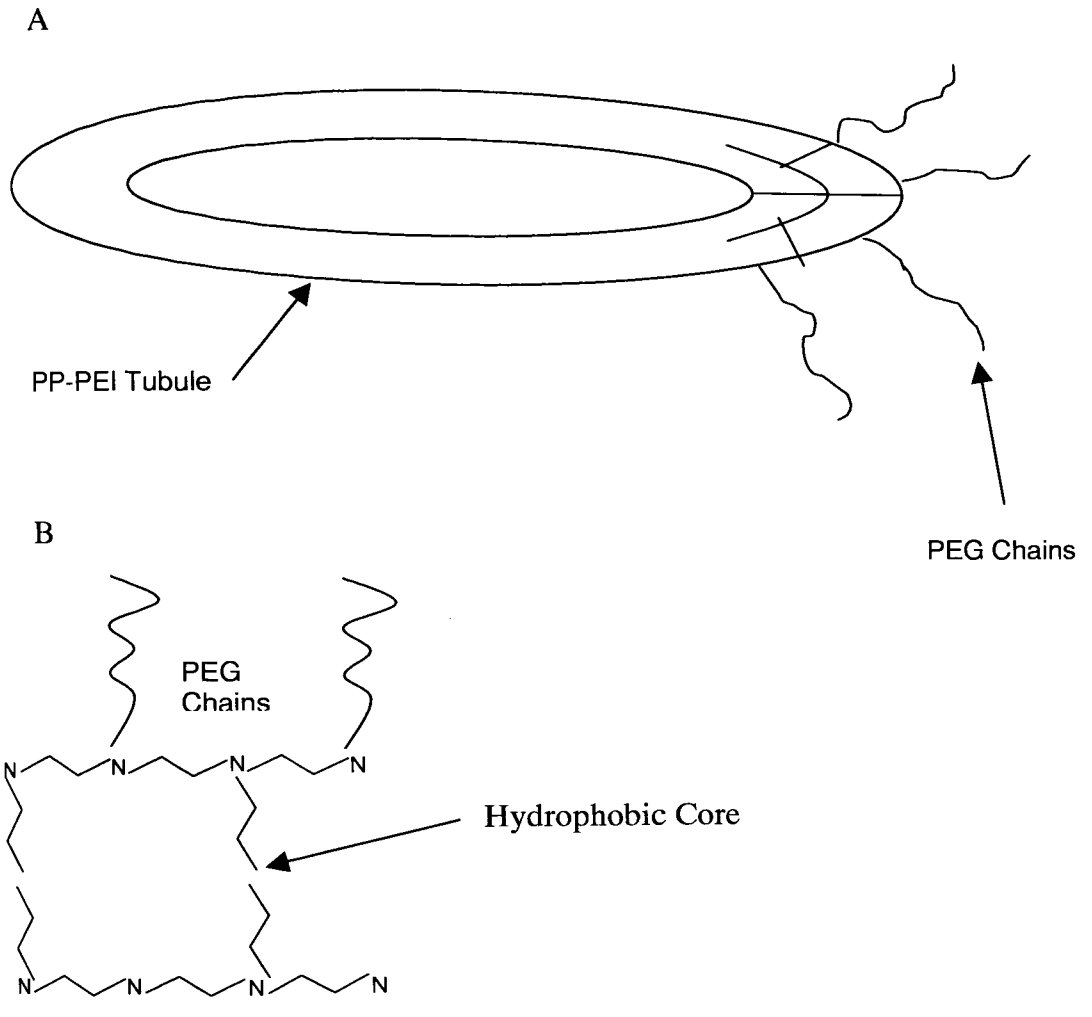

Figure 70: Schematic diagram of A: PP-PEI tubule and B: Section of PP-PEI tubule.

Erbacher and workers [151] have previously reported the properties of PEG conjugated PEI. Two PEI-PEG polymers were synthesised with 0.5 and 1.7% of their amine functions derivatised. Electron micrographs of the polymer/DNA complexes revealed 5-10nm thick polymeric strings around 50-100nm in length. This type of polymer crowding prevents both Van der Waals and electrostatic interactions of incoming molecules but also interferes with the compactness required for full DNA condensation. Similar structures have also been identified with polylysine-PEG block copolymers complexed with DNA [152]. The formation of hair like structures was also thought to result in a reduction of transfection efficiency, as cells may not be able to internalise the complexes. Erbacher suggested several solutions to this problem [151]. To keep a compact morphology while increasing the number of ligands, the use of targeting medium-length oligosaccharides was suggested, as was the use of smaller PEG molecules. PEI has been grafted with galactose-PEG of molecular weight = 600 Da and was able to form small torroidal complexes with DNA that transfected hepatocytes at reasonable levels. The grafting of PEG to pre-formed polymer/DNA complexes is also being investigated.

The inclusion of cholesterol into the formulation resulted in the formation of vesicles (Figure 66b), which were retained upon the condensation of DNA (Figure 66c). The presence of cholesterol in the PP-PEI formulation is responsible for the formation of the vesicular structures. The incorporation of cholesterol into the bilayer of the vesicle would cause separation of the PEG

chains as well as reducing their steric effects, although the addition of PEG chains results in the molecule being unable to form small tightly packed complexes (Figure 71).

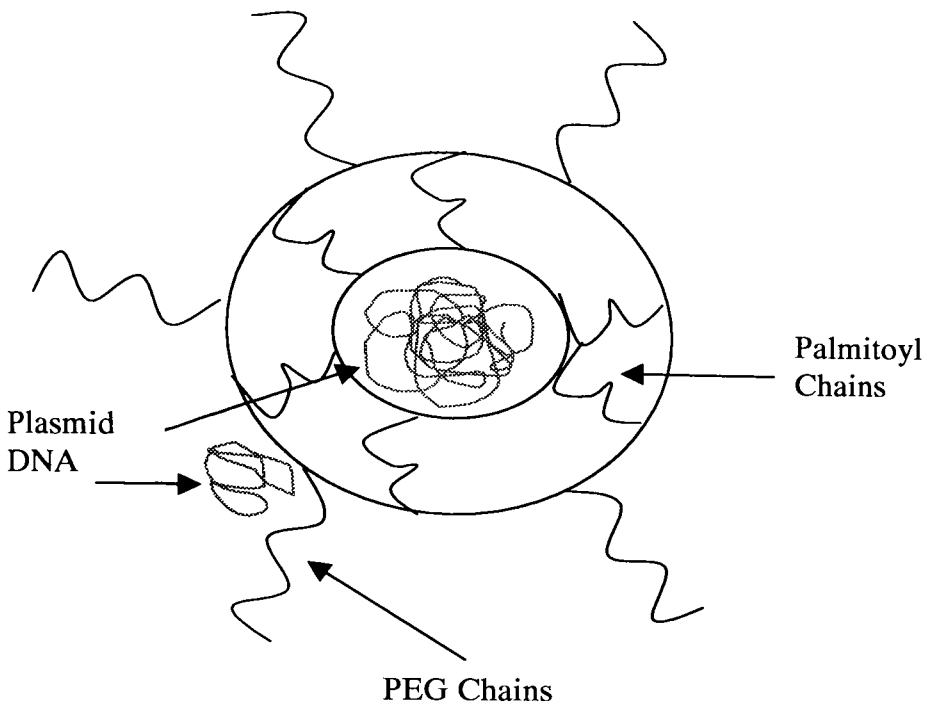

Figure 71: Schematic representation of PP-PEI/Cholesterol/DNA.

Similar vesicular structures have been reported for PEG and Palmitoylated polylysine and polyornithine polymers. The polymers were shown to be able to self-assemble into vesicular morphologies in the presence of cholesterol. The modified polymers were found to be better transfection agents than their unmodified parent polymers.

The QPEI was shown to form small tightly packed spheres when condensed with DNA. The QPEI polymer was the least modified of the polymers. Unlike

P-PEI, PP-PEI and QPPEI, QPEI has no long chain attachments to constrict its formation of small spheres. The complexes produced are similar to those formed with PEI/DNA. The polymer may bind to the plasmid DNA, by means of the available amine groups with the quaternary ammonium groups positioned on the outside of the complex (Figure 72)

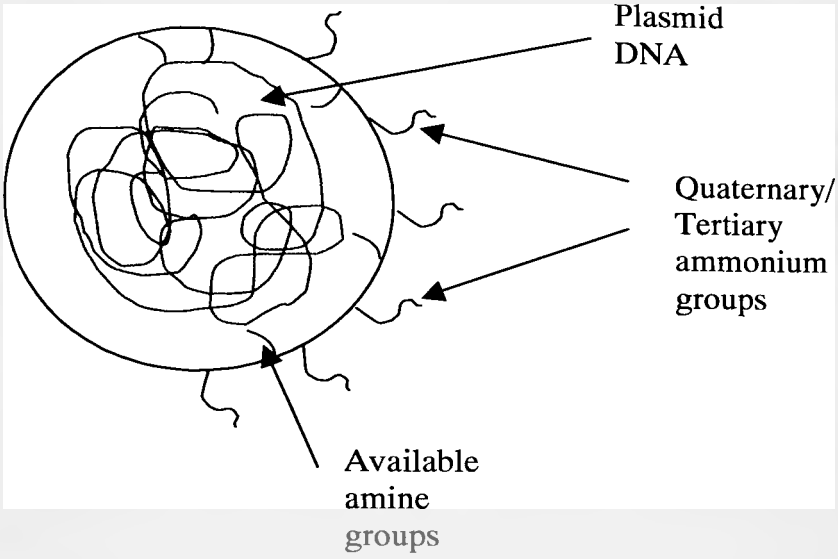

Figure 72: Schematic representation of QPEI/DNA complex.

Upon complexion with DNA the QPPEI polymer formed a complex, which may be described as a collapsed vesicle. This morphology may result from an excess of palmitoyl chains at either end of the complex. At the point of apparent collapse may be due to the presence of the quaternary/tertiary ammonium groups. These groups may form part of the bilayer whose thickness is governed by the length of the chains involved in its formation resulting in the appearance of the collapsed vesicle. Inclusion of cholesterol in the QPPEI formulation resulted in the formation of vesicular structures. As

with the PP-PEI/cholesterol formulations the bilayer is stabilised by the cholesterol molecules resulting in a complete vesicular morphology (Figure 73)

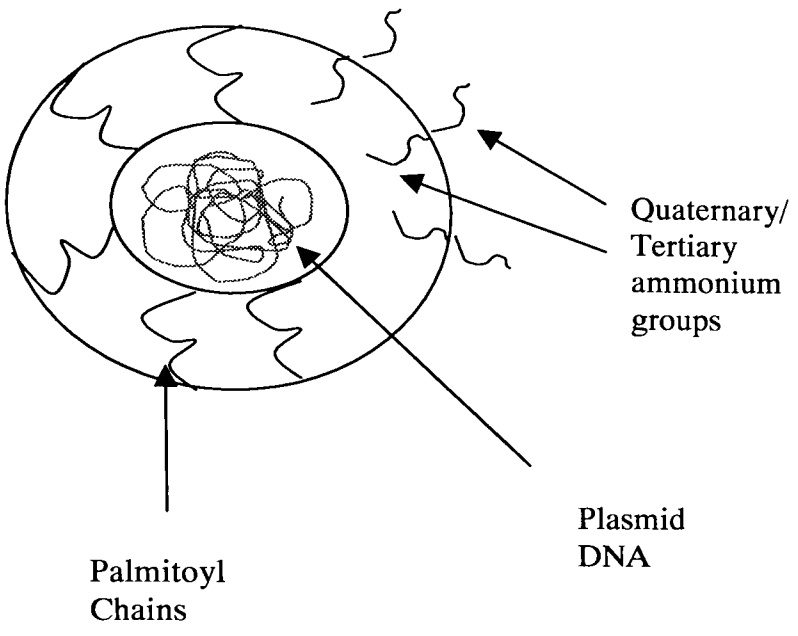

Figure 73: Schematic representation of QPPEI/cholesterol/DNA complexes.

Photon Correlation Spectrocopy

The size of polymer condensed DNA complexes is an important parameter for optimal gene delivery [92]. Complexes of a small size are thought to be a critical parameter for *in vivo* expression due to physical restrictions, for example, in the vascular system where the complexes must pass through fenestrations in order to reach the target cells, as well as diffusion through body tissue. It is also thought that complex size plays a role in endosomal uptake, although it is unclear whether or not it occurs more efficiently for smaller sizes. Wagner and workers reported higher *in vitro* transfection with smaller particles of 100nm or less.

Ogris *et al* [92] investigated several different factors that influenced the size of PEI/DNA and PEI-transferrin/DNA complexes. Small and stable particles produced using an optimised protocol showed significantly lower gene expression levels in *in vitro* transfection experiments. This was thought to result from factors such as a reduced cell binding, by inefficient intracellular release, and/or subsequent steps of intracellular delivery.

The size of particles has been shown to be important for diffusion through the cytoplasm, Luby-Phelps *et al* suggested that particles larger than 54nm may be nondiffusable in the cytoplasmic space. However large particles may migrate in the cytoplasm not only by diffusion but also by other mechanisms

where cytoskeletal components like microtubules and actin filaments are involved, which may facilitate the transport.

The vesicular structures produced by the P-PEI/DNA complexes produced similar sizes over the ratios measured. The size of the complexes produced is largely governed by the palmitoyl chains, as these ligands form the vesicle bilayer. The charge associated with the complex also plays a role in the complex size. An excess of negative charges from the DNA phosphates can result in aggregation of the complexes. As the positive charges of the polymer are increased the DNA is neutralised allowing for more efficient condensation of the DNA.

The large sizes recorded for the PEI/DNA complexes are in contrast to other examples in the literature, that report PEI/DNA complexes around 50nm in size. This difference in size may be due to the different solutions used to formulate the complexes. PEI was able to form stable complexes at ratios of 0.5:1 (w/w) and above. Below this ratio the complexes aggregated and precipitated from the colloidal dispersion. As the polymer/DNA ratios are increased the zeta potential also increases towards the positive, at the lower ratios the complexes are negatively charged which indicates that the DNA in the complexes may not be fully complexed. PEI showed a negative zeta potential at polymer/DNA ratios of 1:1 and below, this negative value is indicative of an excess of negative DNA phosphate charges and would

explain the instability of the complexes. An excess of positive charges is needed to ensure complete condensation of the DNA.

The decrease in size with increasing polymer/DNA ratios shown by the PP-PEI/DNA and PP-PEI/cholesterol/DNA complexes may be explained by the amount of DNA contained in the complex. At the lower ratios there is only a certain amount of polymer available to condense the DNAand the charge repulsion between the two is quite high. As the amount of polymer available is increased the polymer charges out number the DNA charges, resulting in a reduced complex size.

Cholesterol was included in the formulation of both PP-PEI and QPPEI. Both the PP-PEI and QP-PEI samples presented as almost clear liquids upon probe sonication, without the presence of cholesterol indicating a partial solublisation of the polymers. Cholesterol was included in the formulation to encourage self-assembly of the polymers into a vesicular form [67]. The use of cholesterol in gene delivery vectors has previously been reported for use in increasing bilayer stability in self-assembling vesicular systems [49, 50]. Gene delivery systems containing cholesterol have been shown to benefit from an increase in blood half-life in mice. This was thought to result from the cholesterol in the bilayer preventing proteins in the mouse serum moving into the bilayer and breaking up the complex.

Zeta Potential

At low polymer/DNA ratios the complexes of PEI and PP-PEI both showed a negative zeta potential, due to an excess of DNA phosphates to polymer primary amines. As the amount of polymer used in the formulation increased, the complex charge increased towards neutrality, between the ratios of 1:1 and 2.5:1 (w/w), and the complexes assumed a large positive charge with an excess of polymer.

The QPEI, QPPEI and QPPEI/cholesterol complexes exhibited a different pattern to the PEI and P-PEI complexes. The quaternary polymers all showed a large positive charge at all the polymer/DNA ratios tested. The primary amine groups of the modified polymers may be neutralised by the DNA phosphate groups, but due to the extreme positive nature of their quaternary ammonium groups, the complexes retain an overall positive nature.

The PP-PEI and PP-PEI/Cholesterol complexes exhibit a negative charge with an excess of polymer. This may be due to the PEG chains on the polymer backbone shielding the positive charges on the surface of the complex. The inclusion of cholesterol into the PP-PEI and QPPEI complexes results in an overall increase in the net positive charge of the complex. The measured zeta potential for the free uncomplexed polymers (Table 17) is less positive than the zeta potentials measured for the polymer/DNA complexes.

This is due to the presence of DNA in the complexes, which neutralises many of the positive charges of the complexing polymer.

As the charge of the complexes is highly positive, they may suffer from non-specific electrostatic interactions with body tissues [153], which would have a negative effect on the bio-distribution of the complexes. The high positive nature of the complexes may also make them susceptible to circulating proteins in the body, which can bind to the complexes reducing their transfection properties [154].

3.5: Conclusions

In this section we reported the interactions between the modified PEI polymers and plasmid DNA. All of the modified polymers were able to condense plasmid DNA. A kinetic process was identified with the condensation process, as PP-PEI, PP-PEI/cholesterol and QPPEI/cholesterol were only able to completely condense DNA after a certain time period. This process was thought to be governed by the degree of modification made to the polymers as well as the nature of the structural alterations. The presence of palmitoyl groups in the P-PEI, PP-PEI and QP-PEI polymers increased the time required for complexation to take place. This could be due to a slow rearrangement of the self-assembly groups.

The morphologies of the polymer/DNA complexes were analysed using electron microscopy, the conjugation of palmitoyl to the polymers allowed the self-assembly of vesicular structures. The presence of cholesterol enabled the PP-PEI and QPPEI polymers to form vesicular structures, whereas QPEI formed small tightly packed complexes. The complexes containing palmitoyl were found to have a vesicular morphology, along with the observation of a small number of rods and spheres, although incorporation of cholesterol was required in some formulations for the formation of vesicular structures. The sizes of the polymer/DNA complexes obtained by electron microscopy were consistent with the sizes obtained using photon correlation spectroscopy and were all in the colloidal size range.

Sizing of the polymer/DNA complexes was performed using photon correlation spectroscopy. The type of modification made to each of the polymers had an effect on the measured complex size. The PEG containing polymers produced large complexes due to steric hindrance from the large PEG conjugates, whereas the QPEI polymer, which contains no large chain conjugates, produced complexes as small as 50nm in diameter. Zeta potential analysis revealed the surface charge of the various polymer/DNA complexes. The quaternary ammonium formulations were shown to have a highly positive nature at all ratios, whereas the P-PEI/DNA complexes ranged from negative through to positive by changing the polymer/DNA ratio. The PP-PEI/DNA formulations revealed that the complexes were also positively charged at all ratios.

Chapter 4: Biological Characterisation of Polymer/DNA complexes

4.1.1: Protein and Erythrocyte Aggregation

Polyethylenimine (PEI) has been shown to be a highly efficient gene transfection agent in both *in vitro* and *in vivo* experiments, when compared to other cationic polymers and liposomal formulations [72]. The mechanism by which PEI transfects DNA into cells is still poorly understood. Many groups have reported that the ideal complexes for transfection should be small, without a tendency to aggregate before or after *in vivo* administration [78, 92, 155]. Another property of the ideal transfection complex is a minimum of unspecific interactions with its surrounding biological environment.

The body's innate immune system provides the first challenge for *in vivo* administration of a gene delivery system, through the opsonisation of foreign particles with plasma proteins as a means of removing foreign objects from the body [83]. The unwanted interactions of the vector with blood components and non-target cells such as the reticuloendothelial system also cause problems for targeting when the complex is administered intravenously [83]. By studying these unwanted interactions before the gene delivery system is administered to the body, the problem areas that may befall the complex can be identified and give some insight into its transfection ability.

In this section the effects of unspecific protein interactions were investigated, with the vectors in both fetal calf serum (FCS) and human plasma. A method reported by Li *et al* [156] was used. The polymer/DNA complexes were

incubated with either FCS or plasma and the UV absorbance was measured at set time intervals to measure any aggregation of the complexes. To investigate the interaction of the polymer/DNA complexes with blood components, an erythrocyte aggregation assay reported by Ogris *et al* [83] was used. Human erythrocytes were incubated with the complexes and any aggregation of the complexes was observed under the microscope.

4.1.2: Haemolysis Assay

As previously mentioned PEI has been shown to be an effective transfection agent in both *in vitro* and *in vivo* situations. Despite this increased transfection ability, PEI suffers from toxicity problems, with some groups reporting up to 50% fatalities when administered to mice at certain dose levels [78, 157]. The aims of this project were not only to effectively increase the transfection efficiency of the parent PEI polymer by means of modification, but also to decrease the toxic effects in order to produce a safe formulation for *in vivo* use. By measuring toxicity before *in vivo* administration an insight can be gained into the effects of the modifications made to the PEI polymer.

To measure the haemolytic effects of the various polymer/DNA complexes a method reported by Brown *et al* [67] was used. The polymer/DNA complexes were incubated with blood erythrocytes, with triton-X 100 (Figure 74) serving as a positive control to give 100% haemolysis.

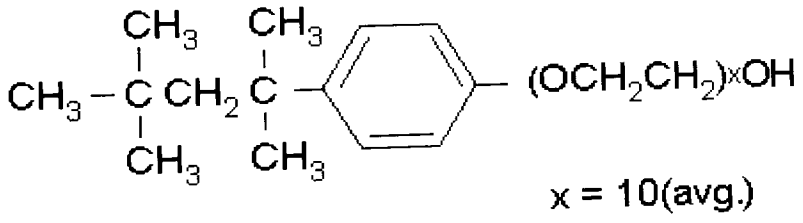

Figure 74: Chemical structure of Triton-X 100.

4.1.3: MTT Assay

The MTT (3-(4,5-dimethylthiazol-2-yl)-2,5 diphenyltetrazolium bromide)) assay is a cytotoxicity assay, which is quick and easy to perform and allows for a large number of assays to be performed in one batch. The assay is particularly useful when comparing differences between cell lines, cytotoxic agents and combinations of drugs. The MTT assay was developed as a rapid throughput micro titration assay to use as a screen for new cytotoxic agents [158]. The assay works by measuring the effect of an agent on the growth of a population of cells and the endpoint is an estimate of live cell numbers [159].

The cytotoxic agent is added to cells that are in an exponential phase of growth, for a length of time calculated to inflict the maximum amount of cell damage. After the set time interval, the cytotoxic agent is removed and the cells are allowed to proliferate for two to three doubling times. This allows for a distinction betweens cells that are viable and capable of proliferation, and the cells that are viable but are incapable of proliferation.

The number of surviving cells can be determined indirectly by reduction of the MTT dye. MTT is a yellow water-soluble tetrazolium dye that is reduced by live cells, to a purple formazan product that is insoluble in aqueous solutions [160]. The amount of MTT-formazan produced can be determined specrophotometrically once solubilised in a suitable solvent. The inclusion of

the growth period the cytotoxic agent has been removed is an important feature of the MTT assay. This allows the cells to either recover from the effects of the drug, or die and also avoids any possible interference from the cytotoxic agent in the reduction of MTT.

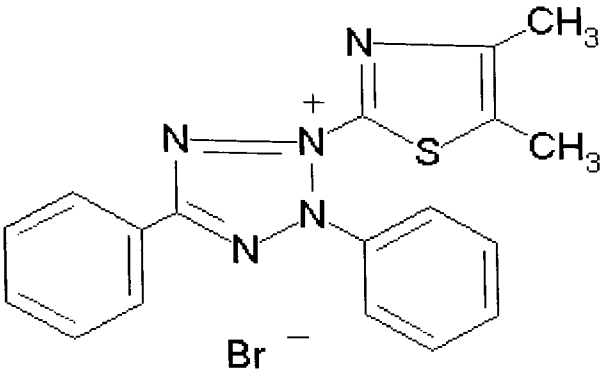

Figure 75: Chemical structure of MTT dye (3-(4,5-dimethylthiazol-2-yl)-2,5 diphenyltetrazolium bromide.

4.1.4: *In Vitro* Transfection

The optimisation of the formulation of vectors for gene delivery requires many experiments to be carried out, so it is preferable to begin work with cell based models rather than animal models, although results obtained from *in vivo* work may differ from those derived from *in vitro* experiments [85]. PEI has been shown by many groups to be a very efficient gene delivery vector when used for *in vitro* experiments [76, 86]. For a vector to effectively transfect DNA it must complete several tasks. The vector must travel from the site of administration to the target site, to be then taken up by the target cell. The vector must then be released from the endosome and be imported into the cell (Figure 76).

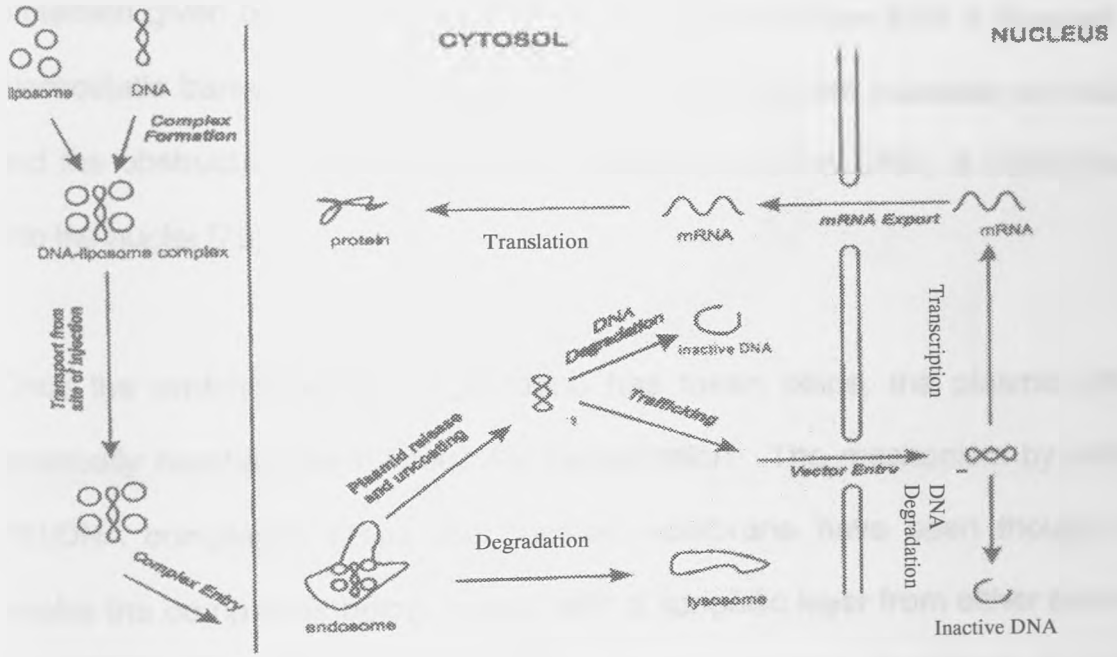

Figure 76: Schematic diagram of the barriers involved in gene delivery.

The success of PEI was first thought to be due to its behaviour as a proton sponge at virtually any physiological pH and the lysosomes would swell and burst due to osmolarity changes upon fusion with endosomes containing PEI [161]. This hypothesis has since been reported as incomplete [162]. A lack of lysomal involvement in the cellular tracking of PEI/DNA complexes has been shown. The lysosomal disruption occurs from an influx of protons from V-ATPases in the lysosomal membrane, which results in a build up of a charge gradient [163]. To relieve this gradient there is also an influx of Cl^- ions which increases lysosomal osmolarity with water rushing in to relieve the gradient resulting in lysosomal swelling and bursting [161]. Godbey *et al* [75] hypothesised that PEI was able to present a physical barrier to nucleases within the cell, as well as offering protection via its buffering capacity. The protection given by the PEI to DNA was thought to derive from a physical or electrostatic barrier to nucleases, which resulted in both nuclease exclusion and the obstruction of endolysosome formation as the DNA, is transported into the nuclei [75].

Once the endolysosomal degradation has taken place, the plasmid DNA eventually reaches the nucleus for transcription. The mechanism by which PEI/DNA complexes cross the nuclear membrane have been thought to involve the complexes being coated with a lipophilic layer from either anionic phospholipids adhering to the cationic exterior of the complexes or from fragments of the membranes of burst endolysosomes [75]. This lipophilic

layer may fuse with the nuclear membrane allowing the complexes to enter the cell nuclei [164, 165].

For the *in vitro* experiments a β-galactosidase plasmid (pCMVβ) was used. pCMVβ (Figure 77) is a human mammalian reporter vector designed to express β-galactosidase in mammalian cells from the human cytomegalovirus immediate early gene promoter. pCMVβ contains an intron (forms the messenger RNA) and polyadenylation signal from SV40, and the full-length E.coli β–galactosidase gene with eukaryotic translation initiation signals.

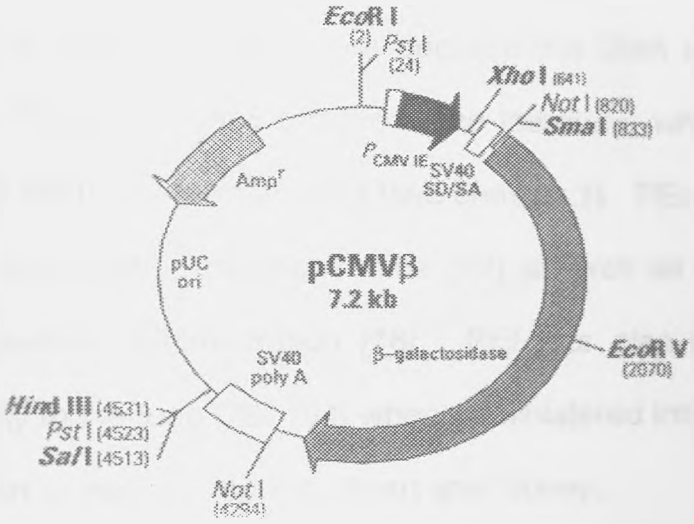

Figure 77: Restriction map of pCMVβ, unique restriction sites are in bold.

4.1.5: *In Vivo* Transfection

Most non-viral vectors are able to transfect plasmid DNA to cells *in vitro*, but only a few have been reported as being able to transfect efficiently *in vivo* [60]. Around 10^4-10^5 plasmid DNA molecules are usually transfected *in vitro*, but for those vectors that are able to transfect *in vivo*, only a small fraction of that number will be transported to the nucleus and be expressed [19].

After administration to the body, there are several obstacles that can stop the complex from reaching its intended target. As mentioned previously in section 4.1.1, interactions with plasma proteins and other blood components can inactivate the complexes and even degrade the DNA contained in the complex [156]. There are many reports in the literature, which detail the *in vivo* response of the many forms of PEI (see chapter 1). PEI was first shown to transfect to the brain in newborn mice [72] as well as the adult brain following intracerebral administration [76]. PEI has also been shown to transfect primarily to the lung [78, 154] when administered intravenously, with some transfection to the liver, spleen, heart and kidney.

For the *in vivo* experiments a green fluorescent protein plasmid (pEGFP) was used. pEGFP-C1 encodes a red-shifted variant of wild-type GFP, which has been optimised for brighter fluorescence and higher expression in mammalian cells.

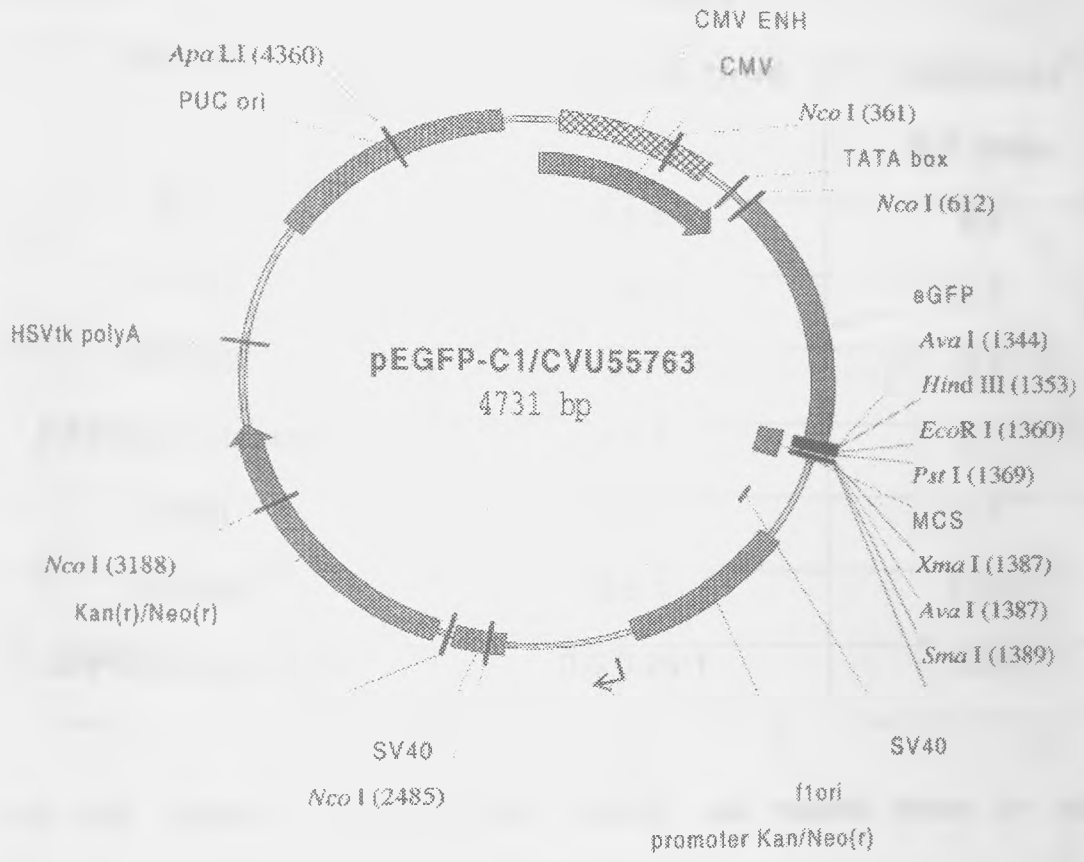

Figure 78: Restriction map of pEGFP-C1.

4.2: Methods and Protocols

4.2.1.1: Protein Aggregation

Polymer/DNA complexes were prepared as described in section 3.2.1. The complexes were formed at optimal *in vitro* transfection ratios (Table 18). The concentration of DNA solution was set at 0.2mg/ml.

Complex	Optimal Ratio (w/w)	Calculated N/P Ratio
PEI	0.5:1	4:1
P-PEI	1.25:1	4:1
PP-PEI	2:1	4:1
PP-PEI/Cholesterol	2:1:1	4:1
QPEI	2:1	7:1
QPPEI	0.5:1	1.2:1
QPPEI/Cholesterol	0.5:0.25:1	1.2:1

Table 18: Optimal polymer/DNA ratios, as found from *in vitro* transfection experiments (see section 4.3.5).

0.5ml of complex solution was added to 1ml of calf serum/ plasma. This mixture was then placed in a water bath at 37°C, with gentle shaking. At time intervals of 0, 40, 80, 120, 160, and 200 minutes, the absorbance of the mixture was read at 500nm (Unicam UV-1, Unicam Ltd, UK)

4.2.1.2: Erythrocyte Aggregation

Approximately 8ml of human blood was centrifuged (1000g x 10min). The erythrocyte pellet was then isolated and washed twice with phosphate buffer saline (PBS, pH = 7.4) at 4^0C by re-suspending the pellet in PBS (pH = 7.4) followed by centrifugation (1000g x 10min). 200µl of the erythrocyte suspension was mixed with 100µl of the polymer/DNA complexes in a 24 well plate. The mixture was then incubated for 1h at 37^0C. After incubation, 5µl of the erythrocyte/polymer/DNA complex mixture was placed on a slide for analysis under the microscope.

Polymer/DNA complexes were prepared as described in section 3.2.1 at the ratios as described in section 4.2.1.

4.2.2: Haemolysis Assay

Approximately 8ml of human blood was centrifuged (1000g x 10min). The erythrocyte pellet was then isolated and washed twice with phosphate buffered saline (PBS, pH = 7.4) at 4^0C by re-suspending the pellet in PBS (pH = 7.4) followed by centrifugation (1000g x 10min). The pellet was weighed and a 3% w/w dispersion of the erythrocytes was prepared in PBS (pH = 7.4).

Varying concentrations of the polymer/DNA complexes (100μl) were added to microtitre plates. PBS and triton X-100 (1%w/w) served as negative and positive controls respectively. After incubation for 4 hours (37^0C), the microtitre plates were centrifuged (1000g x 10min), the supernatant (100μl) was transferred to a new microtitre plate and the absorbance was read at 570nm. Values were corrected for background reading obtained for the polymer/DNA complexes only. The haemolysis given by the triton X-100 was considered to be 100%, while the haemolysis given for the PBS solution was taken as 0%. The results were expressed as % haemolysis. Statistical analysis was performed using one way analysis of variance on Minitab for windows v10.1.

4.2.3: MTT Assay

A microtitre plate was seeded with either A549 or A431 cells at a concentration of 700 cell/well ($3.5x10^3$ cell/ml). The plate was then placed in a 5% CO_2 (37^0C) incubator for 72 hours. Polymer/DNA complexes and polymer solutions were prepared using a polymer concentration of 2mg/ml and 1 in 2 dilutions of the complexes were carried out 9 times to give 10 solutions. These serial dilutions (100μl) were added and incubated with the cells for 4 hours (37^0C). 100μl of Optimem-1 media was added to all wells in addition to the polymer/DNA complex suspensions.

The polymer/DNA complexes and optimem-1 media were removed after 4 hours and 200μl DMEM/F10 + 10% FCS media containing penicillin/streptomycin was added to each well. The plates were fed daily for 96 hours. On the last change of media 50μl/well of MTT (5mg/ml in PBS) was added to each well. The plates were then wrapped in tin foil placed in a 5% CO_2 (37^0C) incubator for 4 hours. The media/MTT was removed and 200μl DMSO was added to each well with an automated dispenser (cell lysis step). 25μl pf glycine buffer (7.5g/L glycine, 5.85g/L NaCl, adjusted to pH = 10.5 with NaOH) was added to the wells and the absorbance was read at 570nm using an automated plate reader. Values were expressed as a percentage of control and the IC_{50} values were determined.

4.2.4: *In vitro* Transfection.

A microtitre plate was seeded with either A549 or A431 cells at a concentration of 3500 cells/well (1.75×10^4 cells/well). The plate was then placed in a 5% CO_2 (37^0C) incubator for 24 hours. Polymer/DNA complexes were prepared at a range of ratios, with DNA concentration set at 0.2mg/ml. The polymer/DNA complexes (100μl) were added and incubated with the cells for 4 hours. 100μl of Optimem-1 media was added to all wells in addition to the polymer/DNA complex suspensions, 200μl of Optimem-1 was added to the wells not containing any polymer/DNA complex suspensions. After 4 hours all media was removed and replenished with 300μl DMEM. The plates were fed daily for 72 hours.

After 72 hours the media was removed and were washed with 200μl of sterile PBS (pH = 7.4). The PBS was removed and 80μl of 1X Passive lysis buffer (PLB) was added to each well and rocked slowly to ensure complete coverage. The plate was then incubated at room temperature with occasional rocking to ensure complete lysis. 50μl of the lysate was transferred to a new microtitre plate. 50μl of β-Galactosidase standard was also added to the microtitre plate. 50μl of 2X assay buffer (200mM sodium phosphate buffer pH = 7.3, 2mM $MgCl_2$, 100mM 2-mercaptoethanol and 1.33mg/ml O-nitrophenyl β-D-galactopyranosil) was added to both the lysate and the standard and mixed by pipetting up and down. The plate was covered and incubated at 37^0C for 1 hour or until a faint yellow colour has

appeared. The absorbance was read at 405nm on an automated plate reader (Molecular Devices, Alpha Laboratories). Statistical analysis was performed using one way analysis of variance on Mintitab for windows v10.1.

4.2.5: *In vivo* Transfection

Polymer/DNA complexes were prepared as described in section 3.2.1. DNA concentration was set at 0.5mg/ml. 200μl of each complex was injected into the tail vein of groups of mice (n=4) per complex, to give a final concentration of 50μg of DNA per mouse. The mice were sacrificed after 24 hours and the organs were removed and placed in paraformaldehyde. Sections of the organs were taken and paraffin embedded onto slides.

Immunohistochemistry of GFP

The slides were de-waxed by placing in histoclear for twenty minutes followed by 10 minutes in fresh histoclear. The slides were then dehydrated by placing in 100% ethanol for 5 minutes, followed by 5 minutes in 70% ethanol, 5 minutes in water and finally 20 minutes in 0.05% Saponin. The slides were then placed in the wash buffer and put on a shaking platform for 5 minutes. The intrinsic peroxidase activity was blocked by placing the sides in 0.3% H_2O_2 for 20 minutes, followed by a further 5 minutes in the wash buffer.

Unspecific binding was blocked using a Vectastain ABC kit (Rabbit IgG), blocking serum followed by mouse serum (4.5ml of BSA buffer + 0.5ml mouse serum). 3 drops of blocking serum was added to 10ml BSA serum in a mixing bottle and placed on the slides for 15 minutes. After the 15-minute

interval, the blocking serum was removed and mouse serum was placed on the slides and left for 15 minutes. The biotinylated antibody was prepared by adding 3 drops of normal blocking serum to 10ml BSA buffer, followed by one drop of biotinylated antibody stock. The mouse serum was removed from the slides and the primary antibody (10μl primary antibody in 2.5ml Dako antibody dilutent) was added. The slides were then left for 1 hour at room temperature inside a tank. The primary antibody was then removed and the slides were washed (3 x 5 minutes) with wash buffer in a shaking tank.

The second antibody was applied to the slides and left for 30 minutes. The Vectastain ABC reagent was prepared from the Vectastain ABC kit. 2 drops of reagent A was added to 10ml of wash buffer, followed by 2 drops of reagent B. The solution was mixed and allowed to stand for 30 minutes. The second antibody was removed and the slides were washed (3 x 5minutes) in wash buffer. The Vectastain ABC reagent was applied to the slides and left to stand for 30 minutes. Preparation of the DAB substrate for Peroxidase was performed in a fume hood. 2 drops of buffer stock solution was added to 10ml of distilled water, followed by 4 drops of DAB stock solution and 2 drops of hydrogen peroxide solution, with mixing at each stage. The Vectastain ABC reagent was removed and the slides were washed (3 x 5 minutes) in wash buffer.

The DAB substrate was added to the slides inside a fume hood and left for 7 minutes. The substrate was removed and the slides were washed (1 x 5 minutes) in distilled water. The slides were then placed in haemotoxylin for

10 seconds and then into Scotts water for 2-5 minutes until the slides turned blue. The slides were then transferred into 70% ethanol for 2 minutes, followed by 100% ethanol for 2 minutes and finally placed in histoclear. A small amount of histomount was placed onto cover slips. The slides were removed from the histoclear and the bottom of the slide was dried. The slide was gently lower, sample facing downwards, onto the cover slip and pressed gently. The slides were allowed to set overnight and viewed under the microscope.

4.2.6: Materials

Material	Supplier
Bovine Serum Albumin	Sigma, UK
Dulbeceos Modified Eagles Serum	Life Technologies, Uk
Fetal Calf Serum	Life Technolgies, UK
β-Galactosidase	Sigma, UK
Optimem-1 Medium	Life Technologies, UK
Passive lysis buffer	Life Technologies, UK
Triton-X 100	Sigma, UK
Vectastain ABC kit	Life Technologies, UK

4.3: Results and Discussion

4.3.1: Protein Aggregation

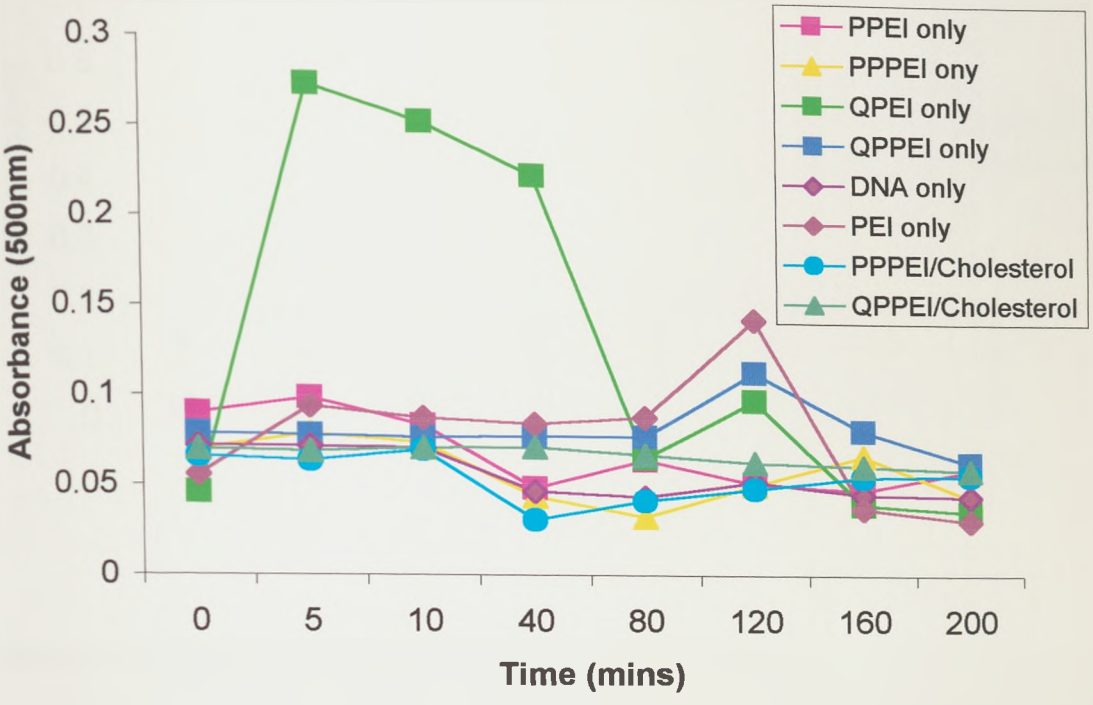

Figure 79: Turbidity of polymers in Fetal Calf Serum.

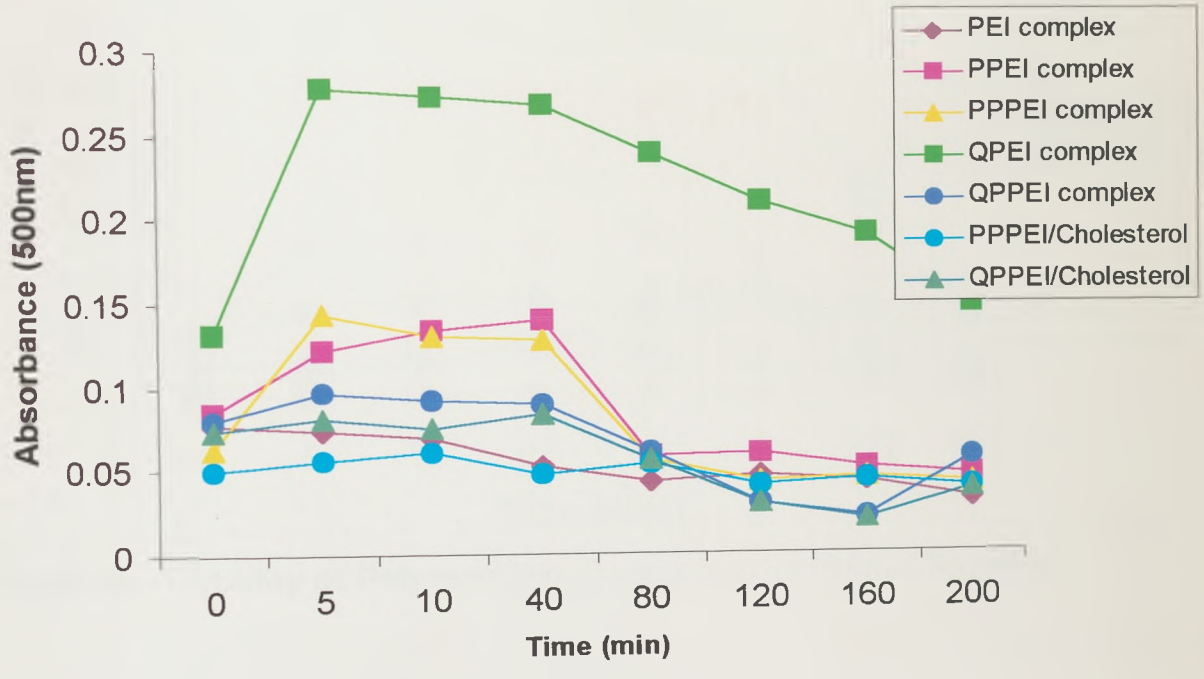

Figure 80: Turbidity of Polymer/DNA complexes in Fetal Calf Serum.

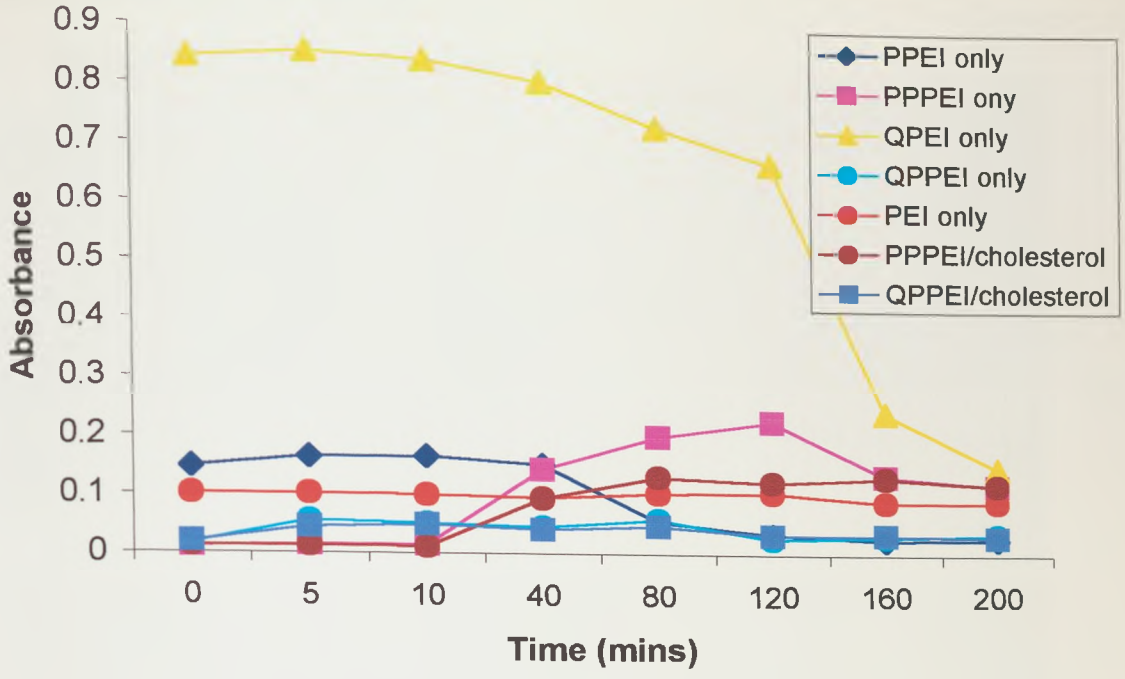

Figure 81: Turbidity of Polymers in Human Plasma.

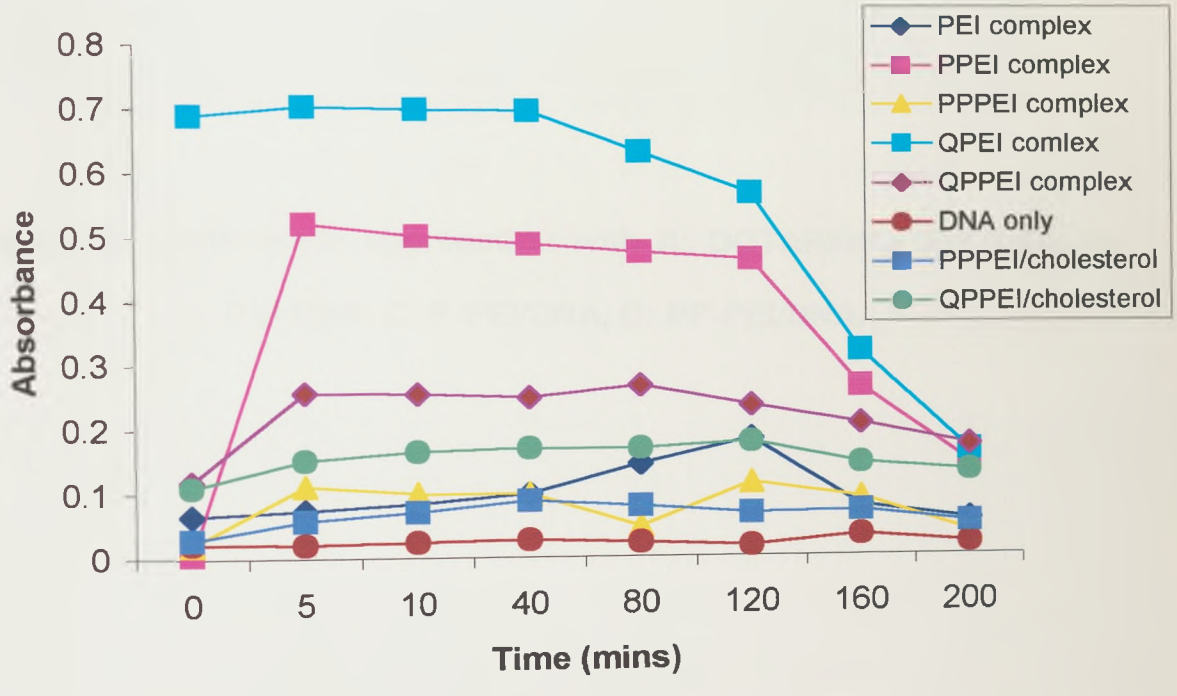

Figure 82: Turbidity of Polymer/DNA Complexes in Human Plasma.

4.3.1.2: Erythrocyte Aggregation

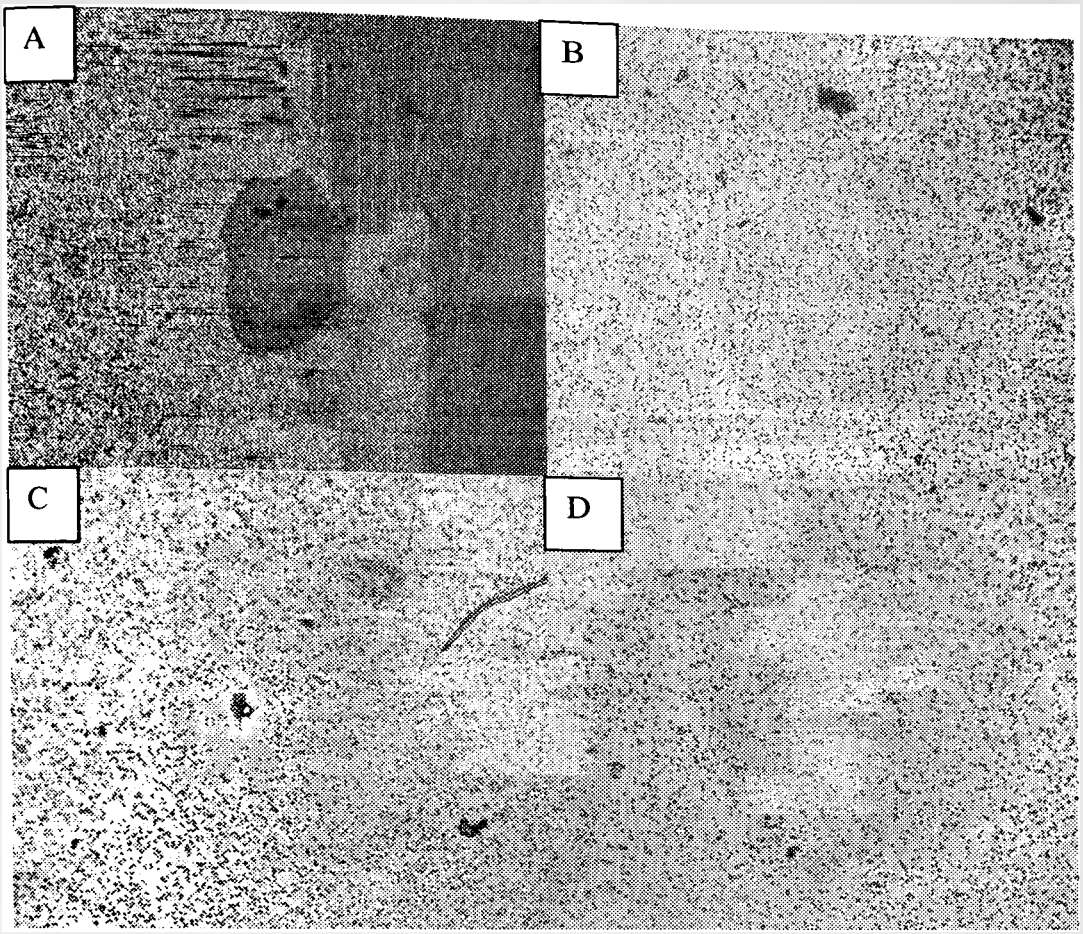

Figure 83: Erythrocyte aggregation with A: DOTAP/DNA (5:1 w/w), B: PEI/DNA, C: P-PEI/DNA, D: PP-PEI/DNA.

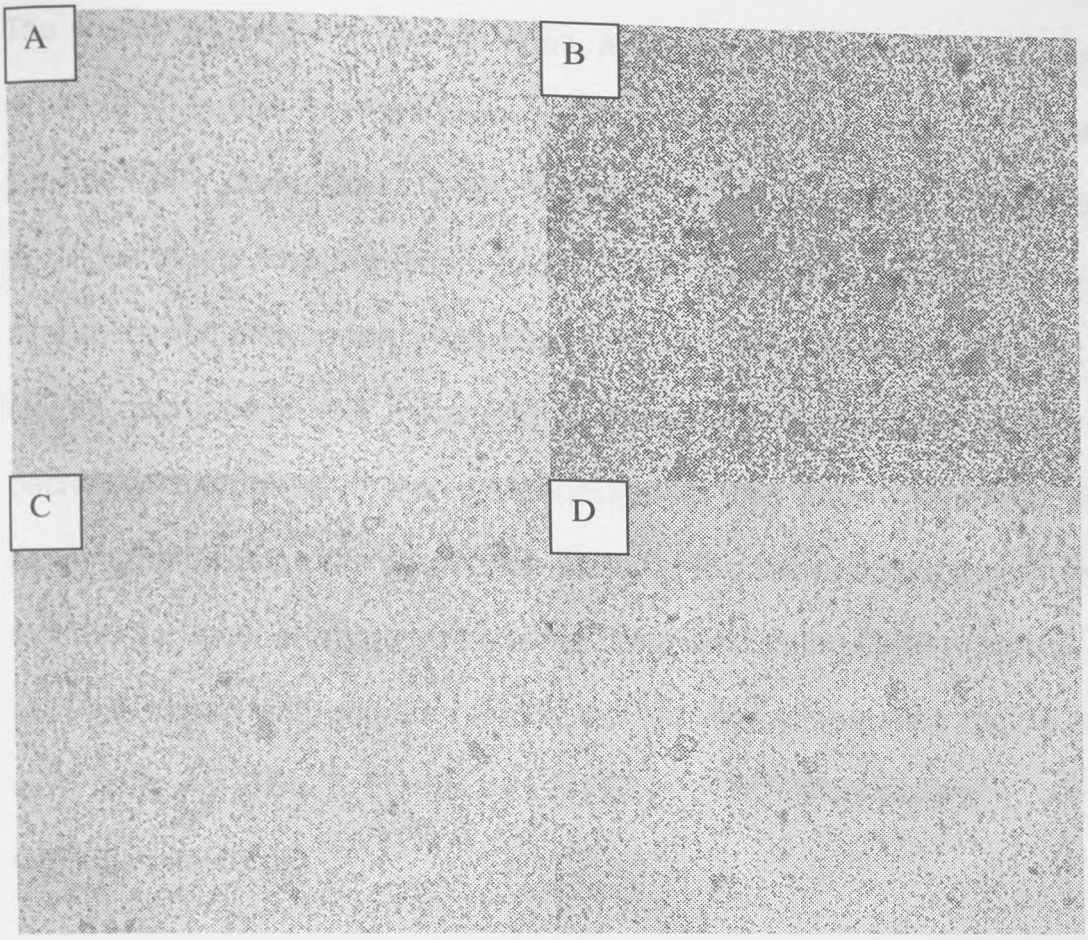

Figure 84: Erythrocyte aggregation with A: PP-PEI/cholesterol, B: QPEI/DNA, C: QPPEI/DNA, D: QPPEI/cholesterol/DNA.

The protein aggregation results show a similar pattern in both the fetal calf serum and in the human plasma. For both the polymer only and the polymer/DNA complexes QPEI appears to be the most susceptible to aggregation with the proteins. Aggregation of the polymer/complex is seen almost immediately upon incubation with the serum/plasma, followed by a steady decrease in the measured absorbance over the time period. This decrease may be due the disintegration of the polymer/complex as the proteins bind during the incubation period. The remaining polymers show a much lower level of aggregation when compared to the QPEI polymer. From both the serum and plasma results, the order of aggregation can be shown as QPEI> PEI> P-PEI> PP-PEI> PP-PEI/cholesterol> QPPEI> QPPEI/cholesterol.

The incubation of the polymer/DNA complexes with blood erythrocytes was performed to compliment the protein aggregation assay and allowed for the visualisation the formation of any aggregates. The erythrocyte aggregation followed a similar pattern as that of the protein aggregation. Large amounts of clumping can be observed with DOTAP/DNA. Of the modified polymers QPEI shows the largest amount of erythrocyte aggregation followed by PEI> P-PEI> QPPEI> QPPEI/cholesterol> PP-PEI> PP-PEI/cholesterol. The protein and erythrocyte aggregation results both show that the PEI and QPEI complexes exhibit a similar level of susceptibility to degradation in the blood. The amphiphilic polymer complexes showed a minimal level of susceptibility to degradation.

4.3.2: Haemolysis Assay

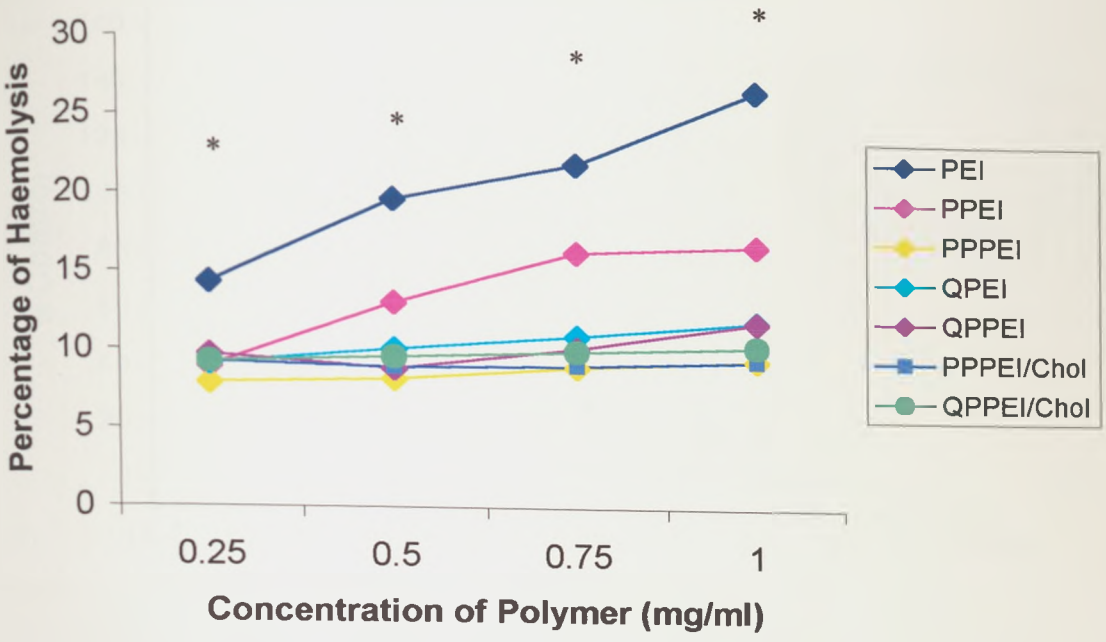

Figure 85: Haemolytic activity of modified and unmodified polymers. (*) Statistically significant difference ($p < 0.05$, one way analysis of variance).

The unmodified parent polymer PEI was found to be a relatively non-haemolytic polymer (27%, 1mg/ml). The modifications made to PEI resulted in a significant decrease in the haemolytic activity of the resulting polymers (Figure 85). Of the modified polymers P-PEI was the most haemolytic (17%, 1mg/ml) followed by QPEI, QPPEI, QPPEI/chol (12%, 1mg/ml), PP-PEI and PP-PEI/chol (10%, 1mg/ml). A slight increase in haemolytic activity was seen as polymer concentration was increased.

4.3.3: MTT Assay

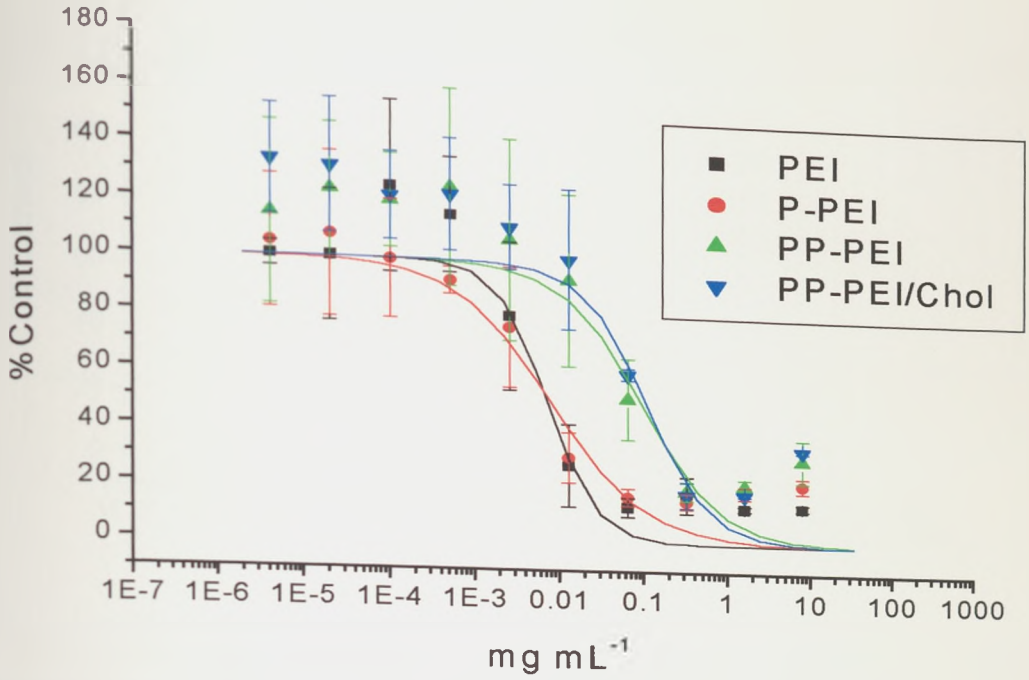

Figure 86: MTT Assay of polymer only in A549 cell line.

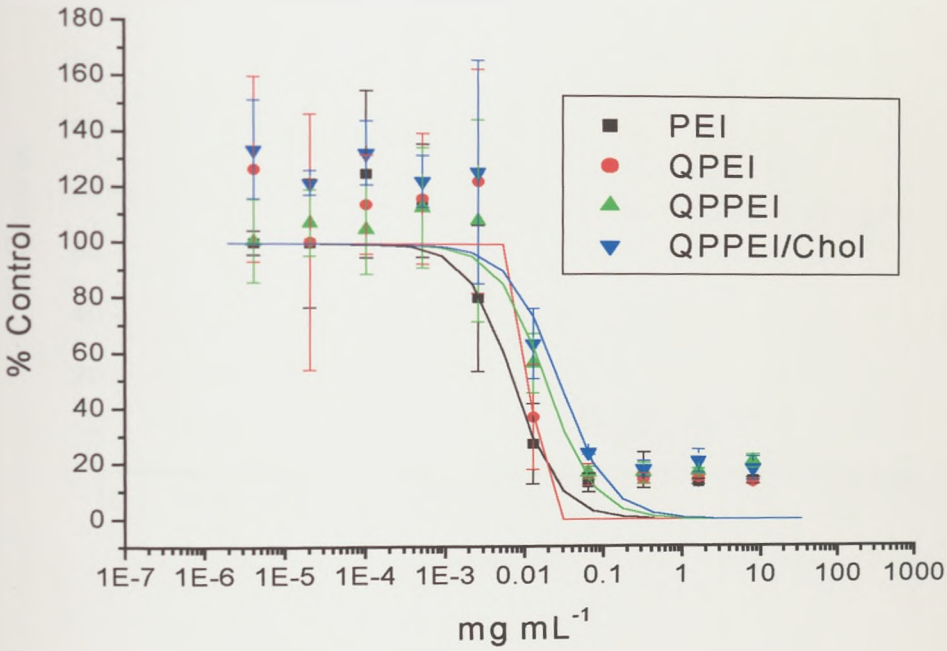

Figure 87: MTT Assay of polymer only in A549 cell line.

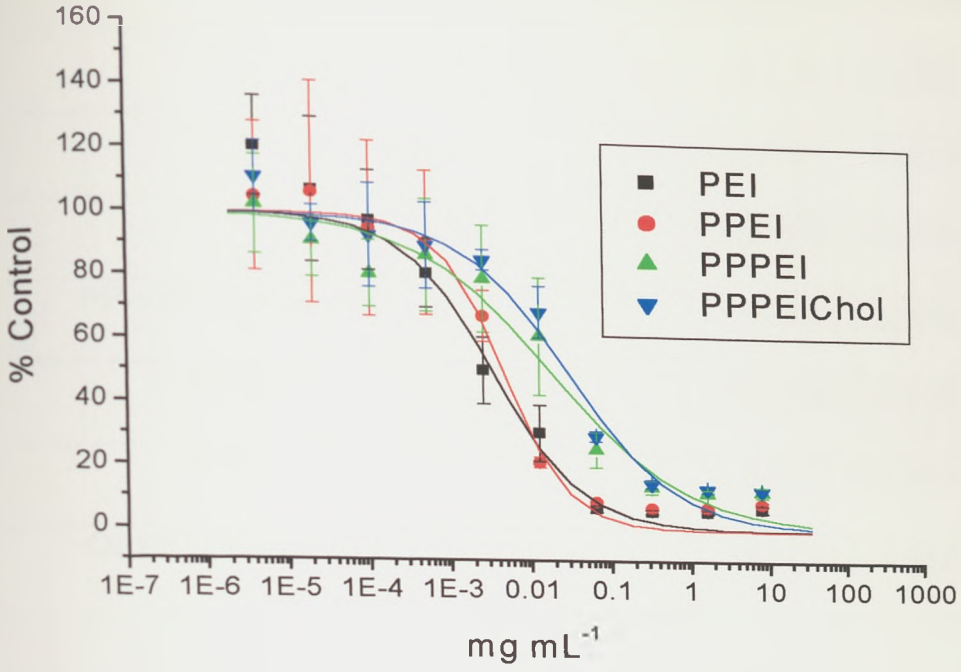

Figure 88: MTT Assay of polymer only in A431 cell line.

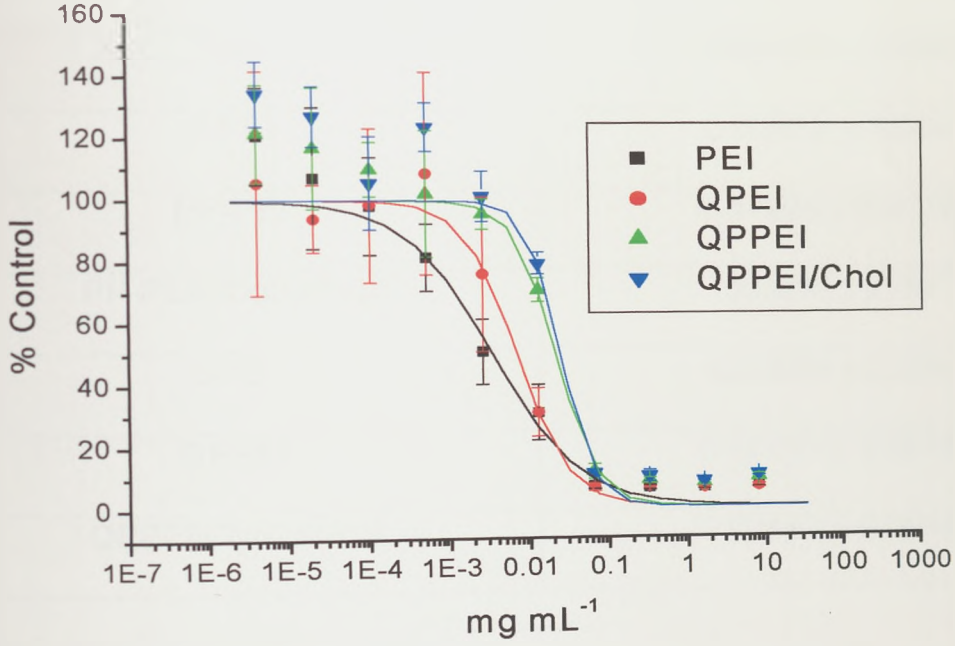

Figure 89: MTT Assay of polymer only in A431 cell line.

Polymer	IC50 (mg mL^{-1}) ± S.D.
PEI	0.0072 ± 0.0032
P-PEI	0.00801 ± 0.0028
PP-PEI	0.09554 ± 0.0161
PP-PEI/Cholesterol	0.10856 ± 0.0201
QPEI	0.01228 ± 0.0157
QPPEI	0.01847 ± 0.0148
QPPEI/Cholesterol	0.02129 ± 0.0023

Table 19: IC50 values of polymers in the A549 cell line.

Polymer	IC50 (mg mL^{-1}) ± S.D.
PEI	0.00345 ± $7.59e^{-4}$
P-PEI	0.00472 ± $9.54e^{-4}$
PP-PEI	0.01905 ± 0.00107
PP-PEI/Cholesterol	0.0304 ± $2.8e^{-4}$
QPEI	0.00694 ± $5.32e^{-5}$
QPPEI	0.02111 ± 0.00157
QPPEI/Cholesterol	0.02442 ± 0.00141

Table 20: IC50 values of polymers in the A431 cell line.

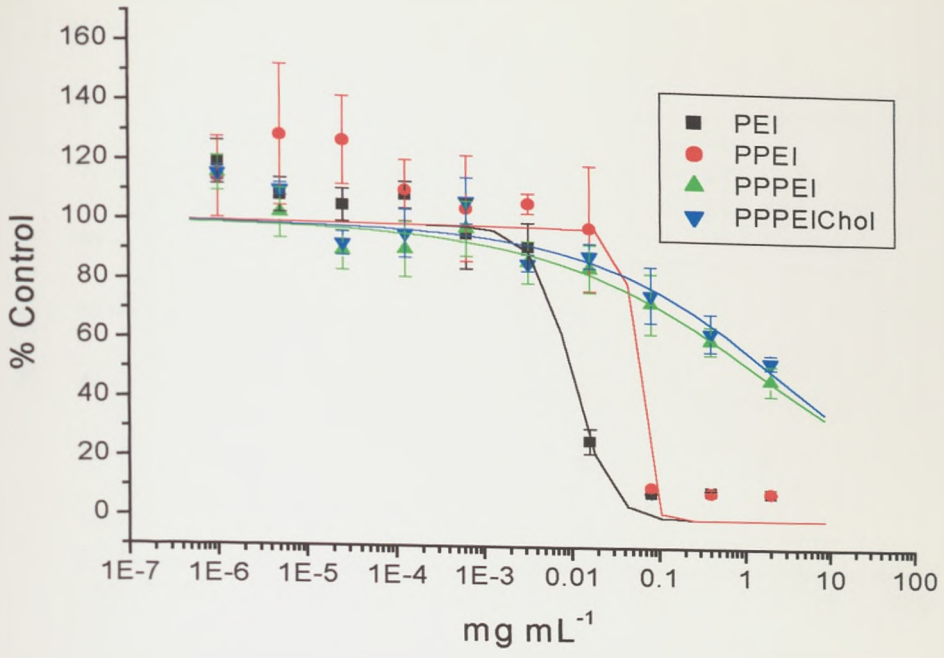

Figure 90: MTT Assay of polymer/DNA complexes in the A549 cell line.

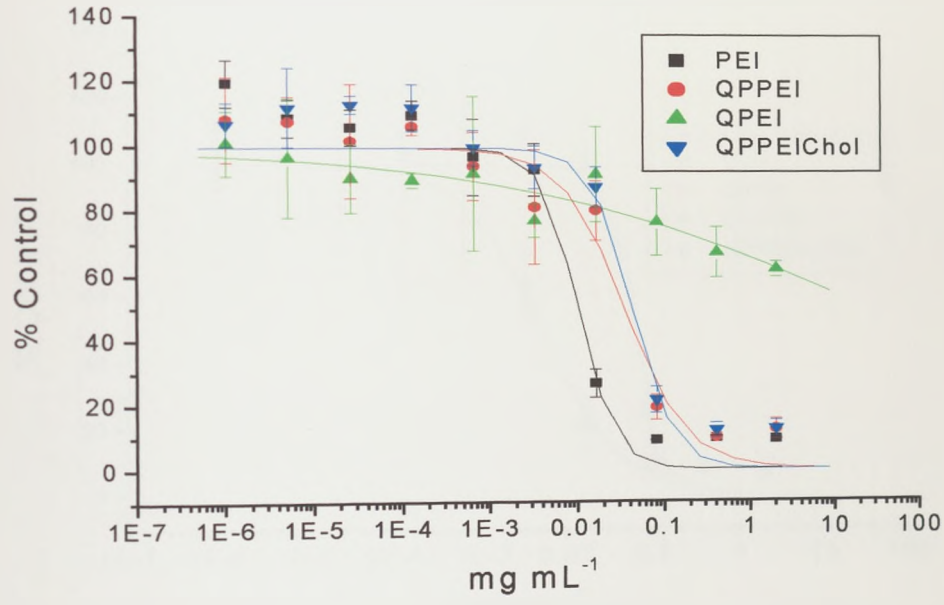

Figure 91: MTT Assay of polymer/DNA complexes in the A549 cell line.

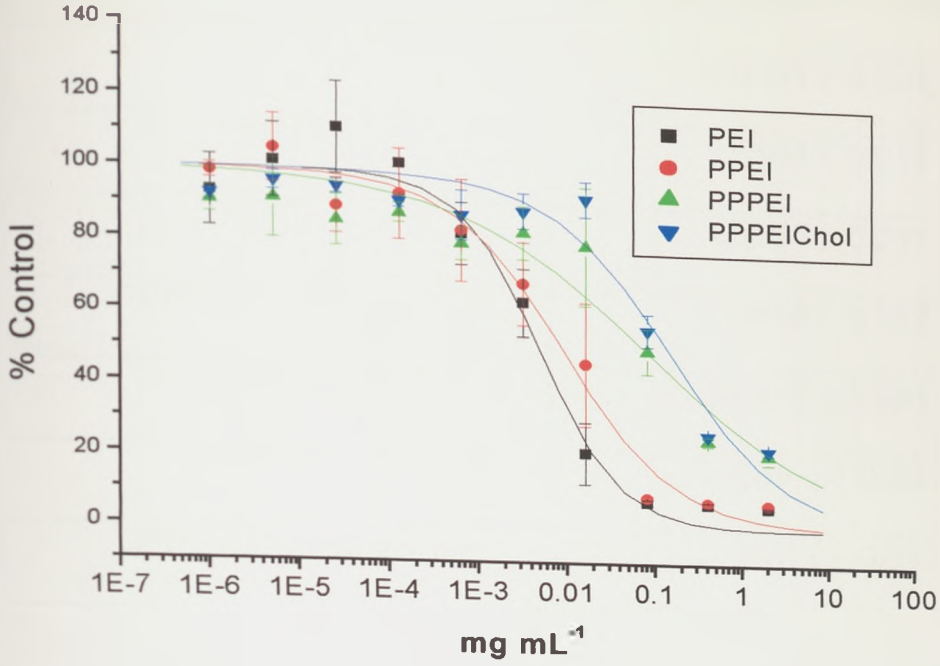

Figure 92: MTT Assay of polymer/DNA complexes in the A431 cell line.

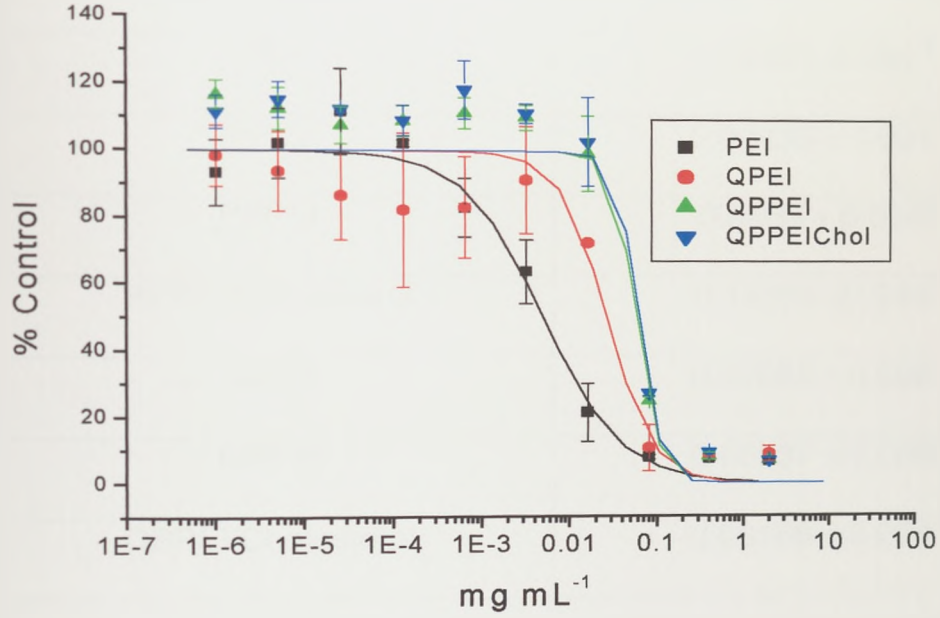

Figure 93: MTT Assay of polymer/DNA complexes in the A431 cell line.

Polymer	IC50 (mg mL^{-1}) ± S.D.
PEI	0.0101 ± 0.031
PPEI	0.0565 ± 0.011
PPPEI	1.6555 ± 0.241
PPPEI/Cholesterol	2.4658 ± 0.512
QPEI	24.447 ± 0.981
QPPEI	0.0345 ± 0.00492
QPPEI/Cholesterol	0.04247 ± 0.012

Table 21: IC50 values of polymer/DNA complexes in the A549 cell line.

Polymer	IC50 (mg mL^{-1})
PEI	0.005 ± $9.59e^{-4}$
PPEI	0.00935 ± 0.0017
PPPEI	0.0862 ± 0.0241
PPPEI/Cholesterol	0.14959 ±0.0457
QPEI	0.02668 ± 0.0081
QPPEI	0.05737 ± 0.0068
QPPEI/Cholesterol	0.06166 ± 0.0043

Table 22: IC50 values of polymer/DNA complexes in the A431 cell line.

The branched form of PEI (25KDa) used in this study has been shown to have a high toxicity when used for *in vivo* studies. From the IC50 values (tables 4.3.3a and 4.3.3b) it can be seen that the modifications made to the PEI polymers have resulted in a reduction in toxicity. In both cell lines the polymers follow the trend of the most heavily modified polymers proving to be the least toxic. This reduction in toxicity appears to be related to the number of available mmoles of nitrogen per gram of polymer (section 2.5). The unmodified parent polymer PEI has the largest amount of nitrogen available (22.2 mmoles) compared to PP-PEI, the most heavily modified (5.51 mmoles) and least toxic of the polymers. Inclusion of cholesterol into two of the formulations resulted in a reduction in toxicity when compared to the equivalent cholesterol free complex.

4.3.4: *In vitro* Transfection

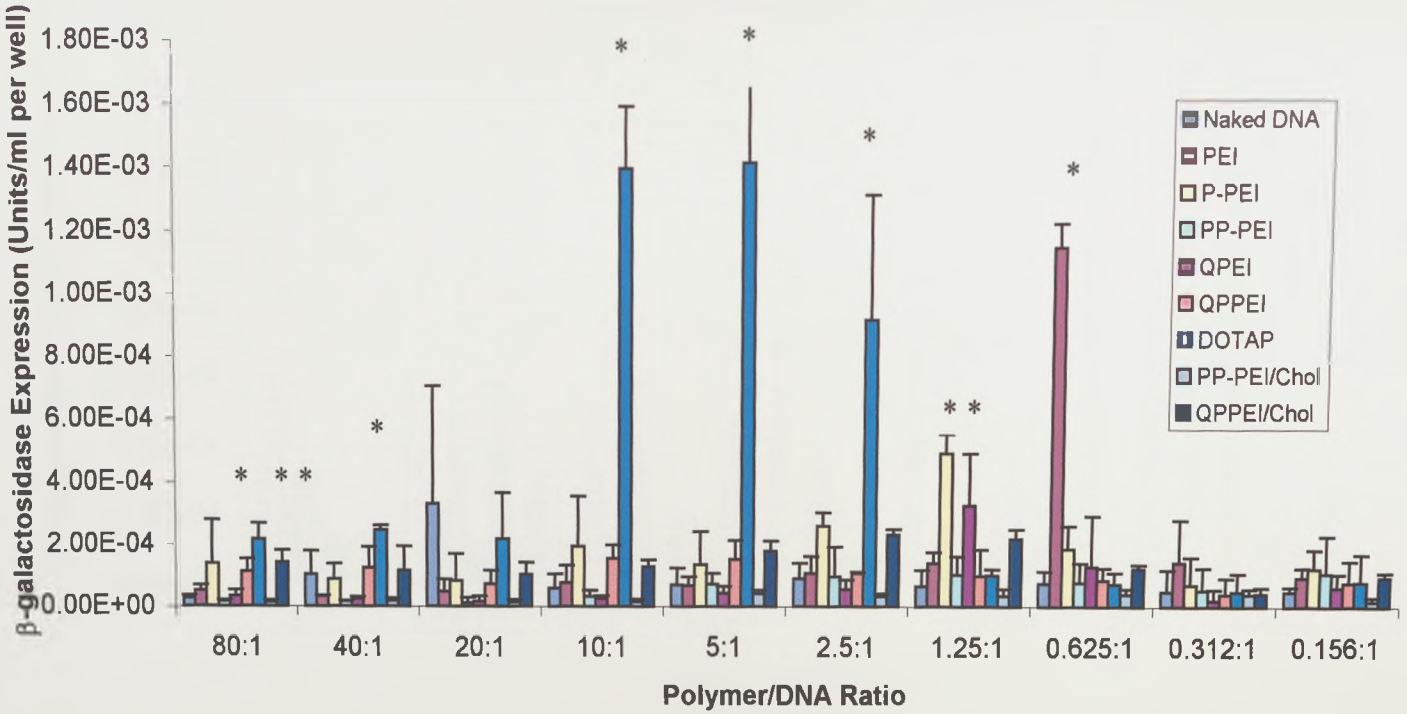

Figure 94: *In vitro* transfection efficiency of polymer or lipid/DNA complexes in the A431 cell lines. (*) Statistically significant difference ($p < 0.05$, one way analysis of variance) relative to other polymers in each ratio class.

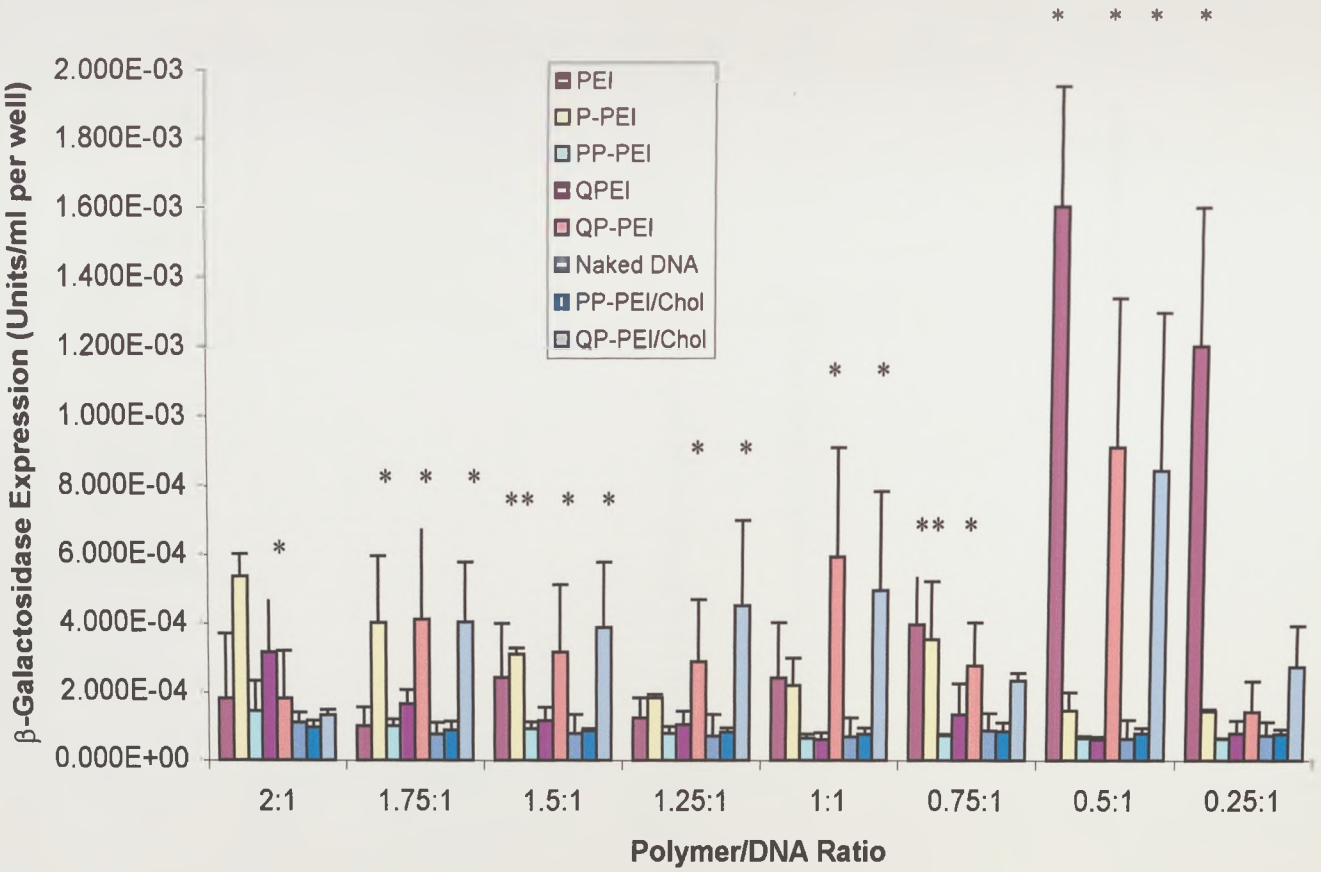

Figure 95: *In vitro* transfection efficiency of polymer/DNA complexes in the A431 cell lines. (*) Statistically significant difference ($p < 0.05$, one way analysis of varaince) relative to other polymers in each ratio class.

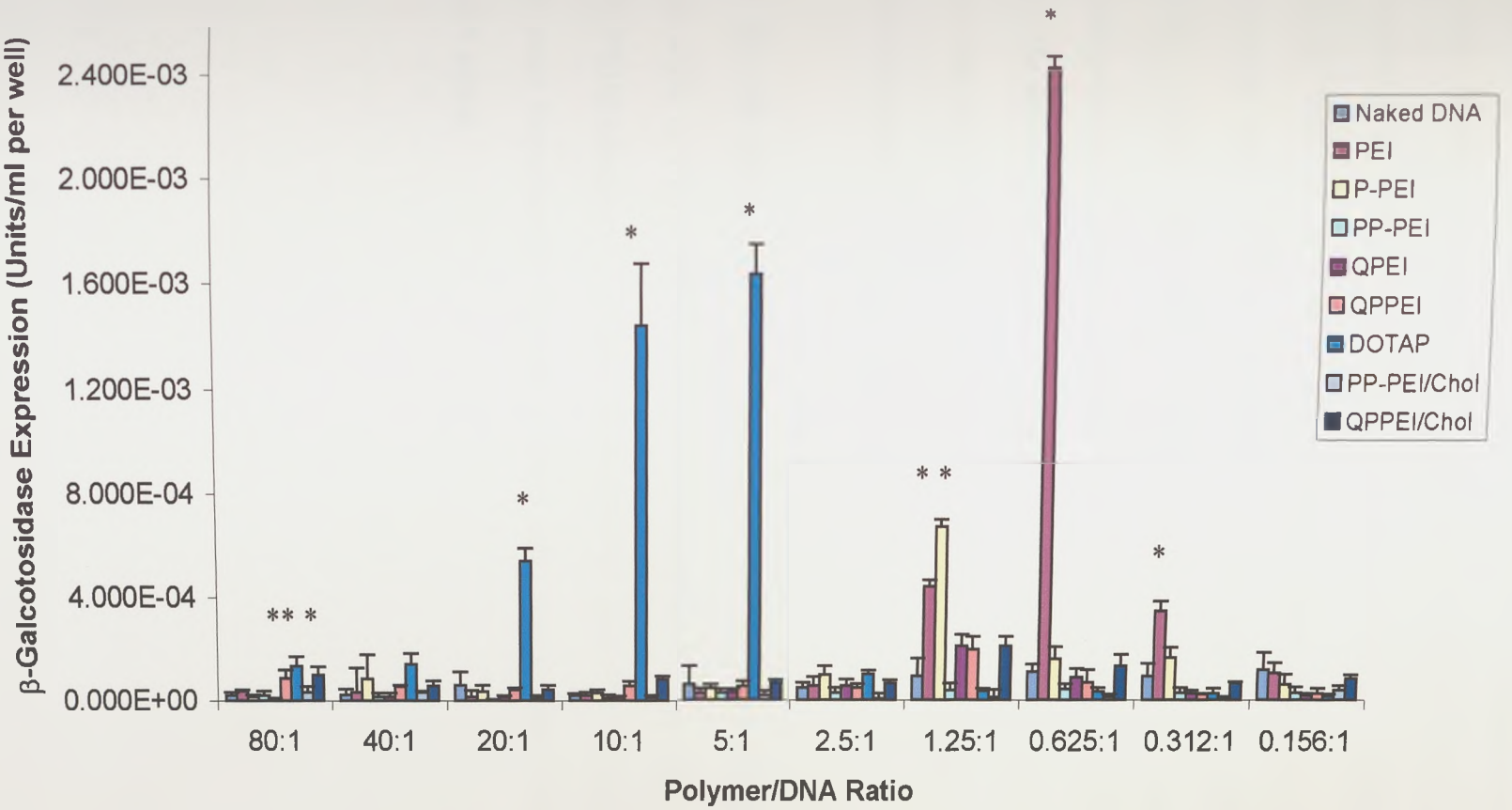

Figure 96: *In vitro* Transfection efficiency of polymer or lipid/DNA complexes A549 cell line. (*) Statistically significant difference ($p < 0.05$, one way analysis of variance) relative to other polymers in each ratio class

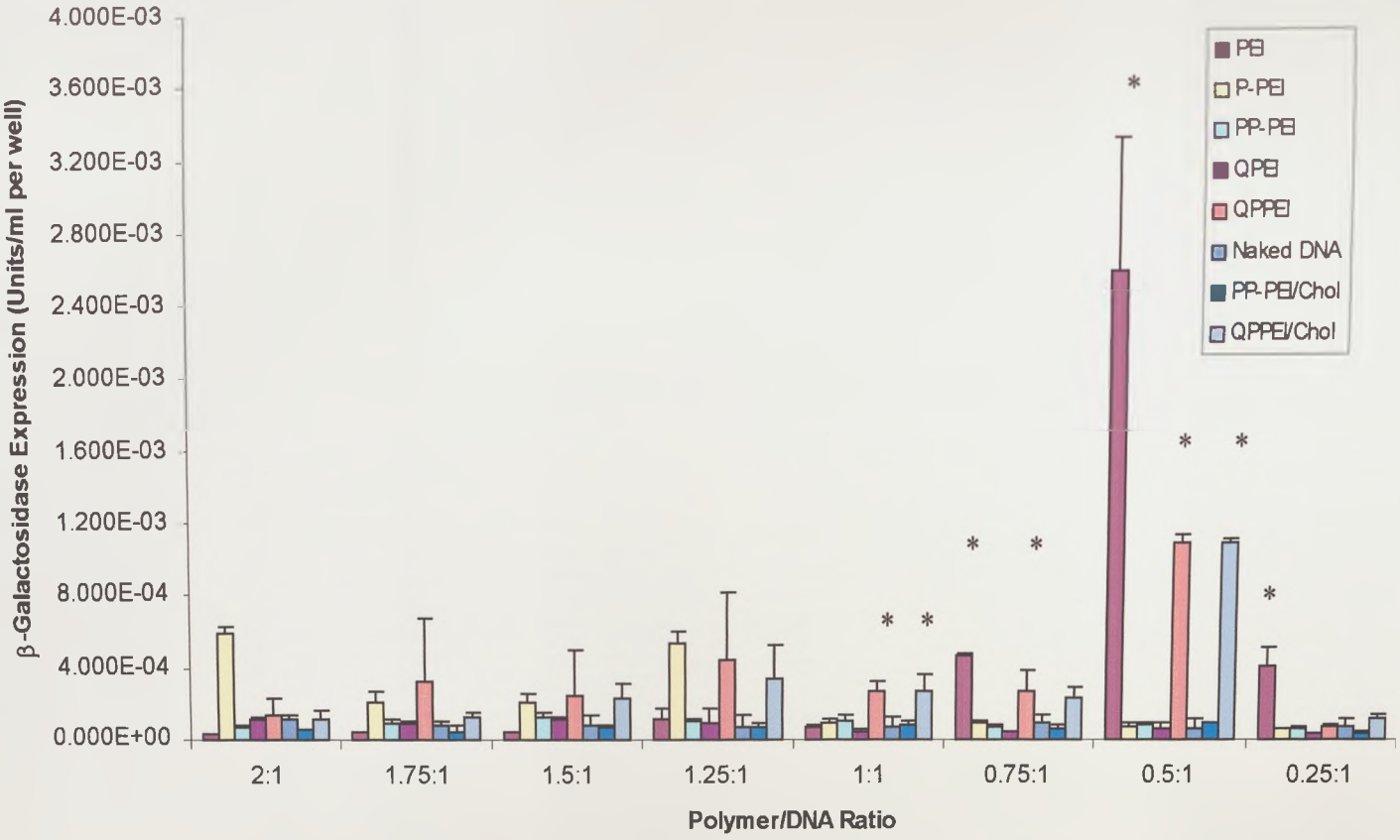

Figure 97: *In vitro* Transfection efficiency of polymer/DNA complexes in the A549 cell line. (*) Statistically significant difference ($p < 0.05$, one way analysis of variance) relative to other polymers in each ratio class.

Figures 94 and 96 show the *in* vitro transfection response over a larger area of polymer/DNA ratios. Once the area showing the highest transfection had been identified the polymer/DNA ratios were confined to a smaller area. The *in vitro* results show that the modifications made to the PEI polymer have resulted in a reduction in transfection efficiency. Efficient transfection is shown only at specific polymer/DNA ratios with very little transfection occurring either side of this ratio. At the higher polymer/DNA ratios used (>10:1, w/w), the transfection efficiency of the complexes will be compromised through the cytotoxicity of the various polymers. The highest transfection efficiency was seen in the A549 cell line due to the fact that this cell line has an increased resistance to the toxic effects of the complexes as shown in the MTT assays (section 4.3.3).

In both the cell lines the complexes give the highest transfection efficiency in the order of PEI > QPPEI > QPPEI/cholesterol > P-PEI > QPEI > PPPEI ~ PP-PEI/cholesterol ~ DNA. Both PP-PEI and PP-PEI/cholesterol proved to be poor transfection agents *in vitro* with transfection levels no better than DNA alone.

4.3.5: *In vivo* Transfection Results

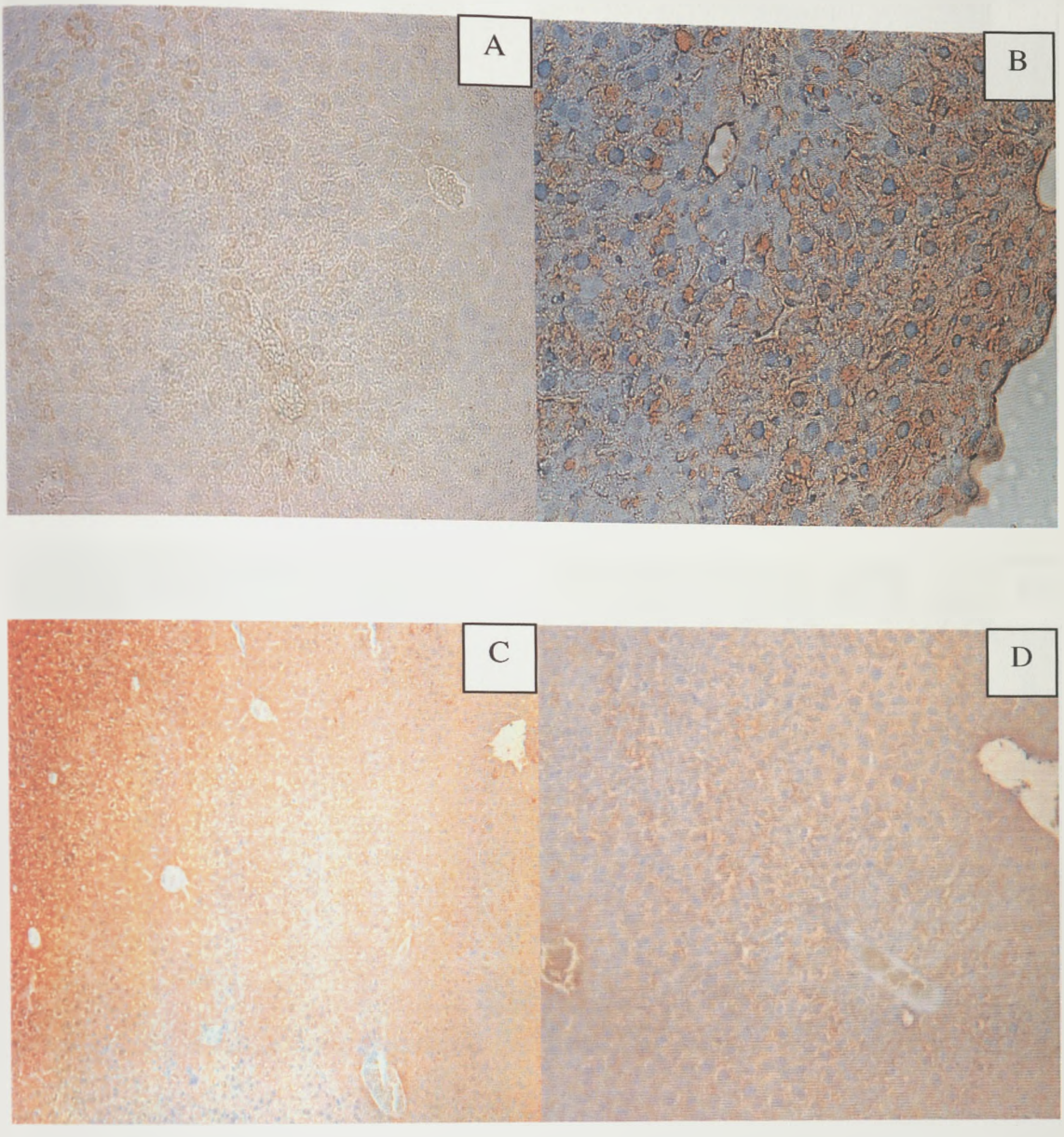

Figure 98: Sections of mouse liver transfected with PEI/GFP complexes (n=4).

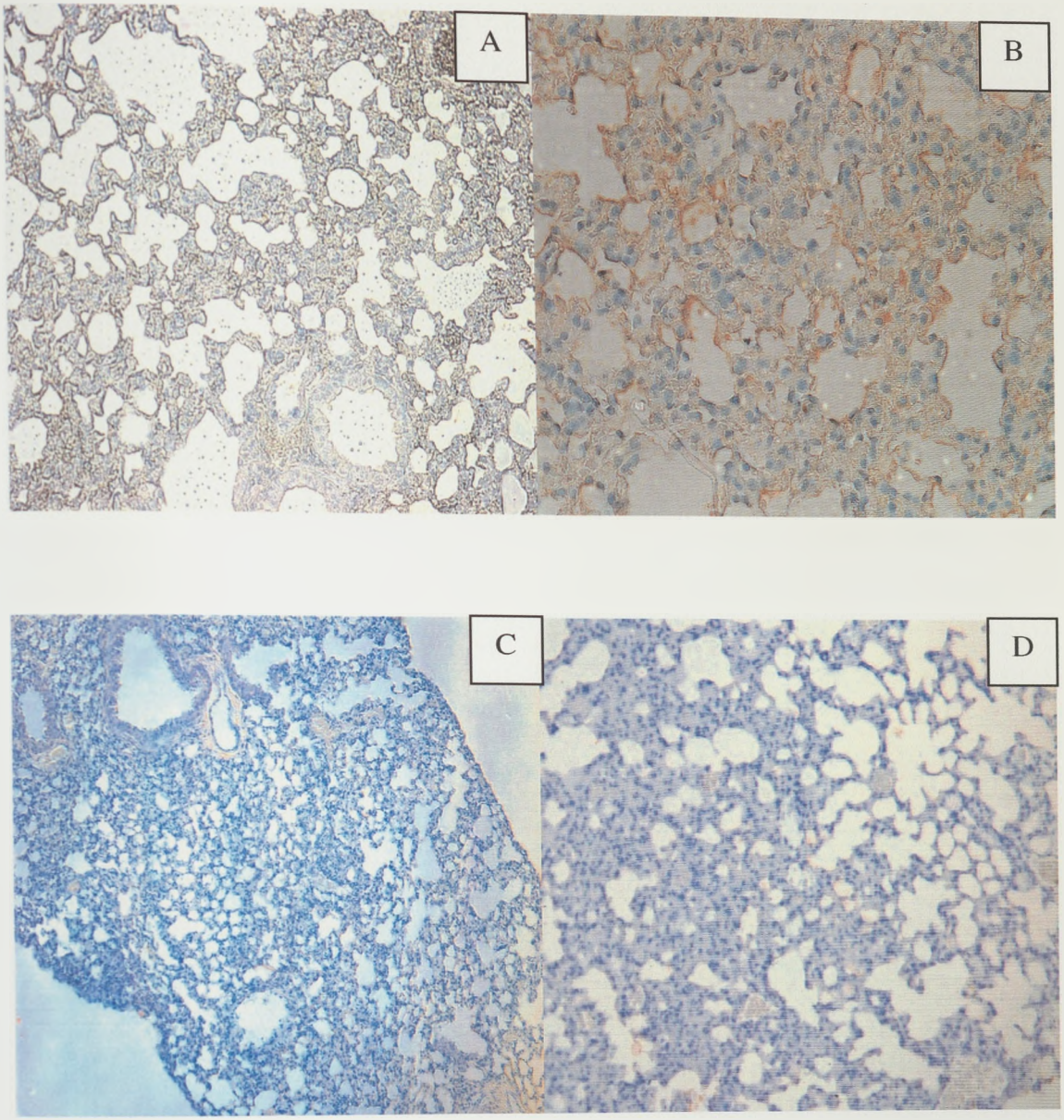

Figure 99: Sections of mouse lung transfected with PEI/GFP complexes (n=4).

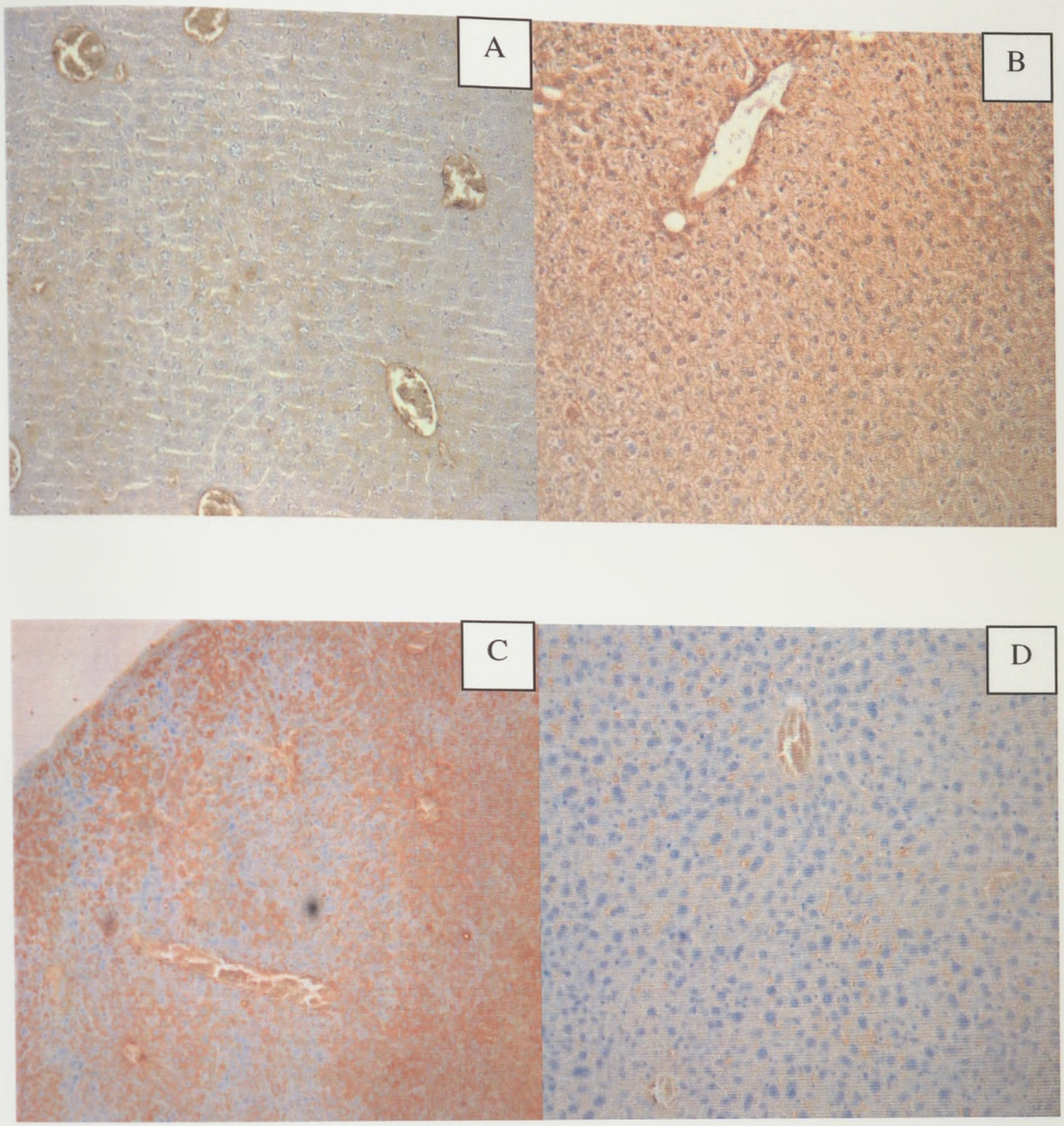

Figure 100: Sections of mouse liver transfected with P-PEI/GFP complexes (n=4).

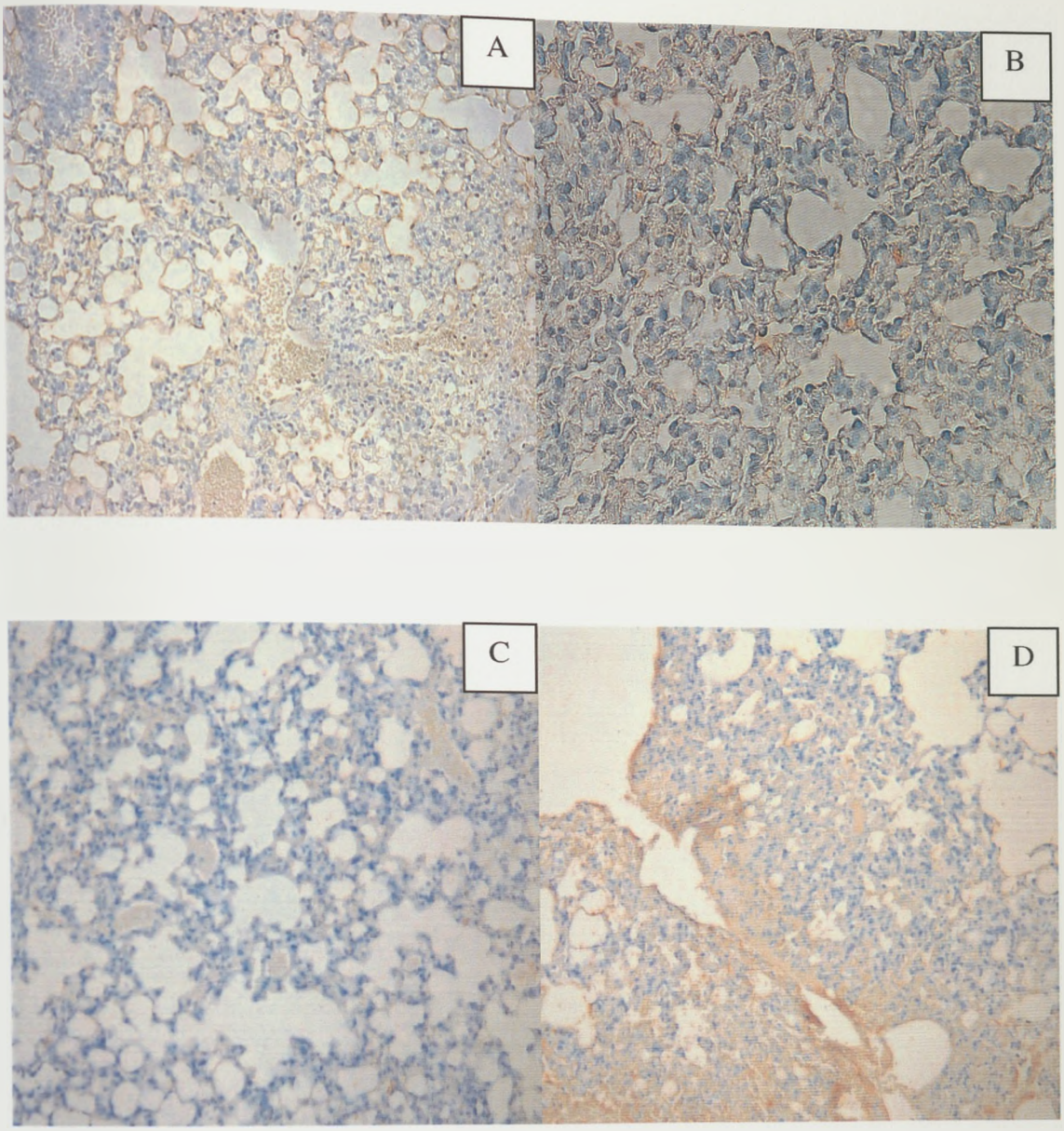

Figure 101: Sections of mouse lung transfected with P-PEI/GFP complexes (n=4).

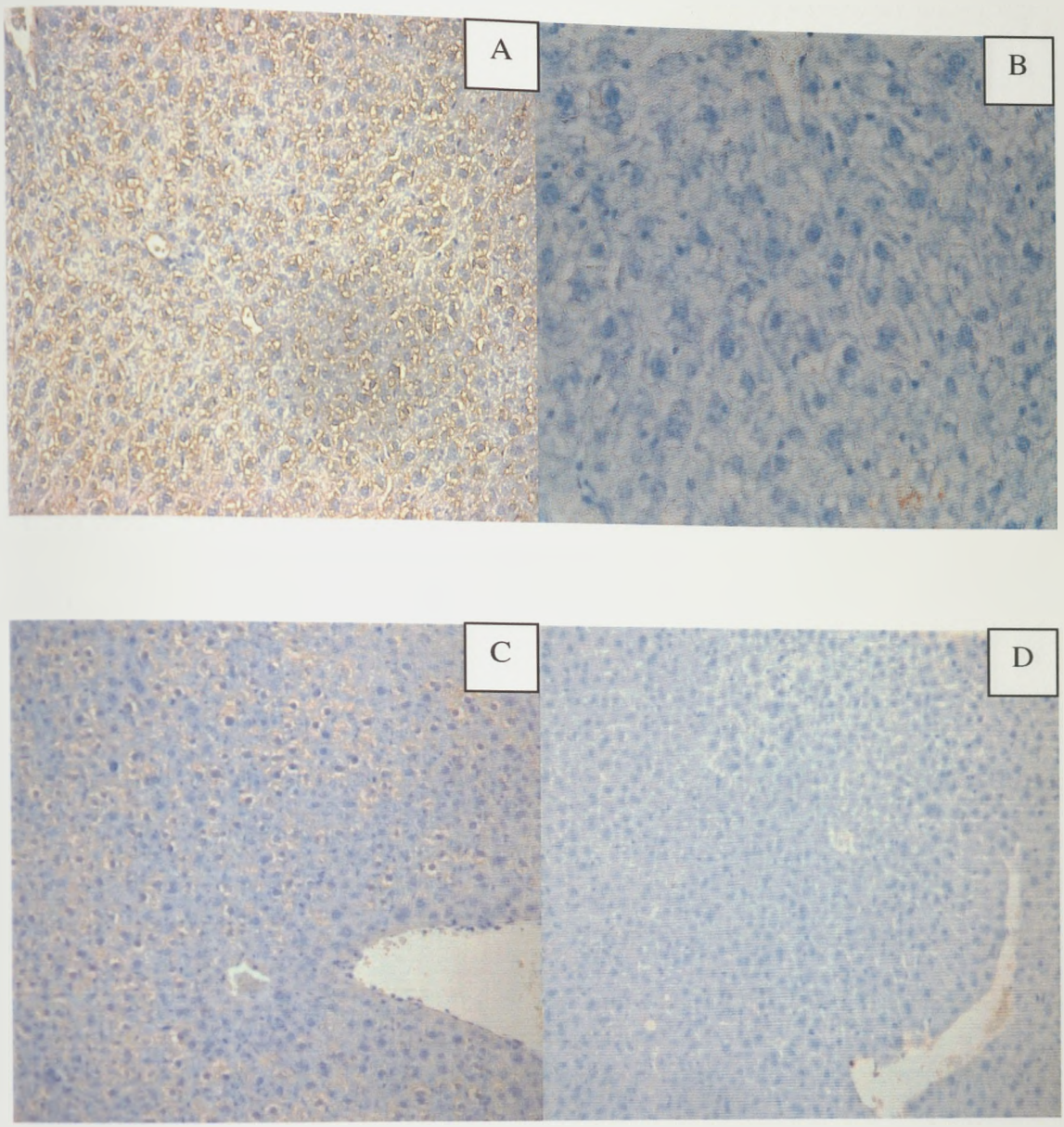

Figure 102: Sections of mouse liver transfected with PP-PEI/GFP complexes (n=4).

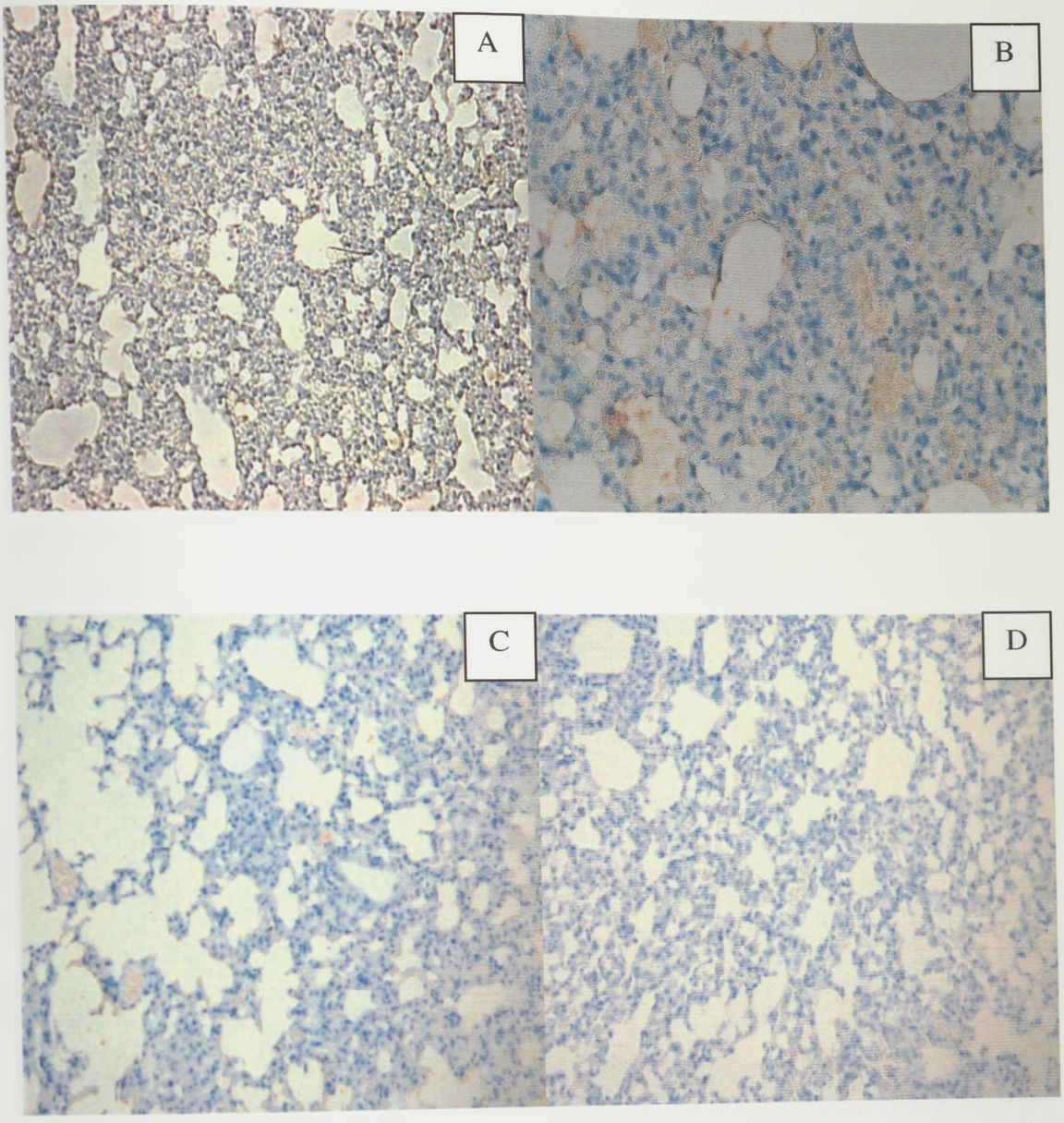

Figure 103: Sections of mouse lung transfected with PP-PEI/GFP complexes (n=4).

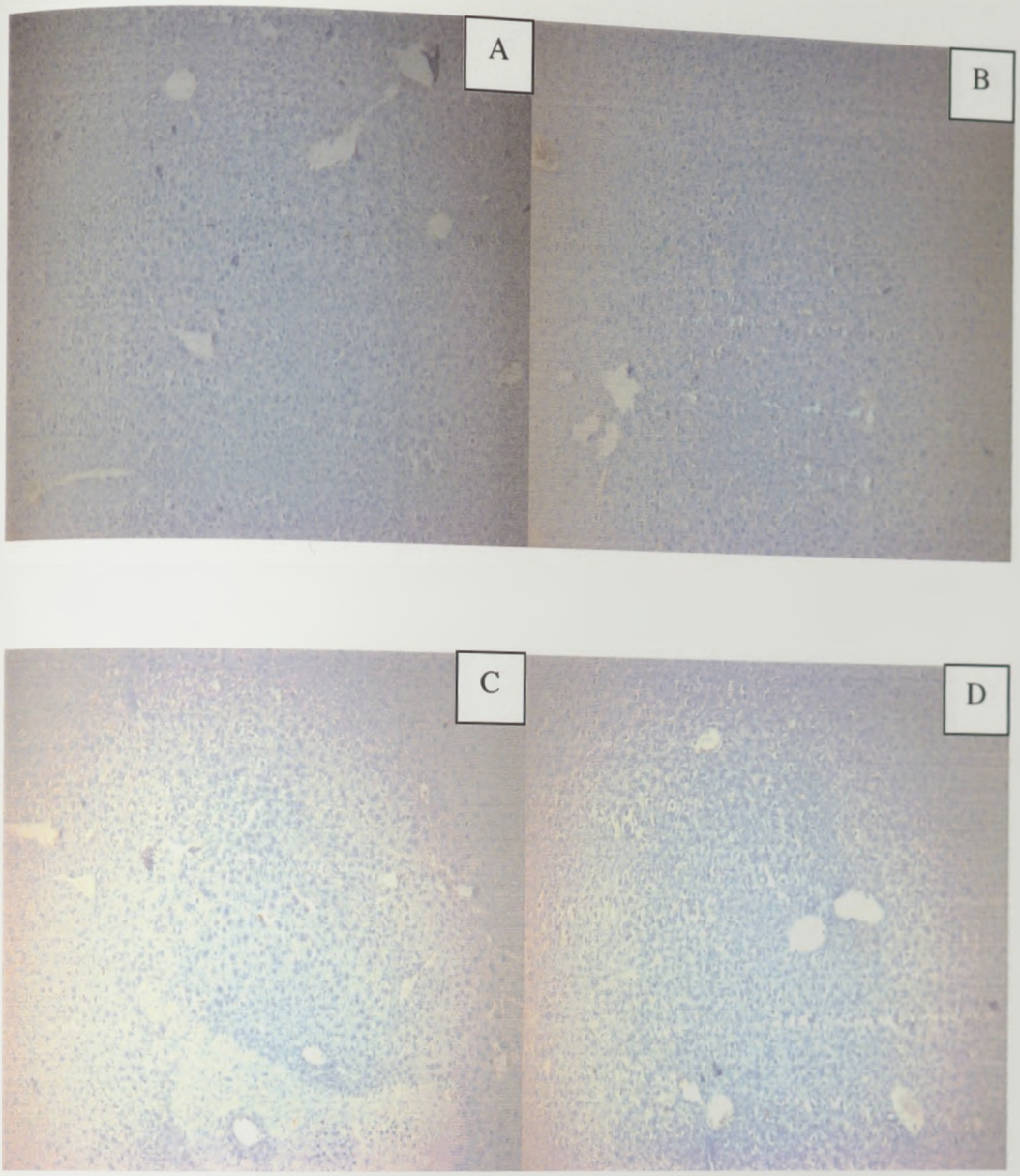

Figure 104: Sections of mouse liver transfected with PP-PEI/Cholesterol/GFP complexes (n=4).

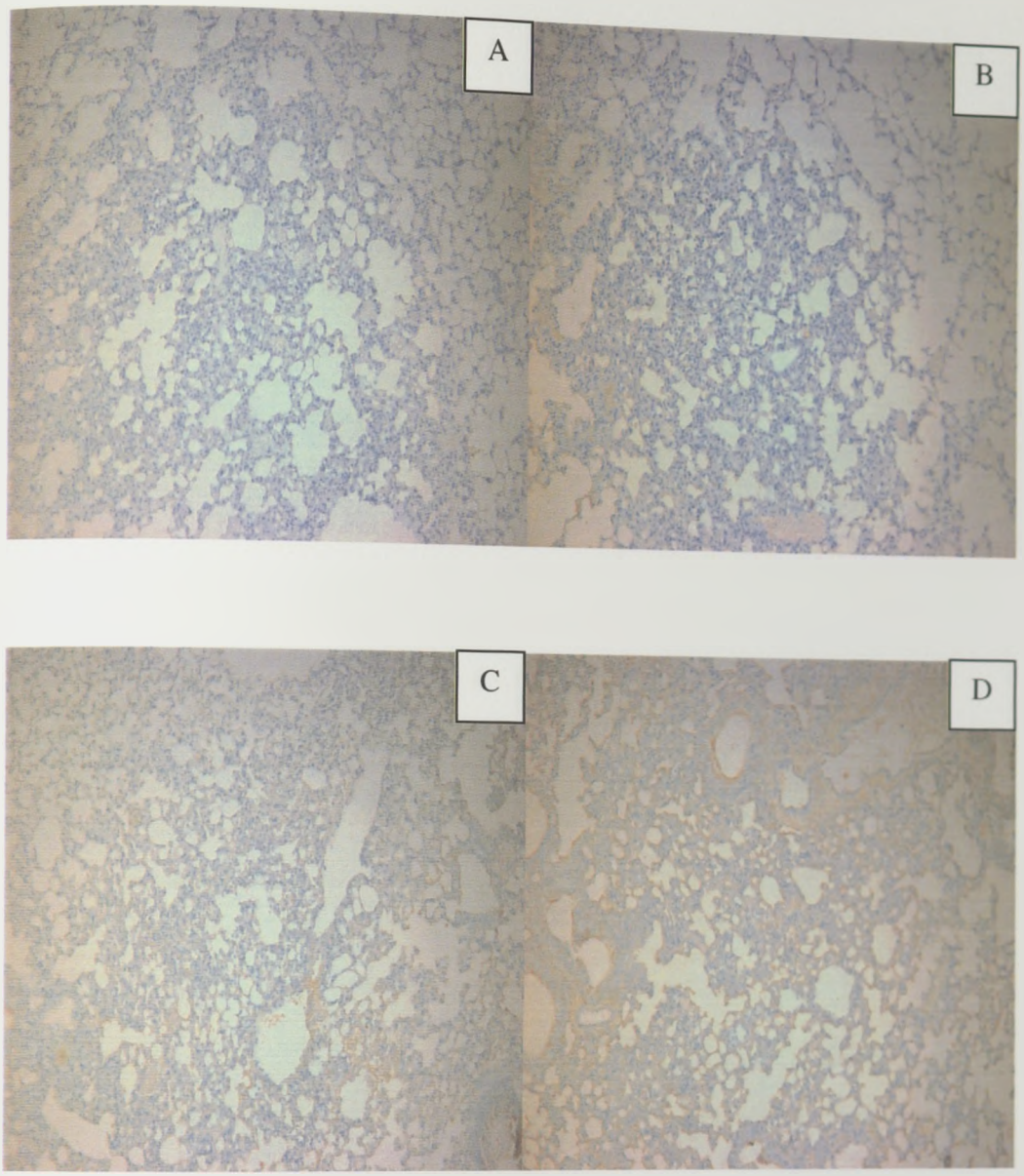

Figure 105: Sections of mouse lung transfected with PP-PEI/Cholesterol/GFP complexes (n=4).

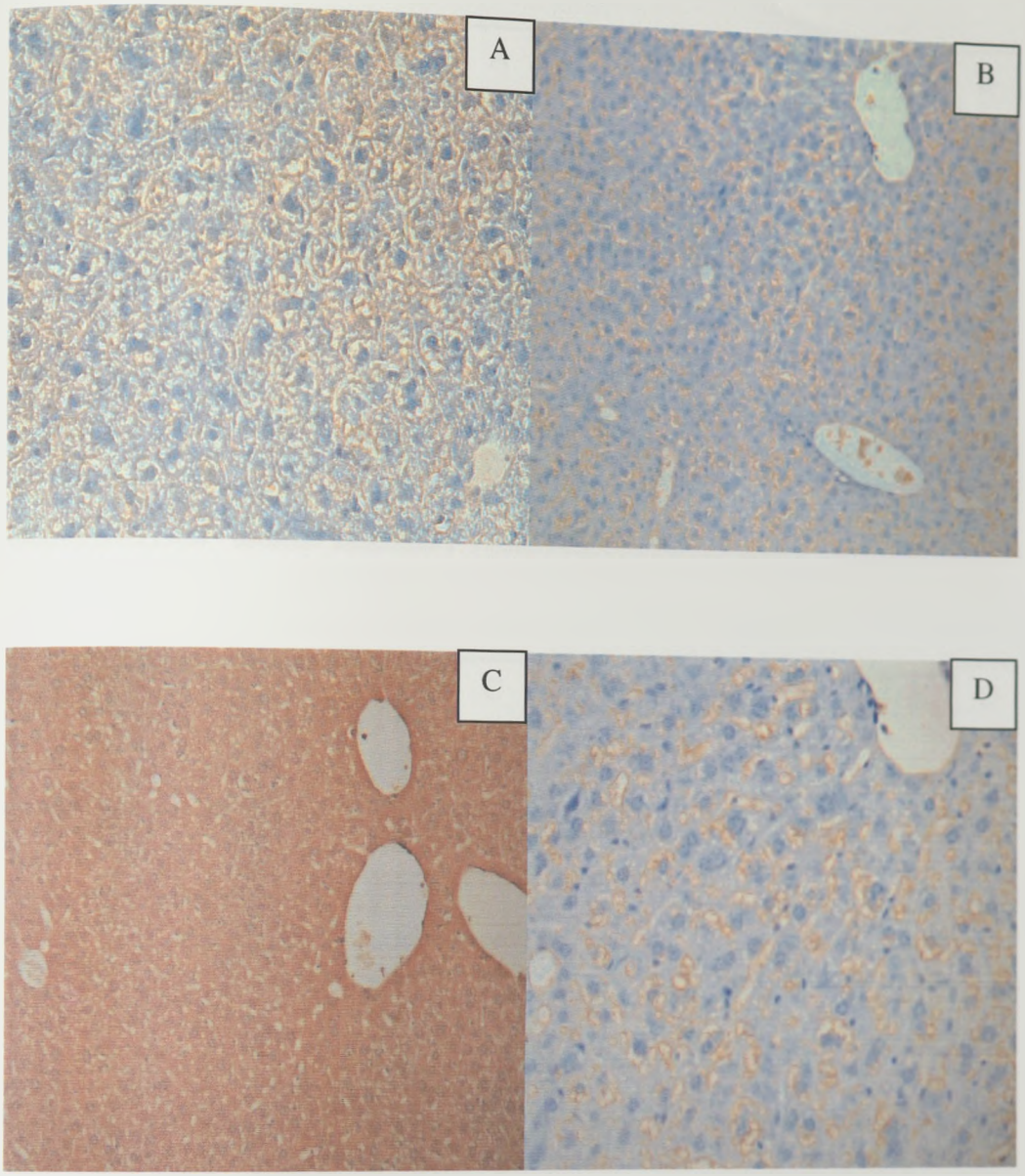

Figure 106: Sections of mouse liver transfected with QPEI/GFP complexes (n=4).

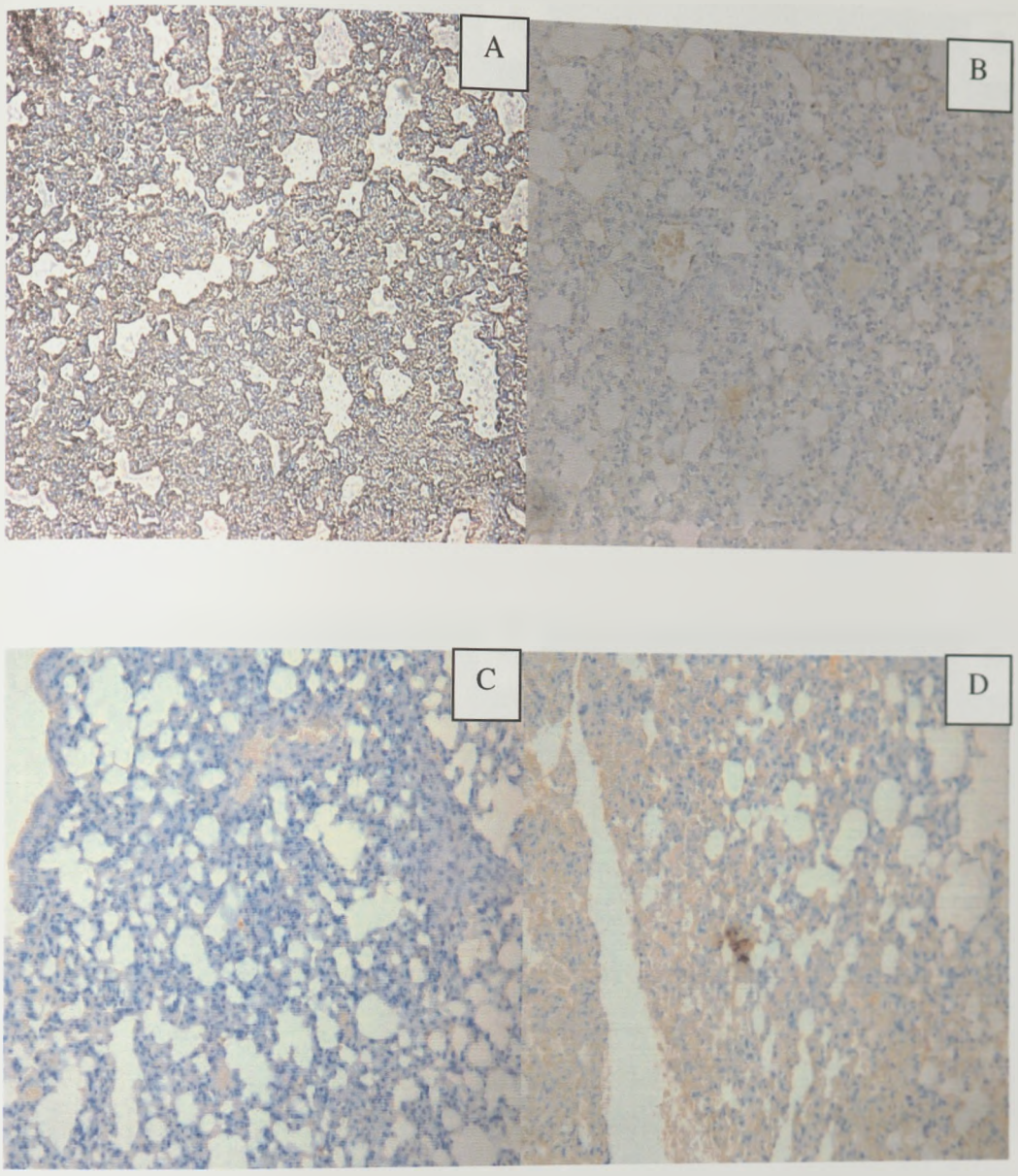

Figure 107: Sections of mouse lung transfected with QPEI/GFP complexes (n=4).

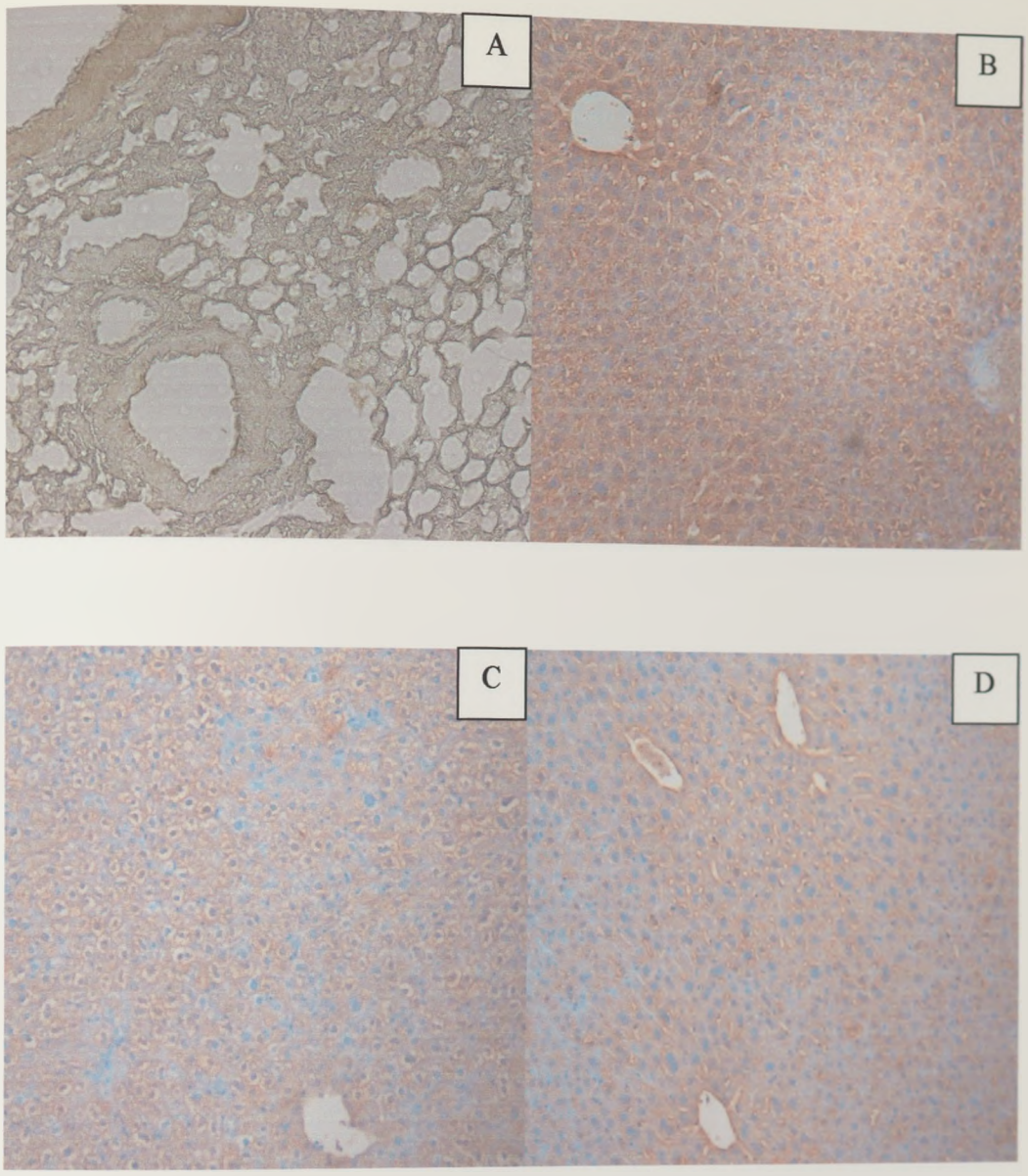

Figure 108: Sections of mouse liver transfected with QPPEI/GFP complexes (n=4).

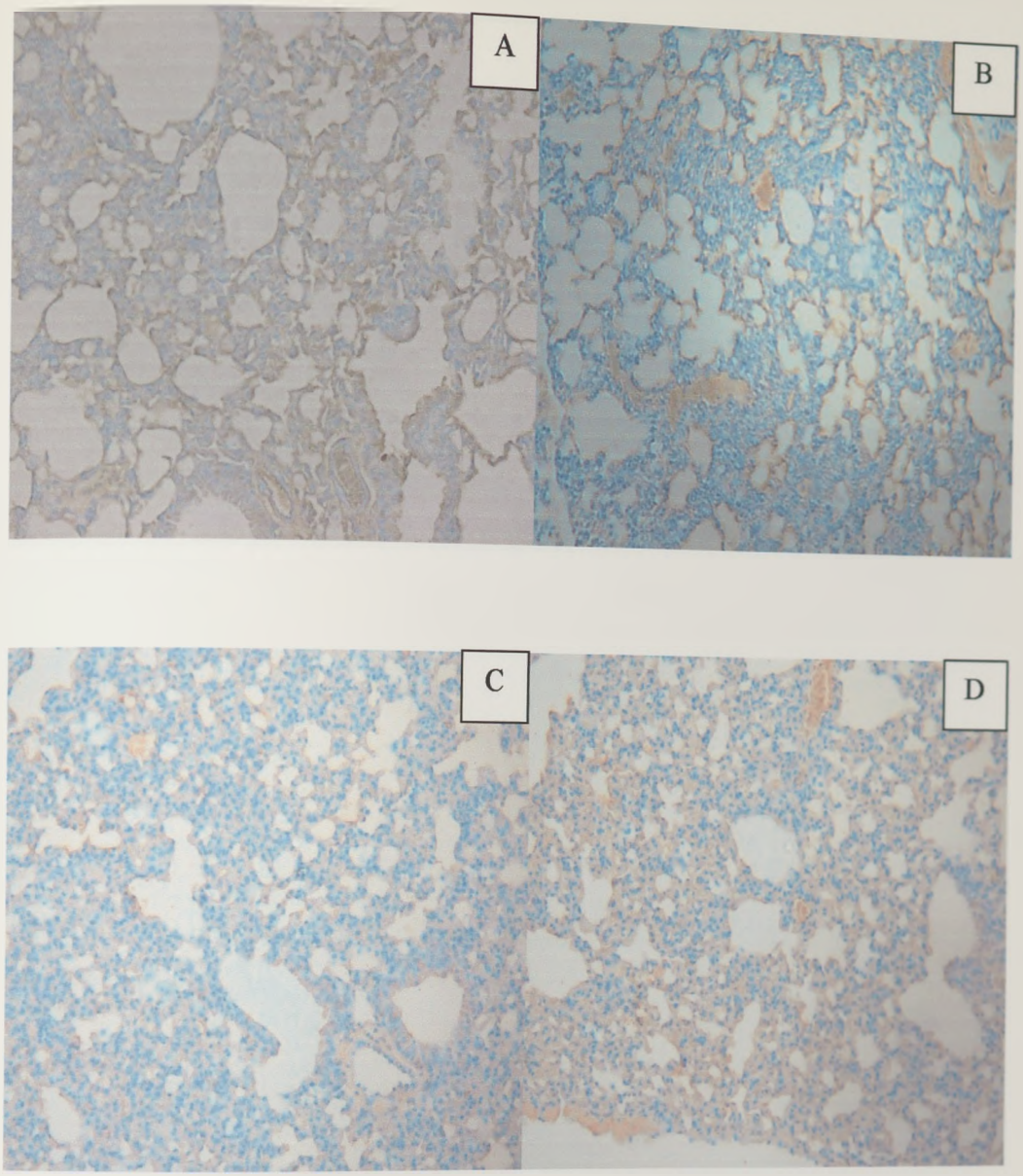

Figure 109: Sections of mouse lung transfected with QPPEI/GFP complexes (n=4).

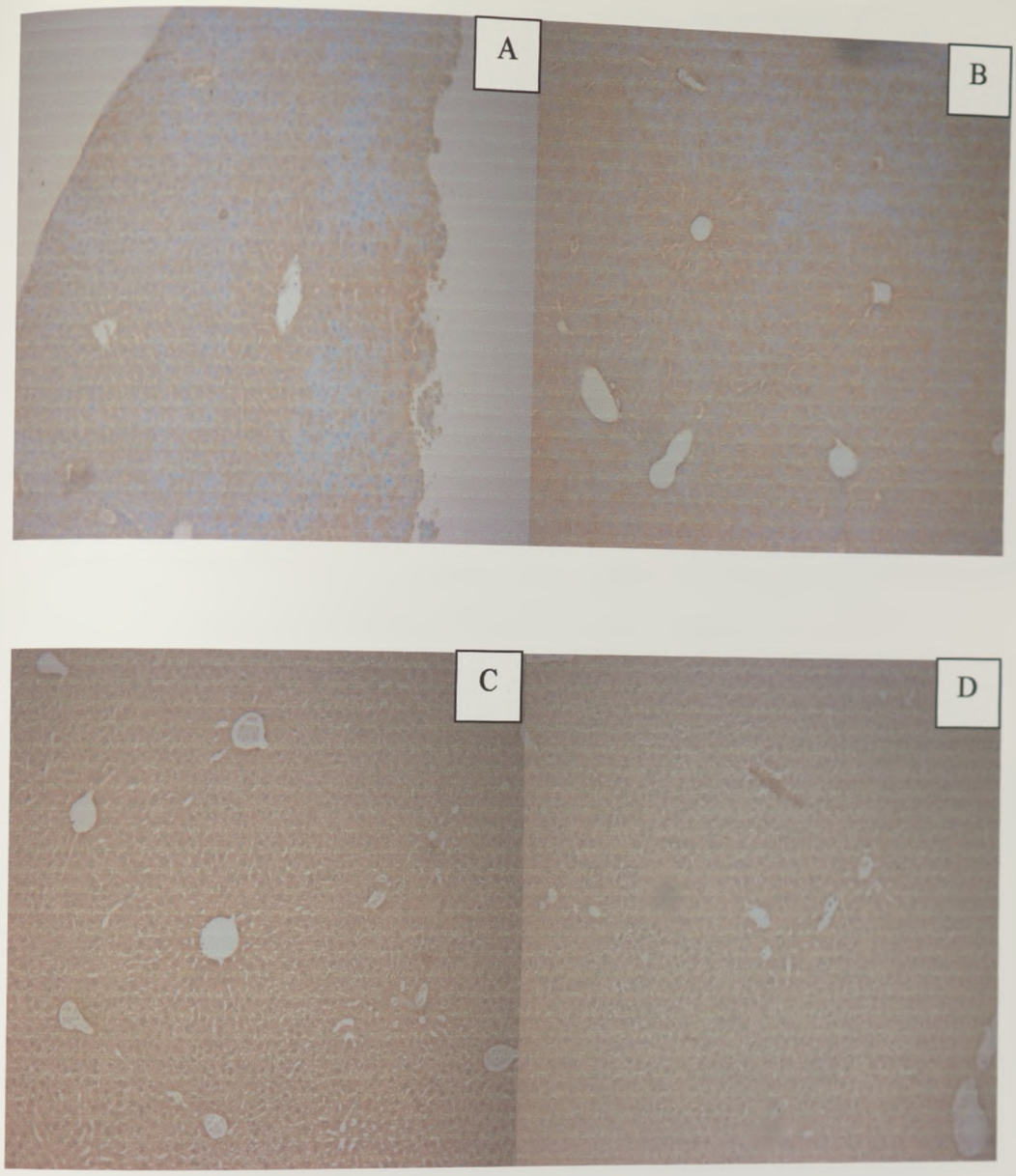

Figure 110: Sections of mouse lung transfected with QPPEI/Cholesterol/GFP complexes (n=4).

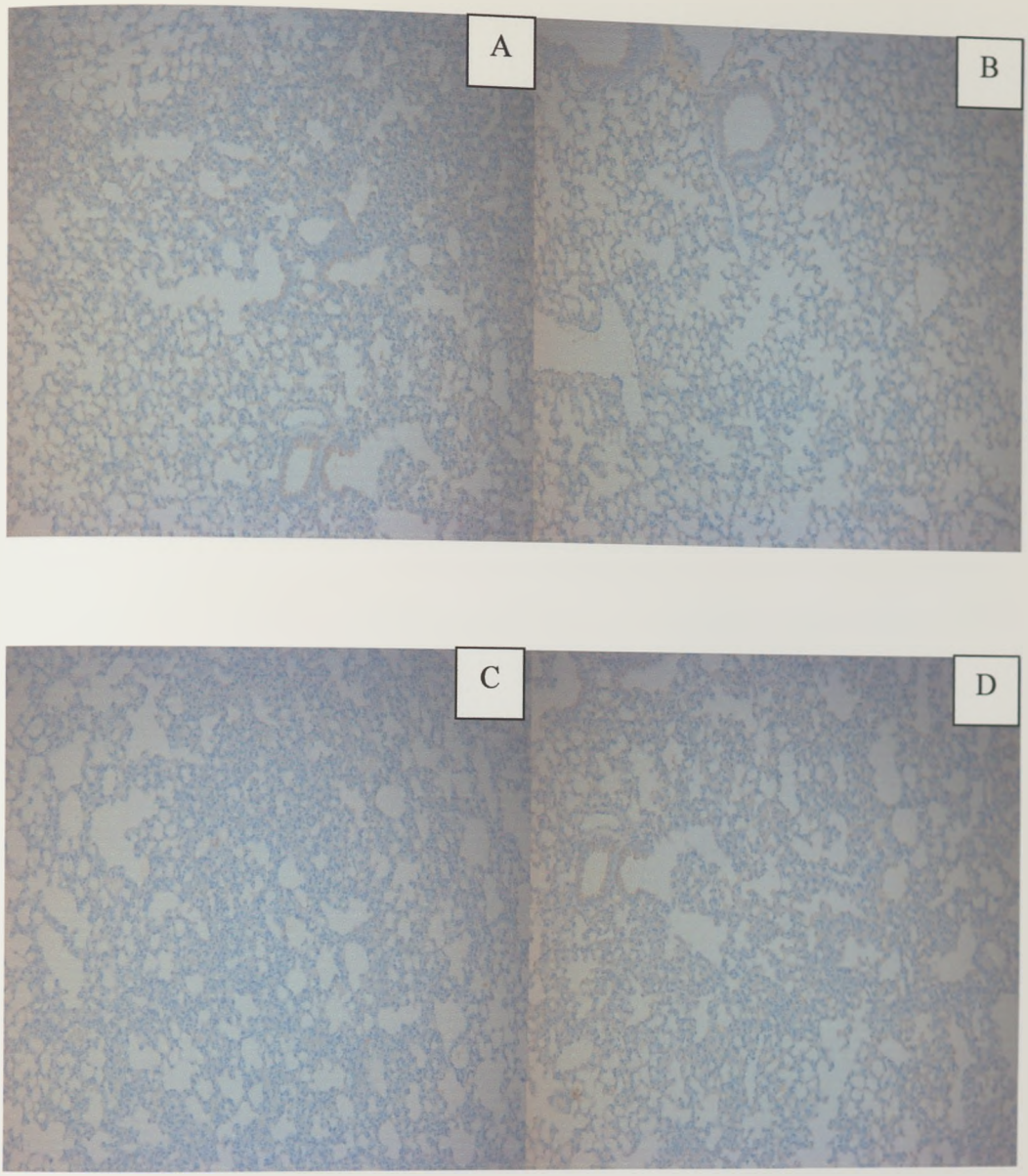

Figure 111: Sections of mouse lung transfected with QPPEI/Cholesterol/GFP complexes (n=4).

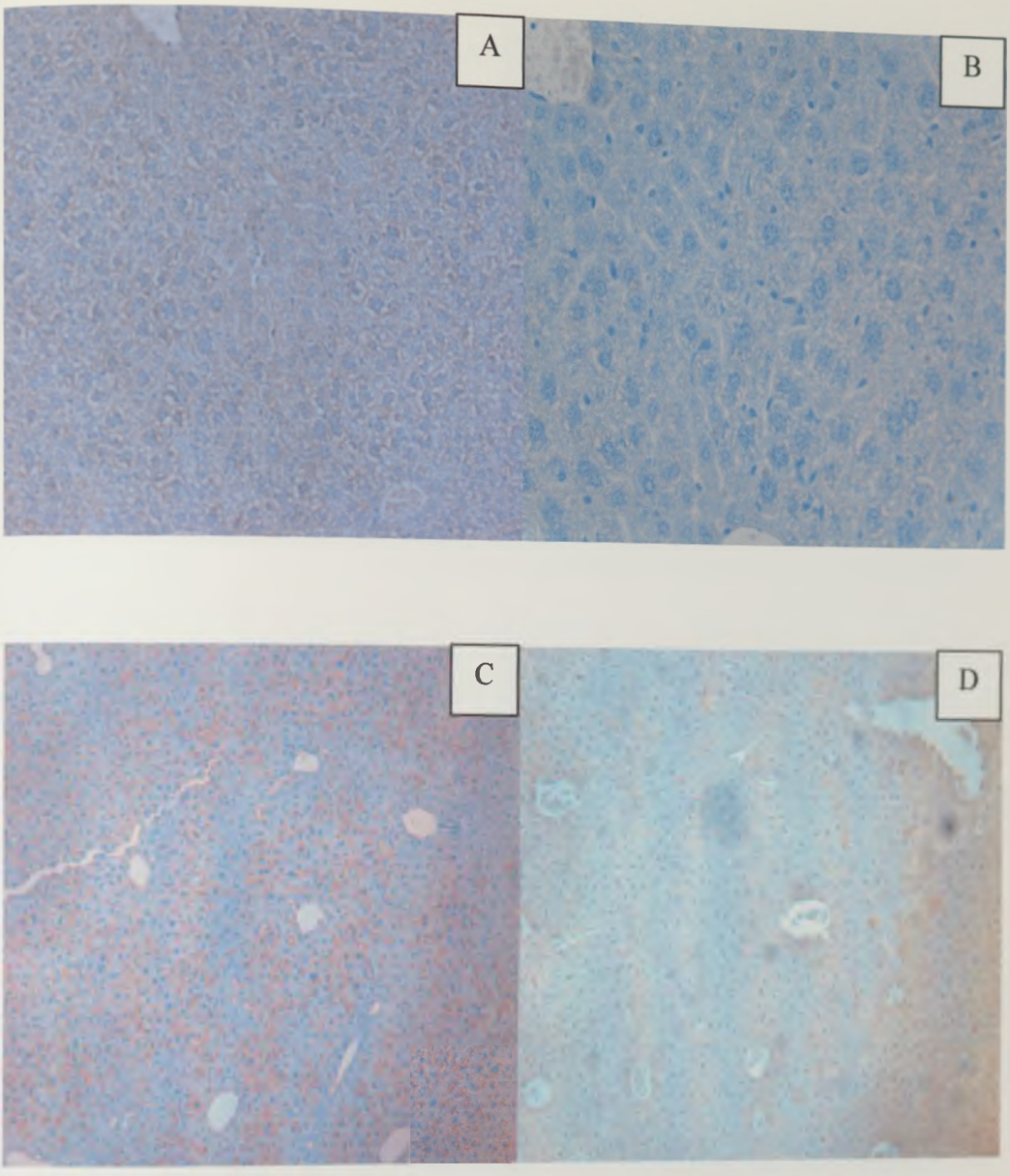

Figure 112: Sections of mouse liver transfected with GFP only (n=4).

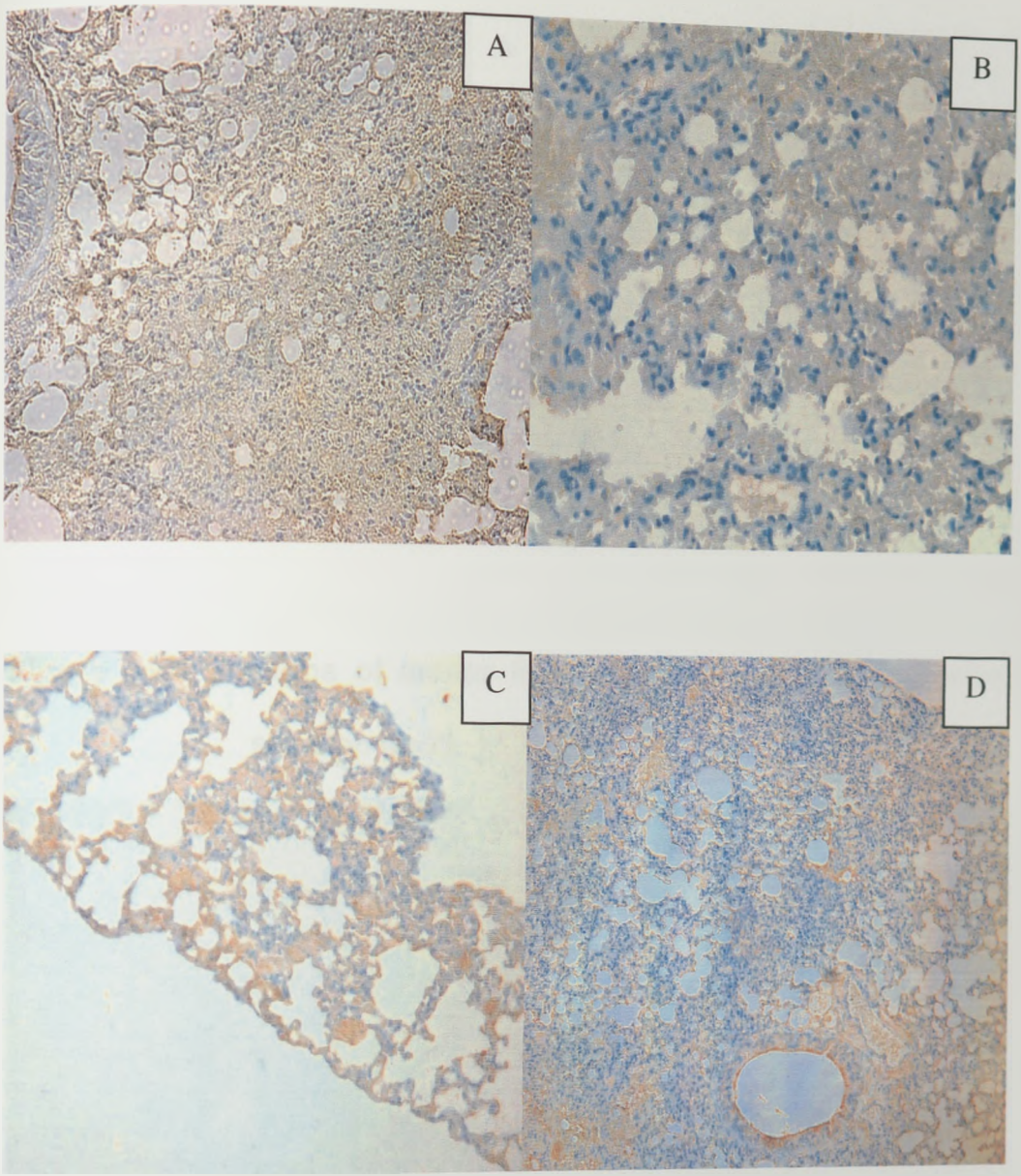

Figure 113: Sections of mouse lung transfected with GFP only (n=4).

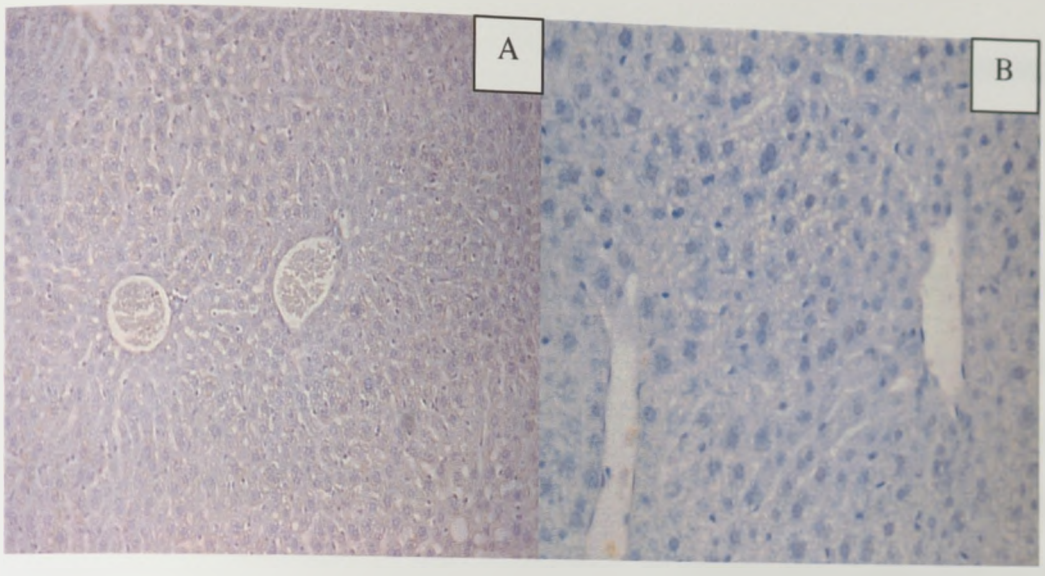

Figure 114: Sections of mouse liver transfected with a 5% dextrose solution (n=2).

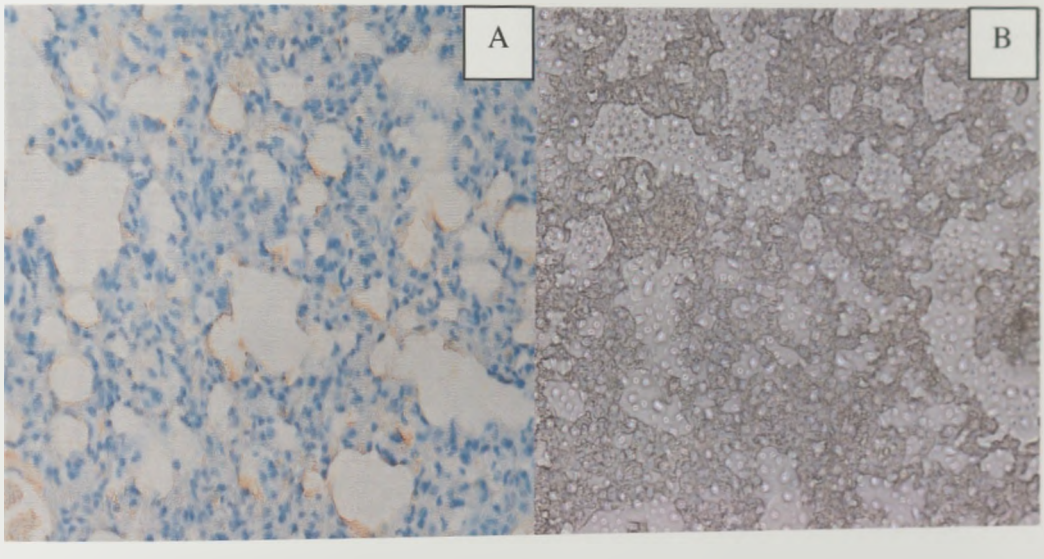

Figure 115: Sections of mouse lung transfected with a 5% dextrose solution (n=2).

In vivo transfection efficiency was measured using a green fluorescent protein (GFP). GFP is a light emitting protein that does not require the presence of any cofactors or substrates for the generation of its green light. The histochemistry procedure applied to the organs stains the GFP expressed by the polymer complexes. This allows the areas of expressed protein in the organs to be viewed visually through a microscope. In using this method the results gained can not be expressed quantitatively only qualitatively, therefore it was necessary to grade the slides due to the number of positive or negative responses shown by the various polymer/DNA complexes (Table 23).

Polymer Complex	Liver response	Lung response
PEI	++	- - - +
P-PEI	++	- - - -
PP-PEI	- - - -	- - - -
PP-PEI/Cholesterol	- - - -	- - - -
QPEI	+	- - - -
QPPEI	+++	- - - -
QPPEI/Cholesterol	++++	- - - -

Table 23: Level of *in vivo* transfection efficiency shown by the polymer/DNA complexes using a GFP reporter gene, where (+) = weak staining, (++) = moderate staining, (+++) = strong staining, (++++) = intense staining and (-) = no staining.

4.4: Discussion of Results

Protein/Erythrocyte Aggregation

The highly positive nature of QPEI, as evidenced by the zeta potential data in chapter 2, may be responsible for the high aggregation with negatively charged proteins such as serum albumin and its subsequent degradation [154]. In both cholesterol-containing formulations the level of protein aggregation was shown to be less than that of their respective cholesterol-free formulations. The presence of cholesterol in the formulations has been previously discussed in section 3.4.1. The cholesterol present in the bilayer of the complex is thought to prevent the proteins from binding to the complex and breaking down the complex [48-50]. The inclusion of PEG in the PP-PEI polymer was carried out with a means of reducing protein aggregation. PEG has been previously attached to PEI/DNA complexes and resulted in a decrease in protein binding to the complex. Ogris *et al* [83] found that the majority of proteins that bound to non-PEGylated complexes had molecular weights >150KDa. The major proteins were identified as IgM, fibronectin, fibrinogen, and complement C3. The inclusion of PEG in this formulation has resulted in a reduced measurement of protein aggregation.

Although the QPPEI and QPPEI/cholesterol complexes proved to be the most highly charged of the complexes (see section 3.3.3), a low protein aggregation was observed in both serum and plasma. The presence of the

palmitoyl chains on the polymer may serve as a barrier to the proteins, in conjunction with the quaternary and tertiary ligands. The mixture of the two modifications may decrease the available sites for any proteins attempting to bind to the complex. The conjugation of palmitoyl side chains in the PPEI formulations provides partial protection from protein binding. This may be due to the fact that the complex is not completely covered with palmitoyl chains and therefore a number of sites may remain available to the proteins. The binding of proteins to the polymer/DNA complex has been thought to increase recognition by cells of the reticuloendothelial system, thus stopping the transfection procedure *in vivo*.

Haemolysis Assay

Each of the modified polymers was shown to have a higher molecular weight than that of the parent PEI polymer (section 2.7.3). This increased molecular weight may reduce the polymers ability to partition into the erythrocytes membranes and the subsequent solublisation that would follow [166]. The overall amphiphillic nature of the P-PEI polymer may explain why the polymer exhibited a slightly increased haemolytic activity when compared to the other modified polymers. This was also observed with modified amphiphillic poly-L-lysines.

MTT Assay

Reports in the literature on the toxic effects of PEI have shown that uncomplexed PEI can harm cells and that when PEI is complexed with DNA its toxicity is greatly reduced [90]. This reduction in PEI's toxicity was seen in both the A549 and A431 cell lines, with the unbound polymers (Figures 86, 87, 88 & 89) and the DNA complexed polymers (Figures 90, 91, 92, & 93). This reduction in toxicity may also be explained by the reduction of available nitrogen's, as most will be complexed with the DNA. The inclusion of cholesterol into some of the formulations also resulted in a reduction in the measured toxicity. The inclusion of cholesterol in the complex would have further reduced the number of available nitrogen's.

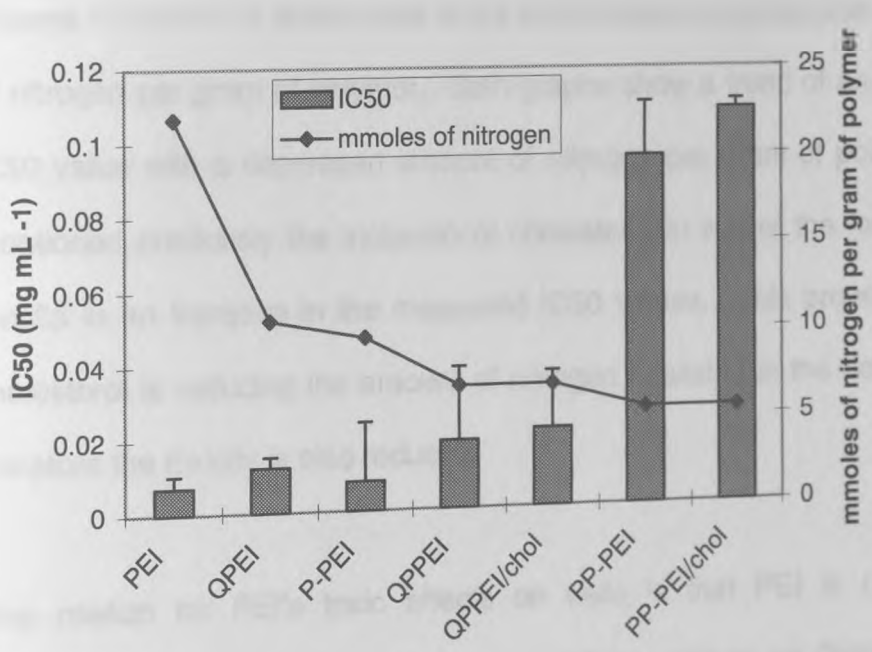

Figure 116: Plot of IC50 values (polymer only A549 cell line) versus available moles of nitrogen per gram of polymer.

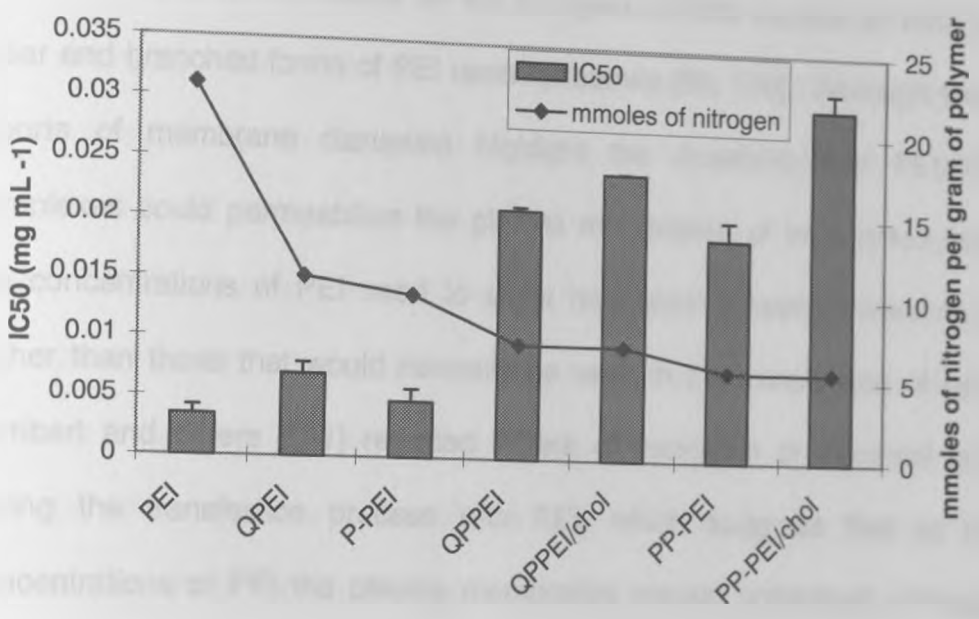

Figure 117: Plot of IC50 values (polymer only A431 cell line) versus available moles of nitrogen per gram of polymer.

Figures 116 and 117 show a plot of the IC50 values versus available mmoles of nitrogen per gram of polymer. Both graphs show a trend of an increased IC50 value with a decreased amount of nitrogen per gram of polymer. As mentioned previously the inclusion of cholesterol in two of the formulations results in an increase in the measured IC50 values. This proves that the cholesterol is reducing the amount of nitrogen available in the polymer and therefore the toxicity is also reduced.

One reason for PEI's toxic effects on cells is that PEI is capable of permeabilising membranes. The permeabilising effects on Gram-negative bacterial outer membranes by PEI have been reported [167, 168]. The

lysosomal disruption of rat hepatocytes has also been linked to PEI [169]. There have also been reports on the fusogenic effects caused by both the linear and branched forms of PEI upon liposomes [94, 170]. Although these reports of membrane disruption highlight the possibility that PEI/DNA complexes could permeabilise the plasma membranes of transfected cells, the concentrations of PEI used to show lysosomal disruption were much higher than those that would normally be used in the transfection of cells. Lambert and others [171] reported a lack of excitation of neuronal cells during the transfection process with PEI, which suggests that at low concentrations of PEI the plasma membranes remain unharmed, although endosomal concentrations of PEI could be increased to a point where the permeabilising effects could occur.

Another possible explanation for the reduction in modified polymer toxicity may be due to the morphology of the complexes. The presence of a vesicular structure in several of the formulations even without the presence DNA may result in a reduction in the number of amine groups available to interact with the cells, as they are contained within the vesicular structure.

***In vitro* Transfection**

By changing the optimal transfection polymer/DNA ratios to nitrogen/phosphate ratios a similar pattern can be seen (Table 18). PEI, P-PEI, PP-PEI and QPEI all exhibit optimal N/P ratios that are close to each other. QPPEI exhibits optimal transfection results at a lower N/P ratio than the other polymers. A possible explanation for this result is that even at higher N/P ratios, where toxicity does not pose a problem, the polymer may bind too efficiently to the DNA and thus the DNA is not being released from the complex [60]. At the lower polymer/DNA ratios there is not enough polymer to fully condense the DNA therefore the transfection efficiency will be compromised. The optimal transfection efficiencies shown by PEI and P-PEI are close to electroneutrality. As QPPEI is highly charged only a small amount of polymer would be needed to neutralise the DNA phosphate charges and stabilise the complex.

This poor result may be due to the presence of the PEG chains, which have been shown to inhibit DNA uptake at a cellular level [151]. QPPEI and QPPEI/cholesterol proved to be the most efficient transfection agent of the modified polymers. The presence of the quaternary and tertiary groups on the molecule may enhance the affinity of the complex towards cellular uptake. The attachment of N-ethyl groups to poly(N-ethyl-4-vinylpyridium bromide) (pVP) was shown increase the complexes ability to penetrate

liposomal membranes, this was thought to be due to the N-ethyl groups mimicking the cell surface [172].

As mentioned in section 3, the size of the polymer/DNA complexes also plays a role in transfection efficiency [92]. Reduced *in vitro* transfection efficiency of smaller PEI and transferrin-PEI complexes was partially attributed to a limited contact with the cells. The larger complexes may have sedimented onto the cells, whereas the smaller complexes stayed in solution and contact with the cells was reduced. The transfection efficiency of smaller complexes has been shown to increase when either the transfection time or the transfection volume was increased [92].

The results gained from the *in vitro* assays can only serve as a rough guide to the efficiency of the modified polymer/DNA complexes when administered *in vivo* and may possibly be totally unrelated.

In vivo Transfection

As can be seen from the *in vivo* results (Table 23) there is a clear difference from the *in vitro* experiments. The transfection efficiency was measured in both the liver and the lung. No positive response was recorded in the lung by any of the polymer/DNA complexes except PEI/DNA which recorded only one positive response, although clear signs of transfection by the majority of the complexes was recorded in the liver. The lack of transfection response in the lung is in contrast to many reports in the literature, which state the lung as being the primary site of transfection. This conflict of results may be explained by the fact that most reports of PEI induced transfection used a luciferase reporter gene. Some groups have reported a reduction in luciferase activity due to the presence of haemoglobin in the organs [173]. The presence of haemoglobin has been suggested to quench any luminescence emitted by luciferase during the reaction with its substrate D-luciferen, as opposed to a direct inhibition of luciferase activity by the haemoglobin [174]. The increased level of haemoglobin in the liver when compared to the lung may explain our results when compared to others.

Both PP-PEI and PP-PEI/Cholesterol failed to produce even a single positive response. This lack of *in vivo* transfection further proves the hypothesis that the inclusion of PEG inhibits the non-specific, ionic interaction-mediated transfection route. The worm like structures formed by PP-PEI upon complexion with DNA may result in cells being unable to internalise the

complexes [101, 151, 175]. Some groups have suggested the use of a smaller molecular weight PEG graft in order to allow the formation of smaller toroidial complexes [176]. Another approach to improving the transfection efficiency in PEGylated PEI polymers was to PEGlyate the polymer after condensation of DNA has taken place [92, 177]. Use of this method allows for the modification of surface available amine groups, thus preventing complex instability due to the PEG chains trapped in the core of the complex.

QPEI also proved to be a poor transfection agent. The zeta potential analysis of the QPEI/DNA complexes showed them to be highly positively charged, rendering it susceptible to aggregation by both plasma proteins and blood erythrocytes (section 4.3.1). Although the QPEI/DNA complexes were non-haemolytic and had a low cytotoxicity the complexes were probably rendered inoperative before they could reach a possible transfection site. Although similarly charged, QPPEI, QPPEI/cholesterol and P-PEI proved to be the most effective transfection agents. The presence of the palmitoyl side chains was shown to give the complexes an increased stability due to the self -assembly, which would help reduce any unspecific interactions with proteins and other blood components. The quaternisation of the P-PEI polymers resulted in an increase in the polymers solubility. This may account for the increased transfection activity from the quaternised polymers. Increased solubility of polymers for gene delivery has been shown to further reduce aggregation and interactions with bio molecules [100, 178].

4.5: Conclusions

The biological characterisation of the modified polymer/DNA complexes revealed both positive and negative results. The majority of the complexes proved to be less susceptible to unspecific protein reactions and interactions with other blood components when compared to the parent compound, except for QPEI, which proved to be more unstable than the unmodified PEI. The polymers were shown to have both a reduced haemolytic activity and cytotoxicity than the parent polymer. *In vitro* analysis of the complexes revealed that the modifications made to PEI resulted in a reduction of transfection efficiency with the best modified polymer (QPPEI) achieving around 60% of PEI's transfection ability. The *in vivo* results showed a poor correlation with the *in vitro* assay. Both QPPEI and QPPEI/cholesterol showed an increased transfection over PEI, with P-PEI proving to be similar in efficiency to that of PEI. The QPEI and PP-PEI formulations were poor transfection agents *in vivo* due to instability in the presence of blood components and steric hindrance of PEG chains.

In conclusion the modifications made to the PEI polymer have resulted in 4 new modified polymers that exhibit a reduction in both toxicity and haemolytic activity. The modified polymers also show an increased resistance to protein and erythrocyte aggregation. *In vitro* analysis of the modified polymers revealed a reduction in the transfection efficiency of the polymer/DNA complexes when compared to the unmodified parent polymer. This is in

contrast to the *in vivo* studies, which showed a marked increase in the transfection efficiency of the P-PEI, QPPEI and QPPEI/cholesterol formulations. We have shown that these structural modifications improve the PEI polymer in its use as a gene delivery vector and these structural variations could be included in the next generation of rationally designed gene transfer agents.

Chapter 5: Final Conclusions

We are able to successfully report the synthesis of four new polymers for use as gene delivery vectors, through the modification of polyethylenimine (25Kda). PEI was modified through the attachment of palmitoyl chains to give P-PEI, the attachment of both palmitoyl and PEG chains to give PP-PEI. PEI and P-PEI were modified through quaternisation, to produce the polymers QPEI and QPPEI. Several analytical techniques were applied to the polymers in order to confirm the modifications were successful. NMR and FTIR analysis confirmed the attachment of the various ligands to the parent PEI polymer. Elemental analysis and a TNBS assay were employed to determine the degree of modification made to the primary amines on the polymers. It was difficult to characterise the level of quaternisation since both quaternary and tertiary amines were produced. Future studies should aim to produce fully quaternised molecules. The degree of modification was expressed in terms of available mmoles of nitrogen per gram of polymer. P-PEI was found to be the least modified polymer (11.4 mmoles), followed by QPEI (10.8 mmoles), QPPEI (8.1 mmoles) and PP-PEI (6.1 mmoles). The molecular weight of the modified polymers was measured through a mixture of Gel Permeation Chromatography (GPC) and laser light scattering techniques. PEI and QPEI were analysed using GPC, the highly charged nature of the polymers was masked through the use of salt in the mobile phase. The presence of palmitoyl chains on the polymers (P-PEI, PP-PEI and QPPEI) resulted in a reduction of solubility in aqueous media and therefore the same technique of masking the polymers charge could not be used. These polymers were analysed using a laser light scattering

technique. Modification of the PEI polymer resulted in an increase in molecular weight. The addition of PEG chains resulted in a large increase in molecular weight (260,000g/mol). The remaining polymers were found to have similar molecular weight values, P-PEI = 46,000, QPEI = 49,000, QPPEI = 48,000g/mol. The GPC-MALLS results were shown to be overestimated when compared to the calculated molecular weight values.

The modified polymers ability to interact with DNA was investigated in chapter 3. All of the polymers were able to condense DNA. The modifications made to the polymers resulted in a difference in the efficiency of DNA condensation. The most heavily modified of the polymers PP-PEI was found to be able to condense DNA only at a higher ratio of polymer to DNA, due to a reduction of the number of available nitrogen's. The second highest modified polymer QPPEI was able to condense DNA at all ratios although at the lower polymer/DNA ratios complete condensation was found only after a certain time period. The inclusion of cholesterol to the PP-PEI and QPPEI formulations was also investigated. The addition of cholesterol to the formulations highlighted a kinetic component to the DNA condensation process. The inclusion of cholesterol in the complex suggests that not all of the polymers nitrogen's are used in the condensation of DNA and may even be inaccessible to the DNA.

Photon correlation spectroscopy and electron microscopy were used to size and visualise the polymer/DNA complexes. The modifications to the

polymers resulted in changes to the morphology of the polymer/DNA complexes. P-PEI was found to able to self-assemble into a vesicular complexes upon probe sonication of the polymer. The inclusion of PEG chains in the PP-PEI polymer resulted in the formation of rod-like assemblies upon probe sonication. This was thought to be due to steric hindrance from the PEG chains. QPEI unhindered by long chains conjugates was able to form small tightly packed spheres similar to that of the parent PEI molecule. QPPEI was able to self assemble with DNA and formed complexes similar to collapsed vesicles. Sonication of PP-PEI and QPPEI with cholesterol resulted in the formation of vesicles. The cholesterol is thought to be included in the bilayer of the vesicle giving added strength to the complex. The surface charge of the polymer/DNA complexes was also measured. PEI and P-PEI were able to form negatively charged complexes at low polymer/DNA ratios and positively charged complexes as the amount of polymer to DNA was increased resulting in an excess of polymer. PP-PEI was positively charged at all the ratios measured with a decrease in charge as the amount of polymer was increased. The quaternary modifications made to the PEI and P-PEI polymers resulted in highly positively charged complexes once condensed with DNA.

In chapter 4 we investigated the biological effects of the modified polymers. The majority of the polymers were shown to be resistant to plasma proteins and blood erythrocytes. Aggregation of erythrocytes was assayed visually under a microscope. The modified polymers showed very little or no

aggregation with the exception of the QPEI/DNA complexes. The same pattern was seen with aggregation of plasma proteins. The QPEI/DNA polymers aggregated quickly followed by the gradual breakdown of the complex. The polymers were also investigated for haemolytic and cytotoxic activity. All of the modified polymers showed very little haemolytic activity when compared to the parent PEI polymer. MTT assays again showed that the polymers were 10 to 500 times less toxic than the unmodified PEI. *In vitro* transfection of the polymer/DNA complexes was investigated over a range of polymer/DNA ratios. The modified polymers were shown to be less efficient gene delivery vectors than the unmodified PEI. QPPEI and QPPEI/cholesterol proved to be the most successful of the modified polymers with a transfection efficiency half that of PEI alone, followed by P-PEI. PP-PEI, PP-PEI/cholesterol and QPEI showed transfection levels little better than naked DNA. The presence of large PEG conjugates was thought to prevent cellular uptake of DNA by the cells. In the case of the QPEI complexes the complexes are thought to have been degraded before transfection can occur.

The polymer/DNA complexes were administered to mice at optimal *in vivo* ratios. The QPPEI and QPPEI/cholesterol formulations proved to be the most efficient transfection agents, giving more positive transfection responses in the liver than the parent PEI polymer. P-PEI was found to have a response similar to that of PEI. The PP-PEI, PP-PEI/cholesterol and QPEI polymers showed no transfection response in either the liver or the

lung. Again the PEG containing polymers whilst being resistant to plasma proteins, would have been hindered by their modification, while the highly positively charged QPEI complexes may have aggregated and been degraded by proteins present in the blood before they could reach their intended target.

The quaternary modification of P-PEI has resulted in a polymer that is a more efficient vector for *in vivo* gene delivery than its parent PEI polymer. The inclusion of cholesterol into the formulation lead to an increased resistance to attack from plasma proteins and blood erythrocytes that resulted in an increased transfection of the plasmid DNA. This work shows that while non-viral vectors still lag behind viral vectors in terms of expressing genes, the careful design of evermore-complicated vectors should result in a safe and efficient molecule for gene delivery.

Future Work

The ^{1}H NMR spectra produced for each of the polymers proved to be inconclusive for most qualitative data. A qualitative ^{13}C NMR technique is available in the form of a two dimensional INADEQUATE (incredible natural abundance double quantum transfer experiment) technique. As use of this method requires a lot of sample (>300mg/ml) to be dissolved in solution, we were not able to use this for our polymers. A more powerful NMR

spectrometer (~600MHz) may be able to perform this experiment at the concentration level we were able to achieve (~30mg/ml).

The modifications made to the PEI polymer (25KDa) lead to greater stability and reduced toxicity. These modifications could be made using a lower molecular weight/linear PEI polymer in order to produce improved toxicity and transfection levels. Other future work could include an investigation into the level of modifications made to the polymer. Lower or increased levels of modification may affect the polymer ability to condense DNA and also the morphology it adopts upon reaction with DNA.

The lack of organ or cell specificity can hamper the application of cationic polymers. Greater transfection efficiency of the polymer/DNA complexes may be achieved through the attachment of ligands that are recognised by a receptor at the cell surface to the carrier. As the liver produced the highest levels of transfection in the *in vivo* experiments, it would be advantageous to act on this through the use of a liver specific targeting ligand. Increased targeting to the liver has been achieved through the use of galactosylated polymers resulting in increased selectivity by the asialoglycoprotein receptor-positive liver parenchymal cells in both *in vitro* and *in vivo tests*.

Chapter 6: References

1. Marchisone, C., et al., *Progress towards gene therapy for cancer.* Journal of Experimental Clinical Cancer Research, 2000. **19**(3): p. 261-270.
2. Mavilio, F. and C. Bordignon, *Gene Therapy.* Nature, 1993. **362**: p. 284.
3. Spack, E.G. and F.L. Sorgi, *Developing non-viral DNA delivery systems for cancer and infectious disease.* DDT, 2001. **6**(4): p. 186-197.
4. Mountain, A., *Gene Therapy: the first decade.* TIBTECH, 2000. **18**: p. 119-128.
5. Boyer, J.D., K.E. Ugen, and A. Shah, *Enhancement of cellular immune response in HIV-1 seropositive individuals: A DNA based trial.* Clinical Immunology, 1999. **90**: p. 100-107.
6. Porteous, D.J., J.R. Dorin, and G. McLachlan, *Evidence for safety and efficacy of DOTAP cationic liposome mediated CFTR gene transfer to the nasal epithelium of pateints with cystic fibrosis.* Gene Therapy, 1997. **4**: p. 210-218.
7. Karp, S.E., et al., *Cytokine secreation by genetically modified non-immunogenic murine fibrosarcoma. Tumor inhibition by IL-2 but not tumor necrosis factor.* Journal of Immunology, 1993. **150**: p. 896-908.
8. Parmiani, G., et al., *Cytokine gene transduction in the immunotherapy of cancer.* Advanced Pharmacology, 1997. **40**: p. 259-307.
9. Rosenberg, S., et al., *Gene transfer into humans - immunotherapy of patients with advanced melanoma, using TIL modified by retroviral gene transduction.* National Journal of Medicine, 1990. **323**: p. 570-578.
10. Rosenberg, S.A., *The development of new cancer therapies based on the molecular identification of cancer regression antigens.* Science America, 1995. **1**: p. 90-100.
11. Palu, G., et al., *Gene therapy of glioblatoma multiforme via combined expression of suicide and cytokine genes: a pilot study in humans.* Gene Therapy, 1999. **6**: p. 330-337.
12. Knudson, A.G. and A.C. Upton, *Tumor suppressor gene workshop.* Cancer Research, 1990. **50**: p. 6765.
13. Weinberg, R.A., *Tumor suppressor genes.* Science, 1991. **254**: p. 1138-1146.
14. Bremner, M.K., et al., *Gene MArking to determine whether autolougous marrow infusion restores long term haematopoiesis in cancer patients.* Lancet, 1993. **342**: p. 1134.
15. May, C., R. Gunther, and R.S. McIvor, *Protection of mice from lethal doses of methotrexate by transplantation with transgenic marrow expressing drug resistant dihyrofolate reductaise activity.* Blood, 1995. **86**: p. 2439-2448.
16. Spencer, H.T., S.E. Sleep, and J.E. Regh, *A gene transfer for marking bone marrow cells resistant to trimexate.* Blood, 1996. **87**: p. 2579-2587.
17. Costantini, L.C., et al., *Gene therapy in the CNS.* Gene Therapy, 2000. **7**: p. 93-109.

18. Smith, A.E., *Viral vectors in gene therapy.* Annual Review of Microbiology, 1995. **49**: p. 807-838.
19. Schatzlein, A.G. and I.F. Uchegbu, *Non-viral vectors in gene delivery.* Anti Cancer Drugs, 2001. **1**(1): p. 17-23.
20. Lasic, D.D., *Liposomes: from physics to applications*. 1993, Amsterdam: Elsevier.
21. Lasic, D.D. and N.S. Templeton, *Liposomes in gene therapy.* Advanced Drug Delivery Reviews, 1996. **20**: p. 221-266.
22. Hwang, S.J. and M.E. Davis, *Cationic polymers for gene delivery: Designs for overcoming barriers to systemic administration.* Current Opinion in Molecular Theraputics, 2001. **3**(2): p. 183-191.
23. Plank, C., et al., *Branched cationic peptides for gene delivery: Role of type and number of cationic residues in formation and in vitro activity of DNA polyplexes.* Human Gene Therapy, 1999. **10**: p. 319-332.
24. Takeuchi, Y. and M. Pizzato, *Retrovirus Vectors*, in *Cancer Gene Therapy: Past achievements and future challenges*, Habib, Editor. 2000, Kluwer Academic/Plenum Publishers: New York. p. 23-35.
25. Collins, M. and C. Porter, *Retroviral Vectors*. Blood Cell Biochemistry, ed. N.G. Testa. Vol. 8. 1998: Plenum Press.
26. Lewis, P., M. Hensel, and M. Emerman, *Human immunodeficiency virus infection of cells arrested in the cell cycle.* Journal of EMBO, 1992. **11**: p. 3053-58.
27. Seth, P., *Adenoviral vectors.* Advances in Experimental Medicine and Biology, 2000. **465**: p. 13-22.
28. Russel, W.C., *Update on adenovirus and its vectors.* Journal of General Virology, 2000. **81**: p. 2573-2604.
29. Stewart, P.L., S.D. Fuller, and R.M. Burnett, *Difference imaging of adenovirus: bridging the resolution gap between X-ray crystallography and electron microscopy.* EMBO Journal, 1993. **16**: p. 1189-1198.
30. Monahan, P.E. and R.J. Samulski, *Adeno-associated virus vectors for gene therapy: more pros than cons?* Molecular Medicine Today, 2000. **6**: p. 433-440.
31. Monahan, P.E. and R. Samulski, *AAV vectors: is clinical success on the horizon.* Gene Therapy, 2000. **7**: p. 24-30.
32. Xiao, W., *Gene Therapy vectors based on adeno associated virus type 1.* Journal of Virology, 1999. **73**: p. 3994-4003.
33. Bloomer, U., L. Naldini, and T. Kafri, *Highly efficient and sustained gene transfer in adult neurons with a lentivirus vector.* Journal of Virology, 1997. **71**: p. 6641-9.
34. Kafri, T., et al., *Sustained expression of genes delivered into liver and muscle by lentiviral vectors.* Nature Genetics, 1997. **17**: p. 314-317.
35. Wolff, J.A., *Long term persistance of plasmid DNA and foreign gene expression.* Human Molecular Genetics, 1992. **1**: p. 363-369.
36. Hengge, U., *Cytokine gene expression in epidermis with biological effects following injection of naked DNA.* National Genetics, 1995. **10**: p. 161-166.

37. Yang, N.S., *In vivo and in vitro gene transfer to mammilian somatic cells by particle bombardment.* Procceeding of the National Academy of Sciences of the USA, 1990. **87**: p. 9568-9572.
38. Nishi, T., *Treatment of cancer using pulsed electric field in combination with chemotherapeutic agents or genes.* Human Cell, 1997. **10**: p. 81-86.
39. Zhang, L., *Depth targeted efficient gene delivery and expression in the skin by pulsed electric fields.* Biochemica Biophysica Research Communication, 1996. **220**: p. 633-636.
40. Rols, M.P., *In vivo electrically mediated protein and gene transfer in murine melanoma.* Nature Biotechnology, 1998. **16**: p. 168-171.
41. Li, S. and L. Huang, *Nonviral gene therapy: promises and challenges.* Gene Therapy, 2000. **7**: p. 31-34.
42. Barenholz, Y., *Liposome application: problems and prospects.* Current Opinion in Colloids and Interface Science, 2001. **6**(12): p. 66-77.
43. Pedroso de Lima, M.C., et al., *Cationic lipid-DNA complexes in gene delivery:from biophysics to biological applications.* Advanced Drug Delivery Reviews, 2001. **47**: p. 277-294.
44. Woodle, M.C. and P. Scaria, *Cationic liposomes and nucleic acids.* Current Opinion in Colloid & Interface Science, 2001. **6**: p. 78-84.
45. Feglner, P.L., T.R. Gadek, and M. Holm, *Lipofectin: a highly efficient, lipid-mediated DNA transfection procedure.* Procceedings of the National Academy of Sciences USA, 1987. **84**: p. 7413-7417.
46. Kaneda, Y., *Virosomes: evolution of the liposome as a targeted drug delivery system.* Advanced Drug Delivery Reviews, 2000. **43**: p. 197-205.
47. Senior, J.H., K.R. Trimble, and R. Maskiewitz, *Interaction of positively charged liposomes with blood.* Biochimica et Biophysica Acta, 1991. **1070**: p. 163-172.
48. Ishiwata, H., et al., *Characteristics and biodistribution of cationic liposomes and their DNA complexes.* Journal of Controlled Release, 2000. **69**: p. 139-148.
49. Hong, K., et al., *Stabilisation of cationic liposome-plasmid DNA complexes by polyamines and poly(ethylene glycol)-phospholipid conjugates for efficient in vivo gene delivery.* FEBS Letters, 1997. **400**: p. 233-237.
50. Semple, S.C., A. Chonn, and P.R. Cullis, *Influence of cholesterol on the association of plasma proteins with liposomes.* Biochemistry, 1996. **35**: p. 2521-2525.
51. Meyer, O., et al., *Cationic liposomes coated with polyethylene glycol as carriers for oligonucleotides.* Journal of Biological Chemistry, 1998. **273**: p. 15621-15627.
52. Brigham, K.L., et al., *In vivo transfection of murine lungs with a functioning prokaryotic gene using a liposome vesicle.* American Journal of Medical Science, 1989. **298**: p. 278-281.
53. Malone, R.W., *mRNA transfection of cultured eukaryotic cells and embryos using cationic liposomes.* Focus, 1989. **11**: p. 62-66.

54. Nabel, E.G., et al., *Gene transfer in vivo with DNA-liposome complexes: lack of autoimmunity and gonadal localisation.* Human Gene Therapy, 1992. **3**: p. 649-656.
55. Stewart, M.K., et al., *Gene transfer in vivo with DNA-lipid complexes: safety and acute toxicity in mice.* Human Gene Therapy, 1992. **3**: p. 267-275.
56. Hyde, S.C., et al., *Correction of the ion transport defect in cystic fibrosis transgenic mice by gene therapy.* Nature Medicine, 1993. **362**: p. 250-255.
57. Alton, E.W.F.W., et al., *Non-invasive liposome-meiated gene delivery can correct the ion transport defect in cystic fibrosis mutant mice.* Nature Genetics, 1993. **5**: p. 135-142.
58. Nabel, G.J., et al., *Direct gene transfer with DNA-liposome complexes in melanoma: expression, biologic activity and lack of toxicity in humans.* Proceedings of the NAtional Academy of Sciences USA, 1993. **90**: p. 11307-11311.
59. Caplen, N.J., et al., *Liposome mediated CFTR gene transfer to the nasal epithelium of pateints with cystic fibrosis.* Nature Medicine, 1995. **1**: p. 39-46.
60. De Smedt, S.C., J. Demeester, and W.E. Hennink, *Cationic polymer based gene delivery systems.* Pharmaceutical Research, 2000. **17**(2): p. 113-126.
61. Zauner, W., M. Ogris, and E. Wagner, *Polylysine based transfection systems utilising receptor mediated delivery.* Advanced Drug Delivery Reviews, 1998. **30**: p. 97-113.
62. Wu, G.Y. and C.H. Wu, *Receptor mediated in vitro gene transformation by a soluble DNA carrier.* Journal of Biological Chemistry, 1987. **262**: p. 4429-4432.
63. Wu, G.Y. and C.H. Wu, *Receptor-mediated gene delivery and expression in vivo.* Journal of Biological Chemistry, 1988. **263**: p. 14621-14624.
64. Perales, J.C., et al., *Gene transfer in vivo: sustained expression and regulation of genes introduced into the liver by receptor targeted uptake.* Proceedings of the National Academy of Sciences USA, 1994. **91**: p. 4086-4090.
65. Hashida, M., et al., *Targeted delivery of plasmid DNA complexed with galactosylated poly-L-lysine.* Journal of Controlled Release, 1998. **53**: p. 301-310.
66. Ferkol, T., et al., *Gene transfer into the airway epithelium of animals by targeting the polymeric immunoglobulin receptor.* Journal of Clinical Investigation, 1995. **95**: p. 493-502.
67. Brown, M.D., et al., *Preliminary characterisation of novel amino acid based polymeric vesicles as gene and drug delivery agents.* Bioconjugate Chemistry, 2000(11): p. 880-891.
68. Stingl, G., et al., *Phase I study to the immunotherapy of metastatic malignant melanoma by a cancer vaccine consisting of autologous cancer cells transfected with the human IL-2 gene.* Human Gene Therapy, 1996. **7**: p. 551-563.

69. Tomalia, D.A. and G.R. Killat, *Encyclopedia of Polymer Science and Engineering*. Vol. 1. 1998, New York: Wiley.
70. Dermer, O.C. and G.E. Ham, *Ethylenimine and Other Aziridines*. 1969, New York: Academic Press.
71. Li, D., S. Zhu, and R.H. Pelton, *Preparation and characterization of graft copolymers of polyacrylamide and polyethylenimine.* European Polymer Journal, 1998. **34**(8): p. 1199-1205.
72. Boussif, O., et al., *A versatile vector for gene and oligonucleotide transfer into cells in culture and in vivo: Polyethylenimine.* Proceedings of the National Academy of Sciences of the USA, 1995. **92**: p. 7297-7301.
73. Haensler, J. and F.C. Szoka, *Polyamidoamine cascade polymers mediate efficient transfection of cells in culture.* Bioconjugate Chemistry, 1993. **4**: p. 372-379.
74. Behr, J.P., *Gene transfer with synthetic cationic amphiphiles - prospects for gene therapy.* Bioconjugate Chemistry, 1994. **5**: p. 382-389.
75. Godbey, W.T., K.K. Wu, and A.G. Mikos, *Poly(ethylenimine) and its role in gene delivery.* Journal of Controlled Release, 1999. **60**: p. 149-160.
76. Abdallah, B., et al., *A powerful nonviral vector for in vivo gene transfer into the adult mammalian brain: Polyethylenimine.* Human Gene Therapy, 1996. **7**: p. 1947-1954.
77. Boletta, A., et al., *Nonviral gene delivery to the rat kidney with polyethylenimine.* Human Gene Therapy, 1997. **8**: p. 1243-1251.
78. Goula, D., et al., *Polyethylenimine-based intravenous delivery of transgenes to mouse lung.* Gene Therapy, 1998. **5**: p. 1291-1295.
79. Godbey, W.T., K.K. Wu, and A.G. Mikos, *Size matters: Molecular weight affects the efficiency of poly(ethylenimine) as a gene delivery vehicle.* Journal of Biomedical Materials Research, 1999. **45**: p. 268-275.
80. Fischer, D., et al., *A novel non-viral vector for DNA delivery based on low molecular weight, branched polyethylenimine: Effect of molecular weight on transfection efficiency and cytotoxicity.* Pharmaceutical Research, 1999. **16**(8): p. 1273-1279.
81. von Harpe, A., et al., *Characterisation of commercially avaiable and synthesised poyethylenimines for gene delivery.* Journal of Controlled Release, 2000. **69**: p. 309-322.
82. Holmberg, K., et al., *Grafting with hydrophillic polymer chains to prepare protein-resistant surfaces.* Colloids and Surfaces A: Physicochemical and Engineering Aspects, 1997. **123-124**: p. 297-306.
83. Ogris, M., et al., *PEGylated DNA/transferrin-PEI complexes: reduced interaction with blood components, extended circulation in blood and potential for systematic gene delivery.* Gene Therapy, 1999. **6**: p. 595-605.

84. Vinogradov, S.V., T.K. Bronich, and A.V. Kabanov, *Self-assembly of polyamine-poly(ethylene glycol) copolymers with phosphorothioate oligonucleotides.* Bioconjugate Chemistry, 1998. **9**: p. 805-812.
85. Remy, J., et al., *Gene transfer with lipospermines and polyethylenimines.* Advanced Drug Delivery Reviews, 1998. **30**: p. 85-95.
86. Zanta, M., et al., *In vitro gene delivery to hepatpcytes with galactosylated polyethylenimine.* Bioconjugate Chemistry, 1997. **8**: p. 839-844.
87. Bandyopadhyay, P., et al., *Enhanced gene transfer into HuH-7 cells and primary rat hepatocytes using targeted liposomes and polyethylenimine.* Biotechniques, 1998. **25**: p. 282-292.
88. Baker, A., et al., *Polyethylenimine (PEI) is a simple, inexpensive and effective reagent for condensing and linking plasmid DNA to adenovirus for gene delivery.* Gene Therapy, 1997. **4**: p. 773-782.
89. Wagner, W., *Effects of membrane-active agents in gene delivery.* Journal of Controlled Release, 1998. **53**: p. 155-158.
90. Godbey, W.T., et al., *Improved packing of poly(ethylenimine)/DNA complexes increases transfection efficiency.* Gene Therapy, 1999. **6**: p. 1380-1388.
91. Tang, M.X. and F.C. Szoka, *The influence of polymer structure on the interactions of cationic polymers with DNA and morphology of the resulting complexes.* Gene Therapy, 1997. **4**: p. 823-832.
92. Ogris, M., et al., *The size of DNA/transferrin-PEI complexes is an important factor for gene expression in cultured cells.* Gene Therapy, 1998. **5**: p. 1425-1433.
93. Klotz, I.M., G.P. Royer, and A.R. Sloniewsky, *Macromolecule-small molecule interactions. Strong bining and cooperativity in a model synthetic polymer.* Biochemistry, 1969. **8**(12): p. 4752-4756.
94. Oku, N., et al., *Low pH induced membrane fusion of lipid vesicles containing proton-sensitive polymer.* Biochemistry, 1987. **26**: p. 8145-8150.
95. Noding, G. and W. Heitz, *Amphiphilic poly(ethyleneimine) based on long chain alkyl bromides.* Macromol. Chem. Phys., 1998. **199**(8): p. 1637-1644.
96. Nucci, M.L., R. Shorr, and A. Abuchowski, *The theraputic value of poly(ethylene glycol)-modified proteins.* Advanced Drug Delivery Reviews, 1991. **6**: p. 133-151.
97. Katre, N.V., *The Conjugation of Proteins with Polyethylene Glycol and Other Polymers.* Advanced Drug Delivery Reviews, 1993. **10**: p. 91-114.
98. Choi, Y.H., et al., *Polyethylene glycol-grafted poly-L-lysine as polymeric gene carrier.* Journal of Controlled Release, 1998. **54**: p. 39-48.
99. Choi, Y.H., et al., *Lactose-poly(ethylene glycol)-grafted poly-L-lysine as hepatoma cell targeted gene carrier.* Bioconjugate Chemistry, 1998. **9**: p. 708-718.

100. Kabanov, A.V., et al., *Water-soluble block polycations as carriers for oligonucleotide delivery.* Bioconjugate Chemistry, 1995. **6**: p. 639-643.
101. Wolfert, M.A., et al., *Characterization of vectors for gene therapy formed by self-assembly of DNA with synthetic block co-polymers.* Human Gene Therapy, 1996. **7**: p. 2123-2133.
102. Domard, A., M. Rinaudo, and C. Terrassin, *New method for the quaternisation of chitosan.* International Journal of Biological Macromolecules, 1986. **8**: p. 105-107.
103. Kotze, A.F., et al., *Comparison of the effect of different chitosan salts and N-trimethyl chitosan chloride on the permability of intestinal epithelial cells (Caco-2).* Journal of Controlled Release, 1998. **51**: p. 35-46.
104. Murata, J., Y. Ohya, and T. Ouchi, *Possibility of application of quaternary chitosan having pendant galactose residues as gene delivery tool.* Carbohydrate Polymers, 1996. **29**(1): p. 69-74.
105. McNeff, C. and P.W. Carr, *Synthesis and use of quaternised polyethylenimine-coated zirconia for high-performance anion-exchange chromatography.* Analytical Chemistry, 1995. **67**(21): p. 3886-3892.
106. McNeff, C., et al., *The efficient removal of endotoxins from insulin using quaternised polyethylenimine-coated porous zirconia.* Analytical Biochemistry, 1999. **274**: p. 181-187.
107. Koenig, J.L., *Spectroscopy of polymers*. 1992, Washington: American Chemical Society.
108. Usami, T. and S. Takayama, *Fine-branching structure in high-pressure, low-density polyethylenes by 50.10-MHz 13C NMR analysis.* Macromolecules, 1984. **17**: p. 1756-1761.
109. Starnes, W.H., B.J. Wojciechowski, and A. Velazquez, *Molecular microstructure of the ethyl branch segments in poly(vinyl chloride).* Macromolecules, 1992. **25**: p. 3638-3641.
110. Randall, J.C., *A review of high resolution liquid 13Carbon nuclear magnetic resonance characterisations of ethylene-based polymers.* JMS-Rev. Macromol. Chem. Phys, 1989. **C29**(2-3): p. 201-317.
111. Cheng, H.N. and T.A. Early, *NMR studies of polymeric materials - an overview.* macromolecular Symposia, 1994. **86**: p. 1-14.
112. Lukovkin, G.M., V.S. Pshezhetsky, and G.A. Murtazaeva, *NMR ^{13}C study of the structure of polyethylenimine.* European Polymer Journal, 1973. **9**: p. 559-565.
113. Arora, K.S. and C.G. Overberger, *Synthesis of linear polyethylenimine containing 9-carboxymethyl carbazole pendants.* Journal of Polymer Science, 1982. **20**: p. 403-409.
114. Domard, A., et al., *13C and 1H n.m.r. spectroscopy of chitosan and N-trimethyl chloride derivatives.* International Journal of Biological Macromolecules, 1987. **9**: p. 233-237.
115. Sieval, A.B., et al., *Preparation and NMR characterisation of highly substituted N-trimethyl chitosan chloride.* Carbohydrate Polymers, 1998. **36**: p. 157-165.

100. Kabanov, A.V., et al., *Water-soluble block polycations as carriers for oligonucleotide delivery.* Bioconjugate Chemistry, 1995. **6**: p. 639-64
101. Wolfert, M.A., et al., *Characterization of vectors for gene therapy formed by self-assembly of DNA with synthetic block co-polymers.* Human Gene Therapy, 1996. **7**: p. 2123-2133.
102. Domard, A., M. Rinaudo, and C. Terrassin, *New method for the quaternisation of chitosan.* International Journal of Biological Macromolecules, 1986. **8**: p. 105-107.
103. Kotze, A.F., et al., *Comparison of the effect of different chitosan salts and N-trimethyl chitosan chloride on the permability of intestinal epithelial cells (Caco-2).* Journal of Controlled Release, 1998. **51**: p. 35-46.
104. Murata, J., Y. Ohya, and T. Ouchi, *Possibility of application of quaternary chitosan having pendant galactose residues as gene delivery tool.* Carbohydrate Polymers, 1996. **29**(1): p. 69-74.
105. McNeff, C. and P.W. Carr, *Synthesis and use of quaternised polyethylenimine-coated zirconia for high-performance anion-exchange chromatography.* Analytical Chemistry, 1995. **67**(21): p. 3886-3892.
106. McNeff, C., et al., *The efficient removal of endotoxins from insulin using quaternised polyethylenimine-coated porous zirconia.* Analytical Biochemistry, 1999. **274**: p. 181-187.
107. Koenig, J.L., *Spectroscopy of polymers*. 1992, Washington: American Chemical Society.
108. Usami, T. and S. Takayama, *Fine-branching structure in high-pressure, low-density polyethylenes by 50.10-MHz 13C NMR analysis.* Macromolecules, 1984. **17**: p. 1756-1761.
109. Starnes, W.H., B.J. Wojciechowski, and A. Velazquez, *Molecular microstructure of the ethyl branch segments in poly(vinyl chloride).* Macromolecules, 1992. **25**: p. 3638-3641.
110. Randall, J.C., *A review of high resolution liquid 13Carbon nuclear magnetic resonance characterisations of ethylene-based polymers.* JMS-Rev. Macromol. Chem. Phys, 1989. **C29**(2-3): p. 201-317.
111. Cheng, H.N. and T.A. Early, *NMR studies of polymeric materials - an overview.* macromolecular Symposia, 1994. **86**: p. 1-14.
112. Lukovkin, G.M., V.S. Pshezhetsky, and G.A. Murtazaeva, *NMR ^{13}C study of the structure of polyethylenimine.* European Polymer Journal, 1973. **9**: p. 559-565.
113. Arora, K.S. and C.G. Overberger, *Synthesis of linear polyethylenimine containing 9-carboxymethyl carbazole pendants.* Journal of Polymer Science, 1982. **20**: p. 403-409.
114. Domard, A., et al., *13C and 1H n.m.r. spectroscopy of chitosan and N-trimethyl chloride derivatives.* International Journal of Biological Macromolecules, 1987. **9**: p. 233-237.
115. Sieval, A.B., et al., *Preparation and NMR characterisation of highly substituted N-trimethyl chitosan chloride.* Carbohydrate Polymers, 1998. **36**: p. 157-165.

116. Williams, D.H. and I. Fleming, *Spectroscopic methods in organic chemistry*. 1997, Maidenhead: McGraw-Hill.
117. Griffiths, P.R., *Fourier transform infrared spectrometry*. 1986, New York: Wiley.
118. Skoog, D.A. and J.J. Leary, *Principles of instrumental analysis*. 1992, Orlando: Saunders College Publishing.
119. Braun, R.D., *Introduction to instrumental analysis*. 1987, New York: McGraw-Hill.
120. Satake, K., et al., Journal of Biochemistry, 1960. **47**: p. 654.
121. Burger, W.C., *Interference by carbonyl compounds in the trinitrobenzenesulfonic acid method for amino groups.* Analytical Biochemistry, 1974. **57**: p. 306-309.
122. Snyder, S.L. and P.Z. Sobocinski, Analytical Biochemistry, 1975. **64**: p. 284-288.
123. Wang, W., L. Tetley, and I.F. Uchegbu, *A new class of amphiphilic poly-L-lysine based polymers forms nanoparticles on probe sonication in aqueous media.* Langmuir, 2000. **16**: p. 7859-7866.
124. Corporation, W.T., *Dn/Dc with an optilab*. 1999.
125. Wang, W., et al., *Controls on polymer molecular weight may be used to control the size of palmitoyl glycol chitosan polymeric vesicles.* Langmuir, 2001. **17**: p. 631-636.
126. Wu, C., *Laser light scattering characterization of spectral intractable macromolecules in solution.* Advances in Polymer Science, 1998. **137**: p. 103-134.
127. Wyatt, P.J., Analytical Chimica Acta, 1993. **272**: p. 1-40.
128. Uchegbu, I.F., et al., *Polymeric chitosan-based vesicles for drug delivery.* Journal of Pharmaceutics and Pharmacology, 1998. **50**: p. 453-458.
129. Bloomfield, V.A., *DNA condensation.* Current Opinion in Structural Biology, 1996. **6**(3): p. 334-341.
130. Plum, G.E., P.G. Arscott, and V.A. Bloomfield, *Condensation of DNA by trivalent cations 2. Effects of cation structure.* Biopolymers, 1990. **30**: p. 631-643.
131. le Pecq, J.B., *Use of ethidium bromide fpr separation and determination of nucleic acids of various conformational forms and measurement of their asscoiated enzymes.* Methods of Biochemical Analysis, 1971. **20**: p. 41-86.
132. Bowen, R.B. and A. Mongruel, *Calculation of the collective diffusion coefficient of electrostatically stabilised colloidal particles.* Colloids and Surfaces A: Physicochemical and Engineering Aspects, 1998. **138**: p. 161-172.
133. Nowicki, W. and G. Nowicka, *Brownian motion of a polymer-bound colloidal particle.* Colloid and Polymer Science, 1999. **277**: p. 469-473.
134. Okubo, T., S. Okada, and A. Tsuchida, *Kinetic study on the colloidal crystallisation of silica spheres in the highly diluted and exhaustively deionised suspensions as studied by light scattering and reflection spectroscopy.* Journal of Colloid and Interface Science, 1997. **189**: p. 337-347.

135. Dickinson, R., *A dynamic model for the attachment of a brownian particle mediated by discrete macromolecular bonds.* Journal of Colloid and Interface Science, 1997. **190**: p. 142-151.
136. Atteia, O., *Evolution of size distributions of natural particles during aggregation: modelling versus field results.* Colloids and Surfaces A: Physicochemical and Engineering Aspects, 1998. **139**: p. 171-188.
137. Filella, M., et al., *Analytical applications of photon correlation spectroscopy for size distribution measurements of natural colloidal suspensions: capabilities and limitations.* Colloids and Surfaces A: Physicochemical and Engineering Aspects, 1997. **120**: p. 27-46.
138. Chu, B., *Laser Light Scattering. Basic principles and Practise*. 1991, New York: Academic Press.
139. Schmitz, K.S., *An introduction to dynamic light scattering by macromolecules*. 1990, San Diego: Academic Press.
140. Fernandes, M.X.J.J., N. Santos, and M.A.R.B. Castanho, *Continuous particle size distribution analysis with dynamic light scattering.* Journal of Biochemical and Biophysical Methods, 1998. **36**(2-3): p. 101-117.
141. Lozada-Cassou, M. and E. Gonzalez-Tovar, *Primitive model electrophoresis.* Journal of Colloid and Interface Science, 2001. **239**: p. 285-295.
142. Thode, K., R.H. Muller, and M. Kresse, *Two-time window and multiangle photon correlation spectroscopy size and zeta potential analysis - highly sensitive rapid assay for dispersion stability.* Journal of Pharmaceutical Sciences, 2000. **89**(10): p. 1317-1324.
143. Gittings, M.R. and D.A. Saville, *The determination of hydrodynamic size and zeta potential from electrophoretic mobility and light scattering measurements.* Colloids and Surfaces A: Physicochemical and Engineering Aspects, 1998. **141**(1): p. 111-117.
144. Dittgen, M. and B. Herbst, *Zeta potential - Fundamentals, methods of measurement and application in pharmacy.* Pharmazie, 1987. **42**(10): p. 641-656.
145. Hunter, R.J., *Zeta potential in colloid science*. 1981, London: Academic Press.
146. Instruments, M., *Improvements in the measurement of zeta potential using the new M3 technique*. 2000.
147. Chescoe, D. and P.J. Goodhew, *The operation of the transmission electron microscope*. 1984, Oxford University press: London. p. 1-14.
148. Keyse, R.J., et al., *Introduction to Scanning Electron Microscopy*. 1998, Oxford: BIOS Scientific.
149. Robinson, D.G., et al., *Methods of Preparation for Electron Microscopy*. 1987, Springer-Verlag: Berlin. p. 76.
150. Gottschalk, S., et al., *A novel DNA peptide complex for efficient gene transfer and expression in mammalian cells.* Gene Therapy, 1996. **3**: p. 48-57.
151. Erbacher, P., et al., *Transfection and physical properties of various saccharide, polyethylene glycol, and antibody derivatised polyethylenimines (PEI).* The Journal of Gene Medicine, 1999. **1**: p. 210-222.

152. Erbacher, P., et al., *Glycosylated polylysine/DNA complexes: Gene transfer efficiency in relation with the size and the sugar substitution level of glycosylated polylysines and with the plasmid size.* Bioconjugate Chemistry, 1995. **6**: p. 401-410.
153. Kabanov, A.K., *Taking polycation gene delivery systems from in vitro to in vivo.* Pharmaceutical Science & Technology Today, 1999. **2**(9): p. 365-372.
154. Ferrari, S., et al., *ExGen 500 is an efficient vector for gene delivery to lung epithelial cells in vitro and in vivo.* Gene Therapy, 1997. **4**: p. 1100-1106.
155. Dunlap, D.D., et al., *Nanoscopic structure of DNA condensed for gene delivery.* Nucleic Acids Research, 1997. **25**(15): p. 3095-3101.
156. Li, S., et al., *Dynamic changes in the characteristics of cationic lipidic vectors after exposure to mouse serum: implications for intravenous lipofection.* Gene Therapy, 1999. **6**: p. 585-594.
157. Shinoda, T., et al., *Specific interaction with hepatocytes and acute toxicity of new carrier molecule galactosyl-polylysine.* Drug Delivery, 1999. **6**: p. 127-133.
158. Mosman, T., *Rapid colormetric assay for cellular growth and survival: application to proliferation and cytotoxicity assays.* Journal of Immunological Methods, 1983. **65**: p. 55-63.
159. Alley, M.C., et al., *Feasibility of drug screening with panels of human tumour cell lines using a microculture tetrazolium assay.* Cancer Research, 1988. **48**: p. 589-601.
160. Liu, Y., et al., *Mechanisim of cellular 3-(4,5-dimethylthiazol-2-yl)2,5-diphenyltetrazolium bromide (MTT) reduction.* Journal of Neurochemistry, 1997. **69**: p. 581-593.
161. Boussif, O., M. Zanta, and J.-P. Behr, *Optimized galenics improve in vitro gene transfer with cationic molecules up to 1000-fold.* Gene Therapy, 1996. **3**: p. 1074-1080.
162. Godbey, W.T., K.K. Wu, and A.G. Mikos, *Tracking the intracellular path of poly(ethylenimine)/DNA complexes for gene delivery.* Proceedings of the National Academy of Sciences of the USA, 2000. **96**: p. 5177-5181.
163. Nelson, N., *Structure and pharmacology of the proton AT-pases.* Trends in Pharmacological Science, 1991. **12**: p. 71-75.
164. Noguchi, A., èt al., *Membrane fusion plays an important role in gene transfection mediated by cationic liposomes.* FEBS Letters, 1998: p. 169-173.
165. Xu, Y. and F.C. Szoka, *Mechanisim of DNA release from cationic liposome/DNA complexes used in cell transfection.* 1996.
166. Uchegbu, I.F., et al., *Quaternary ammonium palmitoyl glycol chitosan - a new polysoap for drug delivery.* International Journal of Pharmaceutics, 2001. **224**: p. 185-199.
167. Helander, I.M., et al., *Polyethyleneimine is an effective permeabilizer of gram-negative bacteria.* Microbiology, 1997. **143**: p. 3193-3199.
168. Helander, I.M., K. Latva-Kala, and K. Lounatma, *Permeablizing acion of polyethylenimine on Salmonella typhimurium involves disruption of*

the outer membrane with lipopolysaccharide. Microbiology, 1998. **144**: p. 385-390.
169. Klemm, A.R., D. Young, and J.B. Loyd, *Effects of polyethyleimine on edocytosis and lysosome stability.* Biochemical Journal, 1998. **56**: p. 41-46.
170. Oku, N., et al., *The fusogenic effect of synthetic polycations on negatively charged lipid bylaers.* Journal of Biochemistry, 1986. **100**: p. 935-944.
171. Lambert, R.C., et al., *Polyethylenimine-mediated DNA transfection of peripheral and central neurons in primary culture: Probing Ca^{2+} channel structure and function with antisense oligonucleotides.* Molecular and Cellular Neuroscience, 1996. **7**: p. 239-246.
172. Yaroslavov, A.A., S.A. Sukhishvili, and O.L. Obolsky, *DNA affinity to biological membranes is enhanced due to complexation with hydrophobized polycation.* FEBS Letters, 1996. **384**: p. 177-180.
173. Smith, D.A. and J.P. Trempe, *Luminometric quatitation of photinus pyralis firefly luciferase and escherichia coli B-galactosidase in blood-contaminated oragan lysates.* Analytical Biochemistry, 2000. **286**: p. 164-172.
174. Colin, M., et al., *Haemoglobin interferes with the ex vivo luciferase luminescence assay: consequence for detection of luciferase reporter gene expression in vivo.* Gene Therapy, 2000. **7**: p. 1333-1336.
175. Katayose, S. and K. Kataoka, *Stable increase in nuclease resistance of plasmid DNA through molecular assembly with poly(ethylene glycol)-poly(L-lysine) copolymer.* Journal of Pharmaceutical Sciences, 1998. **87**(2): p. 160-163.
176. Bettinger, T., J.-S. Remy, and P. Erbacher, *Size reduction of galactosylated PEI/DNA complexes improves lectin-mediated gene transfer into hepatocytes.* Bioconjugate Chemistry, 1999. **10**: p. 558-561.
177. Fisinger, D., et al., *Protective copolymers for non-viral gene vectors: Synthesis, vector characterisationand application in gene delivery.* Gene Therapy, 2000. **7**: p. 1183-1192.
178. Katayose, S. and K. Kataoka, *Water-soluble polyion complex associates of DNA and polyethylene glycol -polylysine block copolymer.* Bioconjugate Chemistry, 1997. **8**: p. 702-707.